

# Functional characterisation of pregnancy zone protein and its relationship with maternal characteristics and pregnancy outcomes

By

# **Demi Georgiou**

Thesis Submitted to Flinders University for the degree of

# **Doctor of Philosophy**

College of Medicine and Public Health
Flinders Health and Medical Research Institute

October 2025

# TABLE OF CONTENTS

TABLE OF	CONTENTS	I
ABSTRACT	Γ	IV
DECLARA?	ΓΙΟΝ	VI
ACKNOWI	EDGEMENTS	VII
PUBLICAT	TONS	IX
PRESENTA	ATIONS	X
AWARDS 8	& FUNDING	XI
LIST OF FI	GURES	XII
LIST OF TA	ABLES	XV
	ATIONS	
CHAPTER		
1.1 0	verview	
1.2 α	M protein family	3
1.2.1	$a_2M$	4
1.2.2	PZP	11
1.3 P	hysiological changes in uncomplicated and complicated pregnancy	26
1.3.1	Maternal adaptations in uncomplicated pregnancy	27
1.3.2	Pathophysiology of preeclampsia	28
1.4 R	ationale and overarching goal	34
CHAPTER	2: CHARACTERISATION AND FUNCTIONAL ANALYSIS OF PUTATIVE PZ CHYMASE COMPLEXES	
2.1 Ir	ntroduction	36
2.2 M	lethods	39
2.2.1	Materials	39
2.2.2	Purification of PZP from human maternal pregnancy plasma	40
2.2.3	Purification of α₂M from human plasma	43
2.2.4	Denaturing gel electrophoresis	
2.2.5	Native gel electrophoresis	44
2.2.6	Western blot analysis	
2.2.7	Protein quantification	
2.2.8	Generation of protease-modified PZP and α <sub>2</sub> M	
2.2.9	Biotinylation of proteins	
2.2.10	DTNB thiol assays	
2.2.11	bisANS assays	
2.2.12	ThT assays	
2.2.13	Biotin-streptavidin pull-down assays	47

2.2.1	4 Mammalian cell culture	48
2.2.1	5 Flow cytometry	49
2.2.1	6 Chymase activity assays	49
2.3	Results	51
2.3.1	Purification of PZP from human plasma	51
2.3.2	Purification of $lpha_2$ M from human plasma	58
2.3.3	Characterisation of the interaction between PZP and chymase	61
2.3.4	The effect of PZP on the proteolytic activity of chymase	72
2.4	Discussion	76
2.4.1	Purification of PZP for <i>in vitro</i> functional analysis	77
2.4.2	Chymase is a putative endogenous substrate for PZP	78
2.4.3	Binding to PZP does not affect the activity of chymase or its inhibition by $\alpha 1ACT$	79
2.4.4	Cleavage of the PZP bait region by chymase promotes the binding of putative PZP-chymase complexes to lipoprotein receptors	80
2.4.5	PZP retains chaperone activity in the presence of chymase	81
2.4.6	A model for the activity of PZP-chymase complexes	82
CHAPTE	R 3: PARITY INFLUENCES MATERNAL PLASMA PZP CONCENTRATION IN PREGNANT WOMEN	84
3.1	Introduction	85
3.2	Methods	87
3.2.1	Recruitment	87
3.2.2	2 Sample preparation and analysis	89
3.2.3	3 Statistical analysis	90
3.3	Results	91
3.3.1	St George Hospital cohort	91
3.3.2	Nationwide Children's Hospital cohort	99
3.3.3	B Late STOP cohort	. 104
3.4	Discussion	. 108
3.4.1	Maternal plasma PZP concentration is lower in nulliparous versus parous pregnancy during mid-late gestation	. 108
3.4.2	Potential mechanism for the parity-associated increase in maternal plasma PZP concentration	. 109
3.4.3	There is no association between maternal plasma PZP concentration and LO-PE in the third trimester of nulliparous pregnancy	. 111
3.4.4	Concluding remarks	. 112
CHAPTE	R 4: MEASUREMENT OF MATERNAL PLASMA PZP CONCENTRATION IN NULLIPAROUS PREGNANCY	113
4.1	Introduction	
4.2	Methods	
4.2.1		
4.2.2	Sample preparation and analysis	. 118

4.2.3	B Statistical analysis	118
4.3	Results	119
4.3.1	STOP cohort	119
4.3.2	2 SCOPE cohort	127
4.4	Discussion	135
4.4.1	Maternal plasma PZP concentration increases across early pregnancy	136
4.4.2	2 Maternal characteristics influence plasma PZP concentration	137
4.4.3	Maternal plasma PZP concentration is associated with adverse pregnancy outcomes.	. 139
4.4.4	Differences between the STOP & SCOPE cohorts	143
4.4.5	5 Concluding remarks	144
СНАРТЕ	R 5: FINAL DISCUSSION	145
5.1	Summary	146
5.2	A framework for the distinct roles of PZP and $\alpha_2 M$ in the regulation of chymase activity	146
5.2.1	Preferential binding to PZP over α2M may prolong chymase activity via reduced LRP1-mediated clearance	
5.2.2	PZP may cooperate with other molecular inactivators to control chymase activity when LRP1-mediated clearance is overwhelmed	. 147
5.3	PZP may play a role in protecting HDL from chymase-mediated degradation	149
5.4	A link between maternal plasma PZP concentration and maternal BMI suggests a metabolic role for PZP	149
5.5	Elevated maternal plasma PZP concentration and increased odds of hypertensive pregnancy	150
5.6	Final remarks	151
SUPPLE	MENTARY INFORMATION	152
6.1	List of Supplementary Figures	153
6.2	List of Supplementary Tables	154
6.3	Chapter 2 Supplementary Information	156
6.4	Chapter 3 Supplementary Information	160
6.4.1	St George Hospital	160
6.4.2		
	Nationwide Children's Hospital	161
6.4.3	· · · · · · · · · · · · · · · · · · ·	
6.4.3 <b>6.5</b>	· · · · · · · · · · · · · · · · · · ·	164
	Chapter 4 Supplementary Information	164 <b>166</b>
6.5	Chapter 4 Supplementary Information	164 <b>166</b> 166

# ABSTRACT

Pregnancy imposes unique physiological challenges, requiring the maternal body to undergo substantial immunological, hormonal, and metabolic adaptations. While these changes are essential to support a successful pregnancy, their underlying molecular mechanisms remain incompletely understood. Pregnancy zone protein (PZP) is a large plasma glycoprotein whose concentration markedly increases during pregnancy, yet its biological importance remains largely undefined. Although PZP is closely related to well-characterised alpha-2-macroglobulin ( $\alpha_2$ M), emerging evidence suggests that differences in their quaternary structures and bait region underlie distinct functional roles. Unlike  $\alpha_2$ M, PZP has been largely overlooked in the literature. However, a small body of research suggests that PZP may contribute to pregnancy-associated maternal adaptations, including processes that are dysfunctional in preeclampsia (PE), a leading cause of maternal and neonatal morbidity and mortality. A consensus on the relationship between circulating PZP levels and PE risk remains elusive.

This thesis aimed to characterise the putative functions of PZP in pregnancy by performing *in vitro* analyses of PZP-protease interactions and their functional consequences (Chapter 2). Additionally, maternal plasma PZP concentration was assessed in relation to maternal and neonatal characteristics, including pregnancy outcome, across multiple independent cohorts of pregnant women (Chapters 3 & 4). PZP was first purified from human pregnancy plasma – a technically challenging and time-intensive process. Subsequent *in vitro* analyses demonstrated, for the first time, that PZP forms a stable complex with chymase and that their interaction does not inhibit the ability of chymase to cleave its endogenous substrate, angiotensin I (Ang I), to generate angiotensin II (Ang II), a peptide implicated in the pathogenesis of hypertension. Flow cytometry analysis showed that co-incubation of PZP with chymase promoted the binding of putative PZP-chymase complexes to lipoprotein receptors on BeWo and SH-SY5Y cells, suggesting that receptor-mediated endocytosis is important for PZP's ability to modulate chymase activity. Comparative analysis with  $\alpha_2$ M highlighted mechanistic differences in their effects on chymase, consistent with their divergent quaternary structures and ability to sterically hinder protease access.

To explore the biological importance of PZP in a physiological setting, maternal plasma PZP concentrations were quantified in three independent late pregnancy cohorts (Chapter 3). The novel finding that parity significantly affects PZP concentration prompted further analysis in

two large, independent nulliparous cohorts (Chapter 4). Among nulliparous women, plasma PZP concentration was associated several maternal characteristics, including age, ethnicity, gestational age, smoking status, and BMI. Notably, higher circulating maternal PZP concentration was associated with hypertensive disorders of pregnancy, particularly in women with a BMI  $<25 \text{ kg/m}^2$ .

Collectively, the findings presented in this thesis support a distinct, context-dependent role for PZP in modulating protease activity during pregnancy. The functional divergence between PZP and  $\alpha_2 M$  underscores the need to recognise PZP as a distinct biological entity, rather than a redundant analogue. By providing new knowledge regarding this enigmatic protein, this thesis offers new insight into the molecular systems that underpin maternal adaptation to pregnancy.

**DECLARATION** 

I certify that this thesis:

1. Does not incorporate without acknowledgment any material previously submitted for a

degree or diploma in any university

2. The research within will not be submitted for any other future degree or diploma without the

permission of Flinders University

3. To the best of my knowledge and belief, does not contain any material previously published

or written by another person except where due reference is made in the text

4. If generative artificial intelligence has been used in my thesis it has been duly acknowledged

with details to identify the extent to which generative artificial intelligence formed the final

thesis.

Signed Demi Georgiou
----------------------

Date. 17/10/2025

# ACKNOWLEDGEMENTS

This thesis would not exist without the patience, expertise, and encouragement of many people.

First and foremost, I am incredibly thankful to my supervisory team – Dr. Amy Wyatt, Professor Claire Roberts, and Dr. Tanja Jankovic-Karasoulos – for their guidance, scientific insight, and support throughout the course of my PhD.

Amy, your enthusiasm and excitement for this work have been contagious and such an important motivator for me. Thank you for your unending experimental guidance, reassurance, and kindness throughout.

Claire, thank you for your endless patience and mentorship during the many times I cried in your office over one thing or another. I'm also grateful to you for bringing me into the SRB/ANZPRA community – it was a highlight of my journey.

Tanja, thank you for your insightful feedback and help preparing for various conferences and talks, and for providing a much-needed fresh perspective during my final thesis revisions.

To Noralyn, thank you for teaching me many of the core lab skills I still use, and for your work optimising the methods I used to generate some of the data in this thesis. I'm so grateful I had your guidance while I found my feet.

To my lab mates – and those in the near vicinity – including the PHaB lab, Forbes lab, and MND lab: thank you for the technical support, shared laughter (and vents), and collective resilience during the more challenging times. So many of you have made this experience bearable. Special shoutouts go to Alana and Rachel, who have suffered through these final stages with me; the quiz night crew, for adopting me into the group – those nights definitely helped on some of the rougher days; and Dylan, for spending countless hours in the basement with me retrieving an ungodly number of samples from the -80 °C freezer. To those not mentioned by name, please know your support and kindness have not gone unnoticed. I am sincerely thankful to everyone who helped me reach this point.

To my partner, Jono – thank you for always being there to support and encourage me through the tears, late nights, and weekend work. I know there were some particularly rough times, so thank you for standing by me.

To my family and friends – thank you for your love and support throughout, and for always being there for a presentation run-through or to answer, "Does this make sense to someone outside academia?" A special shout-out to my grandma, Kami (Raelene), who has been one of my biggest supporters since I first decided to do a PhD.

I am incredibly grateful to the women who donated samples for purification and analysis, without whom this work would not be possible. I also gratefully acknowledge the contributions of those who supported the generation of some of the data used in this thesis. For the St. George Hospital cohort: Dr. Jordan Cater, Professor Amanda Henry, Wendy Winata, and Gimhani Avindri Abeygunasekara. For the Nationwide Children's Hospital cohort: Professor Irina Buhimschi and her research group.

I gratefully acknowledge the funding bodies who made this research possible: Channel 7 Children's Research Foundation, The Hospital Research Foundation, Flinders Foundation, and the NHMRC. This research was also supported by an Australian Government Research Training Program (RTP) Scholarship. I acknowledge minimal use of generative artificial intelligence tools, in accordance with current Flinders University guidelines, to assist with proofreading and to improve the clarity and conciseness of parts of the writing.

# **PUBLICATIONS**

# Publications arising outside this thesis

**Georgiou, D. K.,** & Wynn, E. (2022). Good vibes: Experimenters report back on their experiences. Flinders University Student Health and Well-being Blog. Available at <a href="https://blogs.flinders.edu.au/student-health-and-well-being/2022/09/12/good-vibes-experimenters-report-back-on-their-experiences/">https://blogs.flinders.edu.au/student-health-and-well-being/2022/09/12/good-vibes-experimenters-report-back-on-their-experiences/</a>

Cater, J. H., Mañucat-Tan, N. B., **Georgiou, D. K.**, Zhao, G., Buhimschi, I. A., Wyatt, A. R., & Ranson, M. (2022). A Novel Role for Plasminogen Activator Inhibitor Type-2 as a Hypochlorite-Resistant Serine Protease Inhibitor and Holdase Chaperone. Cells, 11(7). https://doi.org/10.3390/cells11071152

# **PRESENTATIONS**

**Georgiou, D. K.,** Arthurs, A., L., Jankovic-Karasoulos, T., Roberts, C. T., & Wyatt, A. R., (2024). *Pregnancy zone protein; a novel regulator of hypertension during pregnancy via interaction with chymase?* Presented at the Society for Reproductive Biology (SRB) annual conference, Adelaide, SA, Australia.

**Georgiou, D. K.,** Mañucat-Tan, N. B., McCullough, D., Leemaqz, S. Y., Jankovic-Karasoulos, T., Roberts, C. T., & Wyatt, A. R., (2023). *Characterisation of maternal plasma pregnancy zone protein as a potential biomarker of preeclampsia risk*. Presented at the Society for Reproductive Biology (SRB) annual conference, Brisbane, QLD, Australia.

**Georgiou, D. K.,** Jankovic-Karasoulos, T., Roberts, C. T., & Wyatt, A. R., (2022). *Elucidating the biological importance of PZP*. Presented at the European Molecular Biology (EMBL) Australia PhD course, Monash, VIC, Australia.

**Georgiou, D. K.,** (2022). *Uncovering the biological importance of PZP*. Presented multiple times as part of the Three Minute Thesis competition, Adelaide, SA, Australia.

**Georgiou, D. K.,** Mañucat-Tan, N. B., Ghahghaei, A., Jankovic-Karasoulos, T., Roberts, C. T., & Wyatt, A. R., (2022). *Pregnancy Zone Protein: more than just a protease inhibitor?* Presented at the Adelaide Protein Group (APG) Awards Fest, Adelaide, SA, Australia.

**Georgiou, D. K.,** Jankovic-Karasoulos, T., Roberts, C. T., & Wyatt, A. R., (2022). *Elucidating the biological importance of PZP*. Presented at the Flinders University College of Medicine and Public Health Emerging Leaders Showcase, Adelaide, SA, Australia.

**Georgiou, D. K.,** (2022). The importance of keeping a laboratory notebook. Presented at the Australian School of Mathematics and Science (ASMS), Adelaide, SA, Australia.

**Georgiou, D. K.,** Jankovic-Karasoulos, T., Roberts, C. T., & Wyatt, A. R., (2021). *Pregnancy Zone Protein: more than just a protease inhibitor?* Presented at the Flinders University College of Medicine and Public Health Emerging Leaders Showcase, Adelaide, SA, Australia.

# **AWARDS & FUNDING**

## 2021 - 2024

Australian Research Training Program Scholarship

Healthy Development Adelaide & Channel 7's Research Foundation PhD Excellence Award (top-up scholarship)

The Hospital Research Foundation Group

Channel 7 Children's Research Foundation

Flinders Foundation

## 2022

People's Choice Award, EMBL Australia PhD Course (short talk)

Flinders University Runner Up and People's Choice, Three Minute Thesis competition

Student researcher finalist, APG Awards Fest (short talk)

Australian New Zealand Placental Research Association (ANZPRA) New Investigator Award finalist, SRB annual conference (short talk)

# 2021

Best presentation by a higher degree by research student – Flinders University College of Medicine and Public Health Emerging Leaders Showcase

# LIST OF FIGURES

Figure 1.2.1: Models of human $\alpha_2 M$ structure derived using cryo-electron microscopy 6
Figure 1.2.2: Structure of human PZP based on in silico modelling14
Figure 1.2.3: Simplified diagram showing the differences in protease trapping activity of $\alpha_2 M$
and PZP16
Figure 1.3.1: Simplified schematic diagram highlighting core components of the circulating
and placental RAS and their downstream effects
<b>Figure 2.1.1:</b> Diagram showing the formation and fate of $\alpha_2M$ -chymase complexes
Figure 2.2.1: Summary of the process for purifying endogenous PZP from human pregnancy plasma41
Figure 2.2.2: Two-step incubation protocol used to prepare samples for chymase activity
assays51
Figure 2.3.1: Representative Coomassie-stained gel and matched Western blot showing
protein fractions obtained following PEG 6000 precipitation of human pregnancy plasma 54
Figure 2.3.2: Representative Coomassie-stained gel and matched Western blot showing
protein fractions obtained from DEAE anion exchange chromatography of the PZP-enriched
fraction following PEG 6000 precipitation of human pregnancy plasma55
Figure 2.3.3: Representative Western blots detecting PZP (360 kDa) and $\alpha_2 M$ (720 kDa) in
fractions eluted by HIC of the PZP-enriched fraction obtained from DEAE chromatography $56$
Figure 2.3.4: Representative native Western blots detecting PZP and $\alpha_2 M$ in fractions eluted by
ZAC of the PZP-enriched fraction obtained from HIC57
Figure 2.3.5: Representative Coomassie-stained denaturing gels and native Western blots
showing the proteins eluted during SEC using a HiPrep 26/60 Sephacryl S-300 HR column 59
Figure 2.3.6: Representative Coomassie-stained denaturing and native gels, and native
Western blot showing proteins eluted following ZAC and SEC of whole human plasma for the
purification of $\alpha_2 M$ 61
Figure 2.3.7: Representative Coomassie-stained stained native and denaturing gels showing
the migration of proteins following co-incubation of PZP with chymase or chymotrypsin 63
Figure 2.3.8: Representative Coomassie-stained denaturing and native gels showing the
migration of proteins following co-incubation of PZP with chymase or chymotrypsin at different
molar ratios

Figure 2.3.9: Results of biotin-streptavidin pull-down assay and DTNB assay to assess the
interaction between PZP and chymase67
Figure 2.3.10: The effect of pre-incubation with a protease on the exposed surface
hydrophobicity of PZP, as assessed by bisANS fluorescence
Figure 2.3.11: The effect of PZP and PZP-protease complexes on the aggregation of $A\beta_{1-42}$ , as
assessed by ThT assay69
Figure 2.3.12: Representative Western blot detecting PZP captured by biotinylated $A\beta_{1-42}$ and
recovered using Dynabeads™ MyOne™ Streptavidin C1 beads
Figure 2.3.13: The effect of pre-incubation with chymase on cell-surface receptor binding of
PZP, as assessed by flow cytometry72
<b>Figure 2.3.14:</b> RETF-4NA cleavage by chymase, PZP-chymase, or $\alpha_2 M$ -chymase in the presence
or absence of α1ACT74
Figure 2.3.15: Representative elution profiles of Ang I and Ang II following incubation with
chymase, PZP-chymase, or $\alpha_2 M$ -chymase in the presence or absence of $\alpha 1 ACT$
Figure 2.3.16: Relative peak area of Ang II to Ang I following incubation with chymase, PZP-
chymase, or $\alpha_2 M$ -chymase in the presence or absence of $\alpha 1ACT$
Figure 2.4.1: Proposed model illustrating how differences in the quaternary structure of PZP
and $\alpha_2 M$ influence access of endogenous protease inhibitors to chymase
Figure 3.2.1: Participant flow chart for the late STOP cohort
Figure 3.3.1: Unadjusted maternal plasma PZP concentration grouped by pregnancy outcome
in the St George Hospital cohort96
Figure 3.3.2: Correlation between maternal plasma PZP concentration and clinical parameters
in the St George Hospital Cohort98
Figure 3.3.3: Unadjusted maternal plasma PZP concentration grouped by parity in the St
George Hospital cohort100
Figure 3.3.4: Unadjusted maternal plasma PZP concentration grouped by pregnancy outcome
in the Nationwide Children's Hospital cohort102
Figure 3.3.5: Correlation between maternal plasma PZP concentration and maternal
characteristics in the Nationwide Children's Hospital cohort103
Figure 3.3.6: Unadjusted maternal plasma PZP concentration grouped by parity and gravidity
in the Nationwide Children's Hospital cohort104
Figure 3.3.7: Unadjusted maternal plasma PZP concentration grouped by pregnancy outcome
and stratified by parity and gravidity in the Nationwide Children's Hospital cohort 105

Figure 3.3.8: Unadjusted maternal plasma PZP concentration grouped by pregnancy outcome
in the late STOP cohort
Figure 3.3.9: Unadjusted maternal plasma PZP concentration, grouped by ethnicity, in the late
STOP cohort
Figure 4.2.1: Participant flow charts for the SCOPE and STOP cohorts
Figure 4.3.1: Unadjusted maternal plasma PZP concentration grouped by pregnancy outcome
in the STOP cohort
Figure 4.3.2: Unadjusted maternal plasma PZP concentration grouped by ethnicity and
smoking status in the STOP cohort
Figure 4.3.3: Unadjusted maternal plasma PZP concentration grouped by BMI in the STOP
cohort
Figure 4.3.4: Unadjusted maternal plasma PZP concentration grouped by pregnancy outcome
in the SCOPE cohort
Figure 4.3.5: Unadjusted maternal plasma PZP concentration grouped by ethnicity and
smoking status in the SCOPE cohort
Figure 4.3.6: Unadjusted maternal plasma PZP concentration grouped by BMI in the SCOPE
cohort
Figure 5.2.1: Proposed model of context-dependent regulation of chymase activity by PZP and
$\alpha_2 M$ through differential clearance and susceptibility to endogenous inactivators

# LIST OF TABLES

<b>Table 1.2.1:</b> Human protease substrates for $\alpha_2 M$ and PZP
Table 1.2.2: Summary of studies reporting PZP concentration in maternal blood from patients
with uncomplicated and preeclamptic pregnancies23
Table 1.2.3: PZP mRNA expression in various cancers and its association with prognostic
measures24
Table 1.3.1: Examples of major physiological changes that occur in the mother during
pregnancy
Table 1.3.2: Commonly described risk factors for PE
Table 2.2.1: Common buffers used throughout the experimental procedures         39
Table 2.2.2: Summary of antibodies used in Western Blot analysis.         46
Table 2.2.3: Prepared protein samples and controls for use in biotin-streptavidin pull-down
assays49
Table 2.2.4: Cultured cell line types and composition of the media used to maintain them for
standard growth
Table 2.3.1: Endpoint absorbance and reaction rate for RETF-4NA cleavage by chymase, PZP-
chymase, or $lpha 2$ M-chymase in the presence or absence of $lpha 1$ -antichymotrypsin ( $lpha 1$ ACT) 74
Table 3.1.1: Studies that have quantified PZP in blood plasma or serum during pregnancy 88
Table 3.3.1: Maternal and neonatal characteristics grouped by pregnancy outcome in the St
George Hospital cohort94
Table 3.3.2: Logistic regression model assessing the association between maternal plasma
PZP concentration and pregnancy outcome in the St George Hospital cohort
Table 3.3.3: Maternal characteristics grouped by pregnancy outcome in the Nationwide
Children's Hospital cohort101
Table 3.3.4: Univariate linear regression analyses assessing the association between maternal
characteristics and maternal plasma PZP concentration in the Nationwide Children's Hospital
cohort104
Table 3.3.5: Maternal and neonatal characteristics grouped by pregnancy outcome in the late
STOP cohort107
Table 3.3.6: Univariate quantile regression analyses assessing the association between
maternal characteristics and PZP concentration in the late STOP cohort110

<b>Table 4.2.1:</b> Details for the recruitment of participants to the prospective cohort studies SCOPE
and STOP
Table 4.3.1: Maternal and neonatal characteristics grouped by pregnancy outcome in the STOP
cohort
Table 4.3.2: Correlations between maternal and neonatal characteristics and maternal plasma
PZP concentration in the STOP cohort
Table 4.3.3: Univariate quantile regression analyses to assess the association between
maternal characteristics and maternal plasma PZP concentration in the STOP cohort 127
Table 4.3.4: Maternal and neonatal characteristics grouped by pregnancy outcome in the
SCOPE cohort
Table 4.3.5: Correlations between maternal and neonatal characteristics and maternal plasma
PZP concentration in the SCOPE cohort
Table 4.3.6: Univariate quantile regression analyses to assess the association between
maternal characteristics and PZP concentration in the SCOPE cohort
Table 4.4.1: Summary of the main findings following analysis of the associations between
maternal or neonatal characteristics and maternal plasma PZP concentration in the STOP and
SCOPE cohorts
Table 4.4.2: Summary of how increasing maternal plasma PZP concentration affects the odds
of adverse pregnancy outcomes

# **ABBREVIATIONS**

ADAM12 A disintegrin and metalloproteinase domain-containing protein 12

α1ACT Alpha-1-antichymotrypsin

α1AT Alpha-1-antitrypsin

α<sub>2</sub>M Alpha-2-macroglobulin

α<sub>2</sub>ML1 Alpha-2-macroglobulin-like protein 1

αM Alpha-macroglobulin

AD Alzheimer's disease

ATCC American Type Culture Collection

Aβ Amyloid beta

A $\beta_{1-42}$  Amyloid beta 1-42

ACE Angiotensin converting enzyme

ACE2 Angiotensin converting enzyme 2

Ang I Angiotensin I

Ang II Angiotensin II

AT<sub>1</sub>R Angiotensin II type 1 receptor

AT<sub>2</sub>R Angiotensin II type 2 receptor

AGT Angiotensinogen

AEC Anion exchange chromatography

APH Antepartum haemorrhage

ApoA1 Apolipoprotein A1

AFU Arbitrary fluorescence units

AUC Area under the curve

AST Aspartate aminotransferase

ASPRE Aspirin for Evidence-Based Preeclampsia Prevention

AT<sub>1</sub>R-AA AT1R autoantibodies

BRD Bait region domain

BSA Bovine serum albumin

BAT Brown adipose tissue

CUB C1r/C1s, Uegf, Bmp1

CPAMD8 C3 and PZP like alpha-2-macroglobulin domain containing 8

CA19-9 Carbohydrate antigen

CEA Carcinoembryonic antigen

ChIP-seq Chromatin immunoprecipitation sequencing

CV Column volume

DEAE Diethylaminoethanol

DMSO Dimethyl sulfoxide

DKO Double knockout

DMEM Dulbecco's Modified Eagle's Medium

EO-PE Early onset preeclampsia (<34 weeks gestation)

ECM Extracellular matrix
FBS Fetal bovine serum

FGR Fetal growth restriction

FMC Flinders Medical Centre

GWAS Genome wide association study

GDM Gestational diabetes mellitus

GH Gestational hypertension

GST-RAP Glutathione S-transferase tagged receptor associated protein

GdA Glycodelin A

HBSS Hanks balanced salt solution

HMW High molecular weight

HPLC High performance liquid chromatography

HRP horse radish peroxidase

HUVEC Human umbilical vein endothelial cell

HCl Hydrochloric acid

HIC Hydrophobic interaction chromatography

OCl- Hypochlorite

IPF Idiopathic pulmonary fibrosis

IGF Insulin-like growth factor

IFN Interferon

IL Interleukin

IF Intermittent fasting

ISSHP International Society for the Study of Hypertension in Pregnancy

IUGR Intrauterine growth restriction

LO-PE Late onset preeclampsia (≥34 weeks gestation)

LRP1 Low density lipoprotein receptor related protein 1

MG Macroglobulin-like

MasR Mas Receptor

MC Mast cell

MMP Matrix metalloproteinase

MAP Mean arterial blood pressure

MWCO Molecular weight cut off

MS Multiple sclerosis MUG-1 Murinoglobulin-1 NET Neutrophil extracellular trap NO Nitric oxide NC Nitrocellulose NAFLD Non-alcoholic fatty disease PBS Phosphate-buffered saline PlGF Placental growth factor **PAGE** Polyacrylamide gel electrophoresis PES Polyether sulfone PEG Polyethylene glycol **PVDF** Polyvinylidene fluoride POR Poor ovarian responders PPH Post partum haemorrhage Predicted local distance difference test pLDDT PΕ Preeclampsia PAPP-A Pregnancy associated plasma protein-A PP Pregnancy plasma PZP Pregnancy zone protein (refers to the protein or protein concentration) PZP Pregnancy zone protein (refers to the gene or mRNA concentration) PTdNK Pregnancy-trained decidual natural killer (cells) PROM Premature rupture of membranes (P)RR Prorenin receptor ROS Reactive oxygen species RBD Receptor binding domain Rf Relative migration distance RAS Renin-angiotensin system rpHPLC Reverse phase high performance liquid chromatography DCAK1 Serine/threonine-protein kinase STAT Signal transducers and activators of transcription SEC Size exclusion chromatography SGA Small for gestational age

SEC Size exclusion chromatography

SGA Small for gestational age

SDS Sodium dodecyl sulfate

sFlt-1 Soluble fms-like tyrosine kinase 1

sPTB Spontaneous preterm birth

ACOG The American College of Obstetricians and Gynecologists

NICE The National Institute for Health and Care Excellence

TED Thioester domain

TPL Threatened preterm labour

tPA Tissue plasminogen activator

TGF-β Transforming growth factor beta

TFF3 Trefoil factor 3

Tregs Regulatory T cells

TFA Trifluoroacetic acid

TNF-a Tumor necrosis factor alpha

T2DM Type 2 diabetes mellitus

UCP1 Uncoupling protein 1

uMC Uterine mast cell

uNK Uterine natural killer (cell)

uSMC Uterine smooth muscle cell

VEGFA Vascular endothelial growth factor A

WNV West Nile Virus

WAT White adipose tissue

WAC Women's assessment clinic

ZAC Zinc affinity chromatography

# **CHAPTER 1:**

# **INTRODUCTION**

# 1.1 Overview

Proteins are complex macromolecules that play essential roles in nearly all biological processes. Secreted proteins (also known as extracellular proteins) are those released into the peripheral blood circulation or the local extracellular environment, where they perform diverse functions (Uhlén et al., 2015). Compared to the cytosol, which contains a highly complex mixture of proteins, extracellular fluids have a relatively simple composition. Despite this, the secretome, and the functional roles of its constituent proteins, remain poorly defined.

Secreted proteins play a role in maintaining systemic homeostasis, transporting nutrients, and coordinating immune responses, among many other functions. Constitutively expressed proteins are typically involved in processes essential for normal function and tissue maintenance. Conversely, the concentrations of other proteins fluctuate in response to biological stimuli. For example, tissue injury and/or infection triggers increased acute phase protein concentrations in blood plasma. Additionally, the composition of biological fluids varies with age, and during pregnancy (Romero et al., 2017, Tarca et al., 2022, Labbadia and Morimoto, 2015). In part, this may be explained by the low grade, systemic inflammation that is present in the elderly and in those who are pregnant (Franceschi et al., 2000, Jarmund et al., 2021, Dutta et al., 2024). However, we currently lack a complete understanding of the underlying mechanisms by which major changes to the plasma proteome occur.

A pertinent example is pregnancy zone protein (PZP), a component of blood plasma and other biological fluids that is markedly upregulated in humans during pregnancy. Maternal plasma PZP levels are reported to increase from trace amounts under non-pregnant conditions to become one of the most abundant plasma proteins by the third trimester of pregnancy (Ekelund and Laurell, 1994). Despite this tremendous investment by the maternal body, the underlying reasons for the upregulation of PZP during pregnancy remain elusive. Due to the limited number of *in vitro* studies characterising the functions of PZP, clues about its potential biological role have been inferred from the highly studied, closely related protein alpha-2-macroglobulin ( $\alpha_2$ M). This chapter provides an overview of the structure and function of the  $\alpha$ M protein family, with additional detail provided regarding  $\alpha_2$ M and PZP. A summary of major pregnancy-induced physiological changes is then given, followed by the introduction of preeclampsia (PE), a pregnancy complication in which maternal PZP has previously been studied, although its contribution to disease pathology is yet to be defined (Ekelund and Laurell, 1994, Fosheim et

al., 2023, Horne et al., 1972, Griffin, 1983, Armstrong et al., 1986, Blumenstein et al., 2009, Liu et al., 2011).

# 1.2 αM protein family

 $\alpha$ Ms are large multidomain plasma proteins that have diverse functions but are predominantly known as protease inhibitors. In part, their functions are determined by the quaternary structure of the protein which may be tetrameric, dimeric or monomeric (Rubenstein et al., 1993, Devriendt et al., 1989). For example, the quaternary structure of  $\alpha_2$ M, a tetramer, enables it to efficiently trap protease substrates and sterically hinder their access to larger substrates (Sottrup-Jensen, 1989). On the other hand, despite sharing the key feature of a reactive thioester bond, dimeric and monomeric  $\alpha$ M proteins are less effective as protease inhibitors (Nielsen et al., 2022, Jensen and Stigbrand, 1992, Rubenstein et al., 1993). Additionally, the functions of  $\alpha$ M proteins are influenced by conformational changes that are triggered by reaction of the liable thioester bond with proteases or small amine containing compounds (Reddy et al., 1994, Björk and Fish, 1982).

Proteins from the αM family have ancient origins and are found in a wide range of organisms, including mammals, reptiles, amphibians, chondrocytes, fish, birds (Rubenstein et al., 1993), cephalopods (Thøgersen et al., 1992), and arthropods, (Spycher et al., 1987, Armstrong et al., 1991, Sottrup-Jensen et al., 1990, Sekiguchi et al., 2012). These proteins are even found in bacteria, hypothesised to have been captured from metazoan host genes and subsequently spread by horizontal gene transfer (Budd et al., 2004). The existence of αM family proteins in such a broad range of organisms supports the conclusion that they are important components of the innate immune system and share a common evolutionary origin with the C3 and C4 complement proteins (Sottrup-Jensen et al., 1985).

Though  $\alpha M$  proteins are widely conserved across many organisms, care must be taken when interpreting results from animal studies in the context of human biology. This is particularly true for studies in rodents. For example, in humans  $\alpha_2 M$  is a tetramer, whilst PZP is a dimer (Sottrup-Jensen, 1989), whereas murine  $\alpha_2 M$  and PZP are both tetrameric and the predominant  $\alpha M$  is monomeric murinoglobulin-1 (MUG-1) (Bernhard et al., 2007). Expression patterns also vary, with human  $\alpha_2 M$  constitutively expressed and PZP typically undetectable in blood plasma under normal conditions (Sottrup-Jensen, 1989, Ekelund and Laurell, 1994). Conversely, mice have high plasma PZP concentrations and barely detectable  $\alpha_2 M$  (Bernhard et al., 2007). This

may be attributed to the fact that, in mice, PZP is the broad-spectrum protease inhibitor, whilst in humans this role is performed by  $\alpha_2 M$  (Krause et al., 2019). This suggests that  $\alpha_2 M$  and PZP may have opposing functions in mice compared to humans. As another example, in marmosets,  $\alpha_2 M$ -like protein 1 ( $\alpha_2 ML1$ ) is significantly upregulated during pregnancy, rather than PZP – as observed in humans (Kashiwagi et al., 2020). This highlights the need for caution when generalising data from animal models to the human context.

The following section provides relevant background information on the structure and function of  $\alpha_2 M$  and PZP, beginning with  $\alpha_2 M$  – the most extensively characterised  $\alpha M$  family member – to contextualise the current structural and functional models of PZP. Considering the centrality of PZP to this thesis, a more detailed review of the literature relevant to PZP is subsequently presented.

### 1.2.1 $\alpha_2 M$

 $\alpha_2 M$  is the foremost representative of the  $\alpha M$  protein family and has been highly studied since its discovery. As the largest major non-immunoglobulin plasma protein,  $\alpha_2 M$  is constitutively abundant in human biological fluids. It can be purified from human blood plasma via a straightforward chromatography process with relatively high yield, a feature that has facilitated the ability to extensively characterise its functions *in vitro*.

# 1.2.1.1 Structure

In humans,  $\alpha_2 M$  is a 720 kDa protein comprised of four identical subunits. Each 180 kDa subunit contains 1,451 amino acid residues and during post-translational modification eight asparagine residues are glycosylated via the addition of glucosamine-based oligosaccharide groups that vary in charge and size (Sottrup-Jensen et al., 1984). The amino acid sequence encodes several distinct domains, including seven macroglobulin-like (MG) domains, a C1r/C1s, Uegf, Bmp1 (CUB) domain, a receptor binding domain (RBD), thioester domain (TED), and bait region domain (BRD) (Marrero et al., 2012) (Figure 1.2.1A).

The intricate native fold of  $\alpha_2 M$  is stabilised by eleven intrachain disulfide bridges (Jensen and Sottrup-Jensen, 1986) (Figure 1.2.1B). MG1-6 create a compact, ellipsoidal right-handed superhelix, with the extended and flexible RBD inserted into MG6. The C-terminal portion consists of domains downstream of MG6, with MG7 acting as a hinge to close the MG1-6 super-helix and connect it to the CUB domain (Marrero et al., 2012, Luque et al., 2022). The TED, situated within the CUB domain, forms a six-fold  $\alpha$ -propeller structure, creating a thick disk-like shape. The

reactive β-cysteinyl-γ-glutamyl thioester bond within the TED is formed between cysteine and glutamine side chains (Luque et al., 2022). Finally, the C-terminal domain is the RBD, which contains a cryptic receptor binding site (Huang et al., 2022, Luque et al., 2022, Marrero et al., 2012).

To attain its quaternary structure,  $\alpha_2 M$  monomers are covalently linked via two interchain disulfide bridges in the MG3 and MG4 domains to form dimers (Jensen and Sottrup-Jensen, 1986, Marrero et al., 2012). These dimers then non-covalently associate to complete the 720 kDa native tetramer. In this tetrameric structure, each monomer has a disulfide-linked, vicinal, and opposite monomer (Figure 1.2.1C), resulting in a unique cage-like structure with four large openings (Luque et al., 2022). Notably, the thioester bond, which is critical to  $\alpha_2 M$ 's function as a protease inhibitor, is shielded by large hydrophobic side chains within the native tetramer to prevent premature proteolytic hydrolysis. The RBD is also buried in the native tetramer, surrounded by the CUB domain, TED, and MG7, thereby regulating its interaction with receptors (Marrero et al., 2012, Luque et al., 2022) (Figure 1.2.1B).

In biological fluids,  $\alpha_2 M$  is predominantly present in its native tetrameric conformation, however, its diverse functions are linked to its ability to adopt alternate conformations. Firstly,  $\alpha_2 M$  may exist in a more compact, electrophoretically fast form, known as transformed, activated, or 'fast'  $\alpha_2 M$  (Figure 1.2.1D) (Björk and Fish, 1982, Luque et al., 2022). This conformation exposes the previously buried thioester and RBD which allows  $\alpha_2 M$  to trap proteases and interact with receptors for clearance (see Section 1.2.1.2 for a detailed description of this process; Feldman et al., 1985a, Huang et al., 2022).  $\alpha_2 M$  can also take a dimeric form, which is induced by molecules such as hypochlorite (OCl') that rapidly oxidises the methionine residues situated at the interface of the non-covalently linked dimers causing them to dissociate (Reddy et al., 1994, Reddy et al., 1989). Hypochlorite-modified human  $\alpha_2 M$  dimers exhibit increased exposed surface hydrophobicity (Wyatt et al., 2014), which likely underpins the distinct functionality of dimeric  $\alpha_2 M$  compared to tetrameric  $\alpha_2 M$ . As immune cells are known to produce large amounts of hypochlorite, this has been suggested as an important regulator of  $\alpha_2 M$  function during inflammation, though further *in vivo* studies are needed to confirm the biological relevance of the findings generated by *in vitro* approaches.

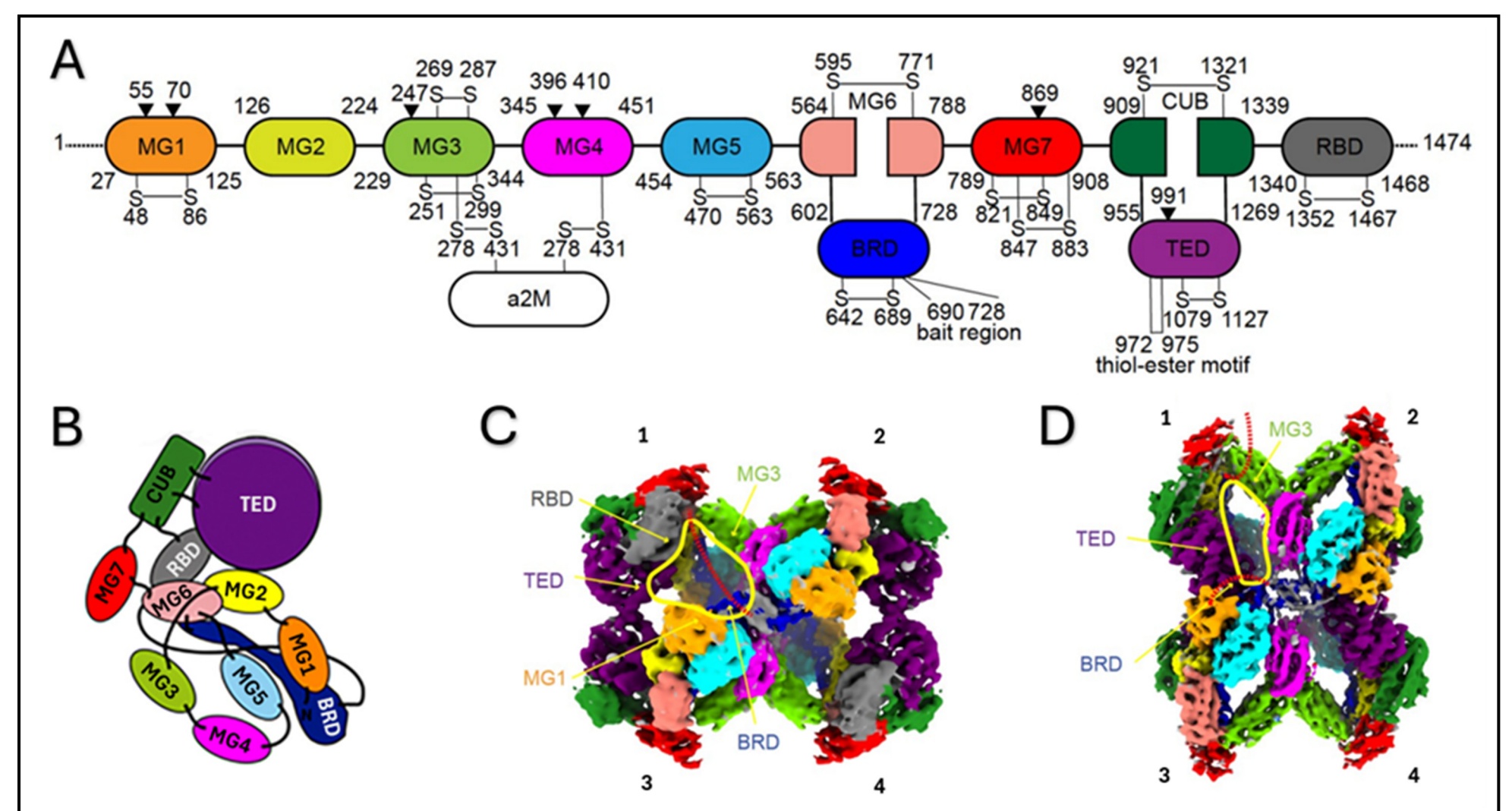


Figure 1.2.1: Models of human  $\alpha_2 M$  structure derived using cryo-electron microscopy.

(A) Known functional domains, with flanking residues and disulfide bonds shown, for one  $\alpha_2M$  subunit. Thioester and bait-region insertion sites are also shown, with N-linked glycosylation sites (arginine residues) depicted by black triangles. Reproduced with permission from Huang et al. 2022, licensed via RightsLink (licence number 5987900893168).

(B) Illustration of domain organisation within one subunit of native  $\alpha_2M$  (adapted with permission from Dr. JR Castón, corresponding author, and licenced under Creative Commons CC BY-NC-ND 4.0). (C & D) Density map of the (C) native and (D) transformed  $\alpha_2M$  tetramers. Colour coding aligns with (A). Monomer 1 has a disulfide-linked (2), vicinal (3), and opposite (4) monomer. Reproduced with permission from Huang et al. 2022, licensed via RightsLink (licence number 5987900893168).

## 1.2.1.2 **Function**

A contemporary view is that  $\alpha_2M$  is a highly multifunctional protein that plays a role in many biological processes, including participating in innate immunity. Nonetheless,  $\alpha_2M$  is predominantly known for its ability to bind to a wide range of proteases, regardless of their structure, source, or catalytic mechanism. Each  $\alpha_2M$  tetramer can bind up to two proteases, highlighting its efficiency as an inhibitor (Sottrup-Jensen, 1989, Travis and Salvesen, 1983). The mechanism by which  $\alpha_2M$  inhibits proteases does not involve direct inactivation of the protease, rather binding to  $\alpha_2M$  traps proteases within a steric cage that is inaccessible to large substrates. This process begins when a protease cleaves the flexible, solvent exposed bait region of  $\alpha_2M$ , contained within the BRD. Proteolytic cleavage of the bait region triggers a conformational change in the corresponding  $\alpha_2M$  monomer subunit, thereby exposing the thioester bond which is typically buried within a hydrophobic pocket (Huang et al., 2022, Luque et al., 2022). Exposure of the  $\alpha_2M$  thioester allows it to react with a nucleophile-containing side chain on the protease substrate, thereby forming a transformed  $\alpha_2M$ -protease complex (Sottrup-Jensen et al., 1980, Luque et al., 2022, Huang et al., 2022).

In addition to trapping proteases, the conformational change associated with reaction of the  $\alpha_2M$  thioester also exposes a receptor recognition site for the multifunctional cell-surface receptor low density lipoprotein related receptor 1 (LRP1) (Luque et al., 2022, Huang et al., 2022). Once the receptor binding site is exposed, LRP1 facilitates rapid clearance of the transformed  $\alpha_2M$ -protease complex. Interestingly, the LRP1 binding site may also be exposed by small nucleophiles, such as methylamine or ammonium chloride, which can react with the  $\alpha_2M$  thioester bond independent of bait region proteolysis and induce a similar compact transformed conformation (Björk and Fish, 1982, Sottrup-Jensen, 1989). Thus,  $\alpha_2M$  can efficiently regulate extracellular proteolytic activity and control many other biological processes by facilitating clearance of non-covalently bound ligands (discussed further below). Following internalisation by LRP1, transformed  $\alpha_2M$ -protease complexes are delivered to lysosomes for degradation (Hanover et al., 1983, Maxfield et al., 1981, Tycko and Maxfield, 1982).

Beyond its role as a protease inhibitor,  $\alpha_2 M$  noncovalently binds to a wide range of structurally diverse ligands. This characteristic of  $\alpha_2 M$  is reflective of its ancient origins, which preceded the evolution of many specialised proteins. For example,  $\alpha_2 M$  has been shown to bind growth factors (Asplin et al., 2001, Crookston et al., 1994, Arandjelovic et al., 2007), cytokines (Gonias

et al., 2000, LaMarre et al., 1991), misfolded proteins (Wyatt and Wilson, 2013, Yerbury et al., 2009, Hughes et al., 1998), hepcidin (Peslova et al., 2009), and apolipoprotein E (Krimbou et al., 1998). In many cases, these ligands preferentially bind transformed  $\alpha_2 M$  (Wyatt et al., 2013a, French et al., 2008, Narita et al., 1997, LaMarre et al., 1991, Wollenberg et al., 1991), suggesting that  $\alpha_2 M$  regulates their activity by facilitating their clearance from biological fluids via an LRP1 mediated pathway.

While the clearance of transformed  $\alpha_2 M$  and its bound ligands via LRP1 is well characterised, less is known about the ability of hypochlorite-modified dimeric  $\alpha_2 M$  to act via a similar mechanism *in vivo*. *In vitro* studies suggest that hypochlorite-modified  $\alpha_2 M$  dimers also bind LRP1, albeit with reduced affinity (Wyatt et al., 2014, Wu et al., 1997). This alternative clearance pathway may be particularly important during inflammation, when levels of hypochlorite are markedly elevated. Interestingly, although reaction with hypochlorite can induce the formation of a dimeric LRP1-recognised form of  $\alpha_2 M$ , it concomitantly reduces the binding of transformed tetrameric  $\alpha_2 M$  to LRP1 (Wu et al., 1997). This supports the idea that during inflammation hypochlorite-induced modification plays a key role in regulating the functions of  $\alpha_2 M$ . The complexity of this system is yet to be fully elucidated.

The distinct ligand binding preferences of transformed and dimeric α₂M have important implications for the molecular cargo that is being cleared from circulation. In vitro studies show that hypochlorite-modified α<sub>2</sub>M dimers are unable to trap proteases (Reddy et al., 1994, Reddy et al., 1989) and, compared to the native tetramer, have reduced binding affinity for certain growth factors including β-nerve growth factor, platelet-derived growth factor-BB, and transforming growth factor  $\beta$ 1 (TGF- $\beta$ 1) and  $\beta$ 2 (TGF- $\beta$ 2) (Wu et al., 1998). Conversely, hypochlorite-modified α<sub>2</sub>M tetramers show increased affinity for the acute phase, proinflammatory cytokines tumor necrosis factor alpha (TNF-α), interleukin (IL) -2, and IL-6 (Wu et al., 1998). This suggests that during inflammation, hypochlorite-induced dissociation of α<sub>2</sub>M into dimers may aid in the transition from tissue damage to repair by enhancing the clearance of pro-inflammatory molecules, and concomitantly reducing the binding of α<sub>2</sub>M to molecules needed for tissue repair. Furthermore, hypochlorite-modified dimeric a₂M has been shown to possess greater chaperone activity in vitro compared to the native α<sub>2</sub>M tetramer (Wyatt et al., 2014). Given the increased likelihood of protein misfolding during inflammation, a₂M may also act as an important hypochlorite-activated chaperone, helping to mitigate the accumulation of misfolded proteins in the extracellular space under conditions of exacerbated physiological

stress. Overall, these findings highlight the versatile and multi-functional nature of  $\alpha_2 M$ , and its importance in a wide range of biological processes.

# 1.2.1.3 Regulation and expression

First isolated in 1946, the gene for human  $\alpha_2 M$  is located on chromosome 12p12-13 (Matthijs et al., 1992), clustered with a number of  $\alpha_2 M$ -related genes, including PZP (Devriendt et al., 1989). Major and minor transcription sites have been identified downstream of a possible TATA-box in the liver, lung, and uterus. Notably, the liver appears to possess an additional minor transcription initiation site, and multiple hepatic promoter 1 sequences, suggesting a liver-specific mechanism of expression (Matthijs et al., 1992). The 5' flanking region also contains putative IL-6 and dexamethasone responsive elements (Matthijs et al., 1992).

Work done as part of the Human Protein Atlas revealed the major tissue types expressing a₂M (normalised as fragments per kilobase of exon per million mapped fragments) include the lung, bladder, liver, smooth muscle, and gallbladder (Uhlén et al., 2015). In terms of single cell expression (transcripts per million), hepatocytes, endothelial cells, and adipocytes are major sources of  $\alpha_2 M$  (Karlsson et al., 2021). As a secreted protein,  $\alpha_2 M$  is predominantly found in blood plasma, where concentrations in healthy adults typically range from 1 - 4 mg/mL and remain relatively stable under normal physiological conditions (Petersen, 1993, Sottrup-Jensen, 1989, Wang et al., 2014). α<sub>2</sub>M is also found in other biological fluids, such as synovial fluid and cerebrospinal fluid, however, this is at much lower concentrations than those in blood plasma/serum (Wang et al., 2014, Gupta et al., 2019). The rate of clearance of a₂M from biological fluids differs depending on whether it's in the native (not receptor recognised) or transformed (receptor recognised) conformation. In both mice and baboons, it has been shown that transformed α<sub>2</sub>M is rapidly cleared following injection into the bloodstream, with a half-life of 2-4 min for mice (Imber and Pizzo, 1981) and 30 min for baboons (Martos et al., 2018). In mice, native α<sub>2</sub>M remains in circulation much longer, with a half-life of several hours (Imber and Pizzo, 1981). The half-life of native α<sub>2</sub>M was not assessed in baboons but it is intuitive that transformed  $\alpha_2 M$  is cleared more rapidly than native  $\alpha_2 M$  in primates too, including humans.

In humans, lifestyle and demographic characteristics have been shown to influence the concentration of  $\alpha_2 M$  in biological fluids. It has been reported that plasma  $\alpha_2 M$  concentration negatively correlates with age in Caucasian (Birkenmeier et al., 2003) and Thai (Rugsarash et al., 2006) populations. This finding is consistent with an earlier study that reported 212 times higher serum  $\alpha_2 M$  concentration in infants compared to adults (Ganrot and Scherstén, 1967).

Sex also impacts  $\alpha_2 M$  levels, with females consistently reported to have significantly higher plasma  $\alpha_2 M$  compared to males (Ganrot and Scherstén, 1967, Birkenmeier et al., 2003). Diet is another factor reported to influence  $\alpha_2 M$  concentration (Pongpaew et al., 1994, Pongpaew et al., 1991, Rugsarash et al., 2006).

The role of a₂M in various disease states has been widely studied and is comprehensively reviewed by Lagrange et al. (2022), Vandooren and Itoh (2021), Rehman et al. (2013). Perhaps the most extensively researched area is the relationship between α₂M and Alzheimer's disease (AD). The amyloid beta peptide (Aβ), a major constituent of brain plaques in AD, co-localises with  $\alpha_2 M$  (Chen et al., 2017, Van Gool et al., 1993).  $\alpha_2 M$  can inhibit A $\beta$  aggregation and facilitate its clearance, attenuating the neurotoxicity of Aβ (Wyatt et al., 2013a, Yerbury and Wilson, 2010, Fabrizi et al., 2001, Lauer et al., 2001, Kang et al., 2000), and elevated plasma levels of α₂M have also been reported in AD (Varma et al., 2017, Shi et al., 2021). These findings reflect potential disease-induced changes in α<sub>2</sub>M concentration and support a mechanistic link between α<sub>2</sub>M and AD pathology. However, the genetic link between a₂M and AD risk remains a subject of debate. Some studies indicate polymorphisms in the A2M gene are associated with AD risk (Mariani et al., 2006, Saunders et al., 2003, Qiu et al., 2023), while others report no association (Blennow et al., 2000, Chen et al., 1999, Wavrant-DeVrièze et al., 1999, Chen et al., 2014). Metaanalyses suggest a complex relationship, providing evidence that polymorphisms may be associated with AD risk but only in certain sub-populations (Xu et al., 2013, Zhang et al., 2023a). Further research is needed to fully elucidate the role  $\alpha_2 M$  may play in AD aetiology.

Alterations in  $\alpha_2 M$  concentration have been reported in several other disease states. For example, increased levels of  $\alpha_2 M$  have been reported in the saliva and serum of patients with diabetes (Feng et al., 2015, Yoshino et al., 2019). Elevated serum  $\alpha_2 M$  has also been associated with greater severity of cirrhosis and fibrosis (Naveau et al., 1994) and increased intra-articular inflammation in osteo arthritis (Zhu et al., 2021). These associations suggest that upregulation of  $\alpha_2 M$  could be a compensatory response to decrease extracellular protease activity or modulate signalling pathways in these disease contexts. Supporting this idea,  $\alpha_2 M$  variants engineered to target specific proteases have been shown to have a chondroprotective effect and reduce degeneration of cartilage when injected into the synovial fluid of the knee (Zhang et al., 2017). On the other hand,  $\alpha_2 M$  is reportedly decreased in inflammatory bowel disease and pancreatitis (Brown et al., 1980, McMahon et al., 1984). A negative correlation between serum  $\alpha_2 M$  levels and flow-mediated vascular dilation has also been reported which may reflect an

association between serum  $\alpha_2 M$  levels and endothelial dysfunction in patients with cardiovascular and chronic stroke risk factors (Shimomura et al., 2018).

Pertinent to the focus of this research on pregnancy, recent reports indicate that  $\alpha_2 M$  concentrations are elevated in maternal serum during the second and third trimesters of pregnancies complicated by early onset PE (EO-PE) (Wang et al., 2023). However, the more than 50% decline in  $\alpha_2 M$  levels over the course of uncomplicated pregnancies has not been reported previously in longitudinal analyses of the human pregnancy proteome (Romero et al., 2017, Tarca et al., 2022). Although the specificity of the ELISA used to measure serum  $\alpha_2 M$  could not be confirmed, the use of polyclonal antibodies for other assays within the same paper raises concerns about ELISA specificity and potential cross-reactivity with PZP. In a subsequent manuscript by the same authors, overexpression of  $\alpha_2 M$  in smooth muscle cells of uterine spiral artery walls in patients with PE was posited to promote its pathology. This effect was reportedly alleviated in a rat model of PE by inhibiting LRP1 (Huang et al., 2025). While a monoclonal antibody was used for flow cytometry and immunohistochemistry, the forward and reverse primers used to detect  $\alpha_2 M$  mRNA were reportedly identical and complementary to a sequence in the *PZP* gene, raising serious concerns regarding the specificity of this analysis and the validity of the conclusions drawn.

# 1.2.2 PZP

PZP is a quantitatively important pregnancy-associated plasma protein in humans. Despite its abundance in maternal plasma during pregnancy, few *in vitro* studies have focussed on characterising the activities of PZP, which has historically been considered less important than its closely related counterpart,  $\alpha_2 M$ . This assumption is largely because, compared to  $\alpha_2 M$ , the protease trapping action of PZP is more restricted, less effective, and less efficient. Highlighting the marked discrepancy in the amount of research focussed on these proteins, a database search of the title and abstract of English papers for PZP ("PZP" OR "pregnancy zone protein" OR "pregnancy-associated alpha2-glycoprotein" OR "pregnancy-associated alpha 2 globulin" OR "pregnancy associated alpha 2 macroglobulin") returned 906 and 434 results between 1967 and 2025, from the SCOPUS and PubMed databases respectively. In stark contrast, a search for  $\alpha_2 M$  with similar parameters ("alpha-2-macroglobulin" OR "a2M" OR "alpha-2M" OR "alpha 2 macroglobulin") returned 8,052 results between 1957 and 2025 in SCOPUS, and 5,632 results from 1958 to 2025 in PubMed. Although PZP was first identified in 1959 (Smithies, 1959), 13

years after the first identification of  $\alpha_2 M$  in 1946 (Cohn et al., 1946), there remains a striking disparity in the volume of research conducted on these two proteins.

The discovery that dissociation of the native  $\alpha_2M$  tetramer into dimers yields a functionally distinct molecular species prompted researchers to reconsider the importance and potential functions of PZP, which exists natively as a dimer (Wyatt et al., 2014, Wu et al., 1998). Current literature supports the view that, while retaining protease inhibitory activity, PZP is a highly multifunctional protein whose properties more closely resemble those of the  $\alpha_2M$  dimer. Emerging evidence supports the idea that PZP fulfills important roles not only in pregnancy but also during pregnancy-independent inflammation. This section summarises existing knowledge on the structure, functions (pregnancy-dependent and -independent), regulation, and expression of PZP.

### 1.2.2.1 *Structure*

In humans, PZP is a 360 kDa homodimer, comprised of two identical 180 kDa subunits that are covalently linked by interchain disulfide bridges. Each subunit of PZP contains 1,482 amino acids residues and is glycosylated at eight conserved asparagine residues, with an additional two potential glycosylation sites identified (Devriendt et al., 1991). Initial studies demonstrated that there was a high degree of homology between partial sequences of PZP and  $\alpha_2 M$  (Sottrup-Jensen et al., 1984). This was later confirmed by cloning full length human PZP cDNA, which revealed that PZP and  $\alpha_2 M$  share 71% identical amino acid residues, with complete conservation of cysteine residues (Devriendt et al., 1991). Notably, the bait region sequences of PZP and  $\alpha_2 M$  are non-homologous. The PZP bait region is 10 amino acids longer than that of  $\alpha_2 M$  (39 versus 49 residues, respectively) and contains more proline and glycine repetition. The bait region of PZP contains 13 unique residues, compared to 15 in  $\alpha_2 M$ , and is less charged, with only 3 charged residues versus 9 in  $\alpha_2 M$  (Sottrup-Jensen et al., 1989). The shorter, more charged, and diverse nature of  $\alpha_2 M$ 's bait region allows for versatile interactions and a greater number of potential protease cleavage sites, giving it a broader protease substrate spectrum compared to PZP.

Although the structure of PZP is not as well characterised as the structure of  $\alpha_2 M$ , they are known to share many characteristics including MG domains, an RBD containing an LRP1 recognition site, a BRD, a thioester group, and a signal sequence (Sand et al., 1985) (Figure 1.2.2A). The highly conserved domain structure between PZP and  $\alpha_2 M$  suggests that the overall structures of their individual subunits are likely very similar and our best estimate of PZP's

tertiary structure is based on cryo-EM images of native  $\alpha_2M$  (Luque et al., 2022) (Figure 1.2.2B). Despite the high degree of similarity between PZP and  $\alpha_2M$ , it is important to note that their native quaternary structures differ in humans. Predictions of the PZP tertiary and quaternary structures using AlphaFold (Varadi et al., 2021, Jumper et al., 2021) and AlphaFold Multimer (Evans et al., 2022) support the conclusion that PZP's quaternary structure is very similar to that of an  $\alpha_2M$  dimer (Figure 1.2.2B–E).

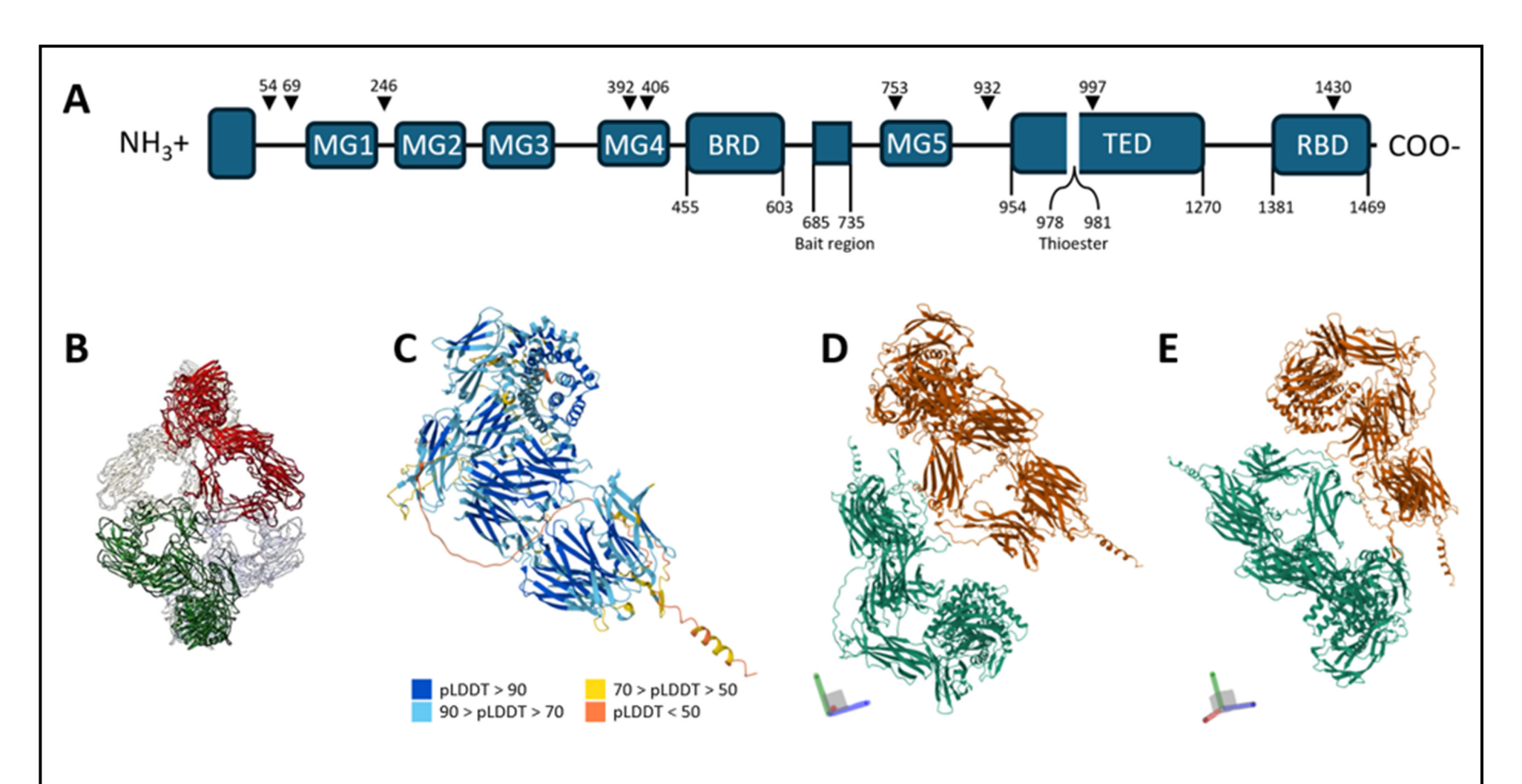


Figure 1.2.2: Structure of human PZP based on in silico modelling.

(A) Schematic of known functional domains of PZP predicted by InterPro (EMBL-EBI) with bait region domain (BRD), bait region, thioester domain (TED), thioester, and receptor binding domain (RBD) amino acid residue positions indicated. Black inverted triangles and amino acid residue positions indicate sites of glycosylation. MG indicate the macroglobulin-like domains. (B) Cryo-EM structure of native α<sub>2</sub>M, with disulfide linked dimers shown in red and green, is the current best estimate of PZP quaternary structure. Reproduced from Luque et al., (2022), licensed under Creative Commons CC BY-NC-ND 4.0. (C) Structure of a PZP monomer predicted by AlphaFold with per-residue model confidence scores (pLDDT). Regions below 50 pLDDT may be unstructured in isolation. (D & E) Structure of the PZP dimer predicted by AlphaFold Multimer from two different angles as indicated by axes at left of each structure.

### 1.2.2.2 Function

Consistent with acting as a protease inhibitor, cleavage of PZP within the bait region exposes a reactive thioester bond that forms a covalent link between PZP and the protease via reaction with a nucleophilic sidechain. During this process PZP adopts an electrophoretically fast conformation that can bind to LRP1 (Chiabrando et al., 2002, Sánchez et al., 2001). While small nucleophiles such as methylamine can react directly with the thioester bond and induce the electrophoretically fast conformation of PZP (Christensen et al., 1989), cleavage of the bait region is required to expose the receptor-binding site and cannot be achieved by methylamine treatment alone (Jensen and Stigbrand, 1992, Carlsson-Bosted et al., 1988). Furthermore, compared to  $\alpha_2 M$ , treatment with the same concentration of methylamine generates a smaller proportion of the electrophoretically fast PZP species (Jensen and Stigbrand, 1992).

While tetrameric  $\alpha_2M$  can bind two proteases per molecule and form an effective cage-like structure for steric hinderance, dimeric PZP forms a far less effective steric cage and can only bind one protease (Sand et al., 1985, Christensen et al., 1989). *In vitro*, a second PZP molecule may be recruited to a PZP-protease complex to form a tetrameric cage resembling  $\alpha_2M$  (Christensen et al., 1989, Sand et al., 1985). Whilst this increases steric hinderance of the protease, it is not an efficient process (Figure 1.2.3). Furthermore, while a handful of human protease substrates have been identified for PZP *in vitro* (Table 1.2.1), its bait region differences confer a narrower specificity, relative to  $\alpha_2M$  (Devriendt et al., 1991, Sand et al., 1985, Sottrup-Jensen et al., 1989). Porcine elastase (Sand et al., 1985), bovine trypsin, and bovine  $\alpha_2M$  (Sand et al., 1985) have also been identified as substrates for PZP. However, considering these proteases are primarily found in the digestive tract, their spatial separation from fluids containing high concentrations of PZP makes them unlikely *in vivo* substrates.

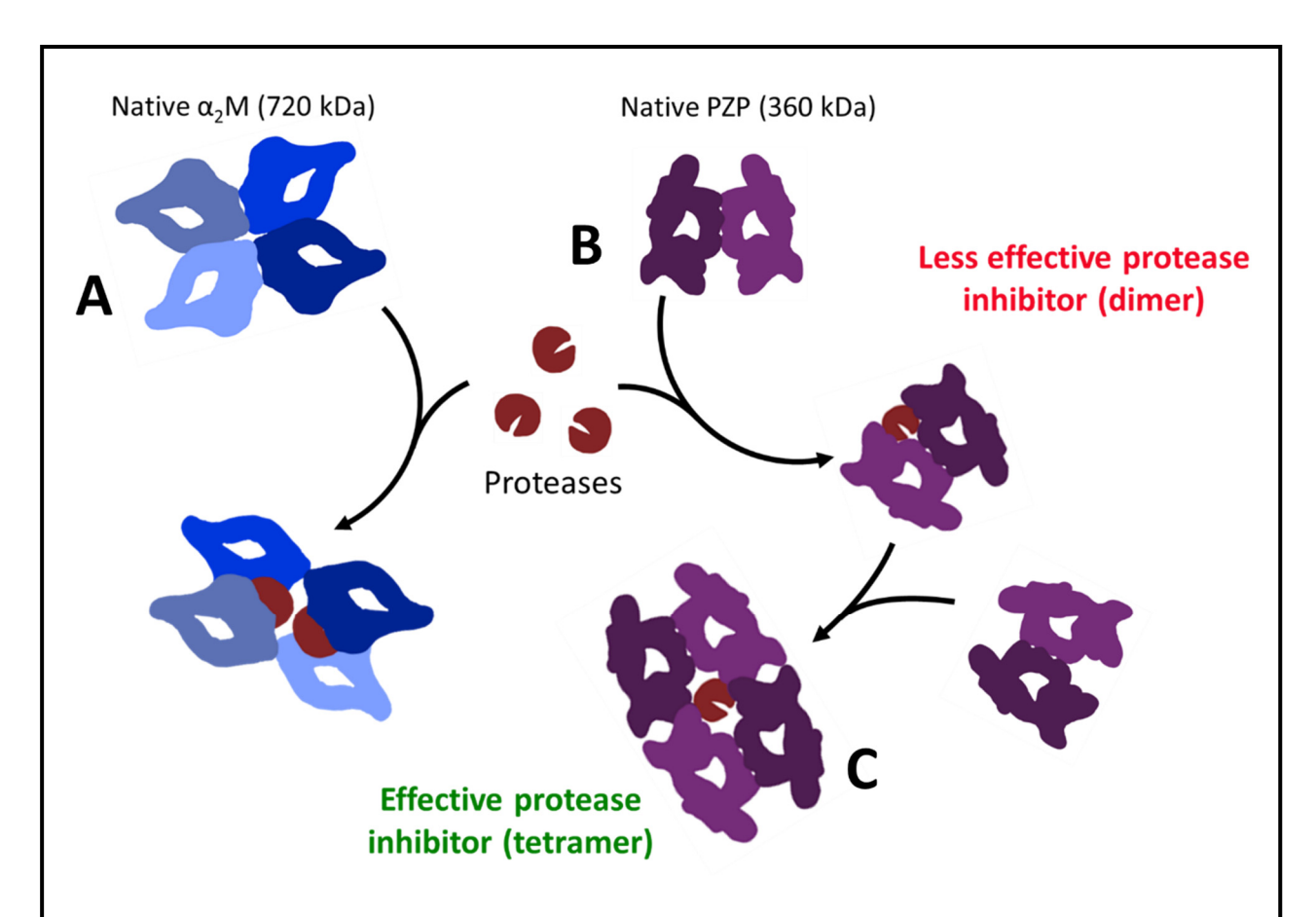


Figure 1.2.3: Simplified diagram showing the differences in protease trapping activity of  $\alpha_2 M$  and PZP. (A) Native tetrameric  $\alpha_2 M$  can bind 2 proteases and form an effective cage-like structure around them to sterically hinder protease activity. (B) Native dimeric PZP can bind one protease, with a less effective steric cage compared to  $\alpha_2 M$ . (C) If available, a free PZP dimer may be recruited to a PZP/protease complex to form a tetrameric cage, similar to that of  $\alpha_2 M$ .

**Table 1.2.1:** Human protease substrates for α<sub>2</sub>M and P7P based on the results of *in vitro* studies.

Protease	$\alpha_2M$	PZP	Location	References
Tissue kallikrein	✓	✓	Pancreas, kidney, urine, saliva	(Arbelaez et al., 1995)
Tissue plasminogen activator	✓	✓	Endothelial cells	(Sánchez et al., 2001, Sánchez et al., 1998)
Matrix metalloproteinase 2	✓	✓	Primarily ECM but can be found throughout the body	(Arbeláez et al., 1997)
Matrix metalloproteinase 9	✓	✓	Primarily ECM but can be found throughout the body	(Arbeláez et al., 1997)
Plasma kallikrein	✓	×	Plasma	(Arbelaez et al., 1995)
Plasmin	✓	×	Serum	(Arbelaez et al., 1995)
Thrombin	<b>√</b>	×	Serum	(Arbelaez et al., 1995, Steiner et al., 1985, Sand et al., 1985)
Urokinase	✓	×	Urine, blood, ECM	(Arbelaez et al., 1995)
Mannose-binding lectin-associated serine protease	<b>√</b>	×	Serum	(Paréj et al., 2013)

ECM – extracellular matrix.

### **Pregnancy-associated functions**

During pregnancy, PZP is significantly upregulated (Ekelund and Laurell, 1994) but the reasons for this remain unclear. A small number of pregnancy-relevant protease substrates for PZP have been identified, such as tissue plasminogen activator (tPA) and tissue kallikrein (Arbelaez et al., 1995, Sánchez et al., 2001, Sánchez et al., 1998). However, there are more efficient inhibitors for these proteases which suggests that protease inhibition is unlikely to be the sole explanation for PZP's upregulation. Considering that constitutively abundant  $\alpha_2$ M (Petersen, 1993, Sottrup-Jensen, 1989, Wang et al., 2014) efficiently inhibits all known classes of human proteases, the importance of PZP's marked upregulation remains enigmatic. Supporting the notion that  $\alpha_2$ M and PZP are functionally distinct, pregnant women with low PZP levels do not compensate by upregulating  $\alpha_2$ M (Cater et al., 2019).

A possible role for PZP could involve the stabilisation and disposal of misfolded proteins. Consistent with this idea, *in vitro* results demonstrate that human PZP has more efficient holdase chaperone activity compared to native  $\alpha_2 M$  (Cater et al., 2019). Furthermore, it has been shown that PZP forms stable complexes with the AD- and PE-associated A $\beta$  peptide *in vitro*, thereby preventing fibril formation (Cater et al., 2019). Considering that pregnancy is a life-stage that involves chronically elevated physiological stresses that can promote protein misfolding, intuitively, maternal adaptations, such as PZP upregulation, may have evolved to mitigate this challenge. However, further research is needed to determine whether the chaperone activity of PZP is cytoprotective, and to elucidate the importance of this function in the context of pregnancy.

PZP is also suggested to have important immunomodulatory functions and has been shown to bind CD3 on T-cells, thereby inhibiting their activation and reducing IL-2 production, a proinflammatory T-helper 1 (Th1) cytokine (Saito et al., 1990). Greater inhibition of activation-induced T-cell proliferation has been observed when PZP acts synergistically with glycodelin A (GdA, also known as placental protein 14), for which it is a non-covalent carrier. Furthermore, PZP-GdA complexes inhibited the production of IL-2 to a greater extent than PZP alone, whilst having minimal effect on IL-4, an anti-inflammatory Th2 cytokine (Skornicka et al., 2004). Further, a negative correlation between GdA and PZP in the decidual stroma between 9 and 13 weeks of gestation has been reported in women with recurrent miscarriage (Löb et al., 2021), a condition characterised by elevated Th1 cytokine expression compared to healthy controls (Kwak-Kim et al., 2003, Lim et al., 2000). Together, these findings suggest that the synergistic

action of PZP and GdA may be important for attenuating the Th1 response in early pregnancy and preventing adverse pregnancy outcomes.

# **Pregnancy-independent functions**

Independent of pregnancy, PZP is reportedly associated with a wide range of disease states, suggesting a generalised role in stress response and immunomodulation. For example, knockout of PZP in breast cancer cell lines results in enhanced cell proliferation, colony formation, and migration (Kumar et al., 2021). Upregulation of the TGF- $\beta$ /SMAD signalling pathway is implicated in this process. Whilst the mechanism by which PZP knockout leads to increased TGF- $\beta$ /SMAD signalling is currently unknown, TGF- $\beta$  is a reported ligand for both PZP (Philip et al., 1994) and  $\alpha_2$ M (LaMarre et al., 1990, O'Connor-McCourt and Wakefield, 1987). It is possible that the normal role of PZP is to control TGF- $\beta$  signalling by facilitating its clearance. Also supporting a role for PZP in controlling cancer progression, overexpression of PZP in hepatocellular carcinoma cell lines significantly inhibited cell proliferation, invasion and migration (Wu et al., 2021). Furthermore, positive correlations between PZP expression, and neutrophil and macrophage levels in hepatocellular carcinoma (Su et al., 2020) and lung adenocarcinoma (LAC; Chen et al., 2023a) have also been reported. In this scenario, it is plausible that PZP is upregulated in response to the pro-inflammatory environment and is being synthesised locally by immune cells.

Supporting localised production of PZP by immune cells, the sputum from patients with bronchiectasis reportedly contains concentrations of PZP that exceed those of serum by at least 10-fold (Finch et al., 2019). This suggests that inflammatory cells including neutrophils, monocytes, and eosinophils, are major sources of PZP during inflammation (Finch et al., 2019). Whilst PZP has not been directly shown to possess antimicrobial activity there was a strong positive correlation between bacterial load and PZP in sputum from bronchiectasis patients (Finch et al., 2019). One explanation for the importance of PZP in neutrophil extracellular traps (NETs) could be that PZP promotes the antibacterial action of T-cells, further supporting the idea that PZP regulates T-cell function in pregnancy. Alternatively, subtilisin (from *Bacillus subtilis*) has been demonstrated as a protease substrate for PZP (Sand et al., 1985) so it is plausible that PZP may attenuate bacterial infection by directly inhibiting the activity of bacterial proteases.

Whilst most studies suggest a protective role for PZP in innate immunity, it is postulated that PZP may exert detrimental effects in specific pathological contexts. For example, double knockout (DKO) of PZP and MUG-1 in mice protected them against mortality induced by West Nile Virus (WNV) infection (Krause et al., 2019). DKO mice had lower levels of inflammatory mediators and a reduced interferon (IFN) response (Krause et al., 2019). Interestingly, transformed  $\alpha_2 M$  has been shown to bind dengue virus (similar to WNV), enhancing infectivity and preventing heat damage to the virion *in vitro* (Huerta et al., 2014). It could be speculated that PZP may also enhance infectivity by facilitating endocytosis of WNV via LRP1. However, as previously noted, differences between murine and human  $\alpha M$ s necessitate further human-specific studies to investigate this hypothesis.

Another potential role for PZP is in regulating cellular senescence. In a study of human fibroblasts, PZP transcription was significantly upregulated in response to DNA damage or upon entry into senescence (Hu et al., 2023). While cellular PZP levels in senescent fibroblasts were ~10-fold lower than in non-senescent cells, the conditioned media surrounding the senescent cells contained around 5-fold higher levels of PZP compared to growing cells, suggesting that PZP is actively secreted during senescence (Hu et al., 2023). Additionally, PZPdepleted pregnancy serum was shown to inhibit senescence, whereas immunoprecipitated PZP reduced cell proliferation and promoted spontaneous senescence. Although the mechanisms underlying the association between PZP and senescence remain unclear, several pathways have been implicated. One potential mechanism involves TNF-α, which induces senescence and upregulates IFN response genes in human umbilical vein endothelial cells (HUVECs) (Kandhaya-Pillai et al., 2017). PZP reportedly contains an IFN response element (Tayade et al., 2005), suggesting that its expression may be regulated by IFN signalling. Additionally, PZP has been shown to induce P38 MAPK signalling in BAT (Lin et al., 2021), a pathway known to induce senescence in fibroblasts (Wajapeyee et al., 2010). These findings suggest that PZP may contribute to senescence through multiple mechanisms but further research is necessary to fully elucidate these pathways.

## 1.2.2.3 Regulation and expression

In humans, the *PZP* gene encodes a 4,609 base pair cDNA sequence with a single open reading frame (Devriendt et al., 1991) and can be found mapped to chromosome 12 (12p12-13), along with  $\alpha_2$ M and  $\alpha_2$ ML1 (Devriendt et al., 1989). Human PZP is present in biological fluids including synovial fluid, cerebral spinal fluid, and blood plasma (Gobezie et al., 2007, Güzel et al., 2020).

Whilst PZP is expressed by a range of tissues including the uterus, brain, kidney, ovary, and placenta, the liver is considered the main site of PZP synthesis (Tayade et al., 2005), except during inflammation where high levels of PZP are synthesised by immune cells (Finch et al., 2019). PZP expression has been reported in several placental structures, including the villous endothelium and mesenchyme, syncytiotrophoblasts, blood vessel walls (Lin and Halbert, 1976), extra villous trophoblasts and some decidual cells (Löb et al., 2022, Löb et al., 2021). Furthermore, fibrous and/or agglomerate forms of PZP have been detected in the villous mesenchymal capillaries and intervillous space (Kashiwagi et al., 2020). It remains unclear whether placental PZP synthesis significantly increases maternal plasma PZP concentration or primarily functions locally. PZP has also been detected in microglial cells, glial cells, and senile plaques in AD patients (Ijsselstijn et al., 2011, Nijholt et al., 2015).

Although PZP is broadly distributed in biological fluids, plasma concentrations are typically very low in males and non-pregnant females (0.01 – 0.03 mg/mL) (Ekelund and Laurell, 1994). However, PZP levels rise markedly during pregnancy and in other inflammatory states, prompting suggestions that it may act as an acute phase protein. In uncomplicated human pregnancy, maternal plasma PZP concentrations have been reported to range from 0.25 to 3 mg/mL, with notable inter-individual variability observed among women of the same gestational age (Ekelund and Laurell, 1994). Characterisation of maternal plasma PZP concentration over the duration of pregnancy is limited to a single study involving a relatively small number of mothers. The results from this study show that maternal plasma PZP concentration appears to increase proportionally, rather than absolutely (Ekelund and Laurell, 1994). The reasons for such high inter-individual variability are not known. During the first two trimesters of pregnancy, maternal plasma PZP concentration can increase by ~25-fold in some women, peaking at around 30 weeks' gestation before declining during the last trimester and returning to baseline by 10 weeks post-delivery (Ekelund and Laurell, 1994). The pronounced pregnancy-associated increase in PZP expression is believed to be primarily regulated by maternal estrogen levels (Damber et al., 1976) but given that estrogen levels rise steadily throughout gestation until parturition, while PZP peaks earlier and subsequently declines, there are likely additional regulatory mechanisms involved. The upregulation of PZP in pregnancyindependent inflammatory states provides further evidence that non-hormonal promoters of PZP expression are important.

Wide variation in PZP blood levels may indicate that its function is context-dependent – playing a more important role in certain physiological states or subgroups. While high levels of PZP do not appear essential to successful pregnancy, several studies have investigated the association between PZP expression and pregnancy outcome. For example, it has been reported that PZP levels are reduced in maternal plasma of mothers who experience spontaneous preterm birth (sPTB) (Than et al., 1976) and in first trimester plasma or serum of mothers with gestational diabetes mellitus (GDM), compared to healthy controls (Liu et al., 2020, Shen et al., 2019, Zhao et al., 2017). Interestingly, by the second trimester of GDM pregnancy serum PZP concentration increases nearly 3-fold, relative to first trimester (Shen et al., 2019), and term placental tissue from GDM patients exhibits an almost 5-fold increase in placental PZP concentration compared to controls (Wei et al., 2022). This suggests that in GDM the maternal body may upregulate PZP expression later in pregnancy as a compensatory response to earlier deficits. However, this does not appear to be the case for other pregnancy complications, with PZP significantly downregulated in term placenta of HELLP patients (Löb et al., 2022). Additionally, mRNA expression of PZP is increased by ~14- and ~11-fold in early placenta from spontaneous and recurrent abortion (Löb et al., 2021) which suggests that it may play a context-dependent role in pregnancy complications.

In the context of PE, inconsistent results have been reported regarding maternal plasma PZP concentrations (Table 1.2.2). Interpretation of these results is further complicated by the different approaches used to classify PE (e.g., late versus early onset, severe versus mild), and the technical challenges associated with the accurate measurement of PZP in biological fluids. Apart from maternal plasma, PZP concentration is also reportedly reduced in maternal serum exosomes (Navajas et al., 2022) and downregulated in the placenta (Löb et al., 2022) of women with EO-PE. A genome wide association study (GWAS) identified *PZP* as a novel risk locus for maternal hypertensive disorders, including PE, suggesting that genetic predisposition may contribute to the observed variability in PZP levels (Tyrmi et al., 2023).

A recent study identified a likely causal missense mutation in *PZP* that was positively associated with increased serum levels of a disintegrin and metalloproteinase domain-containing protein 12 (ADAM12) during early pregnancy, with the strength of the association increasing as pregnancy progressed (Yan et al., 2024). Furthermore, higher ADAM12 levels were associated with reduced odds of a woman having gestational hypertension (Odds Ratio [OR] 0.78,  $p = 8.6 \times 10^{-4}$ ), and were significantly reduced in patients with PE compared to controls (El-

Sherbiny et al., 2012), suggesting a protective role for ADAM12 in pregnancy-related hypertensive disorders (Yan et al., 2024). ADAM12S, a placenta-secreted form of ADAM12, has been shown to cleave insulin-like growth factor (IGF) binding proteins-3 and -5, thereby increasing the bioavailability of IGF during pregnancy (Loechel et al., 2000). ADAM12S has also been posited to play a role in healthy placental development by promoting trophoblast migration and invasion (Biadasiewicz et al., 2014, Aghababaei et al., 2014). It is possible that the association between PZP and ADAM12 is circumstantial, arising from independent responses to shared regulatory pathways in placental development. However, considering that PZP has been shown to interact with matrix metalloproteinases (MMPs) 1, 2, and 9 (Arbeláez et al., 1997), it is plausible that PZP may influence ADAM12 function. The potential role of PZP in regulating ADAM12 dynamics warrants further investigation, especially considering the implications for placental health and hypertensive disorders of pregnancy.

**Table 1.2.2:** Summary of studies reporting PZP concentration in maternal blood from patients with uncomplicated and preeclamptic pregnancies.

Year	Sample size	Gestational age at sampling	Method used to measure PZP	Key findings	Reference	
1972	37 PE 37 healthy	Not reported	Radial immunodiffusion	PZP lower in PE women	(Horne et al., 1972)	
1983	15 PE 18 controls	Term	Single radial immunodiffusion	PZP lower in PE women	(Griffin, 1983)	
1986	14 severe PE 14 healthy	31.5 31	Electro immunoassay	No significant difference	(Armstrong et al., 1986)	
2009	27 PE-AGA 12 PE-SGA 57 controls	20	Multiple DIGE experiments, followed by identification via LC-MS/MS $*\alpha_2M$ & PZP classed together*	PZP higher in PE women but unable to verify if this is due to $\alpha_2 M$ or PZP	(Blumenstein et al., 2009)	
2010	Preclinical PE 30 developed mild PE 40 developed severe PE 79 controls	10.6 11.4 12.1	Serum of 6-8 patients from each group pooled and analysed via 2D-LC-MS/MS and	PZP lower in women who developed mild PE PZP higher in women who developed severe PE	(Rasanen et - al., 2010)	
	Clinical PE 30 mild PE 30 severe PE 58 controls	36 34.1 35.4	label free quantification	PZP lower in women with mild and severe PE	di., 2010)	
2011	5 severe PE 5 controls	36.4 38.6	Sera pooled and analysed via 1D-Gel-LC-MS/MS	PZP lower in PE women	(Liu et al., 2011)	
2023	71 early onset PE 98 late onset PE 258 controls	34.4 39	ELISA (R&D Systems)	PZP lower in women with early-onset PE No significant difference for late-onset PE	(Fosheim et al., 2023)	

AGA – appropriate for gestational age; SGA – small for gestational age; DIGE – difference gel electrophoresis; LC-MS/MS – liquid chromatography with tandem mass spectrometry.

Although PZP is a pregnancy-associated protein, it is also upregulated in pregnancyindependent inflammatory states such as psoriasis (Beckman et al., 1977), pre-symptomatic AD (particularly in females; Nijholt et al., 2015, Ijsselstijn et al., 2011), bronchiectasis (particularly in females; Smith et al., 2017), HIV-1 infected men (Sarcione and Biddle, 2001), inflammatory bowel disease (Shao et al., 2021), and in paediatric chronic kidney disease patients (Chen et al., 2023b). In relation to cancer, early studies reported no correlation between plasma PZP concentrations and metastatic burden or treatment response in a range of cancer patients (Müller et al., 1982; Petersen et al., 1990). However, more recent studies support that PZP expression is dysregulated in several cancers and may impact survival measures (Table 1.2.3). Interestingly, PZP expression has been associated with both favourable and unfavourable survival outcomes, depending on the cancer type and context (Table 1.2.3). This suggests a context-dependent role for PZP, which may act as an immunosuppressive factor in some cancers, helping tumour cells evade immune detection by promoting a more tolerant immune environment. Conversely, in other cases, PZP may enhance the recognition of tumour cells by interacting with immune checkpoints or immune cells. The precise role of PZP in cancer remains unclear and likely depends on the specific immune evasion strategies employed by different cancers. PZP has been reported to positively correlate with various immune checkpoints, including CD274, CTLA4, LAG3, TIGIT, PDL1, and PDL2, across multiple cancer types. Additionally, increased PZP expression or plasma concentration has been associated with increased infiltration of immune cell populations including regulatory T cells (Tregs), macrophages, and neutrophils, suggesting that PZP may play a role in modulating the tumour immune microenvironment (Huang et al., 2024, Su et al., 2020).

Table 1.2.3: PZP mRNA expression in various cancers and its association with prognostic measures.

Cancer types	PZP expression†	Survival outcome	Hazard ratio [95% CI] p-value	n	References
Gastric	Increased	OS	1.984 [1.307, 3.012] 0.0003	253	(Oshima et al., 2024)
Glioblastoma multiforme	Increased		NS		(Huang et al., 2024)
Kidney renal clear cell carcinoma	Increased	OS	0.92 [0.85, 0.99] 0.03	515	(Huang et al., 2024)
Stomach adenocarcinoma	Increased	OS PFS	1.13 [1.05, 1.22] 0.0015 1.11 [1.03, 1.19] 0.0045	372 375	(Huang et al., 2024)
Bladder urothelial carcinoma	Decreased		NS		(Huang et al., 2024)
Breast invasive carcinoma	Decreased	PFS	0.94 [0.88, 1.00] 0.04	1043	(Huang et al., 2024)
Cervical squamous cell carcinoma and endocervical carcinoma	Decreased		NS		(Huang et al., 2024)
Cholangiocarcinoma	Decreased		NS		(Huang et al., 2024)
Colon adenocarcinoma	Decreased		NS		(Huang et al., 2024)
Kidney chromophobe	Decreased		NS		(Huang et al., 2024)
Kidney renal papillary cell carcinoma	Decreased		NS		(Huang et al., 2024)
Liver hepatocellular	Decreased	OS PFS	0.93 [0.88, 0.99] 0.02 0.95 [0.88, 1.00] 0.04	341 340	(Huang et al., 2024)
carcinoma	Decreased	RFS	0.87 [0.78, 0.97] 0.013	363	(Su et al., 2020)
Lung adenocarcinoma	Decreased		NS		(Huang et al., 2024)
Lung squamous cell carcinoma	Decreased		NS		(Huang et al., 2024)
Rectum adenocarcinoma	Decreased		NS		(Huang et al., 2024)
Uterine corpus endometrial carcinoma	Decreased		NS		(Huang et al., 2024)
Stomach and Esophageal carcinoma	Not reported	OS PFS	1.07 [1.01, 1.13] 0.02 1.08 [1.02, 1.14] 0.01	547 548	(Huang et al., 2024)
Sarcoma	Increased <sup>^</sup>	OS	0.93 [0.86, 1.00] 0.04	254	(Huang et al., 2024)
Thymoma	Decreased <sup>^</sup>	OS	2.22 [1.20, 4.13] 0.0075	117	(Huang et al., 2024)
Skin cutaneous melanoma	Decreased <sup>^</sup>	OS	0.95 [0.90, 1.00] 0.03	444	(Huang et al., 2024)

OS - overall survival; PFS – progression-free survival; RFS – relapse-free survival; NS – not significant; †compared to peritumor normal tissue; ^not statistically significant. Hazard ratio determined by Cox regression analyses which indicate the relationship between PZP expression and the risk of an event over time; hazard ratio >1 is increased risk; <1 is decreased risk. Sample size and survival outcome not reported for non-significant results.

Serum PZP levels were significantly elevated in patients with early-onset myocardial infarction and demonstrated strong diagnostic potential, distinguishing patients from controls with an area under the curve (AUC) of 0.874 (Xuan et al., 2019). A similar AUC of 0.861 was reported for identifying poor ovarian responders (POR) during fertility treatment, who exhibited higher PZP levels in their follicular fluid compared to controls (Oh et al., 2017). These findings align with the idea that PZP may be upregulated in response to inflammation. In POR, the ratio of IFN-γ and TNF-α producing Th1 cells to IL-10 producing Th2 cells is reportedly higher, suggesting a pro-inflammatory environment (Huang et al., 2023). Additionally, promising results have been published regarding PZP as a potential biomarker for colorectal cancer (CRC) (Yang et al., 2021a) and LAC (Yang et al., 2021b) in patients with type 2 diabetes mellitus (T2DM). PZP concentration was significantly higher in patients with both T2DM, and CRC or LAC compared to those with T2DM alone, with AUC's 0.713 and 0.742, respectively. For CRC, the combination of PZP with known markers like carcinoembryonic antigen (CEA) and carbohydrate antigen (CA19-9) improved the diagnostic accuracy, increasing the AUC to 0.916 and highlighting the potential for multiplexed biomarkers (Yang et al., 2021a).

A GWAS of patients with non-alcoholic fatty liver disease (NAFLD) identified a significant positive association between a single nucleotide polymorphism in PZP and increased blood levels of aspartate aminotransferase (AST), a marker of liver damage (Chalasani et al., 2010). Since TGF- $\beta$  plays a key role in fibrogenesis, leading to tissue damage and increased AST levels, a deficiency in functional PZP may impair the regulation of TGF- $\beta$ , potentially promoting fibrosis and elevated AST. Supporting this idea, PZP was found to be downregulated in idiopathic pulmonary fibrosis (IPF) (Giriyappagoudar et al., 2023) and is central to a fibrosis-related network module identified in IPF-specific Bayesian analysis (Tomoto et al., 2024). Together these findings highlight PZP as a potential modulator of TGF- $\beta$  activity and fibrosis in humans.

# 1.3 Physiological changes in uncomplicated and complicated pregnancy

Pregnancy is a unique life-stage during which physiological stresses are elevated, and the mother endures a chronic, systemic inflammatory response (Dutta et al., 2024, Jarmund et al., 2021). This is largely due to the significant physiological adaptations required to meet the nutrient and metabolic demands of the growing fetus. The biological changes that occur during pregnancy are highly complex, and despite advances in research, significant gaps remain in our understanding of these processes.

# 1.3.1 Maternal adaptations in uncomplicated pregnancy

Anatomic, metabolic, and physiological adaptations are essential to ensure healthy development of the fetus and placenta while maintaining the health of the mother (Hartgill et al., 2011). Some examples of these adaptations are listed in Table 1.3.1.

**Table 1.3.1:** Examples of major physiological changes that occur in the mother during pregnancy (Heidemann and

McClure, 2003, Soma-Pillay et al., 2016, Zhang et al., 2023b).

System Affected	Change	Caused By
Cardiovascular /haematological	45% increase in plasma volume	Aldosterone renin-angiotensin activation by progesterone and oestrogen
Cardiovascular /haematological	20% increase in red blood cell mass	Increased erythropoietin production in kidney
Cardiovascular /haematological	20% decrease in haemoglobin concentration	Disproportionate increase in plasma volume and red blood cell mass
Cardiovascular /haematological	20% decrease in vascular resistance	Vasodilation by circulating progesterone and oestrogen
Cardiovascular /haematological	Decreased blood pressure	Increased vasodilation
Cardiovascular /haematological	50% increase in cardiac output (stroke volume and heart rate)	Decreased blood pressure
Cardiovascular /haematological	Increased coagulation index	Increased plasma concentration of fibrinogen and clotting factors
Uteroplacental	Increased blood flow to placenta	Remodelling of spiral arteries by extravillous trophoblasts into high-capacitance, low-resistance vessels.
Respiratory	20% increase in oxygen consumption	Increased progesterone levels, increased metabolic rate
Respiratory	Increased tidal volume	Increased progesterone levels
Respiratory	Increased minute and alveolar ventilation	Increased progesterone levels
Renal	Increased glomerular filtration	
Renal	Increased water retention	Increased aldosterone, renin-angiotensin and progesterone activity
Renal	Decreased plasma osmolality, urea, bicarbonate, and urate	Increased water retention and glomerular filtration rate
Gastrointestinal	Reduced lower oesophageal sphincter tone	Increased progesterone levels
Endocrine	Increased insulin production and insulin resistance	Human placental lactogen and other placental hormones
Endocrine	Increased aldosterone and angiotensin II levels	Reduced vascular resistance and blood pressure

Pregnancy is also characterised by important immunological adaptations, including changes in both localised placental and maternal peripheral immunity. These changes have been reviewed extensively elsewhere (Mor et al., 2017, Abu-Raya et al., 2020), with only a brief summary provided here. During implantation, the uterus is rich in immune cells, such as uterine mast cells (uMCs), uterine natural killer (uNK) cells, macrophages, dendritic cells, and T-cells, which are proposed to contribute to creating a favourable environment for implantation and placentation (Zenclussen and Hämmerling, 2015). For example, mice devoid of uMCs or

uNK cells exhibited impaired spiral artery remodelling and placental development (Greenwood et al., 2000, Woidacki et al., 2013). In the uMC devoid mice, normal spiral artery remodelling could be induced by treatment with bone-derived mast cells (MCs) (Woidacki et al., 2013). Tregs also play a crucial role in implantation by promoting early maternal tolerance to paternal antigens derived from the fetus. Depletion of CD25\*Tregs in mice results in allogenic rejection of the fetus and consequently failed gestation (Aluvihare et al., 2004). Collectively, these findings support the idea that pro-inflammatory factors are beneficial for implantation and placentation. Contrary to the idea that pregnancy is an immunosuppressive state, accumulating evidence suggests that dynamic cooperation between the maternal and fetal immune systems is required to maintain immune balance throughout pregnancy. It is now well established that immune function during pregnancy shifts throughout gestation. Early pregnancy is characterised by a pro-inflammatory (Th1) milieu that facilitates implantation and placentation, whereas mid-gestation favours an anti-inflammatory (Th2, tolerogenic) environment to support fetal growth, before shifting back to a pro-inflammatory state at term to promote labour (Saito et al., 1999, Mor and Cardenas, 2010, Dutta et al., 2024).

# 1.3.2 Pathophysiology of preeclampsia

PE is a human specific pregnancy-associated syndrome of unknown aetiology, which has been associated with maternal PZP concentration (Table 1.2.2). A 2013 systematic review of hypertensive disorders of pregnancy reported a global prevalence of between 2.7% and 8.2%, with an average of 4.6% of pregnancies affected by PE. However the incidence varies between countries (Abalos et al., 2013). A major contributor to maternal and fetal morbidity and mortality, PE is estimated to account for approximately 70,000 maternal and 500,000 fetal/neonatal deaths worldwide annually (Rana et al., 2019). Clinically, PE remains a challenge due to its potentially rapid onset and deterioration, difficulty in identifying at-risk mothers, and the absence of effective treatment other than delivery of the placenta, which may not always fully resolve the condition. The acute and long-term effects of PE can also be detrimental to both mother and baby, as such, the social and economic burden of PE is immense.

## 1.3.2.1 Clinical presentation and diagnosis

The clinical presentation of PE can vary greatly among affected mothers. Most cases present as late-onset PE (LO-PE; ≥34 weeks gestation), with a smaller proportion comprised of EO-PE (<34 weeks gestation). In an Ethiopian retrospective cohort study, 72.9% of mothers with PE presented as LO-PE, whilst only 27.1% presented as EO-PE (Teka et al., 2023). Similar results

were reported in an Indian cohort, with 72.4% and 27.6% LO-PE and EO-PE, respectively (Gomathy et al., 2018). In contrast, a retrospective study of births in Washington State reported a lower incidence, at only 12.3% for EO-PE compared to 87.7% for LO-PE (Lisonkova and Joseph, 2013), which highlights the disparities in PE incidence across populations. Another widely used classification divides PE into preterm (delivery <37 weeks gestation) or term delivery (delivery ≥ 37 weeks gestation). A UK cohort reported prevalence rates of 19.9% and 80.1% for preterm and term PE, respectively (von Dadelszen et al., 2023), demonstrating a similar distribution to that of EO-PE and LO-PE in the US (Lisonkova and Joseph, 2013). It should be noted that LO-PE and EO-PE are thought to arise from distinct underlying pathophysiological mechanisms, with EO-PE more strongly associated with a placental cause, whereas LO-PE is thought to be more maternal (Burton et al., 2019). In some cases, PE may also be categorised as mild or severe depending on the severity of symptoms but this is discouraged by the International Society for the Study of Hypertension in Pregnancy (ISSHP) and American College of Obstetricians and Gynecologists (ACOG) because progression from mild to severe can be unpredictably rapid (Brown et al., 2018).

The currently accepted diagnostic criteria for PE (endorsed by the ISSHP) are development of hypertension ≥20 weeks gestation in association with one or more of the following: proteinuria (>300mg/day), fetal growth restriction (FGR), and/or other maternal organ dysfunction including acute kidney injury, liver dysfunction, haemolysis, thrombocytopenia, and neurological features (Brown et al., 2018). Notably, previous diagnostic guidelines required the presence of proteinuria; however, the updated criteria acknowledge that evidence of maternal organ or placental dysfunction alone is sufficient for diagnosis. These revisions to the diagnostic criteria have improved the identification of PE cases that may have previously gone undetected (Lai et al., 2021). Despite more inclusive criteria, diagnosis can still be difficult as early clinical signs are frequently inconspicuous due to other predisposing conditions such as chronic hypertension or nephropathy.

#### **Biomarkers**

Early pregnancy screening for PE risk largely relies on maternal factors, including medical history, age, ethnicity, weight, height, mean arterial blood pressure (MAP), and uterine artery pulsatility index (Dimitriadis et al., 2023). Using these criteria, detection rates for EO-PE and preterm PE are reportedly 88.3% and 73.9%, respectively, at a screen-positive rate of 10.2%. However, for term PE (≥37 weeks), detection rates are markedly lower at just 43.5% (Dimitriadis

et al., 2023). The inclusion of serum biomarkers, such as placental growth factor (PIGF) can improve the detection rates to 90.0% and 81.7% for EO-PE and preterm PE, respectively. However, this approach has minimal impact on the detection of term PE, with rates decreasing slightly to 42.6% (Dimitriadis et al., 2023), highlighting the difficulty of predicting late-onset disease, even with current biomarker-enhanced screening. Similar results were reported in the Aspirin for Evidence-Based Preeclampsia Prevention (ASPRE) trial study population. Using an algorithm that combines maternal factors, MAP, uterine artery pulsatility index, serum pregnancy associated plasma protein-A (PAPP-A) and serum PIGF at 11 – 13 weeks gestation the detection rates for preterm and term PE were 76.7% and 43.1%, respectively, at screen-positive rate of 10.5% and false positive rate of 9.2% (Rolnik et al., 2017). These findings underscore the ongoing unmet need for effective early pregnancy screening tools, particularly for term and LO-PE.

Consequently, the potential for dysregulated proteins to serve as predictive biomarkers for PE has been widely investigated (Danielli et al., 2022, Han et al., 2023, MacDonald et al., 2022). However, only select examples are provided here. Pro- and anti-angiogenic factors have been a key focus as biomarkers for PE as a whole, as well as for the early and late onset subsets. For example, the ratio of the anti-angiogenic soluble fms-like tyrosine kinase 1 (sFlt-1) to proangiogenic PIGF in serum is commonly used to rule out women at immediate risk of developing PE. With a negative predictive value of 99.3%, an sFlt-1/PlGF ratio of ≤38 can rule out the likelihood of a woman <37 weeks gestation developing PE within a week. In contrast, the positive predictive value for a diagnosis of PE within 4 weeks using an sFlt-1/PlGF ratio of >38 was only 36.7% (Zeisler et al., 2016). Consistent with this, a large multicentre study found that the sFlt-1/PlGF ratio had limited ability to predict EO-PE, or any type of PE, with an AUC of just 0.53 for both outcomes (Widmer et al., 2015). A meta-analysis evaluating the diagnostic performance of the sFlt-1/PlGF ratio across PE subtypes reported a pooled sensitivity of 78% (95% CI; 76%, 79%), specificity of 89% (95% CI; 88%, 89%) (Zhang et al., 2025)These findings highlight the potential for circulating proteins to act as biomarkers of adverse pregnancy outcomes.

Despite these promising results, several considerations must be addressed before serum biomarkers can be widely implemented in clinical practice. For example, levels of these markers may be affected by maternal status (e.g., BMI, age) and can vary across gestation, necessitating personalised and/or gestation specific reference ranges. Furthermore, the cost

and accessibility of implementing such tests clinically should be considered, especially in developing countries where the burden of PE is often greatest.

# *1.3.2.2 Risk factors*

Up to 80 risk factors for PE are identified in the clinical practice guidelines; however, the strength of association and quality of evidence varies for each (Elawad et al., 2024). Commonly described risk factors are given in Table 1.3.2. Of note, population attributable factor analysis at 16 weeks gestation found that approximately 32.3% of PE cases can be attributed to nulliparity, the highest contributing risk factor (Bartsch et al., 2016). Despite this, and the fact that nulliparity is considered a moderate risk factor of PE by ISSHP (Brown et al., 2018), the National Institute for Health and Care Excellence (NICE) (Webster et al., 2019), and ACOG (ACOG, 2020), the mechanisms underlying its association with PE remain poorly understood. Immune maladaptation is one proposed mechanism, while aberrant angiogenesis has also been suggested (Luo et al., 2007). A pre-pregnancy BMI >25 kg/m² and history of PE have the next highest population attributable fractions at 23.8% and 22.8% respectively (Bartsch et al., 2016).

**Table 1.3.2:** Commonly described risk factors for PE including pooled unadjusted relative risk (Bartsch et al., 2016, Duckitt and Harrington, 2005).

Risk Factor	Relative Risk [95% CI]
Nulliparity	2.1 [1.9, 2.4]
History of PE	8.4 [7.1, 9.9]
Family history of PE	2.9 [1.7, 4.9]
Multifetal pregnancy	2.9 [2.6, 3.1]
Assisted reproductive technology	1.8 [1.6, 2.1]
Pre-gestational diabetes	3.7 [3.1, 4.3]
Chronic Hypertension	5.1 [4.0, 6.5]
Systemic lupus	2.5 [1.0, 6.3]
Anti-phospholipid syndrome	2.8 [1.8, 4.3]
Chronic kidney disease	1.8 [1.5, 2.1]
History of placental abruption	2.0 [1.4, 2.7]
Pre-pregnancy BMI ≥25 kg/m <sup>2</sup>	2.1 [2.0, 2.2]
Pre-pregnancy BMI >30 kg/m <sup>2</sup>	2.8 [2.6, 3.1]
Maternal age ≥35 years	1.2 [1.1, 1.3]

#### **1.3.2.3** *Sequelae*

PE is responsible for a spectrum of complications that can affect both the mother and her infant, with the potential for rapid and unpredictable clinical deterioration following symptom onset (Brown et al., 2018). As a multi-system disorder, PE can cause microangiopathy in the maternal kidneys, liver, and brain (Hod et al., 2015), and disease progression may lead to seizures (eclampsia), stroke, cerebral haemorrhage, kidney damage, liver failure, or death.

Short term deleterious effects for the infant include FGR, with an approximately 5% - 23% lower birth weight observed in babies of women with PE, and a 3-fold greater risk of being small for gestational age (SGA; Ødegård et al., 2000). PE is also associated with an increased risk of stillbirth, with an 86-fold higher risk of fetal death around week 26 compared to uncomplicated pregnancy (Harmon et al., 2015). Although the risk of fetal mortality decreases as the pregnancy progresses, by 34 weeks gestation there remains a 7-fold increased risk of fetal death in women with PE (Harmon et al., 2015).

## 1.3.2.4 The Renin Angiotensin System in PE

Whilst the underlying causes of PE remain unclear, hypertension is a central component and likely due to dysregulation of the renin-angiotensin system (RAS). In humans, the RAS comprises both circulating and tissue-specific systems, each consisting of numerous components. For clarity, this section focuses on the key components of the circulating and uteroplacental (placenta and decidua) RAS that are most relevant to the research presented in this thesis. Both systems share the same core components, including renin, angiotensinogen (AGT), angiotensin I (Ang I), angiotensin II (Ang II), angiotensin-converting enzyme (ACE), angiotensin-converting enzyme 2 (ACE2), and the Ang II receptors, type 1 (AT<sub>1</sub>R) and type 2 (AT<sub>2</sub>R), although the activation pathway and downstream effects differ.

Renin converts AGT to Ang I in the circulating RAS, while in the uteroplacental RAS, prorenin binds to the prorenin receptor to catalyse this reaction. ACE is traditionally recognised as the enzyme responsible for converting Ang I to Ang II, the primary effector of the RAS; however, chymase may also mediate this conversion. Ang II can then act on AT<sub>1</sub>R to elicit systemic vasoconstrictive effects via the circulatory RAS or to promote angiogenesis, vascular remodelling, and trophoblast invasion within the uteroplacental RAS. Conversely, Ang II may act on AT<sub>2</sub>R, eliciting opposing effects such as systemic vasodilation and inhibition of cell proliferation, invasion, and migration. Ang II can also be cleaved further to Angiotensin 1-7 by ACE2, which acts on the Mas receptor (MasR) to promote a similar effect to that of Ang II binding AT<sub>2</sub>R (reviewed by Lumbers et al., 2019, Yart et al., 2021; Figure 1.3.1). Consequently, the circulating RAS regulates systemic blood pressure, fluid balance, and electrolyte homeostasis, while the uteroplacental RAS governs local blood flow, angiogenesis, and trophoblast invasion to support healthy placentation and fetal growth.

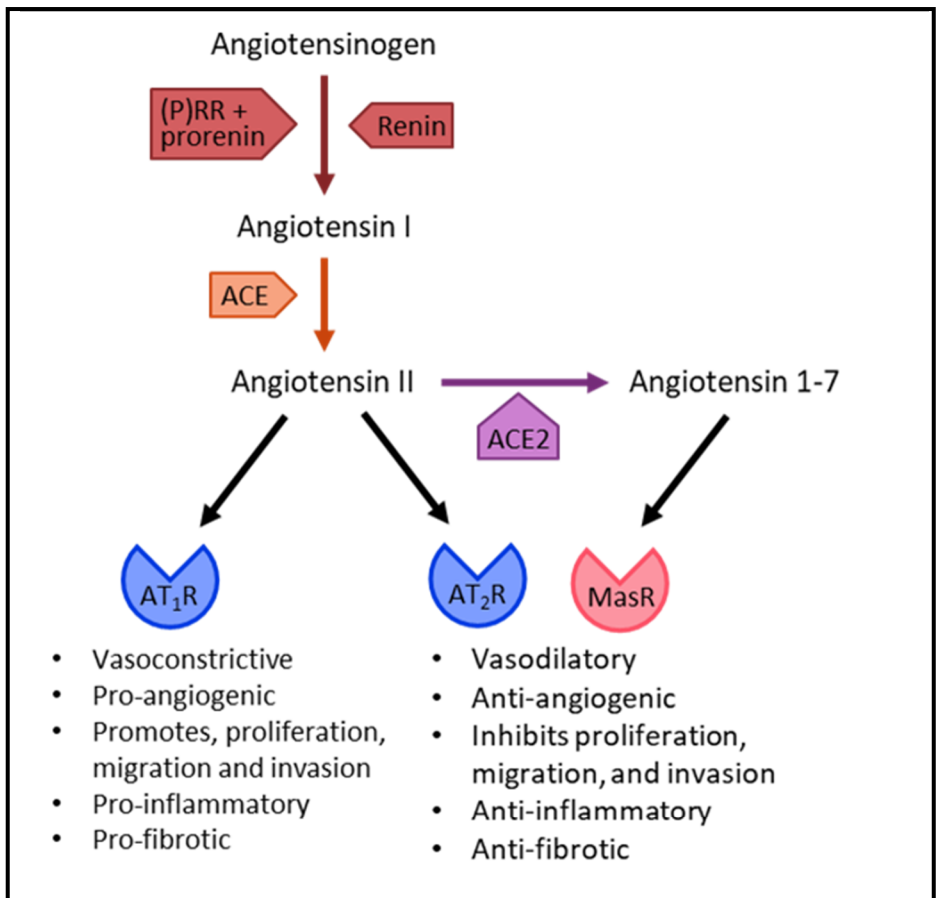


**Figure 1.3.1:** Simplified schematic diagram highlighting core components of the circulating and placental RAS and their downstream effects. Binding of prorenin to the prorenin receptor ((P)RR), or renin, promotes the cleavage of angiotensinogen to Angiotensin I in the placental and circulatory RAS, respectively. Cleavage of Angiotensin I by angiotensin converting enzyme (ACE) produces Angiotensin II which can then act on Angiotensin II type 1 or 2 receptor (AT $_1$ R, AT $_2$ R) to elicit different effects in the circulation, or locally within the placenta. Angiotensin 1-7 may be generated from Angiotensin II by ACE2, which can act on the Mas receptor (MasR) to elicit similar actions to those of Ang II on AT $_2$ R.

Synergistic action between the circulating and uteroplacental RAS is hypothesised to maintain appropriate blood pressure during pregnancy. To facilitate this, RAS activity is increased, with Ang I, Ang II, and Ang 1-7 all significantly elevated in maternal plasma of normotensive pregnancies, compared to non-pregnant women (Merrill et al., 2002). Increased expression of  $AT_2R$  in the uterine arteries (Mishra et al., 2018, Cox et al., 1996), with concomitant reductions in  $AT_1R$  expression (Lumbers, 1970, Lumbers and Pringle, 2013), is thought to promote the vasodilatory effects of Ang II which is necessitated by the significant increases in blood volume and flow to the placenta during pregnancy.

In PE, circulating Ang I, Ang II, and Ang 1-7 are all significantly lower than in normotensive pregnancies (Merrill et al., 2002, Leaños-Miranda et al., 2018). However, AT<sub>1</sub>R expression is

upregulated 5-fold in women with PE compared to controls (Herse et al., 2007), and AT<sub>1</sub>R sensitivity to Ang II is increased (AbdAlla et al., 2001). Furthermore, significantly higher levels of AT<sub>1</sub> autoantibodies (AT<sub>1</sub>R-AA), which are agonistic to AT<sub>1</sub>R, are reported in PE (Herse et al., 2007, Wallukat et al., 1999). Together, these alterations, alongside reduced Ang 1-7 levels, are proposed to tip the balance toward vasoconstriction, thereby contributing to hypertension in PE. While these changes may play a role in PE pathogenesis, it has also been proposed that the abnormal placental development characteristic of PE could itself contribute to dysregulation of the uteroplacental RAS, creating a damaging feedback loop that exacerbates disease progression (Lumbers et al., 2019).

# 1.4 Rationale and overarching goal

Pregnancy involves significant physiological changes that require complex adaptations to support both maternal health and fetal development. Despite pregnancy's critical importance to human survival, we know remarkably little about the processes that drive these adaptations. Plasma proteins, which play key roles in maintaining homeostasis and regulating immune responses, are integral to the dynamic changes that occur throughout pregnancy. Among these proteins, PZP stands out due to its dramatic upregulation but its specific functions and the regulatory mechanisms involved remain poorly understood. The results of prior studies, including investigations of closely related proteins, suggest that PZP is a multifunctional protein that may contribute to supporting pregnancy by inhibiting proteases, stabilising misfolded proteins, and modulating immune responses. Furthermore, although an association between PZP and PE has been reported, the data are conflicting. As such there is no consensus regarding the association between maternal plasma PZP concentration and PE incidence.

The overarching goal of the research presented in this thesis was to gain insight into the potential biological importance of PZP and its relevance to maternal adaptation during pregnancy. To achieve this, PZP was purified from human pregnancy plasma and its functions characterised *in vitro*, including analysis of its binding to chymase, a putative endogenous substrate (Chapter 2). In addition, maternal plasma PZP concentration was measured in several independent pregnancy cohorts (Chapters 3 & 4). Specific hypotheses and aims are provided in the introduction of the individual chapters in this thesis.

# **CHAPTER 2:**

CHARACTERISATION AND FUNCTIONAL ANALYSIS OF PUTATIVE PZP-CHYMASE COMPLEXES

# 2.1 Introduction

Despite its marked upregulation during pregnancy (Ekelund and Laurell, 1994, Fosheim et al., 2023), the biological functions of PZP remain poorly defined. Unlike α<sub>2</sub>M, there are few, if any, well-characterised endogenous substrates for PZP (Table 1.2.1). However, the current evidence supports that interaction with proteases is critical for PZP's function. Thus, identifying physiologically relevant protease substrates and characterising their interaction with PZP will contribute toward advancing our understanding of the biological functions of this protein.

Chymase (30 kDa) is a monomeric chymotrypsin-like serine protease that is predominantly expressed, and secreted, by mast cells (MCs). In humans, chymase is the product of CMA1 (located on chromosome 14) and is classified as an α-chymase. There are two major types of MC, those predominantly containing tryptase (MC<sub>T</sub>) and those containing tryptase, chymase, and carboxypeptidase (MC<sub>TC</sub>). MC<sub>T</sub> are typically located in mucosal tissue exposed to the external milieu, whereas MC<sub>TC</sub> are distributed throughout the connective tissue and submucosa adjacent to the skin and conjunctiva, often near lymphatic and blood vessels. Upon activation, MCs degranulate and release their contents into extracellular fluids where they act on their substrates (Fong and Crane, 2023). Consistent with a role in tissue remodelling, human chymase has been shown to cleave extracellular matrix (ECM) components, including fibronectin (Tchougounova et al., 2003) and biglycan (Roy et al., 2014). It also activates MMP-1 (Saarinen et al., 1994), and -2 (Groschwitz et al., 2013, Tchougounova et al., 2005), which further contribute to ECM degradation. Numerous other substrates for chymase, including vasoactive peptides (Ang I, big endothelin-1), cytokines (e.g., IL-6, -13, -15, -18, -33, IFN-y), growth factors (e.g., IGF-1, CTGF), and other inflammatory molecules (e.g., HMGB1, thrombin) have also been identified (Table S1). The broad range of substrates that chymase acts upon support the notion that it has multiple roles relevant to the regulation of the immune system and stress responses and that its broad-spectrum activity must be tightly regulated.

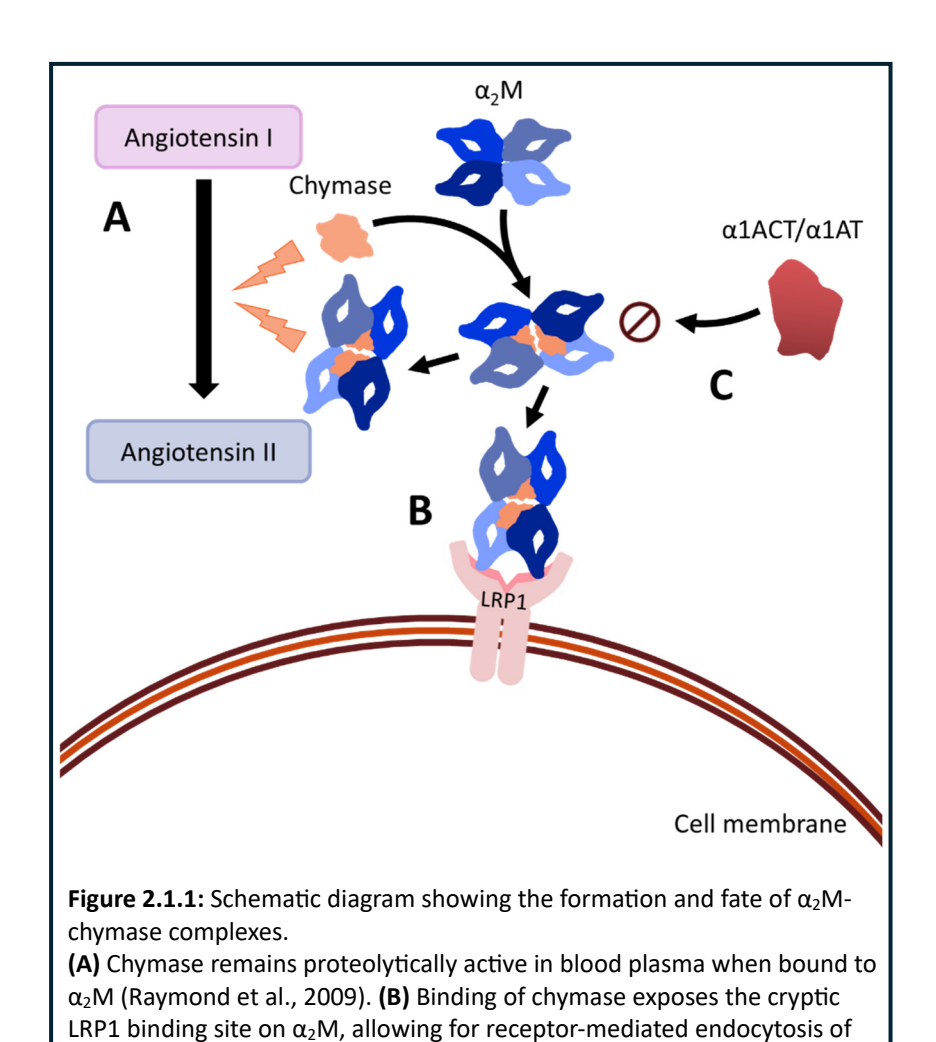
The role of chymase in pregnancy has not been studied extensively. Nevertheless, indirect evidence suggests it may contribute to key processes at the maternal-fetal interface, including placentation and vascular remodelling. Although MCs are an important source of chymase in pregnancy, placental trophoblast cells also express this protease (Wang et al., 2007, Hirai et al., 2016), and the evidence indicates that chymase plays specialised roles at the placenta to support proper placentation. This includes regulating the function of cells at the maternal-fetal

interface, such as uterine smooth muscle cells (uSMCs), extravillous trophoblasts (EVTs), and endothelial cells. During spiral artery remodelling, uSMCs must either migrate away from the vessel walls or undergo apoptosis. This process enables the invasion of EVTs, which replace both the uSMCs and endothelial cells, thereby transforming the vessel walls to support increased blood flow to the placenta (Bulmer et al., 2012). Treatment of uSMCs with human chymase induces a migratory phenotype which promotes their migration (Zhang et al., 2022), while treatment of vascular SMCs with chymase induces apoptosis (Leskinen et al., 2001). It has also been shown that treatment with human chymase promotes EVT migration (Meyer et al., 2017, Zhang et al., 2022), further supporting a role in spiral artery remodelling. Moreover, treatment of HUVECs with recombinant human chymase induces endothelial-tube formation (Zhang et al., 2022), a hallmark of angiogenesis which is critical for ensuring sufficient blood flow to meet the oxygen and nutrient demands of the growing fetus.

In addition to supporting placentation, chymase may also influence pregnancy by contributing to Ang II production. While ACE is widely recognised as the primary enzyme responsible for converting Ang I to Ang II, chymase also performs this function (Takai et al., 1997, Urata et al., 1990b, Caughey et al., 2000, Urata et al., 1990a). As the classical effector of the RAS, Ang II plays a role in regulating blood pressure and fluid homeostasis (see Section 1.3.2.4 for further information regarding the RAS). Ang II has been shown to enhance proliferation and migration of BeWo, a trophoblast-like cell line (Ishimatsu et al., 2006, Ino et al., 2003), and promotes EVT invasion in placental explants (Williams et al., 2010). Additionally, binding of Ang II the AT<sub>1</sub>R receptor is reported to promote angiogenesis by upregulating the production of vascular endothelial growth factor A (VEGFA) (Delforce et al., 2019). These findings support the idea that chymase plays a central role in remodelling the maternal vasculature during placentation, either directly or by generating Ang II.

The activity of chymase is known to be regulated by extracellular serine protease inhibitors such as alpha-1-antichymotrypsin ( $\alpha$ 1ACT), alpha-1-antitrypsin ( $\alpha$ 1AT), and  $\alpha_2$ M (Walter et al., 1999). Among these inhibitors,  $\alpha_2$ M is considered the most efficient (Walter et al., 1999), and is proposed to be the major chymase binding protein in humans (Raymond et al., 2009). However, these conclusions are based on studies of the proteome in non-pregnant individuals. Cleavage of  $\alpha_2$ M by chymase reveals the cryptic binding site for LRP1 (Huang et al., 2022, Luque et al., 2022), which rapidly facilitates the clearance of  $\alpha_2$ M-chymase complexes *in vivo* (Imber and Pizzo, 1981). It has been suggested that if the clearance of  $\alpha_2$ M-chymase complexes is

inefficient, this may create a reservoir of proteolytically active chymase in the blood (Raymond et al., 2009). This is because when in complex with  $\alpha_2 M$ , chymase retains proteolytic activity against Ang I and is protected from inactivation by other endogenous inhibitors due to the steric cage formed by  $\alpha_2 M$  (Raymond et al., 2009) (Figure 2.1.1).



Pregnancy introduces unique proteomic shifts, yet prior studies of chymase inhibitors have overlooked the pregnancy proteome. PZP possesses the canonical features of the  $\alpha M$  family of proteins that enable it to function as a protease inhibitor. Additionally, *in vitro* studies have characterised the protease inhibitory activity of PZP using chymotrypsin (Chiabrando et al., 2002, Christensen et al., 1989, Christensen et al., 1991, Jensen and Stigbrand, 1992) which is a serine protease that shares a similar catalytic triad with chymase (Hellman and Thorpe, 2014). Based on the results of prior studies involving PZP-chymotrypsin complexes or  $\alpha_2 M$ -chymase complexes, in this chapter it was hypothesised that chymase cleaves PZP at the bait

the  $\alpha_2M$ -chymase complex. **(C)** Binding to  $\alpha_2M$  shields chymase from inactivation by other endogenous inhibitors, such as  $\alpha 1ACT$  and  $\alpha 1AT$ .

region to form a stable complex that retains the proteolytic activity of chymase, and the chaperone activity of PZP. Furthermore, cleavage by chymase will expose the cryptic binding site on PZP for LRP1, thereby enhancing its binding to the cell surface. These hypotheses were investigated using a range of *in vitro* assays to characterise the structural and functional consequences of PZP cleavage by chymase, including analyses of proteolytic activity, complex formation, and cell-surface binding.

The specific aims of this chapter were to:

- 1) Purify PZP from human pregnancy plasma
- 2) Demonstrate that co-incubation of PZP and chymase results in the formation of a stable complex
- 3) Assess the effect of binding to PZP on the proteolytic activity of chymase
- 4) Investigate the impact of cleavage by chymase on the chaperone activity and cell-surface binding of PZP

# 2.2 Methods

#### 2.2.1 Materials

The compositions of commonly used buffers referenced in this chapter are detailed in Table 2.2.1.

**Table 2.2.1:** Common buffers used throughout the experimental procedures conducted in this chapter.

Name	Constituents
Phosphate buffered saline (PBS)	137 mM NaCl, 2.7 mM KCl, 1.5 mM KH <sub>2</sub> PO <sub>4</sub> , 8 mM Na <sub>2</sub> PO <sub>4</sub>
	pH 7.4 unless otherwise stated
PBS azide	PBS + 0.01% (v/v) sodium azide
PBST	PBS + 0.1% (v/v) Tween 20

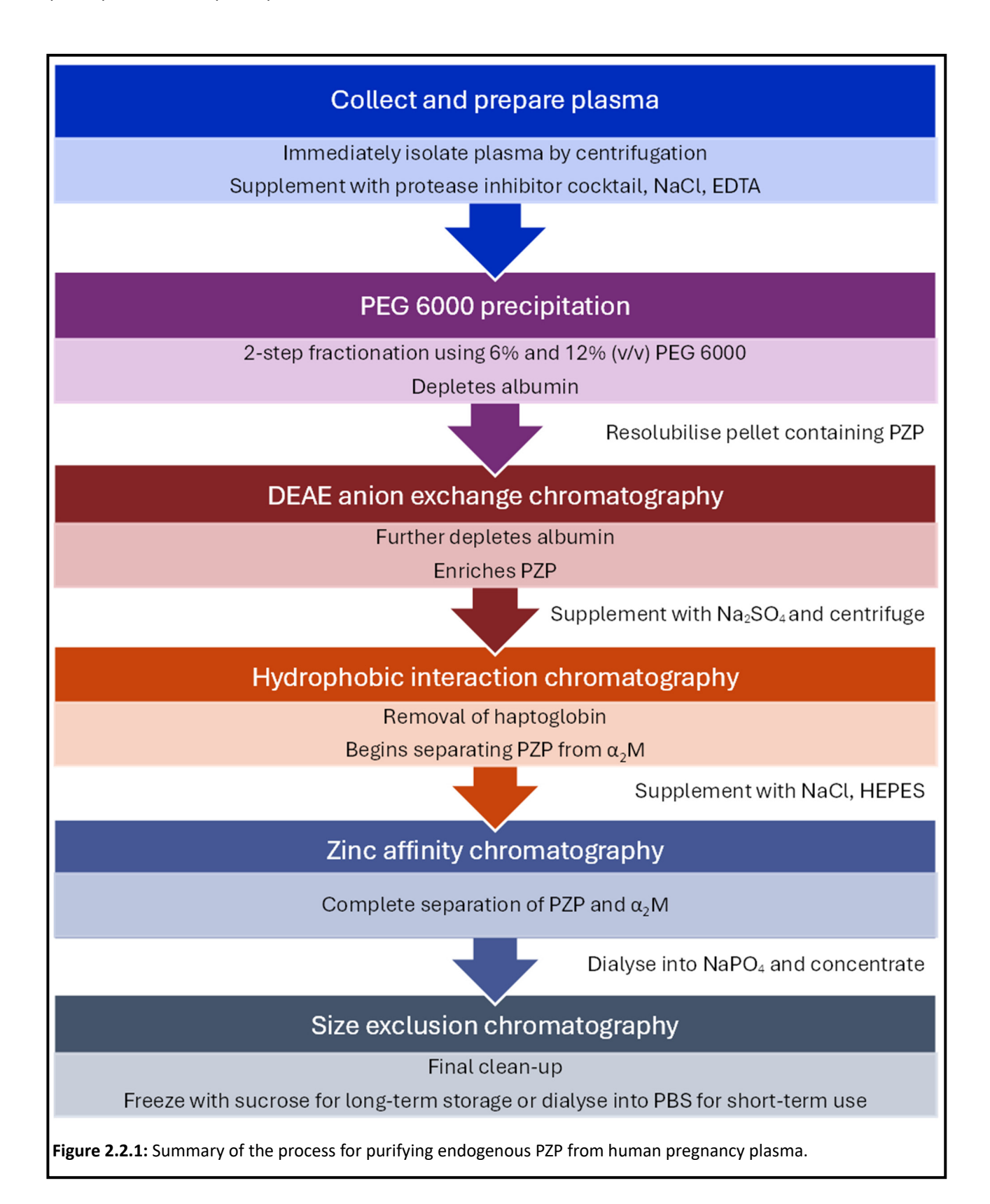
Human synthetic  $Aβ_{1-42}$  (1 mg; AnaSpec, Fremont, CA, USA), biotin labelled  $Aβ_{1-42}$  (0.1 mg; AnaSpec) and HiLyte<sup>TM</sup> Fluor 488 labelled  $Aβ_{1-42}$  (0.1 mg; AnaSpec) were reconstituted under sterile conditions using 50 μL of 10 mM NaOH. Complete dissolution of the peptides was achieved by gentle mixing before being diluted to a final concentration of 1 mg/mL in PBS. The peptide solutions were aliquoted into microfuge tubes, immediately snap frozen in liquid nitrogen and stored at -80 °C for later use. Human α-chymase (Sigma-Aldrich, St. Louis, MO, USA) was supplied in 20 mM Tris-HCl, 0.8 M NaCl, 25% (w/v) glycerol, pH 7.6 at 341 μg/mL and stored at -20 °C in aliquots. Bovine α-chymotrypsin (Sigma-Aldrich) was solubilised at 2 mg/mL in 1 mM HCl and stored in aliquots at -20 °C. α1ACT from human plasma (Sigma-Aldrich) was

solubilised at 2 mg/mL in MilliQ  $H_2O$  that had been syringe-filtered through a Minisart® 0.22  $\mu$ M polyether sulfone (PES) membrane (Sigma-Aldrich), aliquoted into microcentrifuge tubes and stored at -20 °C. Ang I (AnaSpec) was solubilised at 1 mg/mL in sterile MilliQ  $H_2O$ , aliquoted into microcentrifuge tubes and stored at -20 °C.

Fetal bovine serum (FBS) was purchased from Bovogen Biologicals (Keilor East, VIC, Australia) and heat-inactivated by incubation at 56°C for 30 min prior to use in cell culture. Skim milk powder was purchased from Coles Group Limited (Hawthorn East, VIC, Australia). Disodium phosphate, ethanol, HEPES (4-(2-hydroxyethyl)-1-piperazineethanesulfonic acid), and sodium chloride were purchased from ChemSupply Australia (Gillman, SA, Australia). Unless otherwise stated, all other reagents were purchased from Sigma-Aldrich.

# 2.2.2 Purification of PZP from human maternal pregnancy plasma

PZP was purified from human maternal pregnancy plasma as described by Chiabrando et al. (1997) and Cater (2021) with some modifications, as outlined below.



#### 2.2.2.1 Plasma collection

Pregnant women were recruited at the SA Pathology collection centre or the Women's Assessment Clinic (WAC) at the Flinders Medical Centre (FMC) in Bedford Park (SA, Australia). A maximum of 20 mL of blood per donor was collected by a qualified phlebotomist using Vacutainer lithium heparin blood tubes (Becton Dickinson, Macquarie Park, NSW, Australia), as described in Human Research Ethics Committee (HREC)/18/Central Adelaide Local Health Network (CALHN)/421. Blood samples were processed within 20 – 60 min of collection by centrifugation at 3,000 rpm for 10 min at 4 °C. The plasma was then isolated and stored at -20 °C until a sufficient volume was obtained for PZP purification.

# 2.2.2.2 PEG 6000 precipitation

Plasma and reagents were kept on ice throughout the following purification procedures. Frozen human pregnancy plasma (~100 mL) was thawed, pooled, and clarified by centrifugation at 1,500 x g for 10 min at 4 °C. Clarified plasma was pooled and supplemented with cOmplete™ EDTA-free protease inhibitor cocktail tablet (Roche Diagnostics, North Ryde, NSW, Australia) according to the manufacturer's instructions. The plasma was then further supplemented with 5 mM EDTA pH 8.0 and 100 mM NaCl.

Next, 50% (w/v) PEG 6000 (in MilliQ  $H_2O$ ) was added dropwise to the plasma with continuous, slow stirring until a final concentration of 6% (v/v) PEG 6000 was reached. The plasma was then centrifuged at 1,500 x g for 10 min at 4 °C. The resulting supernatant (S1) was collected and further supplemented with 50% (w/v) PEG 6000 to a final concentration of 12% (v/v) PEG 6000. Following centrifugation at 1,500 x g for 10 min at 4 °C, the resulting supernatant (S2) was removed. The pellet (P2; enriched with PZP) was solubilised in ice-cold buffer (20 mM NaPO<sub>4</sub>, 20 mM NaCl, 0.01% (v/v) sodium azide, pH 7.0) overnight at 4°C with gentle rocking.

#### 2.2.2.3 DEAE anion-exchange chromatography

Prior to diethylaminoethyl (DEAE) anion-exchange chromatography (AEC), the protein fraction recovered from PEG precipitation (Section 2.2.2.2; re-solubilised P2) was extensively dialysed against AEC equilibration buffer (20 mM NaPO₄, 20 mM NaCl, 0.01% (v/v) sodium azide, pH 7.0) and syringe filtered through a 0.22 µM PES membrane. A peristaltic pump (Pharmacia, Uppsala, Sweden) was used to load the filtered sample onto a HiPrep DEAE FF 16/10 AEC column (20 mL column volume [CV]; equilibrated with AEC equilibration buffer; GE Healthcare, Parramatta, NSW, Australia) at 3 mL/min. The sample was flushed through the pump with AEC equilibration buffer, to ensure complete loading, before the column was connected to an ÄKTA Pure™ 25 Fast

Performance Liquid Chromatography (FPLC) instrument (Cytiva, Macquarie Park, NSW, Australia) and washed with AEC equilibration buffer at 5 mL/min until the absorbance at 280 nm ( $A_{280}$ ) returned to baseline. The column was then washed using 20 mM NaPO<sub>4</sub>, 60 mM NaCl, 0.01% (v/v) sodium azide, pH 7.0 to remove loosely bound protein. Following this, more tightly bound protein was eluted using 20 mM NaPO<sub>4</sub>, 140 mM NaCl, 0.01% (v/v) sodium azide, pH 7.0, also at 4 mL/min. Finally, the column was regenerated by washing with 20 mM NaPO<sub>4</sub>, 1 M NaCl, 0.01% (v/v) sodium azide, pH 7.0, flushed with MilliQ H<sub>2</sub>O and filled with 20% (v/v) ethanol for storage.

# 2.2.2.4 Hydrophobic interaction chromatography

For hydrophobic interaction chromatography (HIC), the PZP-enriched protein fraction eluted by 140 mM NaCl using DEAE AEC was slowly supplemented with solid  $Na_2SO_4$ , at room temperature (RT) with stirring, to a final concentration of 1 M  $Na_2SO_4$ . The solution was then centrifuged at ~4,500 rpm for 20 min at 4 °C to and the supernatant recovered, which was then syringe filtered using a Minisart® 0.45  $\mu$ M PES membrane (Sigma-Aldrich). The filtered solution was then loaded onto a Phenyl Sepharose CL-4B column (25 mL CV) pre-equilibrated in HIC Buffer 1 (20 mM  $NaPO_4$ , 1 M  $Na_2SO_4$ , 0.01% (v/v) sodium azide, pH 7.0) using a peristaltic pump at 3 mL/min. HIC Buffer 1 was run through the pump, to ensure complete loading of the protein solution, before the column was connected to an ÄKTA Pure and washed with HIC Buffer 1 at 3 mL/min until the  $A_{280}$  returned to baseline. The column was then sequentially washed with 4 CV of HIC Buffer 2 (20 mM  $NaPO_4$ , 40 mM  $Na_2SO_4$ , 0.01% (v/v) sodium azide, pH 7.0) and HIC Buffer 3 (20 mM  $NaPO_4$ , 20 mM  $Na_2SO_4$ , 0.01% (v/v) sodium azide, pH 7.0) at 3 mL/min. Finally, MilliQ  $H_2O$  at 0.5 mL/min was used to elute the remaining protein, which was immediately supplemented with 0.5 M NaCl, 20 mM HEPES, 0.01% (v/v) sodium azide, pH 7.4 upon collection. The column was then washed and filled with 20% (v/v) ethanol prior to storage.

#### 2.2.2.5 Zinc affinity chromatography

For zinc affinity chromatography (ZAC), two 5 mL HiTrap chelating HP columns were connected in series (GE Healthcare, 10 mL total CV) and washed with 5 CV of MilliQ  $H_2O$  at a flow rate of 5 mL/min. The columns were then stripped (50 mM EDTA, 0.5 M NaCl, 20 mM HEPES, 0.01% (v/v) sodium azide, pH 7.4), recharged (0.1 M ZnSO<sub>4</sub>), and equilibrated (ZAC equilibration buffer; 0.5 M NaCl, 20 mM HEPES, 0.01% (v/v) sodium azide, pH 7.4) at 5 mL/min using an ÄKTA Pure. The PZP-enriched fraction eluted with MilliQ from HIC was then loaded onto the columns at 2 mL/min using a peristaltic pump. Once the protein fraction was loaded, the columns were

reconnected to an ÄKTA Pure and washed at 5 mL/min with ZAC equilibration buffer until the  $A_{280}$  returned to baseline. Protein was eluted using 15 mM imidazole in ZAC equilibration buffer at 4 mL/min. To remove tightly bound proteins, the columns were then washed with 500 mM imidazole in ZAC equilibration buffer at 4 mL/min until the  $A_{280}$  returned to baseline. Fractions containing protein, as indicated by the  $A_{280}$  trace, were immediately dialysed against 20 mM NaPO<sub>4</sub>, 0.01% (v/v) sodium azide, pH 7.4 and concentrated using 50 kDa molecular weight cut off (MWCO) Amicon® Ultra-15 centrifugal filter units (Millipore, North Ryde, NSW, Australia), according to the manufacturer's instructions.

# 2.2.2.6 Size exclusion chromatography

PZP-enriched fractions obtained from ZAC (as verified by native Western blot analysis, see Figure 2.3.4) were syringe filtered through a 0.22  $\mu$ M PES membrane prior to undergoing size exclusion chromatography (SEC). Protein fractions containing PZP were loaded onto a HiPrep 26/60 Sephacryl S-300 HR column (320 mL CV; GE Healthcare) that had been equilibrated with 20 mM NaPO<sub>4</sub>, pH 7.4 at a flow rate of 0.5 mL/min (maximum 1.3 mL/min). Typically, 2.5 mL (<3 mg/mL PZP) was injected on to the column via a 3 mL sample loop. For long-term storage at -20 °C, PZP was supplemented with 100 mM sucrose. Alternatively, PZP was dialysed into PBS azide for immediate use or short-term storage at 4 °C.

# 2.2.3 Purification of $\alpha_2 M$ from human plasma

Human blood plasma was collected from non-pregnant healthy donors at SA Pathology, FMC (Bedford Park, SA, Australia). Approximately 100 mL of blood per donor was collected by a trained phlebotomist using Vacutainer lithium heparin blood tubes (Becton Dickinson), in accordance with ethics approval HREC/18/CALHN/421. Immediately following collection, the blood was centrifuged at 3,000 rpm for 10 min at 4 °C and the plasma recovered and pooled. Plasma was supplemented with cOmplete™ EDTA free protease inhibitor cocktail tablet according to the manufacturer's instructions, 1 M NaCl, and 20 mM HEPES, pH 7.4. The supplemented plasma was then syringe filtered through a 0.45 μM PES membrane and ZAC was carried out as described in Section 2.2.2.5, except the ZAC equilibration buffer contained 1 M NaCl, rather than 0.5 M NaCl, and loosely bound proteins were eluted using 20 mM imidazole rather than 15 mM imidazole. α₂M was eluted from the column using 500 mM imidazole, 0.5 M NaCl, 20 mM HEPES, 0.01% (v/v) sodium azide, pH 7.4 and extensively dialysed against PBS azide. Purified α₂M was obtained following SEC using a HiPrep 26/60 Sephacryl S-300 HR column equilibrated with PBS azide. Typical injection volumes were the same as those in

Section 2.2.2.6. Following SEC, if necessary, samples were concentrated using 50 kDa MWCO Amicon® Ultra-15 centrifugal filter units. For short-term use,  $\alpha_2 M$  was stored in PBS azide at 4 °C. For long term storage,  $\alpha_2 M$  was dialysed into 20 mM NaPO<sub>4</sub>, supplemented with 100 mM sucrose and frozen at -20 °C.

## 2.2.4 Denaturing gel electrophoresis

For denaturing gel electrophoresis, proteins were diluted in 4x NuPAGE LDS Sample Buffer (Thermo Fisher Scientific, Scoresby, VIC, Australia) and separated on a precast 1.0 mm thick, 12-well Bolt Bis-Tris 4-12% mini protein gel (Thermo Fisher Scientific) using 2-(N-morpholino)ethanesulfonic acid (MES) running buffer (50 mM MES, 50 mM Tris base, 1 mM EDTA, 0.1% (w/v) SDS) using an Invitrogen XCell SureLock™ Mini-Cell Electrophoresis System (Thermo Fisher Scientific) according to manufacturer's instructions.

Samples were reduced by incubation with 5% (v/v) 2-mercaptoethanol (2-ME) at RT for 5 min. Precision Plus Protein™ Dual Xtra Prestained Protein Standard (Bio-Rad, Gladesville, NSW, Australia) was used to estimate protein band masses. All gels were stained with InstantBlue Coomassie protein stain (Abcam, Melbourne, VIC, Australia) and destained overnight in MilliQ H₂O. Stained gels were imaged using either a ChemiDoc MP or GelDoc Go imaging system (Bio-Rad). Processing of images, calculation of molecular weights, and densitometry was carried out using ImageLab 6.1 (Bio-Rad). Electrophoresis was carried out at RT with a Life Technologies PowerEase 90W power supply (Thermo Fisher Scientific). Due to the sensitivity of αM proteins to heat-induced fragmentation (Harpel et al., 1979), samples were not heated prior to separation unless otherwise specified.

## 2.2.5 Native gel electrophoresis

For native gel electrophoresis, proteins were diluted in 4x native loading buffer (200 mM Tris, 40% (v/v) glycerine, 0.4% (w/v) bromophenol blue, pH 6.8) and separated on a precast 1.5 mm, 10-well NuPAGE Tris-Acetate 3-8% mini protein gel (Thermo Fisher Scientific) in Native Tris running buffer (25 mM Tris base, 192 mM glycine, pH 8.3) using an Invitrogen XCell SureLock™ Mini-Cell Electrophoresis System according to manufacturer's instructions. Gels were stained, imaged, and processed as described in Section 2.2.4. Densitometry analyses were performed using ImageLab 6.1 and relative migration distance (Rf) was calculated manually using ImageJ 1.52a (Schneider et al., 2012).

# 2.2.6 Western blot analysis

Following separation by electrophoresis, proteins were transferred to either 0.2 µM nitrocellulose (NC) or polyvinylidene fluoride (PVDF) membrane iBlot™ 2 transfer stacks (Thermo Fisher Scientific) using an iBlot™ 2 dry blotting system (Thermo Fisher Scientific). Membranes were blocked in PBST containing 5% (w/v) skim milk powder and 0.01% sodium azide (v/v) overnight at 4 °C with gentle shaking. The primary antibody for the protein of interest was diluted in PBST containing 5% (w/v) skim milk powder and 0.01% (v/v) sodium azide, as per Table 2.2.2. The membrane was incubated with the primary antibody for 1 h at RT with gentle shaking, followed by three 5 min washes in PBST. Bound primary antibodies were detected using a horseradish peroxidase (HRP) conjugated secondary antibody diluted in PBST containing 5% (w/v) skim milk powder, as per Table 2.2.2, in which the membrane was incubated for 1 h at RT with gentle shaking. Following a final wash as described above, protein bands were visualised using Clarity Western enhanced chemiluminescence substrate (Bio-Rad) and a ChemiDoc MP imaging system (BioRad) or ImageQuant™ LAS 4000 (GE Healthcare). Processing of images and densitometry analyses were performed using ImageLab 6.1 (BioRad) and Rf was calculated manually using ImageJ 1.52a (Schneider et al., 2012).

**Table 2.2.2:** Summary of antibodies used in Western Blot analysis.

Antibody	Dilution	Species	Clonality	Company (catalogue #)		
Primary antibodies	Primary antibodies					
Anti-PZP	1:2,000	Rabbit	Polyclonal	GeneTex (GTX102547)		
Anti-α <sub>2</sub> M	1:2,000	Goat	Polyclonal	GeneTex (GTX27337)		
Anti-A $\beta_{1-42}$	1:2,000	Mouse	WO2, monoclonal	Sigma-Aldrich (MABN10)		
Anti-chymase	1:10,000	Rabbit	Recombinant monoclonal	Abcam (ab186417)		
Secondary antibodies						
Anti-mouse HRP	1:3,000	Rabbit	Recombinant polyclonal	Invitrogen (A27025)		
Anti-rabbit HRP	1:3,000	Goat	Recombinant polyclonal	Invitrogen (A27036)		
Anti-goat HRP	1:3,000	Rabbit	Recombinant polyclonal	Invitrogen (A27014)		

#### 2.2.7 Protein quantification

A Nanodrop 2000C was used to measure the absorbance of purified protein solutions at 280 nm in quadruplicate and adjusted using the appropriate blank solution. The protein concentration was then estimated using 0.1% absorbance (1 mg/mL) of 0.89 for  $\alpha_2$ M (dimer and tetramer) and 0.81 for PZP.

# 2.2.8 Generation of protease-modified PZP and $\alpha_2 M$

PZP was co-incubated with chymase or chymotrypsin (proteases) in PBS for 45 min at 37 °C. Unless otherwise specified, the molar ratio of PZP-to-protease was 4:1 during the incubation.

Except for Section 2.2.16, protease activity was inhibited by supplementing the protein preparation with cOmplete<sup>™</sup> EDTA-free protease inhibitor cocktail (Roche) according to manufacturer's instructions. Samples were then extensively dialysed against PBS to remove excess inhibitor prior to use in the assay.

Following treatment of PZP as described above, denaturing gel and native gel electrophoresis (see Sections 2.2.4 and 2.2.5) were carried out to analyse the effects of proteolytic processing by chymase or chymotrypsin. For all protein preparations, 0.01 % (v/v) sodium azide was used as a preservative to prevent microbial growth, except for samples used with live cells (i.e. Section 2.2.15). As a control,  $\alpha_2 M$ , which has well characterised protease-inhibitory activity (Jensen and Stigbrand, 1992, Raymond et al., 2009, Wyatt et al., 2013a, Harwood et al., 2021a, Huang et al., 2022), was also co-incubated with proteases as indicated.

## 2.2.9 Biotinylation of proteins

Biotin 3-sulfo-N-hydroxysuccinimide ester sodium salt (Sigma-Aldrich) was solubilised in PBS and incubated with the target protein or putative protein complex at a 40-fold molar excess for 3 h at RT with gentle agitation (60 rpm). Excess biotin was removed by extensive dialysis against PBS prior to use in experiments. Biotinylation was confirmed by Western blotting as per Section 2.2.6, with the exception that HRP was used to directly detect the biotin tag. This approach also enabled assessment of the conformations of the biotinylated species.

## 2.2.10 DTNB thiol assays

5,5'-dithiobis-(2-nitrobenzoic) acid (DTNB; Ellman's Reagent; Gold Biotechnology, St. Louis, MO, USA) assays were carried out according to the manufacturer's instructions. Briefly, PZP or  $\alpha_2 M$  (1.7  $\mu$ M) was incubated in PBS in the presence or absence of chymase (4:1 molar ratio of  $\alpha$ M-to-chymase) for 45 min at 37 °C in triplicate in a 384-well plate (50  $\mu$ L/well). After this incubation period, 100  $\mu$ M DTNB and 100 mM Tris (pH 8.0) was added to each well and the solutions incubated for 5 min at RT. Optical absorbance at 412 nm was measured using a CLARIOstar plate reader (BMG Labtech, Mornington, VIC, Australia). Values were corrected against a blank containing 100  $\mu$ M DTNB and 100 mM Tris in PBS (n = 3, 50  $\mu$ L/well).

#### 2.2.11 bisANS assays

Surface hydrophobicity was estimated using 4,4'-dianilino-1,1'-binaphthyl-5,5'-disulfonic acid (bisANS) assays, as described by (Cater et al., 2019) with minor modification. PZP alone or PZP pre-incubated with proteases (Section 2.2.8) was used at a final concentration of 1.9 µM total

protein and incubated with 10  $\mu$ M of bisANS in PBS for 5 min at RT in the dark. The protein samples were transferred to a 384-well microplate in quadruplicate (50  $\mu$ L/well) and the bisANS fluorescence (excitation = 355 nm, emission = 480 nm) was measured using a CLARIOstar plate reader. Values were corrected against a blank containing 10  $\mu$ M bisANS in PBS (n = 4, 50  $\mu$ L/well).

For bisANS concentration curve experiments, PZP alone (1  $\mu$ M) or PZP that had been preincubated with chymotrypsin at a 1:1 molar ratio (1  $\mu$ M) for 45 min at 37 °C was incubated with bisANS at final concentrations of 0.25, 1, 5, 10, 20, and 40  $\mu$ M. bisANS fluorescence was then measured in triplicate as described above.

# 2.2.12 ThT assays

Thioflavin T (ThT) assays were carried out as described by (Cater et al., 2019, Wyatt et al., 2013a) with some adjustment. A $\beta_{1-42}$  amyloid fibril formation was assessed by incubating 5  $\mu$ M A $\beta_{1-42}$  (in PBS) with 25  $\mu$ M ThT in the presence or absence of PZP alone or PZP pre-incubated with proteases, as described in Section 2.2.8, using a 20-fold molar excess of A $\beta_{1-42}$ . Samples (80  $\mu$ L/well) were incubated (n = 4 technical replicates) at 28 °C in a 384-well microplate with periodic shaking. ThT fluorescence (excitation = 440 nm, emission = 480 nm) was measured at 5 min intervals using a CLARIOstar plate reader. Values were corrected against a blank containing 25  $\mu$ M ThT in PBS (n = 4, 80  $\mu$ L/well).

## 2.2.13 Biotin-streptavidin pull-down assays

Biotin-streptavidin pull-down assays were carried out according to manufacturer instructions using Dynabeads MyOne Streptavidin C1 beads (Thermo Fisher Scientific) and a DynaMag-2 magnet (Thermo Fisher Scientific). Briefly, 500 µg of beads were aliquoted into 1.5 mL microcentrifuge tubes and the supernatant discarded. Beads were washed by resuspending in PBS azide, followed by centrifugation at 21,000 x g for 3 min after which the supernatant was discarded. Washing was then repeated using PBST. Protein samples (Table 2.2.3) were incubated with the beads for 1 h at RT with gentle rotation (30 rpm) using an ELMI RM-2 Intelli-Mixer<sup>TM</sup> (POCD Scientific, North Rocks, NSW, Australia). The supernatant was then removed, and the beads were washed four times with PBS azide containing 0.1% (w/v) bovine serum albumin (BSA). The beads were then washed a final time in PBS azide and resuspended in NuPAGE LDS sample buffer containing 5% (v/v) 2-ME. Samples were reduced and separated by

denaturing gel electrophoresis (Section 2.2.4) and analysed by Western blotting as described in Section 2.2.6.

Table 2.2.3: Prepared protein samples and controls for use in biotin-streptavidin pull-down assays.

Assay	Biotinylated protein	Unbiotinylated protein	Incubation conditions
	bAβ <sub>1-42</sub> (5 μM)	PZP (0.5 μM)	2 h, 37°C; aggregation of Aβ <sub>1-42</sub>
Decement of D7D	bAβ <sub>1-42</sub> (5 μM)	PZP-chymase (0.5 μM)	monitored with ThT (as per
Recovery of PZP	bAβ <sub>1-42</sub> (5 μM)	PZP-chymotrypsin (0.5 μM)	Section 2.2.12)
following pull- down of Aβ <sub>1-42</sub>	-	PZP (0.5 μM)	
	-	PZP-chymase (0.5 μM)	2 h, 37°C
	-	PZP-chymotrypsin (0.5 μM)	
Recovery of	bPZP (1.2 μM)	Chymase (2.4 μM)	
chymase following pull- down of PZP	-	Chymase (2.4 μM)	45 min, 37°C

All proteins were incubated in PBS.

## 2.2.14 Mammalian cell culture

SH-SY5Y cells were kindly donated by Associate Professor Mary-Louise Rogers (Flinders University, SA, Australia), and BeWo cells (CCL-98) were obtained from the American Type Culture Collection (ATCC; Gaithersburg, MD, USA). These cell types were chosen as they are known to express high levels of LRP1 (Quinn et al., 1999, Thul et al., 2017), a cell-surface receptor for PZP. Cells were maintained under sterile conditions in T25 flasks and expanded using T75 flasks as required. Upon reaching 70 - 90% confluence, media was aspirated and cells briefly rinsed with PBS. For routine cell culture, cells were detached by incubation with trypsin-EDTA (0.05% trypsin, 0.02% EDTA; Sigma-Aldrich), diluted in media, and centrifuged at 1000 rpm for 5 min at RT. The cell pellet was then resuspended in 1 mL of fresh media and a portion (typically 5 - 20%) returned to the culture flask with fresh media. Cells were transferred to new flasks every 2 - 3 passages and not used past 20 passages. All cell lines were grown in 5% (v/v) atmospheric  $CO_2$  at 37 °C under aseptic conditions. Cell suspension was mixed at a 1:1 ratio (10 µL) with trypan blue and counted using a CellDrop<sup>TM</sup> FL automated cell counter (DeNovix, Wilmington, DE, USA), according to the manufacturer's instructions.

For long term storage, cells not exceeding passage six were resuspended in freezing media (40% (v/v) FBS, 10% (v/v) dimethyl sulfoxide [DMSO], 50% (v/v) culture media) and aliquoted into sterile cryogenic vials. Vials were transferred to a Mr. Frosty freezing container (Thermo Fisher Scientific) and immediately placed into a -80 °C freezer for 24 – 48 h before being transferred to a liquid nitrogen dewar.

Table 2.2.4: Cultured cell line types and composition of the media used to maintain them for standard growth.

Cell	Туре	Media composition
SH-SY5Y	Subline of neuroblastoma from metastatic bone tumor. Adherent.	Dulbecco's Modified Eagle's Medium (DMEM)/Nutrient Mixture F-12 Ham (Sigma-Aldrich) 10% FBS 1X GlutaMAX™ (Thermo Fisher Scientific)
BeWo	Isolated from the placenta of a patient with choriocarcinoma. Adherent.	Kaighn's modification of Ham's F-12 Medium (In Vitro) 10% FBS 1X GlutaMAX <sup>™</sup> (Thermo Fisher Scientific)

## 2.2.15 Flow cytometry

SH-SY5Y or BeWo cells were detached using 5 mM EDTA (pH 8.0), and pelleted by centrifugation at 300 x g for 5 min at RT. The cell pellet was washed using ice-cold Hanks balanced salt solution (HBSS; 1.3 mM CaCl<sub>2</sub>, 1 mM MgCl<sub>2</sub>, 137 mM NaCl, 5.4 mM KCl, 0.25 mM Na<sub>2</sub>HPO<sub>4</sub>, 0.44 mM KH<sub>2</sub>PO<sub>4</sub>, 4.2 mM NaHCO<sub>3</sub>, 0.1% BSA, pH 7.4) and pelleted by centrifugation at 300 x g for 5 min at 4 °C. Cells were then resuspended in HBSS containing 0.05 mg/mL of biotin-labelled native PZP, PZP-chymase, PZP-chymotrypsin, or glutathione S-transferase tagged receptor associated protein (GST-RAP; a pan-specific ligand of lipoprotein receptors) and incubated on ice for 30 min. Cells were then washed with HBSS, resuspended in streptavidin-Alexa Fluor 488 conjugate (Thermo Fisher Scientific; diluted 1:2000 in HBSS) and incubated on ice for a further 30 min. Finally, cells were washed with HBSS and the cell surface-associated Alexa Fluor 488 fluorescence was measured using a CytoFLEX S flow cytometer (Beckman Coulter, Lane Cove, NSW, Australia). Values were corrected against a blank containing cells treated only with streptavidin-Alexa Fluor 488 conjugate and propidium iodide was used to exclude non-viable cells. In additional experiments using SH-SY5Y, cells were pre-incubated with 0.5 mg/mL unlabelled GST-RAP in HBSS or HBSS alone for 30 min on ice. Following this incubation, the assays were carried out as above. All data were analysed using the CytExpert software (Beckman Coulter).

#### 2.2.16 Chymase activity assays

The effect of PZP on the activity of chymase was assessed in separate assays using RETF-4NA (Focus Bioscience, Tingalpa, QLD, Australia), and Ang I (AnaSpec) as substrates. RETF-4NA is a sensitive and selective colorimetric substrate for chymase and its cleavage can be detected at 410 nm (Raymond et al., 2009). The trifluoracetic acid (TFA) form of RETF-4NA was used due to increased solubility and stability but is referred to throughout as RETF-4NA. In these assays,  $\alpha_2$ M, which is known to bind chymase (Raymond et al., 2009), was included as a positive control.

Proteins to be used for these assays were prepared in a 384-well microplate via two sequential incubations in PBS that had been syringe filtered through a 0.22  $\mu$ M PES membrane. To assess the effect of PZP or  $\alpha_2$ M on the activity of chymase, the proteins were co-incubated with chymase at a 1:1 molar ratio (100 nM) in duplicate (Figure 2.2.2, Incubation 1). Subsequently, a 3x molar excess (300 nM) of  $\alpha$ 1ACT was added to one set of samples to inhibit the activity of any accessible chymase, while the other set of samples received the vehicle control of PBS (Figure 2.2.2, Incubation 2). Chymase alone and chymase co-incubated with  $\alpha$ 1ACT were the positive and negative controls, respectively.

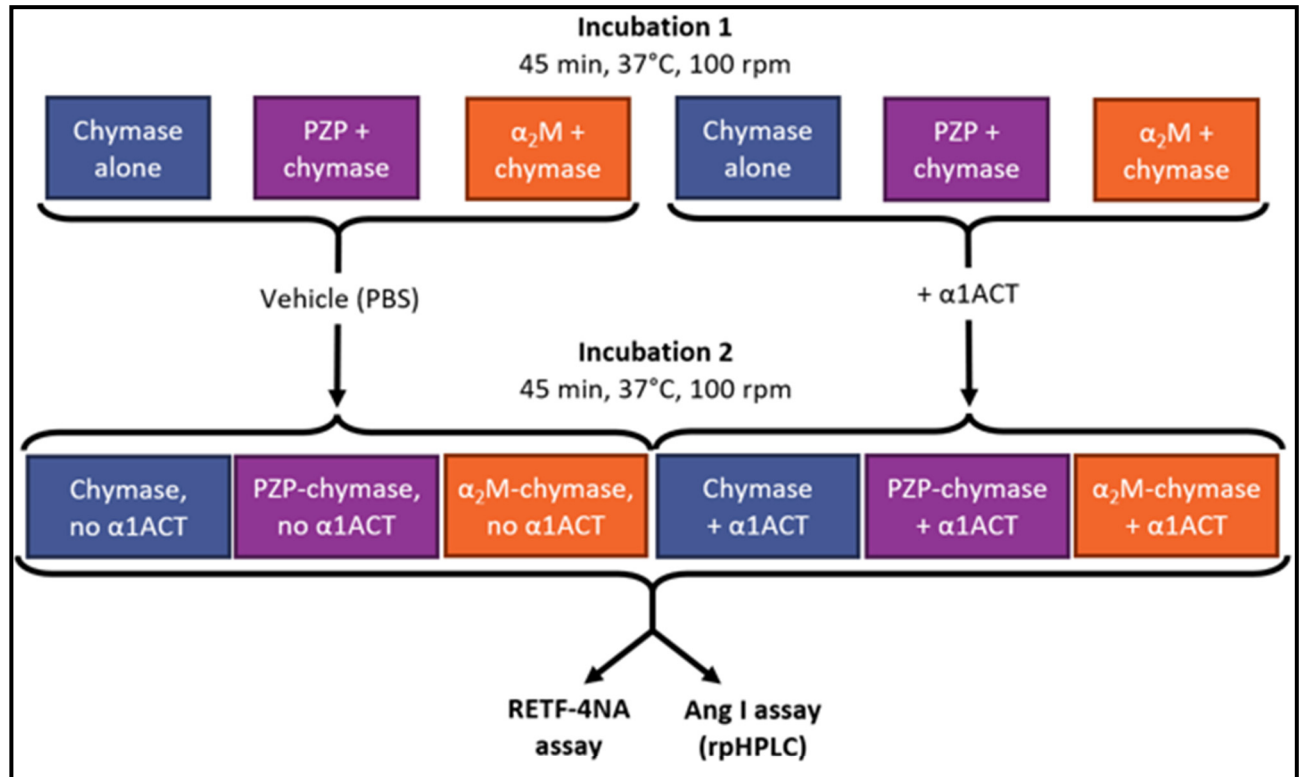


Figure 2.2.2: Two-step incubation protocol used to prepare samples for chymase activity assays. Chymase was incubated alone or in the presence of  $\alpha_2 M$  or PZP, in duplicate, to allow complex formation. Duplicate reactions were then treated with either vehicle or  $\alpha_1 ACT$  to inhibit any accessible chymase – either free or bound. Samples were then assayed for chymase activity using RETF-4NA or Ang I as substrates.

#### 2.2.16.1 RETF-4NA assays

RETF-4NA stock solution was prepared fresh for each biological replicate at 2 mM in PBST + 10% DMSO. Protein samples (prepared as described above) were diluted to 10 nM in PBST + 10% DMSO and aliquoted in triplicate into a 384-well microplate. RETF-4NA was added to each well to a final concentration of 1 mM and the plate immediately placed in a ClarioSTAR plate reader (37 °C, 100 rpm) which measured absorbance at 410 nm every min for 1 h.

#### 2.2.16.2 Ang I assays

Protein samples (prepared as described above) were diluted to 12.5 nM in 0.22  $\mu$ M syringe-filtered (PES membrane) PBS and aliquoted into low-binding microcentrifuge tubes (SSIbio, South San Francisco, CA, USA) containing ~2  $\mu$ g of Ang I. Following a 45 min incubation at 37 °C, 1  $\mu$ L of concentrated hydrochloric acid (HCl; 11.65 M) was added to cease the reaction and the samples were further diluted to ~4.3 nM chymase in 0.1% TFA (115  $\mu$ L total volume). Particulates were removed by centrifugation at 21,000 x g for 2 min and 110  $\mu$ L of the clarified samples was aliquoted into separate high performance liquid chromatography (HPLC) vials (Agilent Technologies, Santa Clara, CA, USA). Reverse phase HPLC (rpHPLC) was performed using a Prep-C18 Scalar column (Agilent Technologies; 4.6 x 250 mm, 10  $\mu$ M, 400 bar) on an Agilent 1260 Infinity Quaternary liquid chromatography system (buffer A: 0.1% TFA, buffer B: 80% acetonitrile in 0.08% TFA). The injection volume was 100  $\mu$ L and was separated using a 10 – 50% (v/v) acetonitrile gradient over 40 min at a flow rate of 0.5 mL/min.

#### 2.3 Results

#### 2.3.1 Purification of PZP from human plasma

A small number of studies have reported purifying PZP from human plasma for *in vitro* functional analyses. The following section describes the results obtained using the multi-step PZP purification procedure optimised by Chiabrando et al. (1997) and Cater (2021).

#### 2.3.1.1 PEG 6000 precipitation

The most prominent protein band visible in whole pregnancy plasma following separation by denaturing gel electrophoresis migrated to a position corresponding to 50 - 70 kDa. This is consistent with the expected mass of human serum albumin (67 kDa) and the heavy chain (HC) of immunoglobulin G (IgG) (50 kDa). Other prominent bands migrated with masses corresponding to 23 kDa and 72 kDa, which are consistent with the expected mass of the abundant plasma proteins IgG light chain (LC; 25 kDa) and/or apolipoprotein A1 (ApoA1; 28 kDa), and transferrin (80 kDa), respectively. A band at 170 kDa, corresponding to the expected mass of  $\alpha_2$ M and PZP (collectively termed  $\alpha$ M), which both migrate as monomers (180 kDa) under reducing conditions, was also visible (Figure 2.3.1A).

Following supplementation of whole pregnancy plasma with 6% (w/v) PEG 6000, protein largely precipitated non-specifically (P1; Figure 2.3.1A). There was marginal depletion of the major proteins present in pregnancy plasma, such as albumin and IgG, which remained in the

supernatant (S1). There appeared to be minimal loss of proteins at the expected mass of the  $\alpha$ M's (Figure 2.3.1A).

After supplementation of fraction S1 with 12% (w/v) PEG 6000, albumin preferentially remained in the supernatant (S2), whilst the remaining protein was recovered in the precipitate (P2). The removal of albumin was only partial (Figure 2.3.1A). To confirm that PZP was retained in the fraction P2 following PEG 6000 fractionation, matched samples were analysed by Western blotting using an antibody raised against a recombinant fragment of PZP, that does not cross-react with  $\alpha_2 M$  (Cater, 2021). The results showed that a small amount of PZP was lost in fraction P1. However, the PZP band was substantially more prominent in fraction P2, with a relative intensity 13.62-fold higher than that in whole pregnancy plasma (PP) when equal volumes of each fraction were analysed (Figure 2.3.1B). Overall, the results from PEG 6000 precipitation of pregnancy plasma suggest that the fraction (P2) was enriched with PZP but removal of other plasma proteins was very inefficient.

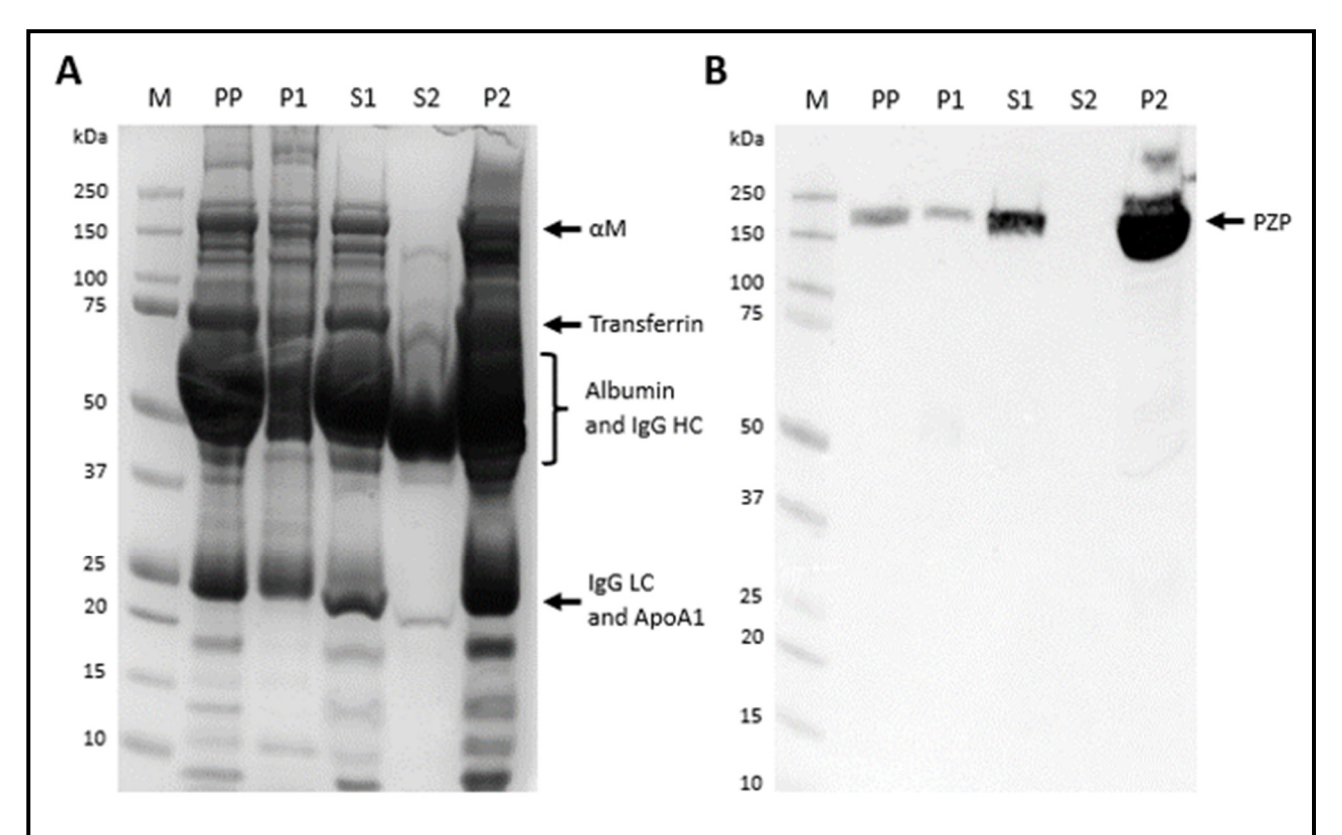


**Figure 2.3.1:** Representative **(A)** Coomassie-stained gel and **(B)** matched Western blot showing protein fractions obtained following PEG 6000 precipitation of human pregnancy plasma.

(A) Samples were prepared by diluting 5  $\mu$ L of each fraction 1:10 in PBS and supplementing with LDS loading buffer containing 5% (v/v) 2-mercaptoethanol. The equivalent of 1  $\mu$ L of undiluted sample was separated on a Bolt Bis-Tris 4-12% mini protein gel and stained with InstantBlue®. Lane order: M = marker, PP = unfractionated pregnancy plasma, P1 = precipitate following 6% PEG 6000 fractionation of whole pregnancy plasma (resolubilised for analysis), S1 = supernatant from P1, P2 = precipitate following 12% PEG 6000 fractionation of S1 (resolubilised for further purification), S2 = supernatant from P2. Expected migration of reduced monomeric  $\alpha$ 2M or PZP ( $\alpha$ M; 180 kDa), transferrin (80 kDa), albumin (67 kDa), IgG HC (50 kDa), IgG LC (25 kDa), and ApoA1 (28 kDa) are indicated. (B) A western blot detecting PZP in matched fractions. Samples were separated as in (A) and transferred to a nitrocellulose membrane.

#### 2.3.1.2 Chromatography

#### **DEAE AEC**

The PZP enriched fraction from PEG 6000 (P2) was subjected to DEAE AEC using a stepwise NaCl gradient to further fractionate the plasma protein. Assessment of the separated protein fractions by denaturing gel electrophoresis indicated that proteins ≤75 kDa were enriched in the fractions eluted using low and mid salt concentrations (i.e., 20 mM NaCl and 60 mM NaCl). The bands migrating at approximately 73 kDa, 62 kDa, 53 kDa, and 24 kDa, representing putative transferrin, albumin, IgG HC, and IgG LC/ApoA1, respectively, were still evident in both protein fractions collected (Figure 2.3.2A). A band consistent with the expected mass of reduced αM protein was visible in all fractions. Western blot analyses confirmed that this band contained PZP and was enriched by 1.87-fold in the protein fraction eluted by high salt

concentration (i.e., 140 mM NaCl) compared to fraction eluted by low salt concentration (Figure 2.3.2B). Although similar amounts of PZP were detected in the fractions eluted by mid and high salt concentrations, comparatively, the protein fraction eluted by high salt concentration contained fewer contaminating proteins, thus, this fraction was selected for further processing to obtain purified PZP.

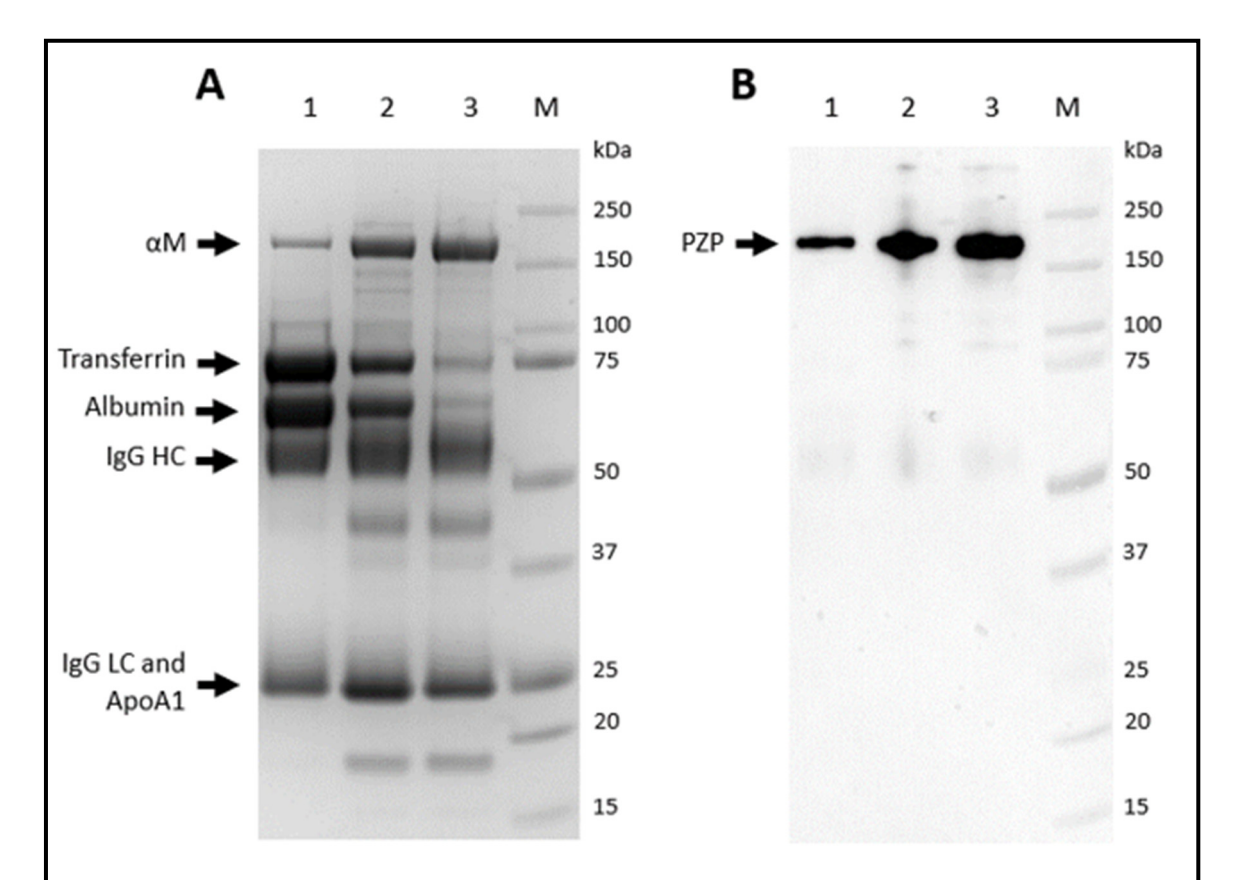


**Figure 2.3.2:** Representative **(A)** Coomassie-stained gel and **(B)** matched Western blot showing protein fractions obtained from DEAE anion exchange chromatography of the PZP-enriched fraction following PEG 6000 precipitation of human pregnancy plasma.

(A) Samples from each step of DEAE chromatography, containing approximately 9.6  $\mu$ g total protein, were supplemented with LDS loading buffer containing 5% (v/v) 2-mercaptoethanol. Protein was separated on a Bolt Bis-Tris 4-12% mini protein gel and stained with InstantBlue®. Lane order: 1 = 20 mM NaCl elution, 2 = 60 mM NaCl elution, 3 = 140 mM NaCl elution, M = marker. Expected migration of reduced monomeric  $\alpha$ 2M or PZP ( $\alpha$ M; 180 kDa), transferrin (80 kDa), albumin (67 kDa), IgG HC (50 kDa), IgG LC (25 kDa), and ApoA1 (28 kDa) are indicated. (B) A western blot detecting PZP in matched fractions. Samples containing approximately 1.3  $\mu$ g total protein were separated as in (A) and transferred to a nitrocellulose membrane.

#### HIC

The PZP-enriched fraction obtained from DEAE AEC was subjected to HIC to further fractionate the protein. Native Western blot analysis was used to assess the separation of PZP and  $\alpha_2 M$ , and to analyse the quaternary structure of PZP. The majority of PZP was retained on the column in the presence of Na<sub>2</sub>SO<sub>4</sub> or Na<sub>2</sub>PO<sub>4</sub> but was eluted in MilliQ H<sub>2</sub>O, as expected (Chiabrando et

al., 1997); Figure 2.3.3A). On the other hand,  $\alpha_2 M$  was abundant in fractions containing Na<sub>2</sub>SO<sub>4</sub> or Na<sub>2</sub>PO<sub>4</sub>, with only a small amount co-eluting with PZP in MilliQ H<sub>2</sub>O (Figure 2.3.3B). The results of Western blot analysis showed that following HIC, PZP predominantly migrated with an Rf of 0.51 (Figure 2.3.3A), which is comparable to the migration of native PZP in whole pregnancy plasma (Figure S1). Several more slowly migrating bands were also detected, of these, the highest molecular weight band had an Rf of 0.36, which is comparable to the Rf of tetrameric PZP which can be detected at low levels in human plasma (Figure S1). The Rf values for the upper and lower bands detected by the  $\alpha_2 M$  antibody were 0.36 and 0.51, respectively, supporting the identification of these bands as tetrameric and dimeric  $\alpha_2 M$  (Figure 2.3.3B).

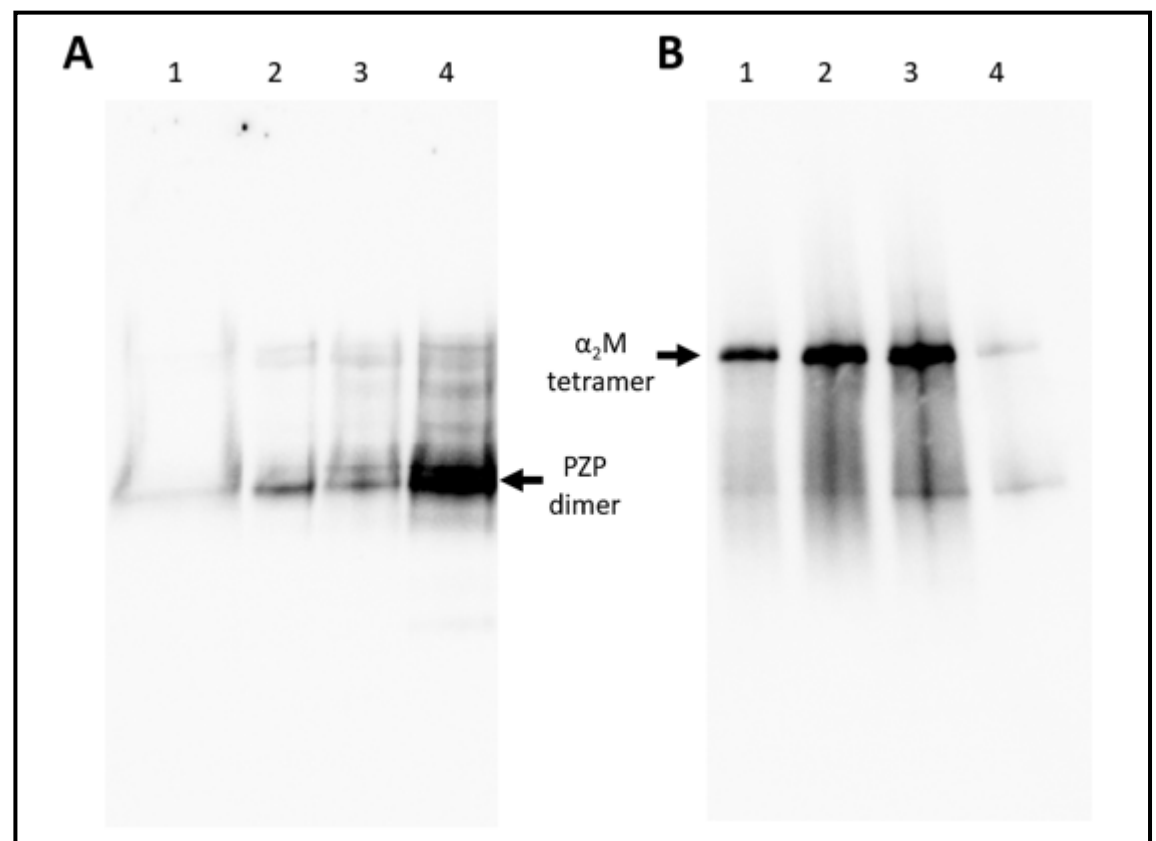


Figure 2.3.3: Representative Western blots detecting (A) PZP (360 kDa) and (B)  $\alpha_2$ M (720 kDa) in fractions eluted by HIC of the PZP-enriched fraction obtained from DEAE chromatography. Samples were prepared in duplicate and supplemented with native loading buffer. Protein was separated on a NuPAGE Tris-Acetate 3-8% mini protein gel and transferred to a nitrocellulose membrane. Lane order: 1 = 0.4 M Na<sub>2</sub>SO<sub>4</sub> elution, 2 = 0.2 M Na<sub>2</sub>SO<sub>4</sub> elution, 3 = 0 M Na<sub>2</sub>SO<sub>4</sub> (20mM NaPO<sub>4</sub> only) elution, 4 = MilliQ H<sub>2</sub>O elution. Expected migration of tetrameric  $\alpha_2$ M and dimeric PZP is indicated.  $\alpha_2$ M is expected to elute in lane 3 (0 M Na<sub>2</sub>SO<sub>4</sub>) and PZP in lane 4 (MilliQ H<sub>2</sub>O). (A) Approximately 4 μg total protein per lane (B) approximately 2 μg total protein per lane.

#### ZAC

The PZP-enriched protein fraction from HIC (eluted in MilliQ  $H_2O$ ) was subjected to ZAC and the protein fractions obtained were analysed by native Western blot and densitometry analysis.

The results showed that the majority of PZP was eluted by 15 mM imidazole, and only trace amounts were eluted by the 500 mM imidazole wash (Figure 2.3.4). The predominant protein band detected by the anti-PZP antibody in native Western blot analysis migrated with an Rf value of 0.54, consistent with the migration of the PZP dimer (Figure 2.3.4A). A PZP species migrating faster than native PZP was also detected in the 15 mM imidazole elution. This band, hereafter referred to as 'fast PZP', was far less prominent than the main PZP band, suggesting that it comprised only a small fraction of the total protein in that elution. Native Western blot analysis using an anti- $\alpha_2$ M antibody detected weak bands in the 500 mM imidazole fraction, corresponding to tetrameric (Rf 0.35) and dimeric (Rf 0.53)  $\alpha_2$ M. There was no detectable  $\alpha_2$ M in the 15 mM imidazole fraction, consistent with effective separation of PZP from  $\alpha_2$ M by HIC (Figure 2.3.4B).

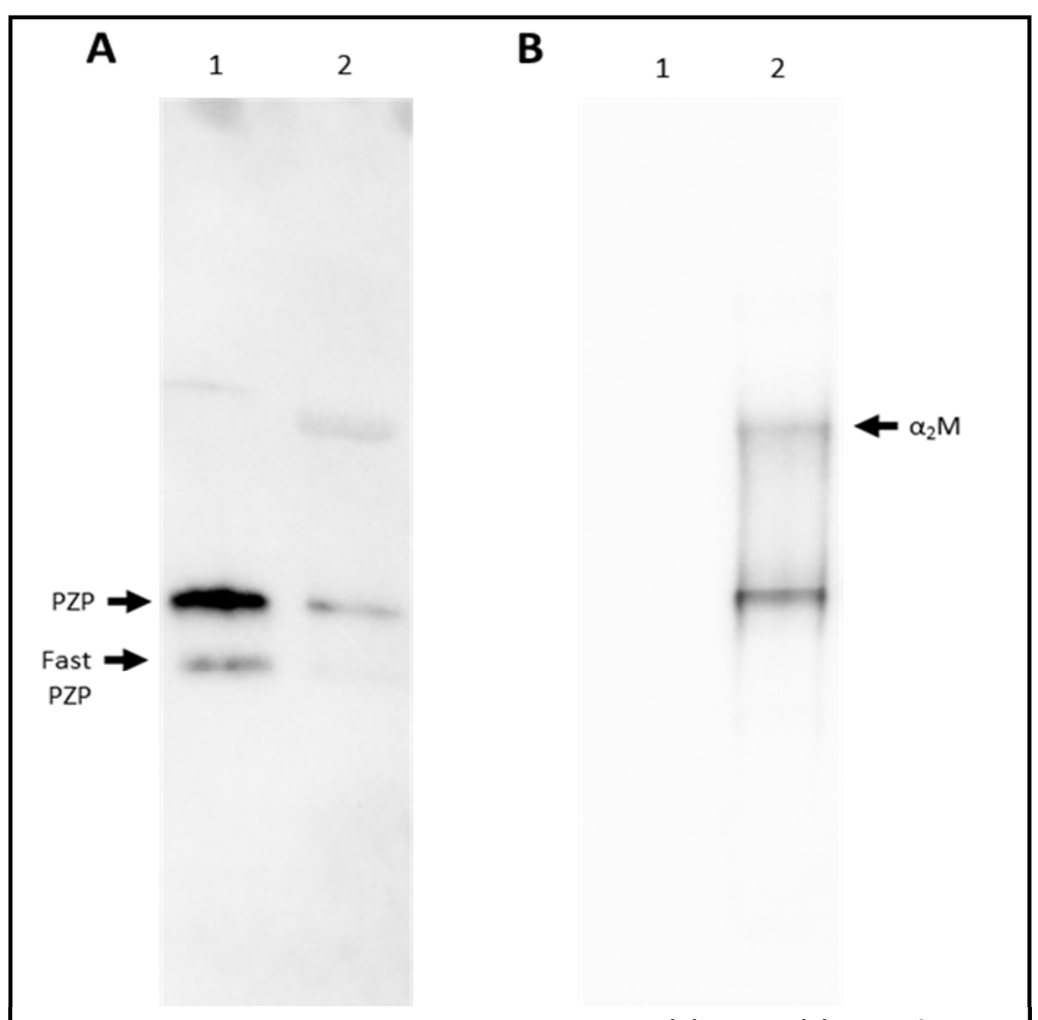
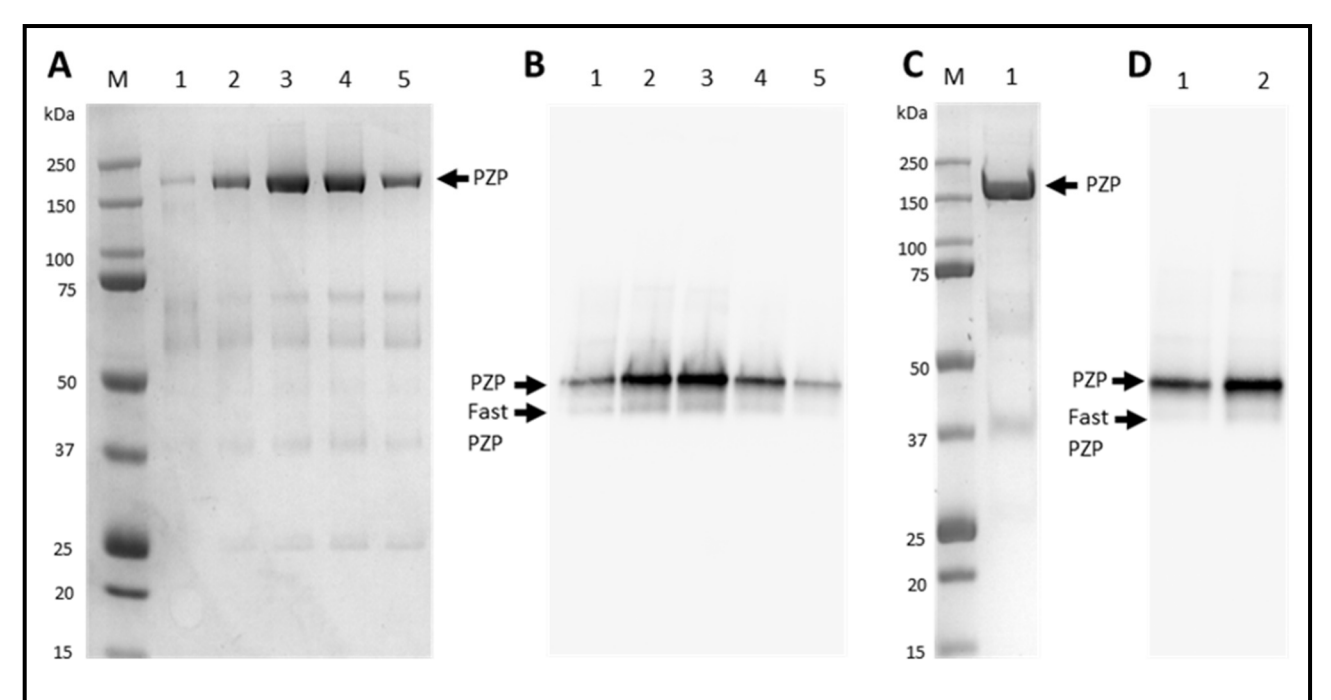


Figure 2.3.4: Representative native Western blots detecting (A) PZP and (B)  $\alpha_2 M$  in fractions eluted by ZAC of the PZP-enriched fraction obtained from HIC. Samples containing approximately 1.6  $\mu$ g of total protein were prepared in duplicate and supplemented with native loading buffer. Protein was separated on a NuPAGE Tris-Acetate 3-8% mini protein gel and transferred to a nitrocellulose membrane. Lane order: 1 = 15 mM imidazole elution, 2 = 500 mM imidazole elution. Expected migration of tetrameric  $\alpha_2 M$ , dimeric PZP, and fast PZP is indicated. PZP is expected to elute in lane 1 (15 mM imidazole) and  $\alpha_2 M$  in lane 2 (500 mM imidazole).

#### SEC

The PZP-enriched fraction obtained from ZAC was subjected to SEC as a final step to remove low molecular weight contaminants. Analysis of consecutively eluted SEC fractions by denaturing gel electrophoresis revealed a prominent band at 185 kDa, the expected mass of the reduced PZP monomer, in fractions 2, 3, 4, and 5, which were eluted from 110 to 130 mL. Additional bands corresponding to lower molecular weight contaminating proteins were also visible but their staining intensity was minimal compared to PZP. These proteins accounted for 5.35 ± 0.96% of the total Coomassie-stained protein signal in these 4 fractions, as assessed by densitometry (Figure 2.3.5A). Matched native Western blot analyses confirmed the presence of PZP in the aforementioned SEC fractions. The predominant band migrated with an Rf value of 0.52, consistent with the PZP dimer (Figure 2.3.5B). A band corresponding to fast PZP was also observed; however, this band contributed only 4.4% of the total Coomassie-stained protein signal, as assessed by densitometry (Figure 2.3.5B).

The fractions with the strongest PZP immunoreactivity (2, 3, and 4) were pooled and concentrated. Denaturing gel electrophoresis of the final purified product revealed the presence of minor amounts of contaminating proteins that migrated to 60 kDa and 38 kDa under reducing conditions, contributing approximately 4.2% and 7.9% to the total Coomassiestained protein signal, respectively (Figure 2.3.5C). Native Western blot analysis of the purified PZP was used as an additional quality control measure pre- and post-concentration of the protein sample. The results showed that following centrifugal concentration PZP was enriched approximately 1.41-fold, as determined by densitometry analysis. Furthermore, the method used to concentrate PZP did not alter its electrophoretic migration which is consistent with that of the PZP dimer (Rf 0.54; Figure 2.3.5D). The total amount of purified PZP obtained from 100 mL of human pregnancy plasma was approximately 9.6 mg, as quantified by spectrophotometry  $A_{280}$ .



**Figure 2.3.5**: Representative **(A, C)** Coomassie-stained denaturing gels and **(B, D)** native Western blots showing the proteins eluted during SEC using a HiPrep 26/60 Sephacryl S-300 HR column.

(A) Equal volume (20  $\mu$ L) of samples from consecutively eluted fractions were supplemented with LDS loading buffer containing 5% (v/v) 2-mercaptoethanol. Protein was separated on a Bolt Bis-Tris 4-12% mini protein gel and stained with InstantBlue®. (B) Equal volume (20  $\mu$ L) of matched samples (to A) were supplemented with native loading buffer and separated on a NuPAGE Tris-Acetate 3-8% mini protein gel. Protein was transferred to a nitrocellulose membrane and detecting PZP. Lane order (A, B): M = marker, 1 – 5 = consecutively eluted fractions. (C) Fractions 2, 3, and 4 were pooled and concentrated. A sample containing approximately 10  $\mu$ g total protein was supplemented with LDS loading buffer containing 5% (v/v) 2-mercaptoethanol. Protein was separated on a Bolt Bis-Tris 4-12% mini protein gel and stained with InstantBlue®. Lane order: M = marker, 1 = concentrated PZP. (D) A western blot detecting PZP. Equal volume (10  $\mu$ L) of samples from pre- and post-centrifugal concentration were supplemented with native loading buffer, separated on a NuPAGE Tris-Acetate 3-8% mini protein gel and transferred to a nitrocellulose membrane. Lane order: 1 = pre-concentration, 2 = post-concentration (corresponding to lane 1 in C). Expected migration of monomeric (A, C), dimeric (B, D), and fast (B, D) PZP is indicated.

#### 2.3.2 Purification of α<sub>2</sub>M from human plasma

Compared to the multi-step procedure needed to purify PZP from human plasma,  $\alpha_2 M$  can be purified via a much more straightforward process due to the much higher affinity of  $\alpha_2 M$  for zinc. Following ZAC,  $\alpha_2 M$  was enriched by 3.62-fold in the protein fraction eluted by 500 mM imidazole, compared to the protein fraction eluted by 20 mM imidazole. Lower molecular weight proteins that migrated at 122 kDa and 71 kDa by denaturing gel electrophoresis were also present in the fraction eluted by 500 mM imidazole. These proteins comprised approximately 29.1% of total protein, as assessed by densitometry (Figure 2.3.6A). To remove contaminating proteins, the fraction eluted by 500 mM imidazole was subjected to SEC with the fractions eluted between 20 and 25 mL containing a single protein band, as assessed by denaturing gel electrophoresis. The migration of this band was consistent with the reduced  $\alpha_2 M$  monomer (Figure 2.3.6B). The relative electrophoretic migration of  $\alpha_2 M$  under native conditions

was consistent with that of the  $\alpha_2M$  tetramer (Rf 0.36; Figure 2.3.6C). The fractions from SEC were pooled and confirmed to be  $\alpha_2M$ , as assessed by native Western blot analysis (Rf 0.40; Figure 2.3.6D), prior to use in experiments.

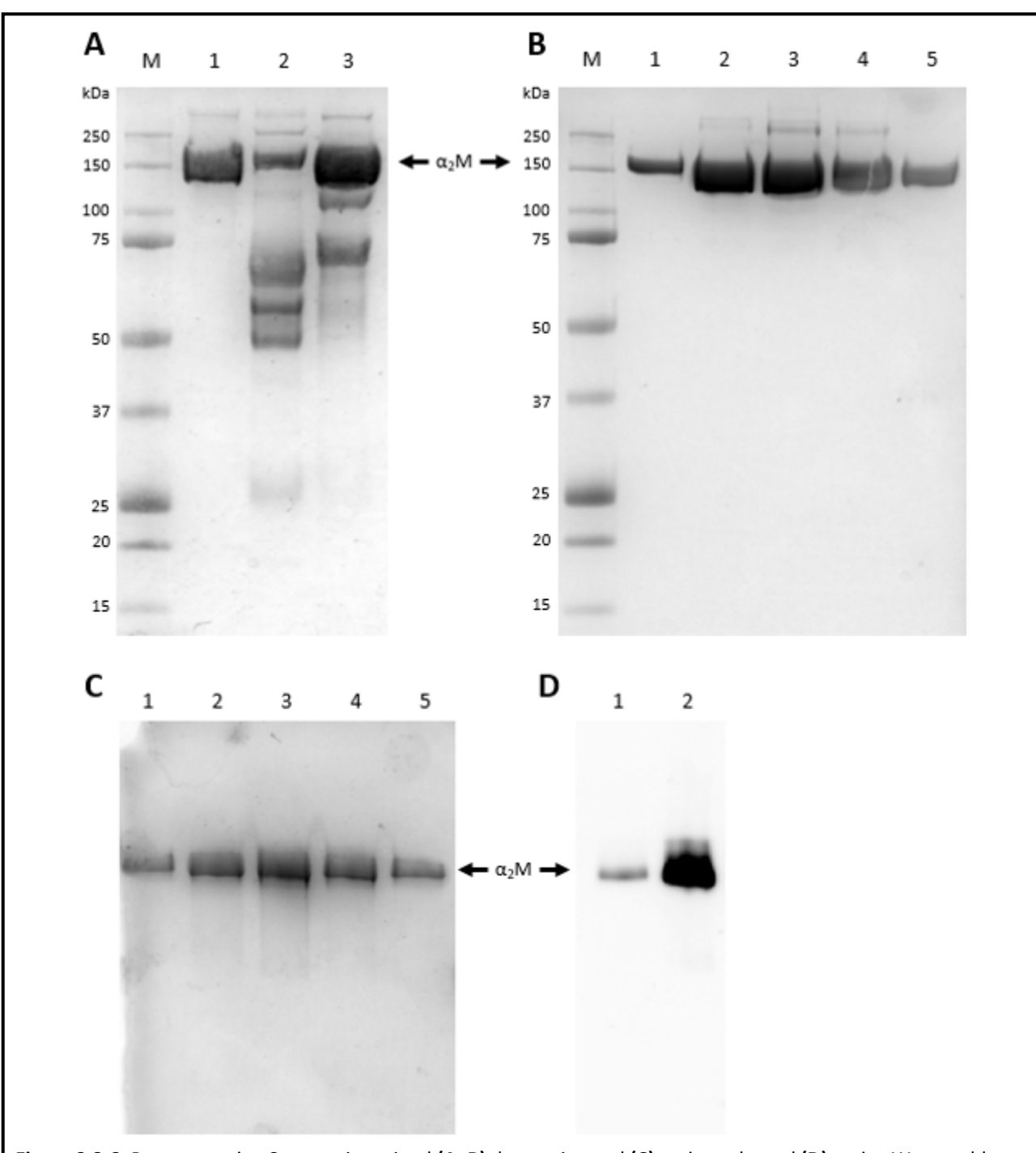


Figure 2.3.6: Representative Coomassie-stained (A, B) denaturing and (C) native gels, and (D) native Western blot showing proteins eluted following ZAC and SEC of whole human plasma for the purification of  $\alpha_2M$ . (A) Purified  $\alpha_2M$  and samples from ZAC fractionation containing approximately 1.4  $\mu g$  total protein were supplemented with LDS loading buffer containing 5% (v/v) 2-mercaptoethanol. Protein was separated on a Bolt Bis-Tris 4-12% mini protein gel and stained with InstantBlue<sup>®</sup>. Lane order: M = marker, 1 = purified  $\alpha_2$ M control, 2 = 20 mM imidazole elution, 3 = 500 mM imidazole elution. (B) Equal volume (7.5  $\mu$ L) of samples from consecutively eluted fractions following SEC using a HiPrep 26/60 Sephacryl S-300 HR column were supplemented with native loading buffer. Protein was separated on a NuPAGE Tris-Acetate 3-8% mini protein gel and stained with InstantBlue<sup>®</sup>. Lane order: M = marker, 1 - 5 = consecutively eluted fractions. (C) Equal volume (7.5  $\mu$ L) of matched samples (to B) were supplemented with native loading buffer and separated on a NuPAGE Tris-Acetate 3-8% mini protein gel and stained with InstantBlue<sup>®</sup>. Lane order: M = marker, 1 - 5 = consecutively eluted fractions. (D) A western blot detecting  $\alpha_2M$ . Purified  $\alpha_2M$  and a sample from the pooled consecutive SEC fractions, containing approximately 1.3µg of total protein, was supplemented with native loading buffer. Protein was separated on a NuPAGE Tris-Acetate 3-8% mini protein gel and transferred to a nitrocellulose membrane. Lane order: 1 = purified  $\alpha_2 M$ , 2 = pooled SEC fractions containing  $\alpha_2 M$ . Expected size of monomeric (A, B) or tetrameric (C, D)  $\alpha_2 M$  is indicated.

#### 2.3.3 Characterisation of the interaction between PZP and chymase

## 2.3.3.1 Co-incubation of PZP with chymase induces conformational changes consistent with protease inhibition

It has previously been demonstrated that chymase is an endogenous substrate for the protease inhibitory activity of α<sub>2</sub>M in human serum (Raymond et al., 2009, Walter et al., 1999). However, it is currently unknown if this activity is shared by PZP. To investigate if chymase cleaves PZP and induces a conformational change consistent with protease inhibition, the two proteins were co-incubated at a 1:1 molar ratio and the resultant molecular species were analysed using native and denaturing gel electrophoresis (Figure 2.3.7). As controls, PZP was incubated under the same conditions in buffer alone, or co-incubated with chymotrypsin which has previously been used to demonstrate the protease trapping activity of PZP in vitro (Christensen et al., 1991, Christensen et al., 1989). Following co-incubation with chymase or chymotrypsin a PZP species that migrated faster than the native dimer was formed, consistent with the adoption of a relatively more compact, electrophoretically fast conformation following cleavage of the bait region and binding to a protease (Christensen et al., 1989, Christensen et al., 1991). Generation of the PZP dimer-protease complex was relatively more efficient for chymase compared to chymotrypsin, whereby more than half of the PZP present in the sample co-incubated with chymase was converted to the electrophoretically fast form. A small amount of fast PZP was present in the control sample containing PZP alone; however, the intensity of this band was marginal compared to the band corresponding to native PZP (Figure 2.3.7A). Analysis of matched samples by denaturing gel electrophoresis confirmed that co-incubation of PZP with chymase results in the generation of relatively uniform protein fragments ~80 kDa that are consistent with cleavage of the PZP monomer within the central bait region (Figure 2.3.7B). By comparison, the fragments generated following co-incubation of PZP with chymotrypsin were generally more varied in size. While some lower molecular weight bands were present in the sample containing PZP and chymotrypsin (~60 kDa), co-incubation of PZP with chymase did not generate additional protein fragments (Figure 2.3.7B).

It has been proposed that PZP covalently binds to proteases with a stoichiometry of 1:1; however, a second PZP molecule may be recruited to form a molecular cage around the protease. This results in a complex >720 kDa, composed of a tetrameric PZP cage that surrounds a central covalently bound protease (Sand et al., 1985). Although generation of PZP-protease complexes containing a single PZP dimer (i.e., PZP dimer-protease complex) was the predominant effect of protease treatment, the results of native gel electrophoresis indicated

that a small fraction of the total protein (~10%) migrated to a position corresponding to the PZP protease complexes containing two PZP dimers (i.e., PZP tetramer-protease complex) (Figure 2.3.7A). Additionally, around 10 – 20% of the protein migrated as high molecular weight (HMW) species (>250 kDa) by denaturing gel electrophoresis under reducing conditions, supporting that co-incubation of PZP with chymase generated some crosslinked species that were resistant to reducing conditions (Figure 2.3.7B).

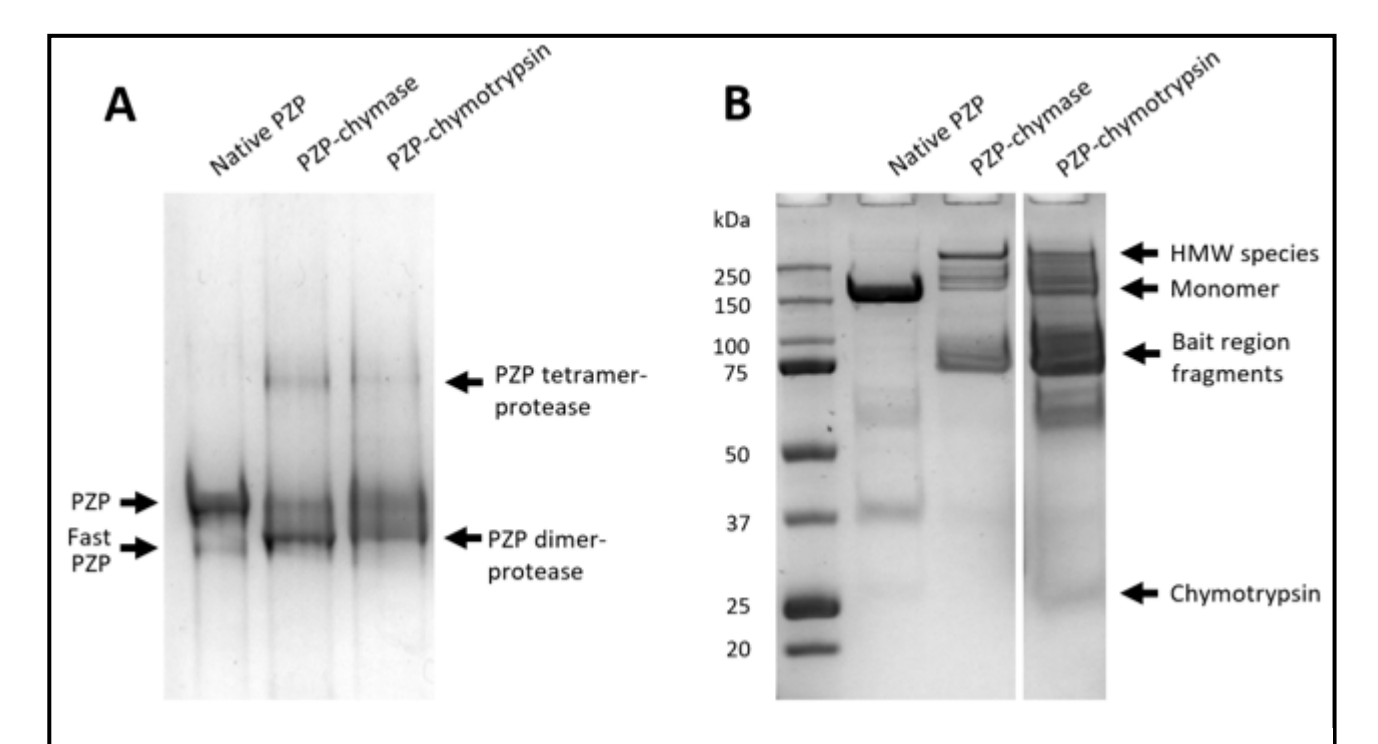


Figure 2.3.7: Representative Coomassie-stained stained (A) native and (B) denaturing gels showing the migration of proteins following co-incubation of PZP with chymase or chymotrypsin.

(A) PZP was co-incubated with protease at a 1:1 molar ratio for 45 min at 37 °C. Approximately 9.7 μg of total protein was separated on a NuPAGE Tris-Acetate 3-8% mini protein gel and stained with InstantBlue®. Native PZP, fast PZP, putative PZP dimer-protease complexes and PZP tetramer-protease complexes are indicated. (B) Matched samples were supplemented with LDS loading buffer containing 5% (v/v) 2-mercaptoethanol and separated on a Bolt Bis-Tris 4-12% mini protein gel and stained with InstantBlue®. The positions of high molecular weight (HMW) species (>250)

kDa), monomeric PZP (180 kDa) and bait region fragments (80 kDa) are indicated.

To further investigate the interaction between chymase and PZP, the two proteins were coincubated at a range of different molar ratios, including those involving an excess of either protein (Figure 2.3.8). Analysis by denaturing gel electrophoresis supported that chymase induces dose-dependent fragmentation consistent with cleavage at the bait region of PZP. HMW species, consistent with cross-linked PZP-chymase complexes, only represented a small fraction of the total protein in all samples (<10%) and were not visible when chymase was present at a molar excess compared to PZP. A band corresponding to free chymase (37 kDa) was only visible when chymase was present in excess compared to PZP (Figure 2.3.8A).

The dose-dependent effect of chymase on the generation of PZP dimer-chymase and PZP-tetramer-chymase complexes was not as clear when matched samples were analysed by native gel electrophoresis (Figure 2.3.8B). A small fraction of fast PZP was evident in the control sample containing native PZP. Interestingly, the results showed that the tetrameric PZP species were more commonly formed when PZP was present at sub-stoichiometric concentrations compared to chymase (Figure 2.3.8B). Given that HMW crosslinked species were not formed when chymase was incubated with PZP at a molar excess (Figure 2.3.8A), it's plausible that the putative PZP tetramer-chymase complex observed in native gel electrophoresis is non-covalently associated, rather than covalently crosslinked via reaction of labile thioesters (Christensen et al., 1989, Christensen et al., 1991).

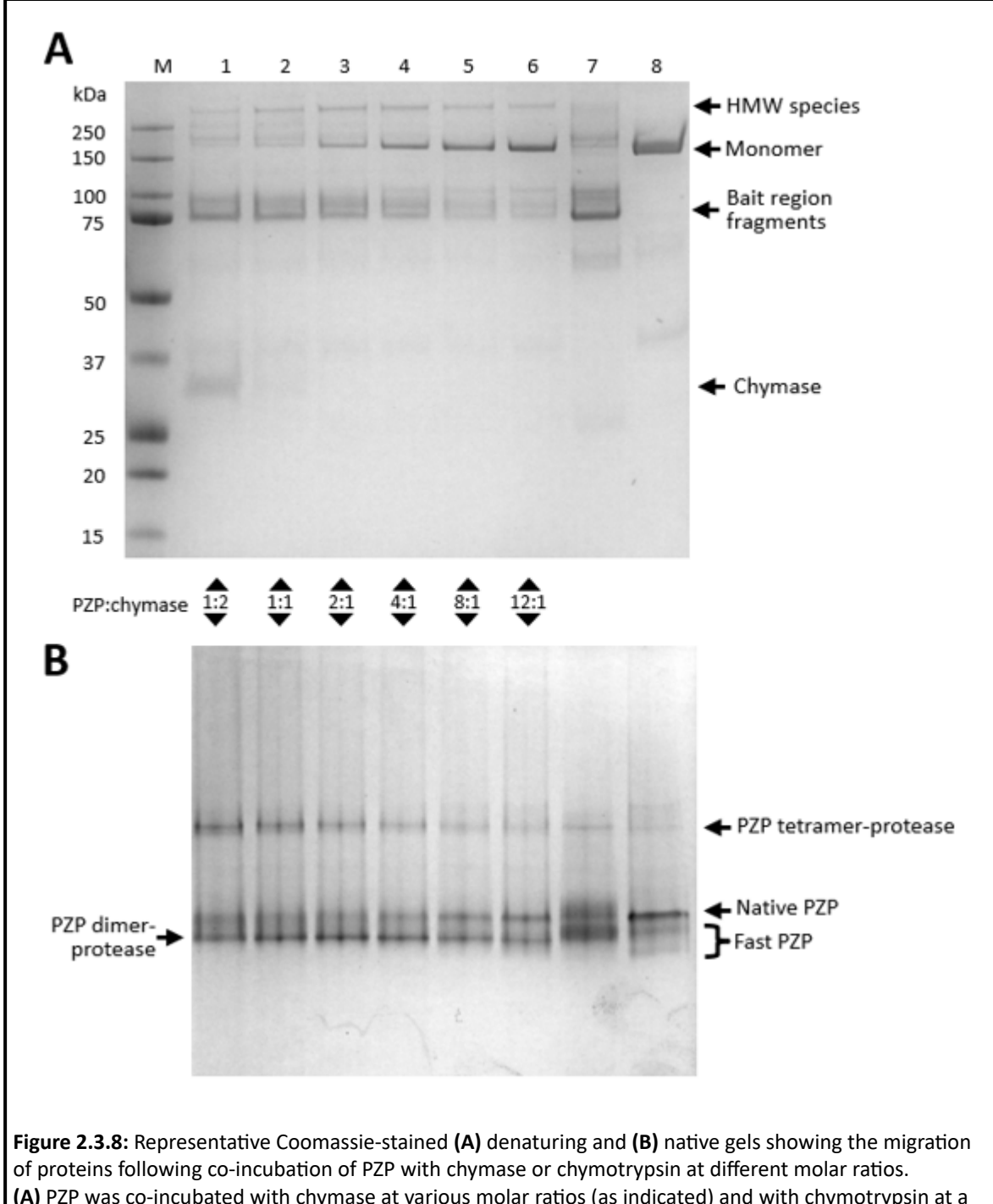


**Figure 2.3.8:** Representative Coomassie-stained **(A)** denaturing and **(B)** native gels showing the migration of proteins following co-incubation of PZP with chymase or chymotrypsin at different molar ratios. **(A)** PZP was co-incubated with chymase at various molar ratios (as indicated) and with chymotrypsin at a 1:1 molar ratio 45 min at 37 °C. Samples containing approximately 2.8 μg of PZP were supplemented with LDS loading buffer containing 5% (v/v) 2-mercaptoethanol, separated on a Bolt Bis-Tris 4-12% mini protein gel and stained with InstantBlue®. High molecular weight (HMW) species (>250 kDa), monomeric PZP (180 kDa) and bait region fragments (80 kDa) are indicated. **(B)** Matched samples were separated on a NuPAGE Tris-Acetate 3-8% mini protein gel and stained with InstantBlue®. Native PZP, fast PZP, putative PZP dimerprotease complexes and PZP tetramer-protease complexes are indicated.

Lanes 1 – 6 contain PZP:chymase at molar ratios of 1:2, 1:1, 2:1, 4:1, 8:1, 12:1, respectively, lane 7 contains PZP:chymotrypsin at a molar ratio of 1:1, and lane 8 contains native PZP.

To further characterise the binding of chymase to PZP, a streptavidin-biotin pull-down assay was performed. Chymase was preferentially recovered when co-incubated with biotinylated PZP, compared to the low-level non-specific binding of chymase to the streptavidin-coated beads (Figure 2.3.9A). When subjected to Western blot analysis following denaturing electrophoresis under reducing conditions, a prominent band was visible at the expected mass of free chymase (~37 kDa) but not at the expected size of a cross-linked PZP-chymase complex (Figure 2.3.9A). Thus, the data support that chymase binds to PZP in solution to form a stable complex but the interaction is not mediated by reaction between the PZP thioester bond and chymase. To confirm whether co-incubation of chymase and PZP increases the free thiol content DTNB assay was performed. In this assay,  $\alpha_2 M$ , which covalently binds to chymase, was included as a positive control. Consistent with the observation that the complex between chymase and PZP is not covalently linked, co-incubation of chymase with  $\alpha_2 M$  but not PZP, resulted in an increase in DTNB absorbance at 412 nm, indicative of thioester cleavage (Figure 2.3.9B).

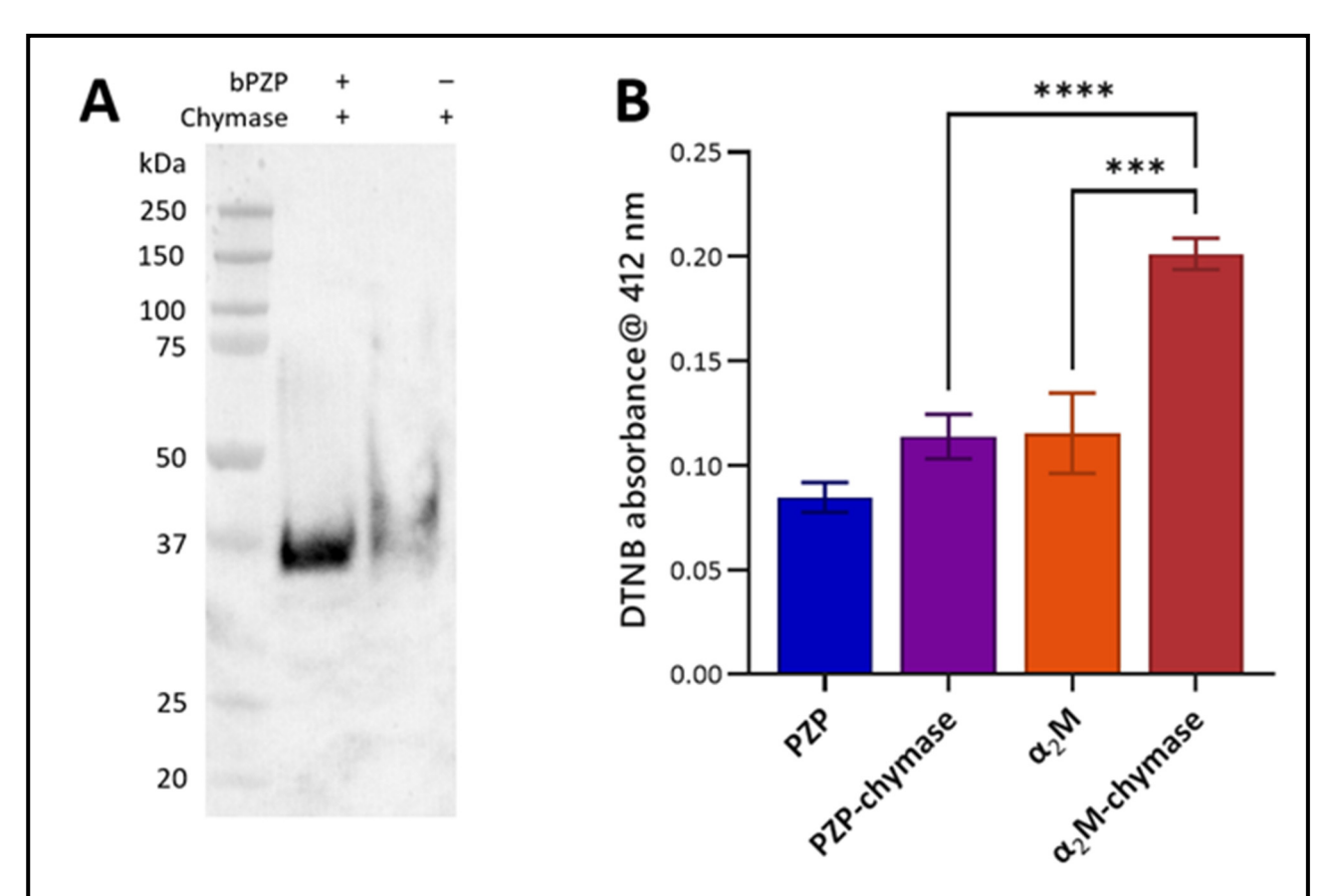


**Figure 2.3.9:** Results of **(A)** biotin-streptavidin pull-down assay and **(B)** DTNB assay to assess the interaction between PZP and chymase.

(A) Image of a western blot detecting chymase captured by biotinylated PZP (bPZP) and recovered using Dynabeads<sup>TM</sup> MyOne<sup>TM</sup> Streptavidin C1 beads. Chymase was incubated in the presence or absence of bPZP at a 2:1 molar ratio (bPZP:chymase) for 45 min at 37 °C with agitation. Samples containing approximately 1.4  $\mu$ g of chymase were supplemented with LDS loading buffer containing 5% (v/v) 2-mercaptoethanol, separated on a Bolt Bis-Tris 4-12% mini protein gel and transferred to a nitrocellulose membrane. (B) DTNB absorbance indicating thiol group reactivity in samples containing native PZP, PZP with chymase, native  $\alpha_2$ M, or  $\alpha_2$ M with chymase. Proteins were incubated at a 4:1 molar ration (1.7  $\mu$ M  $\alpha$ M:chymase) for 45 min at 37°C. Data are mean DTNB absorbance at 412 mm  $\pm$  SD (n = 3) expressed in arbitrary units (AU) and are representative of two independent experiments. One-way ANOVA with post-hoc Tukey's HSD, significance indicated by asterisks (\*\*\* p <0.0001, \*\*\*\* p <0.0001).

#### 2.3.3.2 Interaction with chymase increases the surface-exposed hydrophobicity of PZP

To further characterise the effect of chymase on PZP, the two proteins were co-incubated with PZP at a 4-fold molar excess and bisANS assay performed to assess changes in surface-exposed hydrophobicity. In these experiments, chymotrypsin, which reportedly reduces the surface-exposed hydrophobicity of PZP (Jensen et al., 1993), was included as a control. Unexpectedly, pre-incubation of PZP with chymotrypsin resulted in enhanced bisANS fluorescence compared to PZP alone (Figure 2.3.10; Figure S2). Under the conditions used, pre-incubation of PZP with chymase also resulted in an increase in bis-ANS fluorescence, indicative of inducing a conformational change that enhances the exposed surface hydrophobicity of PZP by around 2-fold (Figure 2.3.10).

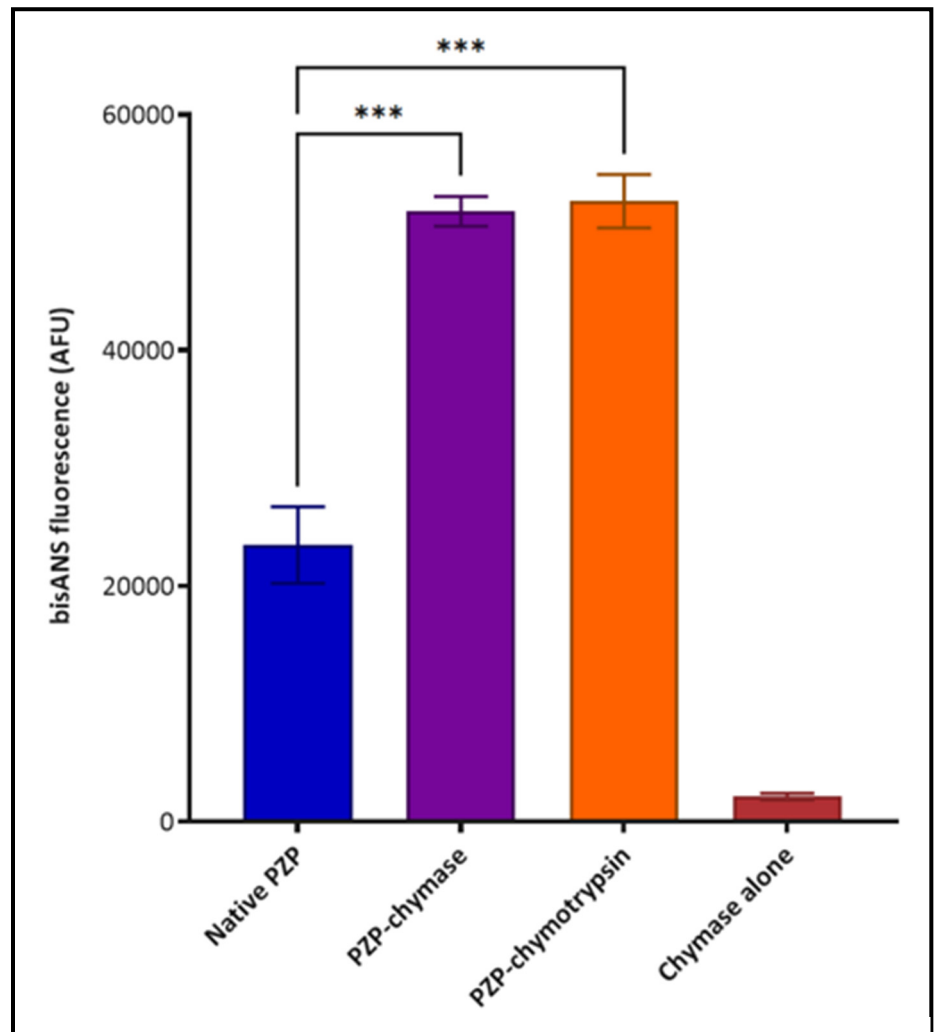


**Figure 2.3.10:** The effect of pre-incubation with a protease on the exposed surface hydrophobicity of PZP, as assessed by bisANS fluorescence. PZP or pre-formed PZP-protease complexes (4:1 molar ratio, incubated 45 min at 37 °C) were incubated with 10  $\mu$ M bisANS at RT in the dark for 5 min. Data are mean bisANS fluorescence  $\pm$  SD (n = 3) in arbitrary fluorescence units (AFU) and is representative of three independent experiments. One-way ANOVA with post-hoc Tukey's HSD, significance indicated by asterisks (\*\*\* p <0.001).

## 2.3.3.3 Interaction with chymase does not enhance the chaperone activity of PZP against $A\beta_{1-42}$

Prior studies have shown that native PZP stabilises  $A\beta_{1-42}$  (Cater et al., 2019), an aggregation prone peptide implicated in PE (Cheng et al., 2021, Buhimschi et al., 2014). To investigate if preincubation with chymase influences the chaperone activity of PZP, ThT assay was performed. Incubation of  $A\beta_{1-42}$  in buffer containing ThT, a dye that fluoresces when it binds to  $\beta$ -sheet-rich amyloid structures, resulted in a rapid increase in fluorescence, indicating the aggregation of the peptide occurred within <1 h (Figure 2.3.11). Co-incubation of  $A\beta_{1-42}$  with either native PZP or PZP pre-incubated with a protease prevented any increase in ThT fluorescence over the course of the assay (Figure 2.3.11). At the endpoint of the assay, all samples containing PZP

showed reduced ThT fluorescence compared to the control containing  $A\beta_{1-42}$  alone but under the conditions used there was no difference in fluorescence between samples containing native PZP, PZP-chymase, or PZP-chymotrypsin.

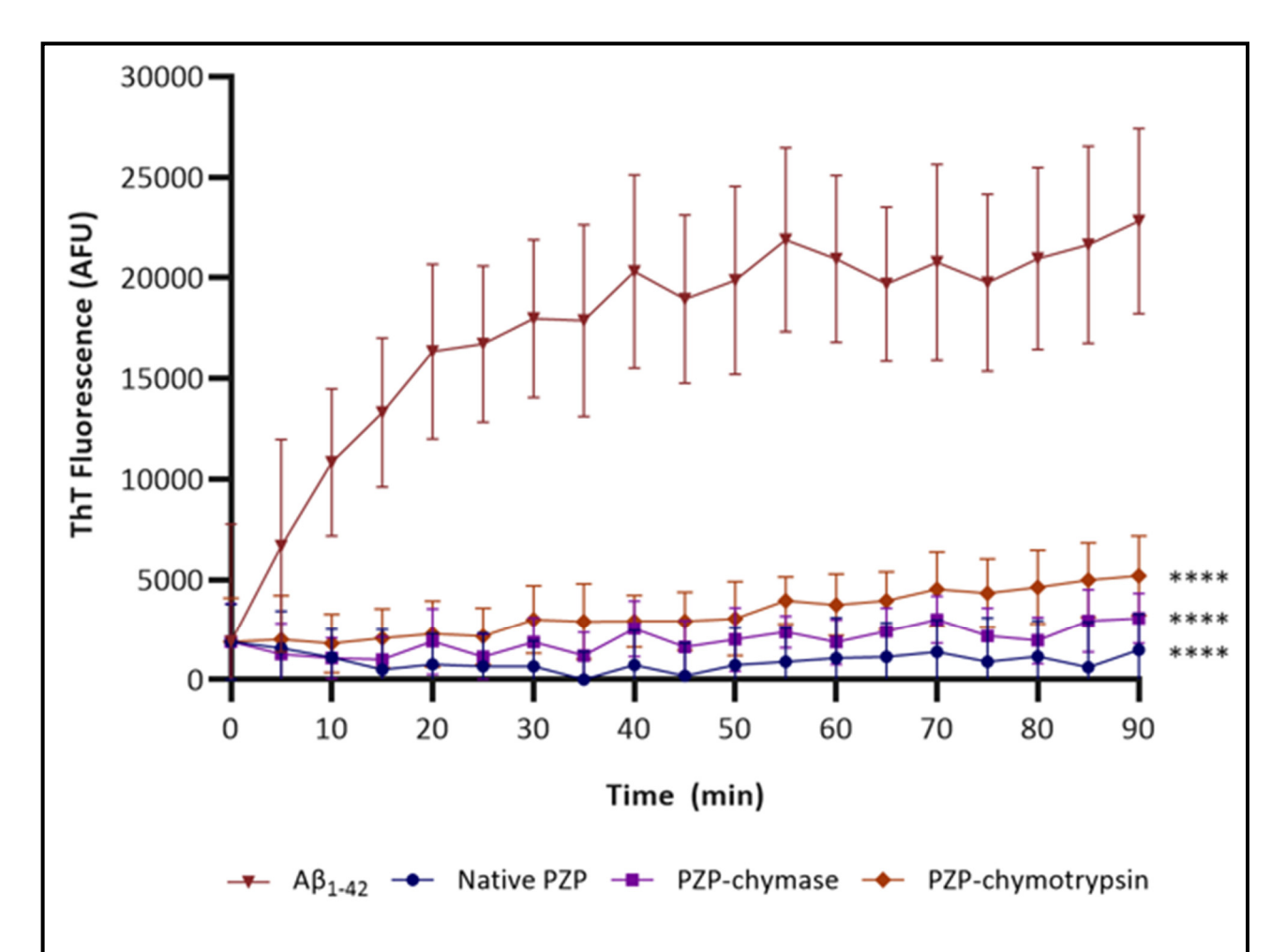


**Figure 2.3.11:** The effect of PZP and PZP-protease complexes on the aggregation of  $Aβ_{1-42}$ , as assessed by ThT assay.  $Aβ_{1-42}$  (5 μM) was incubated in buffer containing 25 μM ThT at 23 °C for 90 min in the presence or absence of PZP or PZP-protease complexes at a 1:20 molar ratio (PZP or PZP-protease: $Aβ_{1-42}$ ). PZP-protease complexes were preformed by co-incubation at a 4:1 molar ratio for 45 min at 37 °C. Data are mean ThT fluorescence (AFU)  $\pm$  SD (n = 3) and are representative of three independent experiments. One-way ANOVA with post-hoc Tukey's HSD was used to compare endpoint values to  $Aβ_{1-42}$  alone (\*\*\*\*p <0.0001).

Binding to  $\alpha M$  family proteins does not inactivate proteases (Christensen et al., 1989) and prior studies have shown that  $\alpha_2 M$ -protease complexes can inhibit amyloid formation by either binding to and stabilising misfolded proteins or by degrading them (Wyatt et al., 2013a). To investigate the mechanism responsible for PZP's inhibition of  $A\beta_{1-42}$  amyloid aggregation, a biotin-streptavidin pull-down assay was performed. The results showed that pre-incubation with proteases did not overtly affect the amount of PZP that co-precipitated with biotinylated  $A\beta_{1-42}$ . There was minimal to no non-specific binding of PZP to the streptavidin coated beads;

however, bands corresponding to full-length monomeric PZP and bait-region cleaved PZP were recovered in samples incubated with biotinylated  $A\beta_{1-42}$  (Figure 2.3.12). This supports the conclusion that the effect of native PZP, PZP-chymase and PZP-chymotrypsin on  $A\beta_{1-42}$  aggregation is due, at least partially, to canonical holdase-type chaperone activity that involves the formation of a stable non-covalent complex.

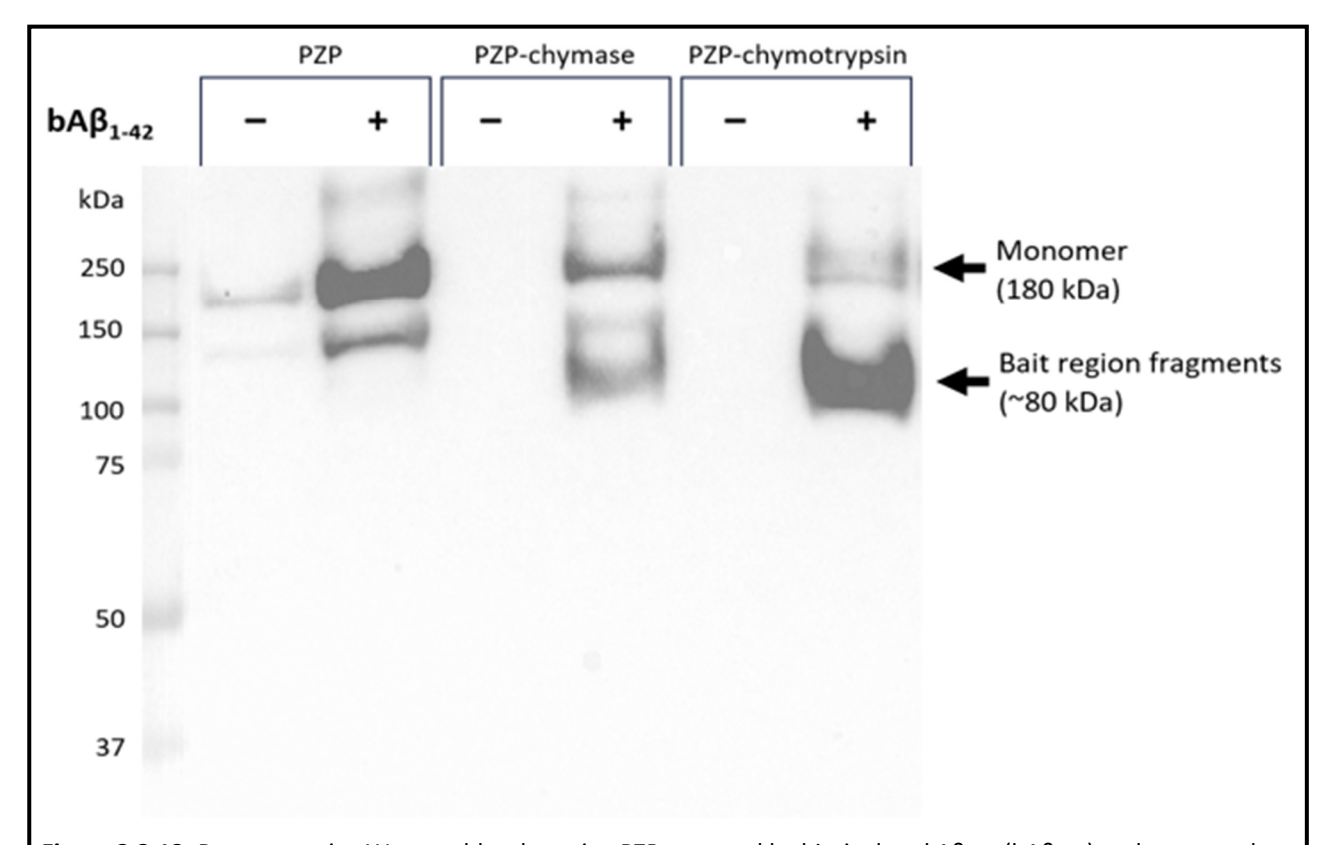


**Figure 2.3.12:** Representative Western blot detecting PZP captured by biotinylated  $Aβ_{1-42}$  ( $bAβ_{1-42}$ ) and recovered using Dynabeads<sup>TM</sup> MyOne<sup>TM</sup> Streptavidin C1 beads. PZP, PZP-chymase, and PZP-chymotrypsin were co-incubated with  $bAβ_{1-42}$  at a ratio of 1:10 PZP/PZP-protease to  $bAβ_{1-42}$  for 45 min at 37°C with agitation. Samples containing approximately 9 μg of PZP were supplemented with LDS loading buffer containing 5% (v/v) 2-mercaptoethanol. Protein was separated on a Bolt Bis-Tris 4-12% mini protein gel, transferred to a nitrocellulose membrane and probed for PZP. Expected mass of monomeric PZP and bait region fragments are indicated.

## 2.3.3.4 Interaction with chymase promotes the binding of PZP to cell-surface lipoprotein receptors

The conformational change that PZP undergoes following proteolytic cleavage of the bait region exposes a cryptic binding site for LRP1 (Christensen et al., 1989, Sand et al., 1985). To investigate the effect of chymase on the cell surface binding of PZP, flow cytometry analysis was performed using SH-SY5Y (neuroblastoma) and BeWo (trophoblast-like choriocarcinoma) cell lines, both of which express LRP1 (Thul et al., 2017, Quinn et al., 1999). In both BeWo and SH-SY5Y cells, low levels of fluorescence were measured when the cells were incubated with

native PZP. In contrast, cells treated with PZP pre-incubated with chymase exhibited more than 25-fold higher fluorescence, indicative of cell-surface binding of the biotinylated ligand (Figure 2.3.13A&B). To determine if this binding was mediated by lipoprotein receptors, cells were pre-incubated with RAP, a pan-specific lipoprotein receptor antagonist. Pre-incubation with an excess of RAP reduced the fluorescence associated with the binding of chymase-treated PZP by 70.7% (Figure 2.3.13C), which supports the conclusion that the binding to SH-SY5Y cells was predominantly mediated by lipoprotein receptors, such as LRP1.

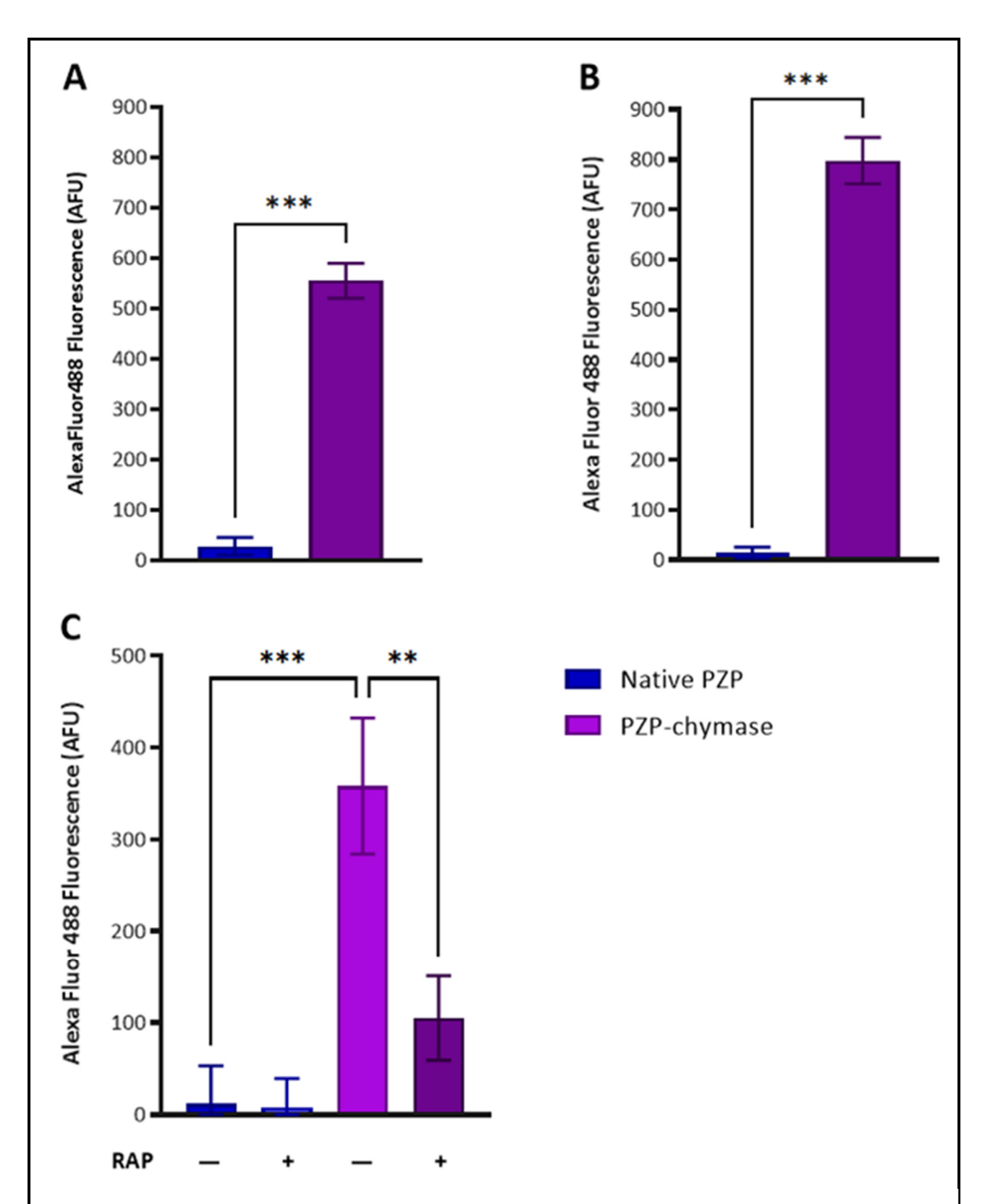


**Figure 2.3.13:** The effect of pre-incubation with chymase on cell-surface receptor binding of PZP, as assessed by flow cytometry.

(A) BeWo or (B) SH-SY5Y cells were treated with Alexa Fluor 488 labelled PZP or PZP pre-incubated with chymase (45 min at 37°C at a 4:1 molar ratio of PZP:chymase) for 30 min. (C) Cells were pre-incubated in the presence and absence of unlabelled RAP prior to treatment with PZP or PZP-chymase. Data are mean Alexa Fluor 488 fluorescence  $\pm$  SD (n = 3) in arbitrary fluorescence units (AFU) and is representative of three independent experiments. One-way ANOVA with post-hoc Tukey's HSD used to compare treatments, significance indicated by asterisks (\*\* p <0.01, \*\*\* p <0.001).

#### 2.3.4 The effect of PZP on the proteolytic activity of chymase

#### 2.3.4.1 PZP does not affect the cleavage of RETF-4NA by chymase

To investigate the effect of PZP on chymase activity, initial *in vitro* assays were performed using RETF-4NA, a chymase-specific substrate that produces a coloured product when cleaved. In these assays,  $\alpha_2 M$  was included as a positive control as it has previously been shown that chymase remains proteolytically active against small substrates when bound to  $\alpha_2 M$  (Raymond et al., 2009).

Incubation of chymase with RETF-4NA in the absence of any inhibitor resulted in a steady increase in absorbance at 410 nm, which reached a maximum after ~40 min (Figure 2.3.14). Pre-incubation of chymase with  $\alpha$ 1ACT, an endogenous inhibitor that inactivates chymase by distorting its active site (Schechter et al., 1997, Huntington, 2011), effectively prevented any increase in absorbance over the same time period (Figure 2.3.14). When chymase was pre-incubated with PZP at equimolar concentrations there was no effect on the reaction rate or endpoint absorbance compared to RETF-4NA incubated with chymase alone (Figure 2.3.14; Table 2.3.1). The addition of  $\alpha$ 1ACT to the PZP-chymase sample reduced RETF-4NA cleavage by 3-fold over the course of the assay and reduced the initial rate of reaction by around 6-fold. However, the proteolytic activity of chymase in the presence of PZP was not completely abolished by  $\alpha$ 1ACT (Figure 2.3.14; Table 2.3.1).

Co-incubation with  $\alpha_2 M$  reduced the rate and amount of chymase-mediated RETF-4NA cleavage but the addition of  $\alpha 1$ ACT resulted in no further reductions. RETF-4NA cleavage was more than 2-fold greater in the sample containing chymase,  $\alpha_2 M$ , and  $\alpha 1$ ACT compared to the corresponding sample containing chymase, PZP, and  $\alpha 1$ ACT (Figure 2.3.14, Table 2.3.1). Therefore, the effects of PZP and  $\alpha_2 M$  on the cleavage of RETF-4NA by chymase are distinctly different, whereby  $\alpha_2 M$  partially inhibits the cleavage of RETF-4NA by chymase and effectively protects chymase from inactivation by  $\alpha 1$ ACT. Whereas PZP does not inhibit cleavage of RETF-4NA by chymase and only partially protects chymase from inactivation by  $\alpha 1$ ACT.

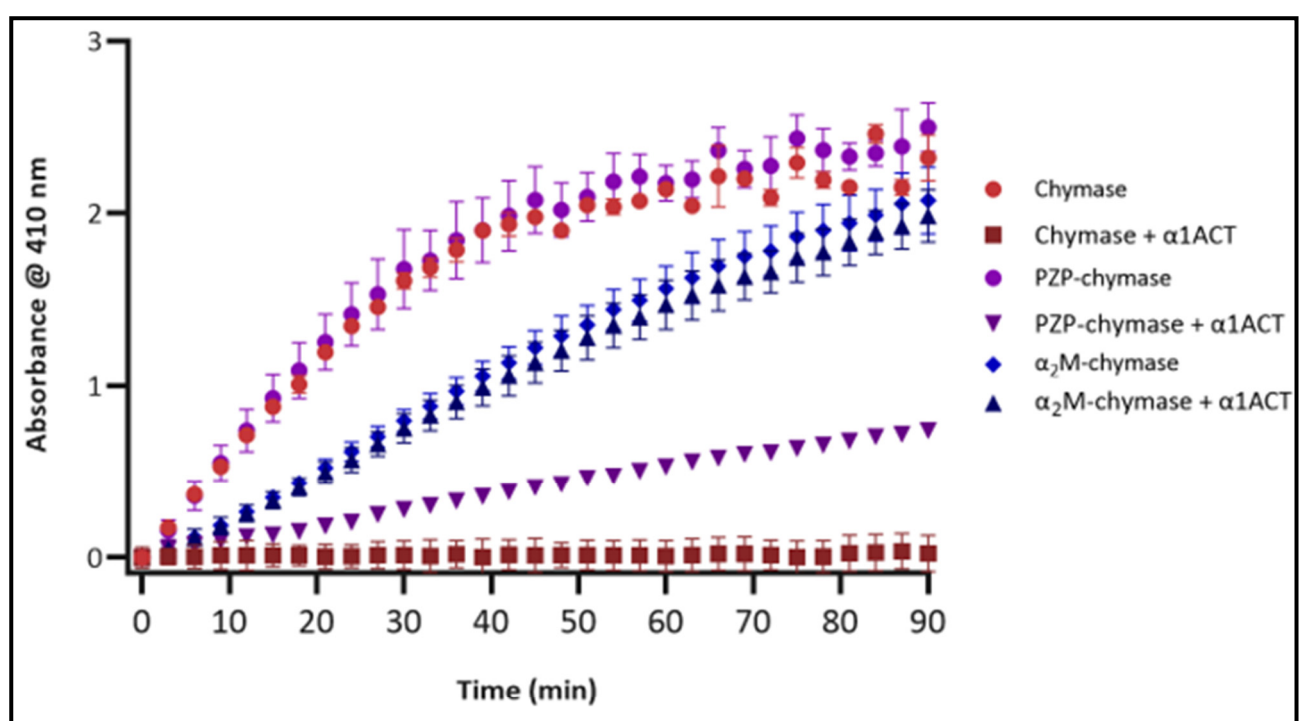


Figure 2.3.14: RETF-4NA cleavage by chymase, PZP-chymase, or  $\alpha_2$ M-chymase in the presence or absence of  $\alpha_1$ ACT. Chymase (10 nM) was incubated with 1 mM RETF-4NA for 90 min at 37 °C either alone or following pre-incubation with PZP or  $\alpha_2$ M at a 1:1 molar ratio for 45 min at 37 °C. Samples were subsequently incubated in the presence or absence of a 3-fold molar excess of  $\alpha_1$ ACT for 45 min at 37 °C. RETF-4NA cleavage was monitored by absorbance at 410 nm. Data are mean absorbance  $\pm$  SD (n = 3) and are representative of three independent experiments. Statistical comparisons of reaction rate and endpoint values are provided in Table 2.3.1.

**Table 2.3.1:** Endpoint absorbance and reaction rate for RETF-4NA cleavage by chymase, PZP-chymase, or  $\alpha$ 2M-chymase in the presence or absence of  $\alpha$ 1-antichymotrypsin ( $\alpha$ 1ACT). RETF-4NA cleavage was assessed by measuring endpoint absorbance at 410 nm and reaction rate following incubation of chymase alone or pre-formed PZP-chymase and  $\alpha$ 2M-chymase complexes (1:1 molar ratio, 45 min, 37 °C) in the presence or absence of a 3-fold molar excess of  $\alpha$ 1ACT for 45 min at 37 °C.

Treatment	Endpoint absorbance ± SD (AU)	Rate of reaction ± SD (mAU/min)
Chymase	2.321 ± 0.133	5.36 ± 0.17
Chymase + α1ACT	0.023 ± 0.105 <sup>a</sup>	0.05 ± 0.34 <sup>a</sup>
α <sub>2</sub> M-chymase	2.076 ± 0.194 <sup>b</sup>	2.66 ± 0.25 <sup>a,b</sup>
α <sub>2</sub> M-chymase + α1ACT	1.984 ± 0.152 <sup>b</sup>	2.51 ±0.29 <sup>a,b</sup>
PZP-chymase	2.498 ± 0.141 <sup>b,e</sup>	5.59 ± 0.77 <sup>b,e</sup>
PZP-chymase + α1ACT	0.739 ± 0.031 <sup>a,c,e,g</sup>	0.92 ± 0.25 <sup>a,d,f,g</sup>

Endpoint absorbance is after 90 min incubation with RETF-4NA, rate of reaction calculated between 0 and 40 min. One-way ANOVA with post-hoc Tukey's HSD used to compare treatments;  $^ap < 0.0001$  vs. chymase,  $^bp < 0.0001$  vs. chymase +  $\alpha 1$ ACT,  $^cp < 0.001$  vs. chymase +  $\alpha 1$ ACT,  $^dp < 0.05$  vs. chymase +  $\alpha 1$ ACT,  $^cp < 0.0001$  vs.  $\alpha_2$ M-chymase/ $\alpha_2$ M-chymase +  $\alpha 1$ ACT,  $^dp < 0.0001$  vs.  $\alpha_2$ M-chymase/ $\alpha_2$ M-chymase +  $\alpha 1$ ACT,  $^dp < 0.0001$  vs. PZP-chymase.

#### 2.3.4.2 PZP does not affect chymase-mediated cleavage of Ang I

To further investigate the effect of PZP on the proteolytic activity of chymase, *in vitro* assays were conducted using Ang I, a physiologically relevant substrate. Matched samples from the RETF-4NA assays were assessed. In these assays, Ang I processing was monitored using rpHPLC which separates Ang I from Ang II – the cleavage product formed by chymase.

When a control solution containing Ang I alone was analysed, a peak was eluted from the column after approximately 33 min (Figure 2.3.15A). Co-incubation of Ang I with chymase resulted in the generation of a second peak that eluted after 31 min, corresponding to the generation of Ang II (Figure 2.3.15B). Under the conditions used, the Ang II peak area was 62.6% relative to Ang I (Figure 2.3.16). Pre-incubation with  $\alpha$ 1ACT completely abolished the cleavage of Ang I by chymase (Figure 2.3.15C; Figure 2.3.16).

Consistent with the results of the RETF-4NA assays,  $\alpha_2 M$  but not PZP, had an inhibitory effect on the proteolytic activity of chymase against Ang I (Figure 2.3.15D&E; Figure 2.3.16). Furthermore, the addition of  $\alpha 1$ ACT to the sample containing  $\alpha_2 M$  and chymase had no effect on Ang I cleavage (Figure 2.3.15F). However, when  $\alpha 1$ ACT was added to the sample containing PZP and chymase, the amount of Ang II generated relevant to Ang I was reduced to approximately half that of the sample containing  $\alpha_2 M$ , chymase, and  $\alpha 1$ ACT (Figure 2.3.15F&G; Figure 2.3.16). Therefore, although PZP forms a stable complex with chymase, this neither impedes its ability to generate Ang II and only marginally protects chymase from inhibition by  $\alpha 1$ ACT.

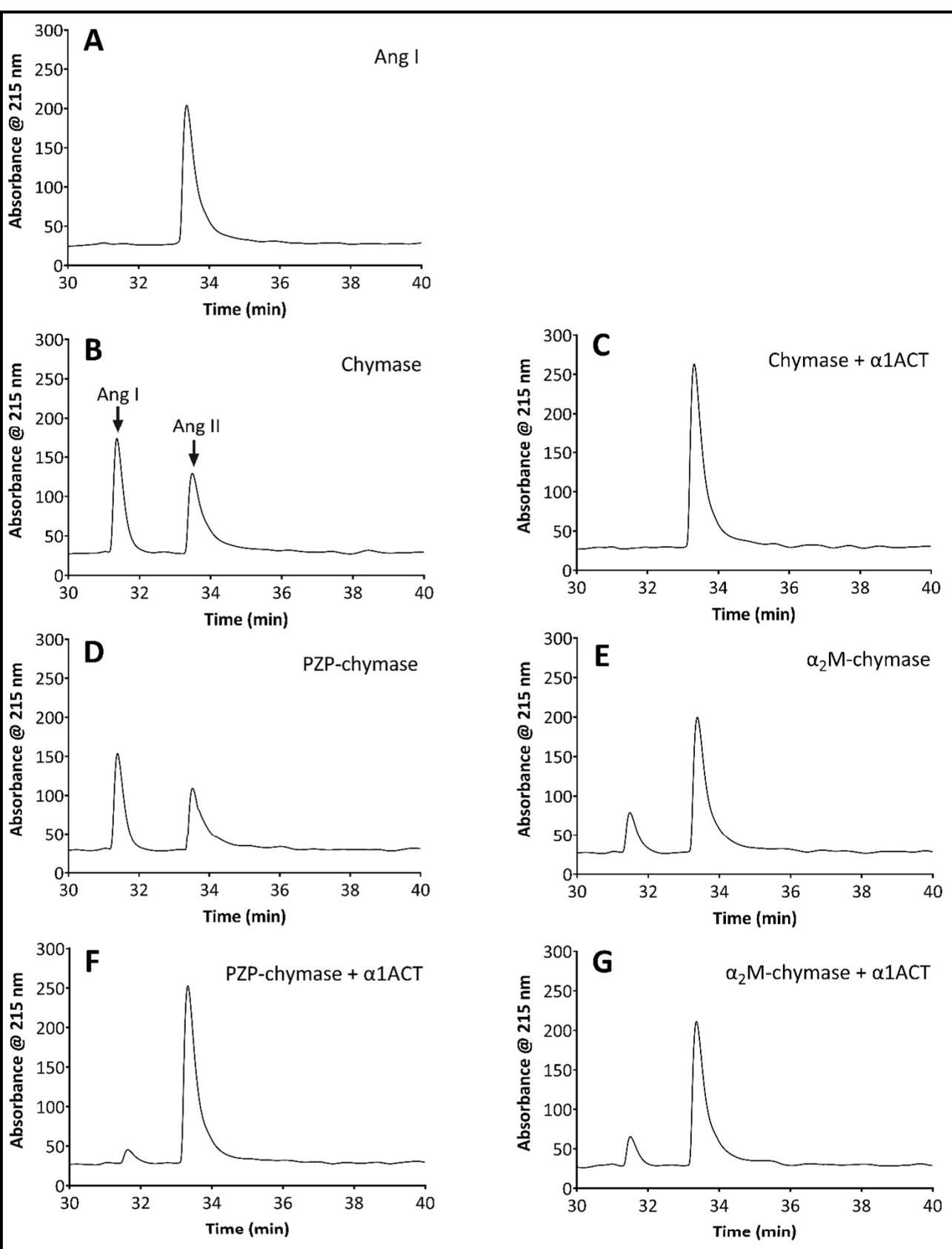


**Figure 2.3.15:** Representative elution profiles of Ang I and Ang II following incubation with chymase, PZP-chymase, or  $\alpha_2$ M-chymase in the presence or absence of  $\alpha_1$ ACT.

Chymase (12.5 nM), either alone or pre-incubated with PZP or  $\alpha_2 M$  at a 1:1 molar ratio for 45 min at 37 °C, was incubated with 2  $\mu g$  Ang I for 45 min at 37 °C in the presence or absence of a 3-fold molar excess of  $\alpha 1$ ACT. Ang I and II were separated by rpHPLC using a Prep-C18 Scalar column. Chromatograms are representative of three independent experiments. Treatments and peak identities are indicated.

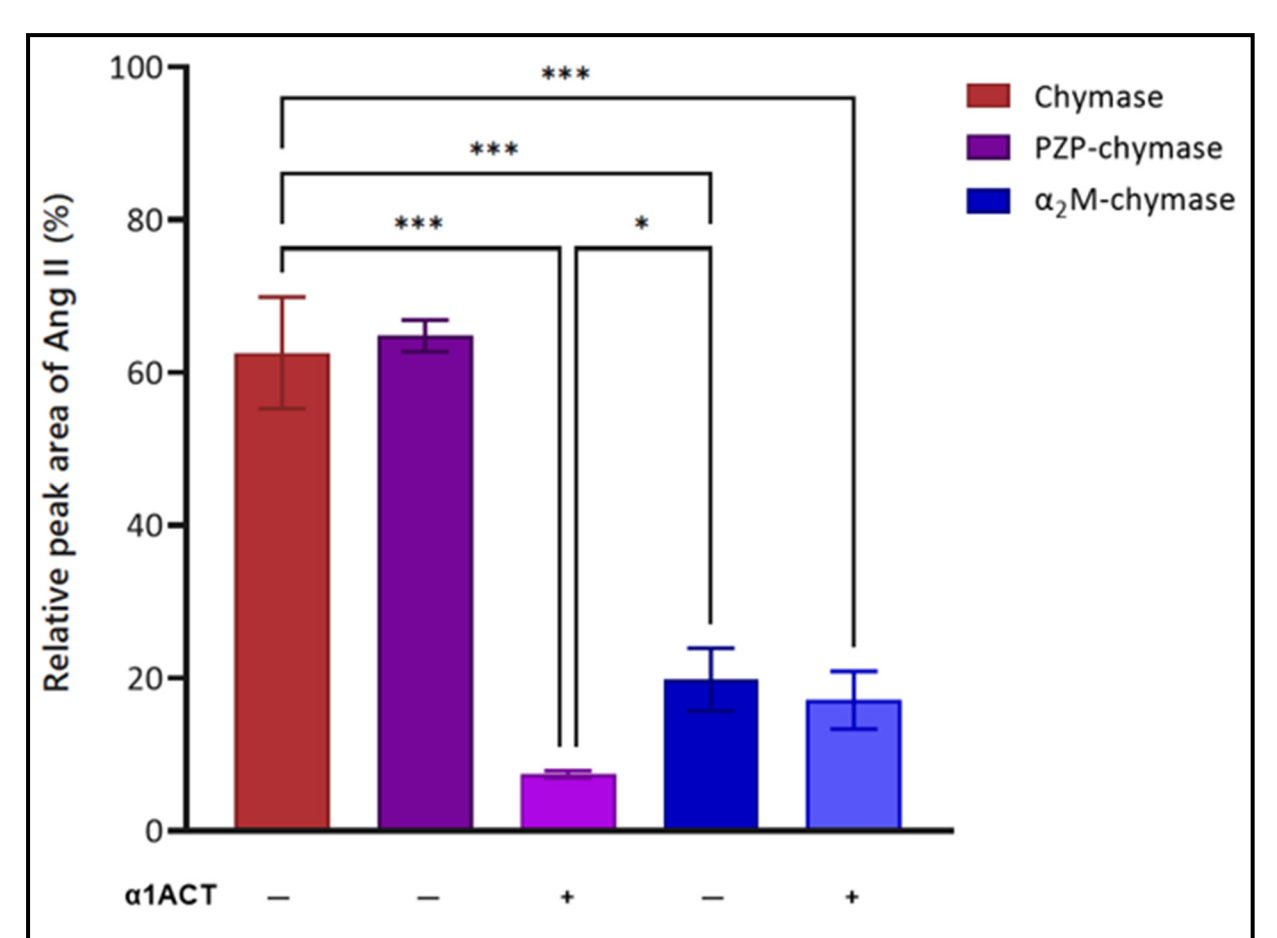


**Figure 2.3.16:** Relative peak area of Ang II to Ang I following incubation with chymase, PZP-chymase, or  $\alpha_2$ M-chymase in the presence or absence of  $\alpha_1$ ACT.

Chymase (12.5 nM), either alone or pre-incubated with PZP or  $\alpha_2 M$  at a 1:1 molar ratio for 45 min at 37 °C, was incubated with 2  $\mu$ g Ang I for 45 min at 37 °C. Samples were then separated by rpHPLC using a Prep-C18 Scalar column. Ang II peak area is expressed relative to Ang I (%). Data are mean  $\pm$  SD (n = 3) and are representative of three independent experiments. One-way ANOVA with post-hoc Tukey's HSD was used to compare treatments (\*p <0.05, \*\*\*p <0.0001).

#### 2.4 Discussion

In vitro studies investigating the functions of PZP are extremely limited, largely due to the challenges associated with purifying this protein from pregnancy plasma under conditions that preserve its native structure and activity. The results presented in this chapter provide the first evidence that chymase is a putative endogenous substrate for PZP. Specifically, chymase cleaves PZP at the bait region, forming a stable, non-covalent complex. In contrast to  $\alpha_2 M$ , binding of PZP to chymase does not sterically restrict access to small substrates or endogenous protease inactivators. Instead, the regulation of chymase by PZP likely involves clearance of PZP-chymase complexes via receptor-mediated endocytosis. Furthermore, chymase-treated PZP retains its ability to bind misfolded proteins and prevent their aggregation, supporting a role for PZP in extracellular proteostasis.

#### 2.4.1 Purification of PZP for in vitro functional analysis

Purifying a protein from a complex biological fluid such as blood plasma is an inherently difficult task, particularly when biochemically similar counterparts are abundant, and it is necessary to preserve the native structure and function of the molecule. Early methods for purifying PZP from human pregnancy plasma, involving PEG fractionation combined with DEAE, ZAC, and SEC, reportedly achieved ~23% yield and 80% purity but contamination with haptoglobin was a notable limitation (Sand et al., 1985). Incorporating HIC effectively reduced haptoglobin contamination but the problem of low yield remained (Chiabrando et al., 1997). Recent efforts to optimise the protocol involved replacing the pH gradient elution in ZAC with non-denaturing isocratic elution steps to minimise the likelihood of PZP to partially denature (Cater et al., 2019). Additionally, other gradient elution steps have been replaced with isocratic elution, reducing elution volumes and minimising the need for concentration procedures that may promote protein loss or denaturation (Lee, 2017). Nevertheless, the multi-step protocol to purify PZP from pregnancy plasma is time consuming and yields remain low.

In this study, quality control analyses were routinely performed to ensure that the results generated *in vitro* accurately reflect the function of the native PZP dimer. This was important because  $\alpha_2 M$  and PZP are prone to adopting alternative conformations in response to purification methods and storage (Chiabrando et al., 1997, Wyatt et al., 2015, Sand et al., 1985). Despite best efforts, the result of native gel electrophoresis showed that small amounts of erroneous dimeric (i.e., fast PZP) or tetrameric PZP species were present in solution following purification of the protein. Given that these were typically present at very low levels, the precise identity of these species was not further investigated. It is plausible that these represent alternative glycoforms of PZP, compact/tetrameric PZP conformations that are formed in the absence of protease interaction, or complexes formed between PZP and other ligands. Alternatively, it is also feasible that these non-native species are simply present as a limitation of the process required to obtain purified PZP. The use of liquid chromatography coupled with tandem mass-spectrometry could be explored to further characterise different PZP species but the heavy glycosylation of PZP complicates this approach.

The current approach for purifying PZP requires a large volume (≥ 100 mL) of mid to late gestation pregnancy plasma, which can be ethically and logistically challenging to obtain. While further optimisation of the process for purifying PZP from pregnancy plasma may be possible, a more attractive solution is the development of a recombinant production system to

eliminate the reliance on blood plasma and incorporate an affinity tag that facilitates simpler purification of the protein. However, PZP's complex macromolecular structure, involving extensive intra- and inter-chain disulfide bonding, an internal thioester bond, and 10% glycosylation (Devriendt et al., 1991, Sottrup-Jensen, 1989), poses significant challenges for producing the protein using a recombinant system. Prior attempts to generate recombinant PZP using a baculovirus-insect cell system resulted in deficient thioester synthesis (Van Rompaey and Marynen, 1994). Similarly, prior attempts to generate recombinant PZP in HEK293 cells only produced low amounts of PZP that was present as a heterogeneous mix of dimeric, tetrameric, aggregated, and misfolded species (Cater, 2021). Comparable challenges have also been reported following attempts to produce recombinant α<sub>2</sub>M using Expi293F cells (derived from HEK; Marino-Puertas et al., 2019). However, full-length recombinant α₂M has since been generated using HEK293 FreeStyle cells with a reported yield of 4 - 6 mg/L of conditioned media (Harwood and Enghild, 2024). The recombinantly produced α<sub>2</sub>M retained the structure and functionality of wild-type α<sub>2</sub>M, as assessed using gel electrophoresis following treatment of the α<sub>2</sub>M with methylamine and trypsin (Harwood et al., 2021b, Harwood et al., 2021a). While this approach requires further validation, it offers a promising framework for producing recombinant PZP.

#### 2.4.2 Chymase is a putative endogenous substrate for PZP

Chymase participates in numerous processes that are important to pregnancy, and elevated chymase activity has been associated with PE (Wang et al., 2007, Wang et al., 2010, Gu et al., 2009). However, its regulation by secreted protease inhibitors during pregnancy remains poorly understood. This study provides the first evidence that chymase is a putative endogenous substrate for PZP, which has ramifications for our understanding of the currently enigmatic biological role of PZP.

#### 2.4.2.1 Chymase specifically cleaves PZP at the bait region

Chymotrypsin has historically been used as a model to investigate the protease trapping activity of PZP (Christensen et al., 1989, Christensen et al., 1991). While these studies have provided valuable insights regarding the conformational changes that occur upon cleavage of the PZP bait region, chymotrypsin primarily functions in the digestive tract and is therefore, unlikely to be a physiological substrate for PZP *in vivo*. On the other hand, PZP and chymase are co-localised in biological fluids during pregnancy and inflammatory responses, which

increases the likelihood that the interaction characterised in this chapter is physiologically relevant.

The data obtained from this study suggest that cleavage of PZP by chymase is more selective for the bait region, compared to cleavage of PZP by chymotrypsin which produces a more diverse fragmentation pattern. This is consistent with the relatively stringent substrate recognition profile of chymase that specifically cleaves at tyrosine and phenylalanine residues over tryptophan residues (Andersson et al., 2008). In contrast, chymotrypsin cleaves at a broader range of amino acids, including tyrosine, phenylalanine, tryptophan, and histidine, as well as methionine and leucine (Vreeke et al., 2023). Further studies utilising *in situ* approaches will be important to confirm that PZP and chymase interact in biological fluids. While it may be possible to investigate this interaction using an animal model, it is important to note that interspecies differences exist in the regulation and functions of aMs and chymase (Kunori et al., 2005, Kunori et al., 2002, Gallwitz and Hellman, 2006); see also Section 1.2).

In addition to the main cleavage products, a small proportion of PZP migrated as HMW species (>250 kDa) on reducing SDS-PAGE following co-incubation with either chymase or chymotrypsin. Their persistence under reducing/denaturing conditions and occurrence with multiple serine proteases suggests that they represent thioester-mediated covalent PZP-protease adducts and/or inter-PZP crosslinks formed after bait-region cleavage, although protease-induced tetramerisation or aggregation cannot be excluded. Future studies using approaches such as thioester quenching, SEC with fraction collection and immunoblotting, and/or LC-MS/MS could help clarify their molecular basis and relevance.

#### 2.4.2.2 Chymase forms a stable complex with PZP via non-covalent interactions

It has previously been reported that cleavage of the bait region by chymotrypsin exposes PZP's thioester bond, which then rapidly reacts with a nucleophilic sidechain of the protease, forming a covalent complex between the two molecules (Jensen and Stigbrand, 1992, Christensen et al., 1991). However, the data presented in this chapter provide evidence that this covalent reaction is not needed for complex formation between PZP and chymase. While PZP and chymase form a stable complex *in vitro*, as assessed by streptavidin-biotin pull-down assay, the results of Western blot analysis and DTNB assay support the conclusion that this interaction is non-covalent, and that the PZP thioester bond remains intact. It has previously been shown that human plasma carboxypeptidase B binds to native  $\alpha_2 M$  via non-covalent interactions (Valnickova et al., 1996). Interestingly, the same study reported that both  $\alpha_2 M$  and

PZP co-purify with carboxypeptidase B from human plasma However, *in vitro* analysis to characterise the binding of PZP to carboxypeptidase B was not performed (Valnickova et al., 1996). This raises the possibility that the interaction between PZP and chymase is transient and/or reversible. However, further studies would be needed to determine if this is the case and whether is it specific to the protease substrate.

#### 2.4.3 Binding to PZP does not affect the activity of chymase or its inhibition by α1ACT

 $\alpha$ M family proteins are best known as protease inhibitors but the mechanism by which they control protease activity does not involve directly inactivating the protease. Consistent with the results of prior studies (Raymond et al., 2009), co-incubation with  $\alpha_2$ M reduced the ability of chymase to cleave small substrates and shielded chymase from inactivation by  $\alpha$ 1ACT. In contrast, data presented in this chapter show that the dimeric quaternary structure of PZP renders it ineffective at shielding chymase from accessing Ang I or being inactivated by  $\alpha$ 1ACT. Thus, these findings suggest that PZP regulates chymase activity through the clearance of PZP-chymase complexes from circulation, rather than by steric inhibition.

A limitation of this study is that all experiments were performed *in vitro*, and do not recapitulate the dynamics of protease inhibition in complex biological fluids such as human plasma. Further experiments are needed to characterise the affinity of chymase for PZP and compare this to the binding of chymase to  $\alpha_2 M$ . Although surface plasmon resonance, which requires less purified protein than ELISA-based approaches, was explored as a potential method for characterising the binding of PZP to ligands, technical challenges and time constraints led to abandoning this approach. Given that the relative abundance of PZP and  $\alpha_2 M$  are dependent on the biological context it's plausible that both proteins contribute to the regulation of chymase activity at different times. In non-pregnant individuals,  $\alpha_2 M$  has been suggested as the primary chymase inhibitor in human blood plasma (Walter et al., 1999). However, during pregnancy or in pregnancy-independent inflammatory states, PZP may be more abundant than  $\alpha_2 M$  on a molar basis and therefore alter the dynamic between  $\alpha_2 M$  and chymase.

## 2.4.4 Cleavage of the PZP bait region by chymase promotes the binding of putative PZP-chymase complexes to lipoprotein receptors

Cleavage at the bait region by chymotrypsin exposes a cryptic binding site for LRP1 on PZP, a critical step that is required for receptor-mediated endocytosis of PZP-protease complexes (Chiabrando et al., 2002, Sánchez et al., 2001). This mechanism is proposed to regulate the activity of PZP's protease substrates and facilitate the removal of other molecular cargo, such

as misfolded proteins, from biological fluids. The flow cytometry analyses described in this chapter provide the first evidence that chymase is a plausible endogenous partner that induces the conformational change necessary to facilitate the clearance of PZP via LRP1. While the results of native gel analysis support that this conformational change involves the collapse of the native PZP molecule to form an electrophoretically fast PZP dimer, a small fraction of the PZP migrated consistent with the formation of a PZP tetramer-protease complex. At present, it is not possible to determine whether one or both species are the ligand for lipoprotein receptors. However, this could be resolved by fractionating the protein using SEC prior to performing receptor binding assays. Additionally, given that a pan-specific lipoprotein receptor antagonist was used in this study, further experiments are needed to precisely characterise the involvement of LRP1 in the binding of PZP-protease complexes to the cell surface.

Given that LRP1 is abundantly expressed in the liver and placenta, it is plausible that LRP1 provides the major route for the clearance of PZP-chymase complexes in vivo. However, additional mechanisms may contribute to this activity. For example, scavenger receptors have been shown to clear blood-borne misfolded protein-chaperone complexes in rodents (Wyatt et al., 2011). Considering that PZP retains its holdase-type chaperone activity in the presence of chymase, scavenger receptors, including those expressed in the placenta (Landers et al., 2018, Stylianou et al., 2009), may also contribute to the clearance of PZP and its molecular cargo. While the current model proposes that internalisation of PZP-protease complexes is followed by lysosomal degradation, the fate of these complexes once endocytosed remains unknown. It is possible that some components of the endocytosed complex are recycled rather than degraded, or that binding to LRP1 activates intracellular signalling cascades. Although the downstream consequences of a<sub>2</sub>M-protease complex uptake via LRP1 have been shown to include lysosomal degradation (Van Leuven and Cassiman, 1980, Feldman et al., 1985b) and modulation of cell signalling pathways (Bonacci et al., 2007, Cáceres et al., 2010), whether the internalisation of PZP elicits similar effects remains to be determined. Therefore, internalisation assays involving placental explants or placental organoids may provide opportunity for more detailed characterisation of the uptake and clearance of PZP-protease complexes in the context of uncomplicated and complicated pregnancy (discussed further in Chapter 5).

#### 2.4.5 PZP retains chaperone activity in the presence of chymase

The ability of  $\alpha_2 M$  to stabilise misfolded proteins is enhanced when the native  $\alpha_2 M$  tetramer dissociates into PZP-like dimers (Wyatt et al., 2014). Although previous studies reported that cleavage by chymotrypsin reduces the surface-exposed hydrophobicity of PZP (Jensen et al., 1993), under the conditions used in this study, chymase-mediate cleavage of PZP was associated with an increase in surface-exposed hydrophobicity, as assessed by bisANS binding. Notably, the study of Jensen at al., (1993) utilised a 4-fold molar excess of chymotrypsin relative to PZP and did not include electrophoretic analysis to assess the quality of the purified PZP prior to treatment, nor the extent of PZP degradation following incubation with chymotrypsin. Alternatively, the discrepancy in findings may arise from differences in the methods used to quantify surface-exposed hydrophobicity. Nevertheless, the data presented here support that under controlled conditions in which PZP is present in molar excess, cleavage by chymase or chymotrypsin results in a conformational change associated with increased surface hydrophobicity – consistent with observations previously reported for  $\alpha_2 M$  (Constantinescu, 2016).

Although treatment with chymase increased the surface-exposed hydrophobicity of PZP – a feature typically associated with enhanced chaperone activity – it had no notable effect on PZP's ability to inhibit  $A\beta_{1-42}$  aggregation. A limitation of this study is that all assays were conducted using concentrations of PZP that virtually abolished  $A\beta_{1-42}$  aggregation. Reducing the concentration of PZP in these assays may reveal differences in chaperone activity between native and chymase-treated PZP preparations. Additional experiments involving different ratios of PZP/PZP-protease complex to  $A\beta_{1-42}$  would also be informative. Regardless, the data presented in this chapter collectively support that, following cleavage by chymase, PZP binds to  $A\beta_{1-42}$ , thereby preventing its aggregation. This is important because our current understanding suggests a fundamentally important role for extracellular chaperones is to facilitate the clearance of misfolded proteins via receptor-mediated endocytosis (as reviewed by (Wyatt et al., 2013b)). Thus, there are at least two plausible routes for the clearance of misfolded proteins following their stabilisation by PZP – uptake by either scavenger receptors that bind to misfolded proteins (Wyatt et al., 2011), or lipoprotein receptors that bind the PZP-protease complexes.

#### 2.4.6 A model for the activity of PZP-chymase complexes

In the absence of kinetic data describing the affinity of chymase for PZP, it is only possible to speculate on the extent to which PZP upregulation might influence chymase binding to other molecules, such as α<sub>2</sub>M, in vivo. Nonetheless, the in vitro results presented in this chapter demonstrate that PZP and  $\alpha_2M$  modulate chymase activity in fundamentally different ways. While both proteins bind to chymase, dimeric PZP does not significantly alter its activity against small substrates. Instead, PZP may regulate chymase indirectly by facilitating its clearance via LRP1. In contrast, tetrameric α<sub>2</sub>M forms a steric cage that partially restricts chymase from acting against small substrates in solution and also facilitates its rapid clearance via LRP1. Considering that  $\alpha_2 M$  is also able to bind 2 chymase molecules per tetramer, the evidence supports that α<sub>2</sub>M may be more effective at limiting chymase activity than PZP. However, if LRP1 becomes overwhelmeddownregulated, or dysfunctional - as may occur in complicated pregnancies (discussed further in Chapter 5) – inefficient clearance of α<sub>2</sub>M-chymase complexes may result in prolonged chymase activity (Figure 2.4.1). It should also be noted that the wide inter-individual variation in maternal plasma PZP concentrations complicates direct extrapolation of these biochemical findings to physiological settings. Nevertheless, the results provide important and novel mechanistic insight into how PZP may act, independently of absolute concentration. Together, these findings support the idea that α<sub>2</sub>M and PZP likely exert context-dependent and distinct effects on chymase activity in vivo, underscoring the need for further investigation into receptor-binding dynamic and clearance mechanisms under both physiological and pathological conditions.

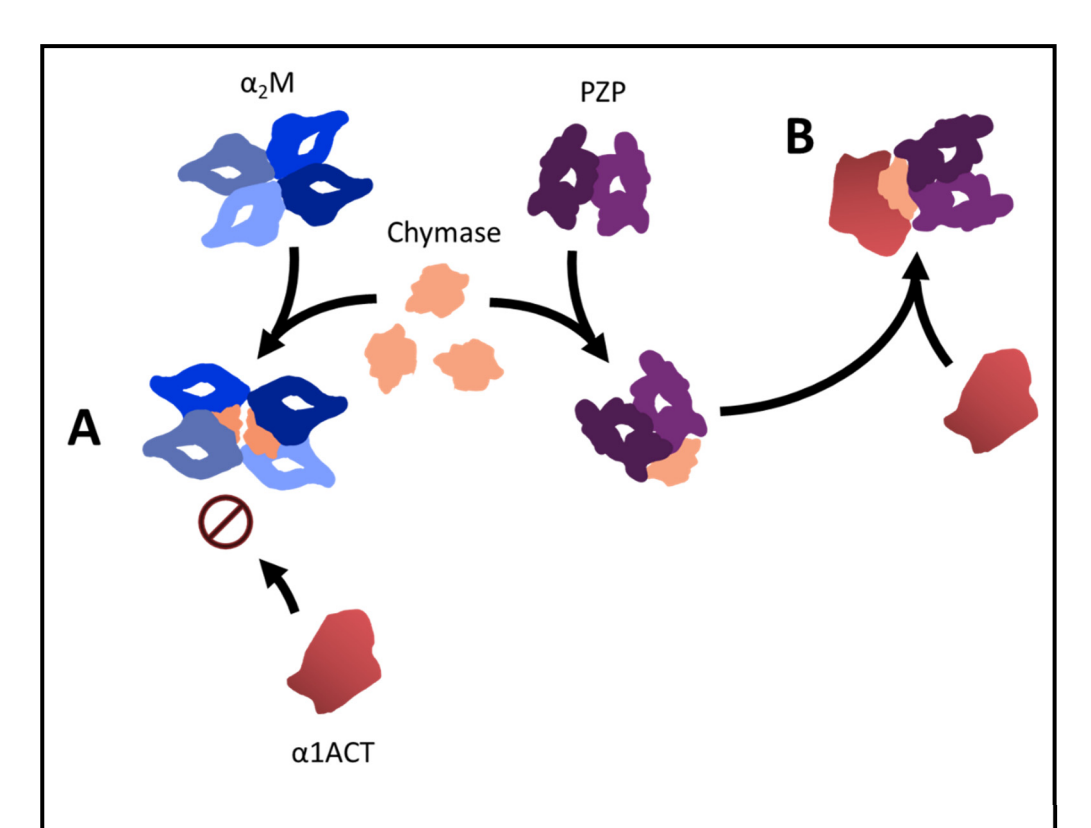


**Figure 2.4.1:** Proposed model illustrating how differences in the quaternary structure of PZP and  $\alpha_2M$  influence access of endogenous protease inhibitors to chymase.

(A) Tetrameric  $\alpha_2 M$  forms a steric cage around bound chymase, restricting access of endogenous protease inhibitors such as  $\alpha 1$ ACT. (B) In contrast, dimeric PZP provides less structural shielding, leaving chymase more accessible to inactivation.

### **CHAPTER 3:**

# PARITY INFLUENCES MATERNAL PLASMA PZP CONCENTRATION IN PREGNANT WOMEN

#### 3.1 Introduction

PZP is a quantitatively important pregnancy-associated protein, yet few studies have attempted to measure its concentration in maternal blood during pregnancy (Table 3.1.1). Of note, most existing studies relied on gel-based immunoassays, which provide less accurate estimates of protein concentration than techniques such as ELISA. Gel-based immunoassays typically have lower sensitivity, limited dynamic range, and low precision. Moreover, the use of antisera – blood serum containing a heterogenous mix of antibodies – increases the likelihood of protein cross-reactivity, thus raising concerns regarding the accuracy of the PZP concentrations previously reported (Table 3.1.1). Further, in some of these studies PZP concentrations are expressed in arbitrary or relative units, such as percentages of undefined reference pools or international units of unspecified calibration materials. These reporting methods are uninformative and lack standardisation, hindering cross-study comparisons and making it difficult to interpret the physiological relevance of the data. To date, only two studies have utilised ELISA to measure maternal circulating PZP concentration, both involving antibodies that were confirmed to have no cross-reactivity with a<sub>2</sub>M (Petersen et al., 1990, Fosheim et al., 2023). Considering that α<sub>2</sub>M is constitutively abundant in pregnancy plasma at 1 – 4mg/mL (Petersen, 1993, Wang et al., 2014), ensuring that the quantification method used is specific for PZP is crucial to prevent erroneous measurements.

**Table 3.1.1:** Studies that have quantified PZP in blood plasma or serum during pregnancy.

Year	n	Included complications	GA at sampling (weeks)	Biological fluid	Method	Detection method	PZP (μg/mL)	Reference
1972	74	PE	Not reported	Serum	Radial immunodiffusion	Antisera	127 ± 73#	(Horne et al., 1972)
1974	72	None	9 - 42	Serum	Single radial immunodiffusion	Antisera	25 ± 10 – 1,198 ± 429°	(von Schoultz, 1974)
1976	425	Prolonged pregnancy, spontaneous abortion	6 - 40	Serum	Radial immunodiffusion	Antisera	Undetectable <sup>b</sup> 863.2 ± 443.4 <sup>c</sup>	(Than et al., 1976)
1976	5	None	Up to 6 weeks prior to delivery	Plasma	Rocket immunoelectrophoresis	Antisera	No units reported	(Lin et al., 1976)
1982	70	None	16 - 40	Serum	Rocket immunoelectrophoresis	Antisera	95.9 ± 29.86##	(Westergaard et al., 1982)
1983	33	PE	Term	Plasma	Single radial immunodiffusion	Antisera	131.1 ± 60.2°	(Griffin, 1983)
1986	28	PE	31	Plasma	Rocket immunoelectrophoresis	Antisera	52.5 ± 2.29###	(Armstrong et al., 1986)
1990	49	Hydatidiform mole	35	Serum	ELISA	PZP-specific antibodies	8.4 – 920°	(Petersen et al., 1990)
1994	101	None	5 - 42	Plasma	Rocket immunoelectrophoresis	Antisera	1206.2 ± 932.8 <sup>a</sup> 3000 <sup>c</sup>	(Ekelund and Laurell, 1994)
2023	549	PE, GH, GDM	34 - 39	Serum	ELISA (R&D Systems)	PZP-specific antibodies	892 <sup>a</sup> 32 – 3240 <sup>b</sup>	(Fosheim et al., 2023)

GA – gestational age. For studies with pregnancy complications included PZP concentrations are given for the control group. Mean<sup>a</sup>, minimum<sup>b</sup>, and maximum<sup>c</sup> reported where available/appropriate. \*Reported as a percentage of "pregnant human serum known to contain appreciable quantities of PZP". \*Reported as AU, where AU/100 mL is the "concentration of PZP in a pool (n = 212) of late pregnancy serum". \*#Reported as "i.u./l of WHO reference material for pregnancy associated proteins 78/610".

Following the development of a commercial ELISA capable of quantifying PZP in complex biological solutions (R&D Systems, Minneapolis, MN, USA), maternal PZP concentration has been reported in only one population of pregnant women, based on serum samples collected between 24 and 42 weeks of gestation (Fosheim et al., 2023). The major findings were that in the late third trimester circulating PZP concentration was lower in mothers with EO-PE compared to controls, whereas no association was observed with LO-PE (Fosheim et al., 2023). Conflicting data describing the nature of the association between circulating PZP and PE also exists in prior reports (see Table 1.2.2). The novel interaction between PZP and chymase described in Chapter 2 supports the idea that PZP may modulate chymase activity relevant to PE and, more broadly, pregnancy-associated hypertension. This finding strengthens the rationale for re-evaluating the association between maternal PZP concentration and PE with increased rigor. In the current chapter, it was hypothesised that currently unrecognised maternal and/or neonatal characteristics influence maternal plasma PZP concentration during pregnancy and that this contributes to the cohort-dependent associations observed between PZP and PE. To investigate this hypothesis, PZP concentration was measured in late gestation plasma samples from three independent cohorts of pregnant women, including a sub-set with PE. Plasma samples were selected for this study in preference of serum to eliminate the possibility that proteases involved in coagulation interfere with the accurate measurement of PZP (Lagrange et al., 2022, Arbelaez et al., 1995).

The specific aims of this study were to:

- 1) Measure maternal plasma PZP concentrations in late gestation in three independent groups of women including subgroups with PE
- 2) Investigate the associations between late gestation maternal plasma PZP concentration and maternal and neonatal characteristics, including pregnancy outcome

## 3.2 Methods

#### 3.2.1 Recruitment

## 3.2.1.1 St George Hospital cohort

Participants were recruited in 2017 and 2018 from St George Hospital (Kogarah, NSW, Australia) in accordance with National Ethics Application HREC/16/WGONG/256, approved by the Joint University of Wollongong and Illawarra Shoalhaven Local Health District HREC. Diagnosis of PE (n = 31) was according to ISSHP guidelines (Brown et al. 2018); systolic blood pressure ≥140

mmHg and/or diastolic blood pressure  $\geq 90$  mmHg accompanied by maternal organ dysfunction and/or proteinuria and/or uteroplacental dysfunction (such as FGR). SGA babies were defined as those with a birthweight  $<10^{th}$  centile based on population-specific centiles. The control group (n = 31) comprised normotensive women with no major pregnancy or health complications.

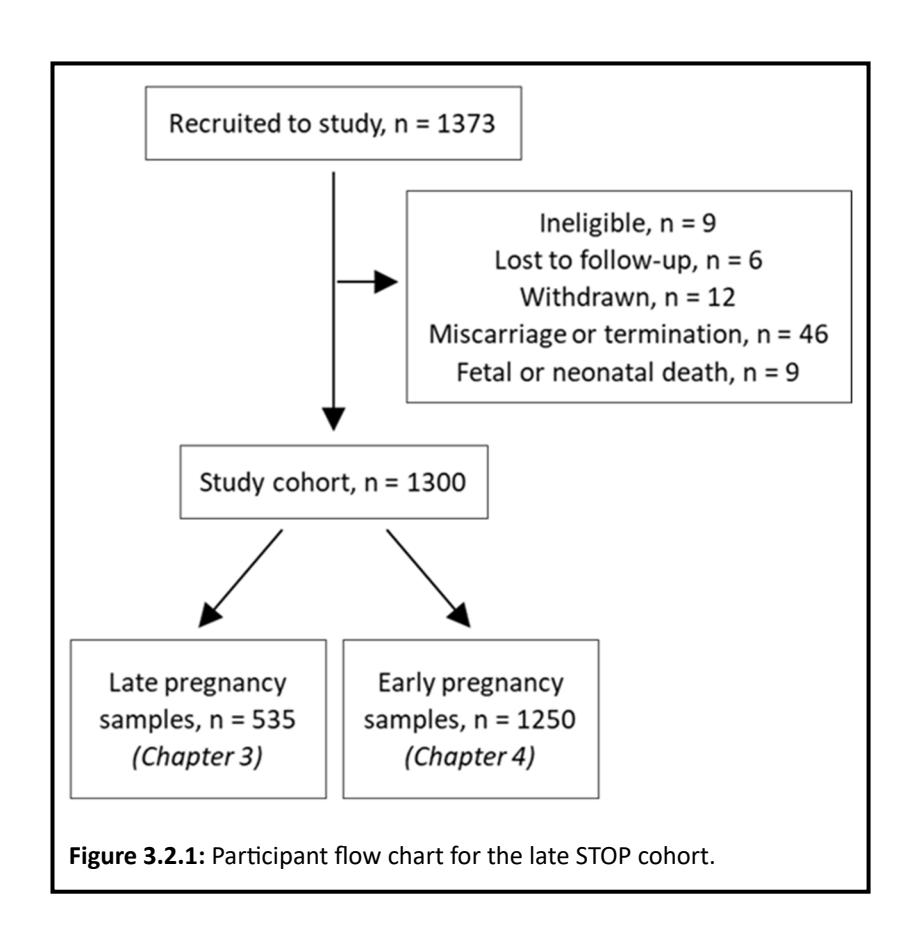
## 3.2.1.2 Nationwide Children's Hospital cohort

Participants were recruited between March 2004 and December 2010 from the Yale-New Haven Hospital or the Nationwide Children's Hospital (Columbus, Ohio, USA) in accordance with Protocol 2019-0290 approved by the Human Investigation Committee of Yale University. Diagnosis of PE (n = 30) was according to the ACOG criteria valid at the time of sample collection; systolic blood pressure ≥140 mmHg and/or diastolic blood pressure ≥90 mmHg accompanied by proteinuria (urinary excretion of ≥0.3 g protein in 24 h sample) (ACOG, 2002). Intrauterine growth restriction (IUGR) for the PE + IUGR group (n = 31) was defined ultrasonographically as an estimated fetal weight <10<sup>th</sup> percentile for gestational age (ACOG, 2013). sPTB (n = 30) was defined as delivery <37 weeks gestation. The control group (n = 30) consisted of normotensive women with no major pregnancy complications or pre-existing health conditions.

#### 3.2.1.3 Late STOP cohort

Samples analysed in this cohort were collected in late gestation from patients recruited to the prospective cohort study **S**creening **T**ests to identify poor **O**utcomes of **P**regnancy (STOP) (Australian and New Zealand Clinical Trials Registry ACTRN12614000985684), with Ethics approval from the Women's and Children's Health Network HREC (HREC/14/WCHN/90). Women were recruited to the STOP study between 2015 and 2018 from Lyell McEwin Hospital (Elizabeth Vale, SA, Australia) and the Women's and Children's Hospital (North Adelaide, SA, Australia). All women were recruited as healthy, nulliparous mothers with a singleton pregnancy. Women were excluded from the study if they had any of the following: ≥3 terminations or miscarriages, major fetal or uterine anomalies, treated hypertension prepregnancy, renal disease, anti-phospholipid syndrome, type I or II diabetes mellitus, systemic lupus erythematosus, previous cervical cone biopsy. PE was defined as systolic blood pressure ≥140 mmHg and/or diastolic blood pressure ≥90 mmHg after 20 weeks gestation on at least 2 occasions 4 h apart, accompanied by proteinuria and/or any multi-system complication of PE, including FGR. sPTB was defined as spontaneous preterm labour or preterm premature rupture

of membranes (PROM) resulting in birth <37 weeks. Gestational hypertension (GH) was defined as new-onset hypertension (systolic ≥140 mmHg and/or diastolic blood pressure ≥90 mmHg) after 20 weeks gestation. SGA was defined as birthweight <10<sup>th</sup> percentile using customised centiles adjusted for maternal weight, height, parity, ethnicity, and infant sex. GDM was diagnosed by 75 g oral glucose tolerance test with fasting glucose ≥5.1 mmol/L and/or 2 h glucose ≥7.8 mmol/L (Mohammed et al., 2020). If multiple complications were present a hierarchy was used to classify cases where PE > sPTB > GH > SGA > GDM. Women who experienced a complication other than those listed were classified as 'other'. All women were recruited between 9 – 16 weeks gestation, with a subset (n = 535) of women donating a second sample between 32- and 38-weeks' gestation. The data presented in this chapter are based solely on the late gestation samples.



## 3.2.2 Sample preparation and analysis

The St George Hospital cohort was analysed in 2019 by Dr. Jordan Cater, and Gimhani Avindri Abeygunasekara while the Nationwide Children's Hospital cohort was analysed in 2021 by Professor Irinia Buhimschi's research group. Heparinised blood samples were collected, and the plasma isolated then stored at -20 °C prior to analysis. Individual pregnancy plasma

samples were analysed for PZP concentration in triplicate using an ELISA kit and ancillary reagents (R&D Systems; cat# DY8280-05 and DY008) as per manufacturer's instructions. Triplicate measurements were feasible for these cohorts due to their smaller sample sizes. For a subset of women in the St George Hospital cohort (n = 20 PE, 20 normotensive), sFlt-1 and PIGF levels were measured via Elecsys immunoassay using a Cobas e 411 analyser (Roche Diagnostics). The candidate gratefully acknowledges the contribution of these data.

In contrast, the late STOP cohort was measured in duplicate due to the larger sample size (n = 535). Heparinised blood samples were collected from STOP participants and held on ice prior to processing. Plasma was isolated by centrifugation and stored at -80 °C in 250 μL aliquots for future analyses. Maternal plasma PZP concentrations were quantified as per manufacturer's instructions using the same commercial ELISA kit and ancillary reagents (R&D Systems; cat# DY8280-05 and DY008) as the St George Hospital and Nationwide Children's Hospital cohorts. Briefly, plasma samples were thawed once, centrifuged (21,000 x g, 5 min, 4 °C), and serially diluted (~1:25,000 final) using PBS as the dilution matrix. A seven-point standard curve (156– 10,000 pg/mL) was prepared in plasma-PBS, generated by a 25,000-fold dilution of normal plasma in PBS to match the sample matrix, with a blank included. Bound PZP was detected using a biotinylated anti-PZP antibody, streptavidin–HRP, and colorimetric detection with TMB substrate, read at 450 nm with 540/570 nm correction. The antibodies used have been confirmed by the manufacturer to exhibit no cross-reactivity with the natural protein a₂M or the recombinant proteins CD109, LDL R, α<sub>2</sub>ML1, complement C3a and complement C5a. All assays were performed by the candidate to reduce inter-user variability, and pooled plasma controls were included on each plate to monitor inter-plate consistency. The inter-assay and intra-assay coefficients of variation were 11.3% and <10%, respectively. Duplicate samples with readings that differed by >10% coefficient of variation were re-analysed (in duplicate) as a quality control measure.

## 3.2.3 Statistical analysis

Descriptive statistics for maternal and neonatal characteristics are grouped by pregnancy outcome and reported separately for each cohort. Categorical variables were compared using Fisher's exact or chi squared test and are reported as n (%). Continuous normally distributed variables were compared using Student's T-test and are reported as mean (SD). Continuous skewed variables were compared using the two-tailed Mann-Whitney U test adjusted using the

Bonferroni correction to account for multiple comparisons or Kruskal-Wallis test with Dunn's post-hoc comparisons and are reported as median (IQR). Spearman's rank correlation coefficient (rho) was used to assess correlations between maternal plasma PZP concentration and relevant variables.

For the St George Hospital and Nationwide Children's Hospital cohorts, natural logarithmic transformation was performed to normalise the distribution of PZP concentrations and sFlt-1/PIGF measures for models in which they were the dependent variable. Univariate linear regression models were used to assess the association between maternal and neonatal characteristics and maternal plasma PZP concentration in the St George Hospital and Nationwide Children's Hospital cohorts. Log transformation was not sufficient to normalise PZP in the late STOP cohort, therefore quantile regression at the 0.25, 0.5, and 0.75 quantiles was used to assess the associations between maternal and neonatal characteristics and PZP concentration for this cohort. Models which assessed the influence of parity on PZP were adjusted for gestational age at sampling, and/or BMI as indicated. Logistic regression models were used to assess the association between PZP and pregnancy outcome, and were adjusted for parity, gestational age at sampling, and/or BMI as indicated. The Akaike Information Criterion (AIC), calculated as −2 log-likelihood + 2k, and the Bayesian Information Criterion (BIC), calculated as  $-2 \log$ -likelihood + k × log(n), where k is the number of parameters and n is the sample size, were used to assess model fit as indicated, with lower AIC/BIC indicative of a better fitting model. Parity and gravidity were treated as binary variables in all regression analyses (nulliparous and parous, primigravida and multigravida) due to limited mothers with parity ≥2 or gravidity ≥3. Similarly, due to the small sample sizes within each ethnic group, participants were broadly categorised as 'Caucasian' and 'non-Caucasian' for all analyses. All statistical analyses were carried out in SPSS (version 28.0.1.1), and all figures were generated using GraphPad Prism (version 9.0.0).

## 3.3 Results

## 3.3.1 St George Hospital cohort

PZP concentration was measured in blood plasma samples collected from mothers during the mid to late third trimester and were grouped according to whether they experienced normotensive or PE pregnancy. Relevant maternal and neonatal characteristics, grouped by pregnancy outcome, are presented in Table 3.3.1 with additional information regarding

comorbidities supplied in Table S2. The normotensive and PE groups were comparable in terms of the gestational age at sampling, maternal age, BMI, neonatal sex, and the proportion of primigravid mothers. As expected, given the clinical presentation of PE, systolic and diastolic blood pressures were significantly higher in the PE group compared to the normotensive group. Preterm birth occurred exclusively in the PE group and the average gestational age at birth was lower for PE women compared to normotensive women. Concomitantly, neonatal birthweight was significantly lower in the PE group and SGA babies were born exclusively to mothers with PE. Consistent with PE occurring more commonly in first time mothers, the PE group had more than double the number of nulliparous women compared to the normotensive group. The frequencies of parity and gravidity for both groups are provided in Table S3.

**Table 3.3.1:** Maternal and neonatal characteristics grouped by pregnancy outcome in the St George Hospital cohort. Maternal characteristics collected at time of sampling.

	Normotensive	Preeclampsia	р
n	31	31	
Gestational age at sampling (weeks)	35.72 ± 2.70	35.64 ± 2.80	0.70
Maternal age (years)	32.19 ± 4.37	32.35 ± 5.45	0.90
Body mass index (kg/m²)	24.52 ± 3.54	25.64 ± 5.58	0.35
Systolic blood pressure (mmHg)	108 (98 – 112)	145.0 (140 – 154)	<0.001
Diastolic blood pressure (mmHg)	70 (60 – 80)	92 (90 – 115)	<0.001
Nulliparous	7 (22.6)	17 (54.8)	0.02
Primigravida	5 (16.1)	10 (32.3)	0.23
Gestational age at birth (weeks) <sup>a</sup>	39.28 ± 1.12	36.21 ± 2.40	<0.001
Birthweight (g) <sup>a</sup>	3430 (3165 – 3650)	2550 (1790 – 3340)	<0.001
Neonatal sex (Female) <sup>a</sup>	9 (31.0)	11 (37.9)	0.50
Preterm birth (<37 weeks)	0 (0)	15 (48.4)	<0.001
Small for gestational age (<10 <sup>th</sup> centile)	0 (0)	11 (35.5)	<0.001
Early onset (<34 weeks gestation)	N/A	11 (35.5)	N/A

Normally distributed variables compared using Student's T-test and reported as mean  $\pm$  SD. Non-normally distributed variables compared using two-tailed Mann-Whitney U test and reported as median (IQR). Categorical variables compared using Fisher's exact test (2-sided) and reported as n (%). Gravidity includes the current pregnancy. <sup>a</sup>Missing data for n = 2 normotensive participants.

There was substantial inter-individual variation in maternal plasma PZP concentration between mothers of similar gestational age, ranging from 16.23  $\mu$ g/mL to 826.86  $\mu$ g/mL. When PZP concentration was compared, the median was lower for the PE group (123.11, IQR 48.24 – 257.25  $\mu$ g/mL), compared to the normotensive group (254.51, IQR 88.85 – 425.12  $\mu$ g/mL, p = 0.01) (Figure 3.3.1A). To further analyse the relationship between maternal plasma PZP concentration and pregnancy outcome (PE versus normotensive) logistic regression modelling was performed. The results indicated a statistically significant association, although the effect

size was small (odds ratio [95% CI]: 0.996 [0.993, 0.999]; p = 0.02). When gestational age at sampling or BMI were included as covariates (both have previously been reported to associate with PZP concentration; Ekelund and Laurell, 1994, Fosheim et al., 2023) there was little effect on the model outcome. Model fit statistics (AIC and BIC) supported that models including either PZP concentration alone or PZP concentration with BMI provided the best fit to the data, with little difference between them (Table S4).

Given that the association between maternal plasma PZP concentration and PE was weak, further analysis was performed to explore whether other variables contributed to this association. When PE cases were stratified according to time of diagnosis (i.e., EO-PE versus LO-PE), no significant difference in median PZP concentration was observed between these subgroups. A difference was only found between the median PZP concentration of the LO-PE group and the normotensive group (Figure 3.3.1B). When the data were separated according to birthweight (i.e., PE + SGA versus PE + appropriate for gestational age [AGA]), the median PZP concentration was lowest for the PE + SGA group, with no difference between the PE + AGA and normotensive groups (Figure 3.3.1C). Due to the small sample sizes generated when stratifying the PE group by time of diagnosis or birthweight, only univariate logistic regression was performed. PZP concentration showed a very weak association with the odds of a woman having PE + SGA (odds ratio [95% CI]: 0.994 [0.988, 0.999]; p = 0.03) but not PE + AGA (odds ratio [95% CI]: 0.997 [0.994, 1.001]; p = 0.10). Similarly, when stratified by time of diagnosis, LO-PE (odds ratio [95% CI]: 0.995 [0.991, 0.999]; p = 0.02) but not EO-PE (odds ratio [95% CI]: 0.997 [0.993, 1.003]; p = 0.20), was found to be associated with plasma PZP concentration.

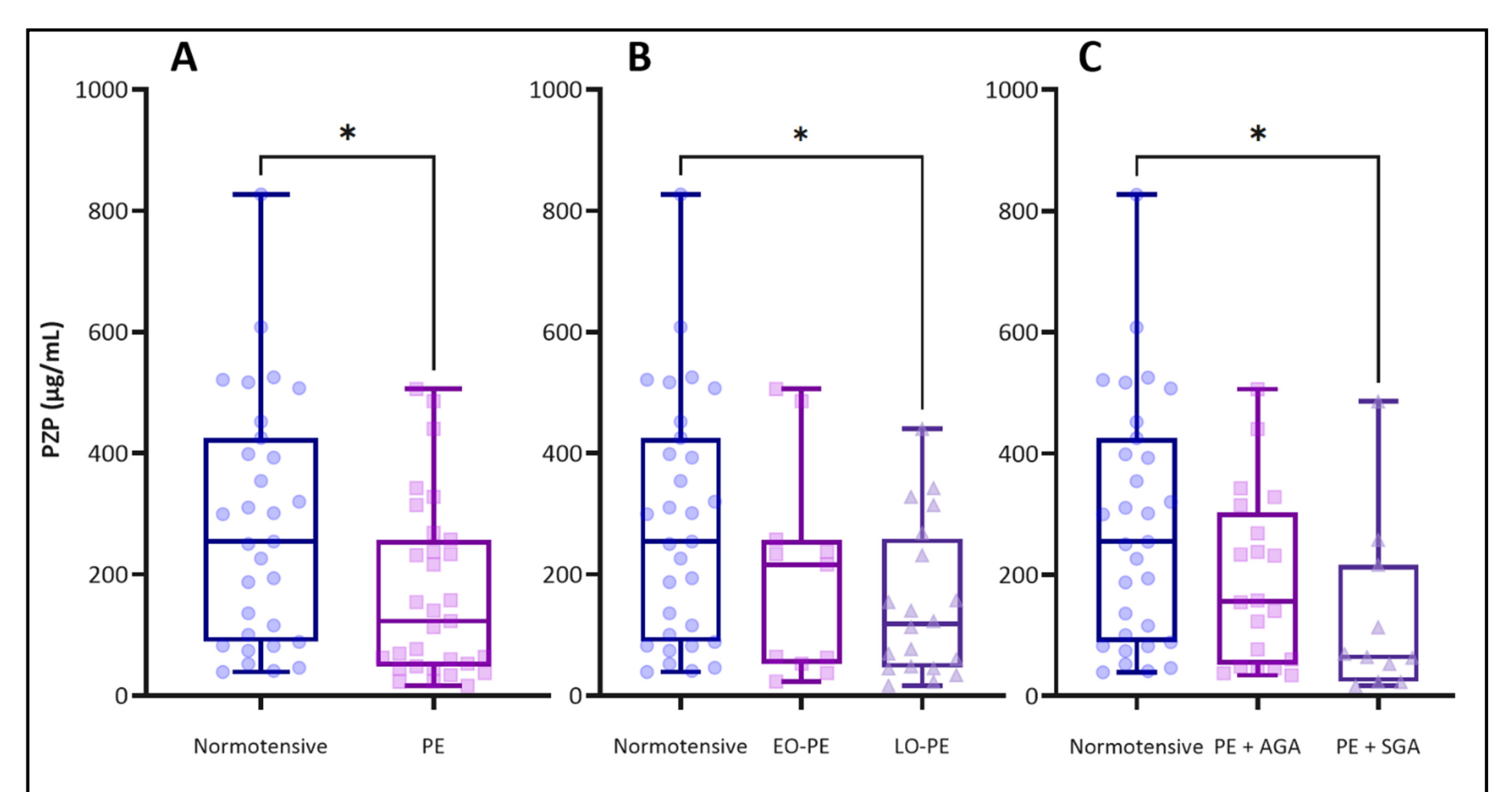


**Figure 3.3.1:** Unadjusted maternal plasma PZP concentration grouped by pregnancy outcome in the St George Hospital cohort. **(A)** Normotensive (n = 31) versus PE (n = 31) pregnancies; **(B)** normotensive versus PE pregnancies stratified by gestational age at onset (EO-PE n = 11; LO-PE n = 20); **(C)** normotensive versus PE pregnancies stratified by birthweight for gestational age (PE + SGA n = 11; PE + AGA n = 20). Two-tailed Mann-Whitney U test; significance indicated with asterisks (\*p < 0.05).

# 3.3.1.1 Maternal plasma PZP concentration weakly correlated with sFlt-1/PlGF ratio, gestational age at birth, and parity

To explore whether maternal plasma PZP concentration was associated with maternal and neonatal characteristics in the St George Hospital cohort correlation analyses were performed. Independent of pregnancy outcome, PZP concentration showed a weak negative correlation with the sFlt-1/PlGF ratio, a biomarker of PE (Figure 3.3.2A), and a weak positive correlation with gestational age at birth (Figure 3.3.2B) and parity (Figure 3.3.2C). Despite the apparent association between PE + SGA and reduced maternal PZP concentration, birthweight did not correlate with PZP concentration. No other variables were found to correlate with PZP concentration (Table S5).

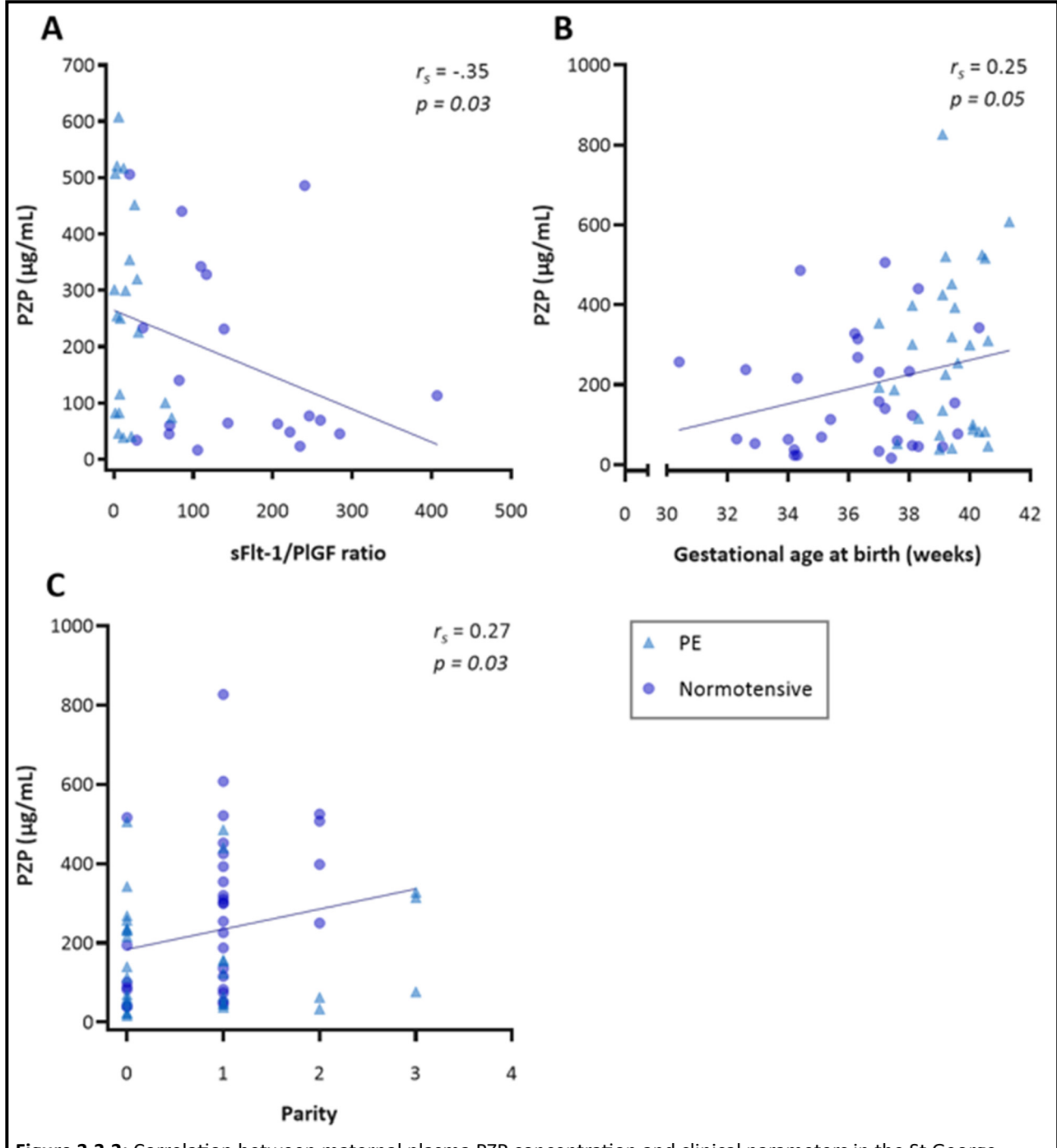


**Figure 3.3.2:** Correlation between maternal plasma PZP concentration and clinical parameters in the St George Hospital Cohort.

(A) sFlt-1/PIGF ratio (n = 40; 20 PE, 20 normotensive); (B) gestational age at birth (n = 60; 31 PE, 29 normotensive); (C) parity (n = 61; 31 PE, 30 normotensive). Spearman's rho. Data points are shaded by pregnancy outcome for visual reference only; the trend line represents the overall dataset.

# 3.3.1.2 Parity was associated with maternal plasma PZP concentration in normotensive pregnancies

To further explore the relationship between maternal plasma PZP concentration and correlated variables, linear regression analyses were performed. When log-transformed PZP concentration was modelled as the independent variable, the results showed that the

association between PZP concentration and the sFlt-1/PlGF ratio was very weak, with the ratio of geometric means close to 1 (Table S6). Given the uncertainty regarding the direction of the relationship between PZP and sFlt-1/PlGF ratio, analyses were repeated with PZP as the dependent variable. Similar results were obtained, suggesting that it is unlikely that a causal relationship exists (Table S6). Similarly, the results of linear regression analyses assessing the association between PZP concentration and gestational age at birth were only marginally significant, with a negligible effect size of 0.3% (Table S6). In contrast, the results of linear regression modelling showed a much stronger association between maternal plasma PZP concentration and parity, whereby, on average, PZP concentrations in parous women were  $\sim$ 1.7-fold higher compared to nulliparous women (ratio of geometric means [95% CI]: 1.748 [1.085, 2.814]; p = 0.02). To further investigate this association, gestational age at sampling and BMI were included as covariates in the model to assess their contributions to explaining the variability in maternal plasma PZP concentration. However, the AIC and BIC supported that a model including parity alone fit the data best (Table S7).

The finding that maternal plasma PZP concentration in late pregnancy is influenced by parity was further supported by the significantly higher median value measured in parous (252.42, IQR 76.32 – 405.11  $\mu$ g/mL) versus nulliparous (106.99, IQR 47.19 – 236.67  $\mu$ g/mL, p = 0.03) women (Figure 3.3.3A). Although sample sizes were insufficient for reliable statistical analyses, visual assessment of PZP concentration in normotensive versus PE pregnancies stratified by parity showed that the elevated levels of maternal plasma PZP are plausibly driven by the normotensive group of women (Figure 3.3.3B). This observation prompted further investigation of the relationship between parity and PZP concentration within each outcome group.

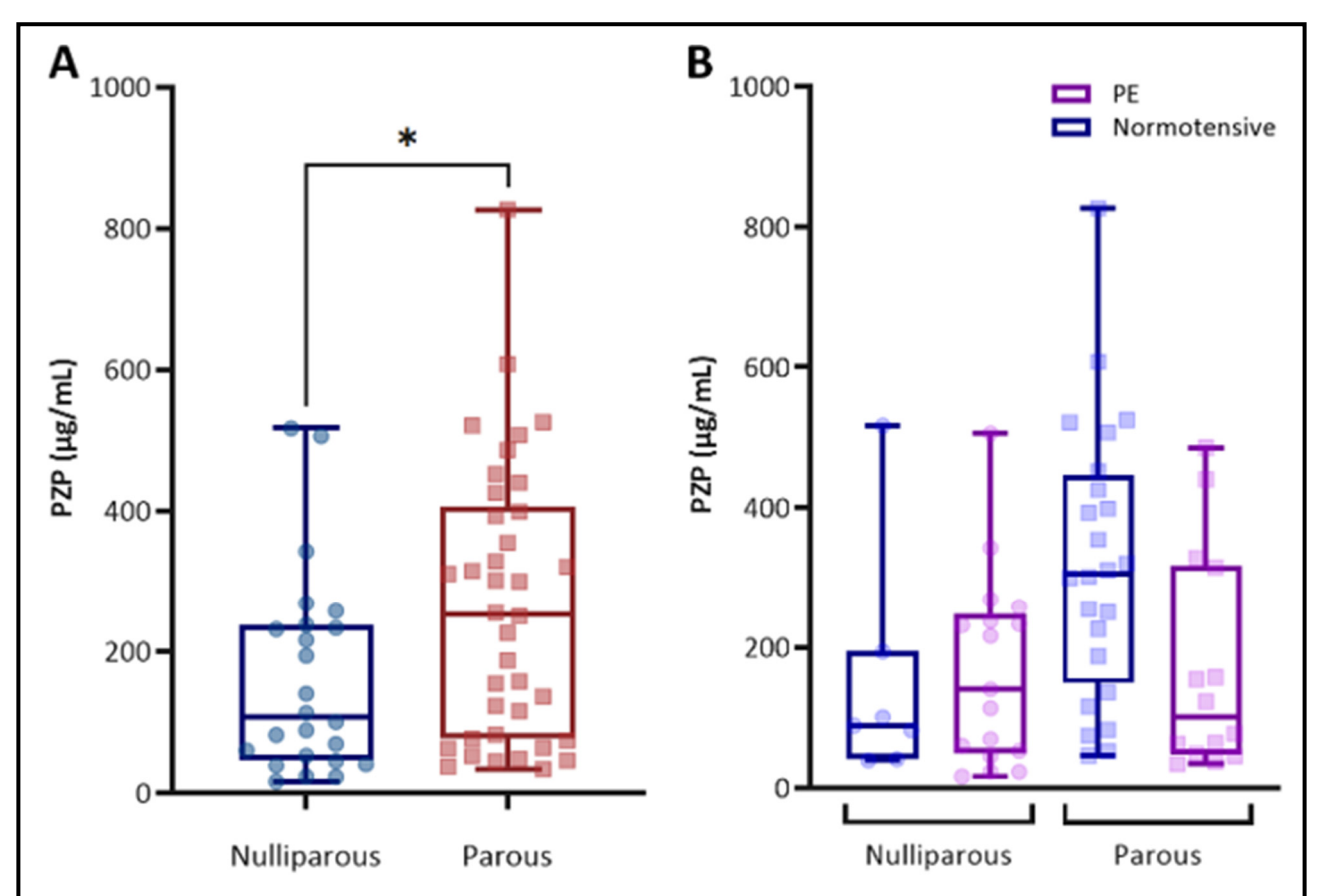


**Figure 3.3.3:** Unadjusted maternal plasma PZP concentration grouped by parity in the St George Hospital cohort. **(A)** Nulliparous (n = 24) versus parous (n = 38). Two-tailed Mann-Whitney U test; significance indicated with asterisks (\* p < 0.05). **(B)** Normotensive versus PE pregnancies, stratified by parity. Statistical analysis not performed due to limited n.

In the normotensive group there was a moderate positive correlation between maternal plasma PZP concentration and parity ( $r_s$  = 0.46, p = 0.009) and parous women were associated with approximately 2.4-fold higher plasma PZP levels, compared to nulliparous women (ratio of geometric means [95% CI]: 2.460 [1.271, 4.762]; p = 0.008). Conversely, in the PE group there was no significant correlation between PZP levels and parity ( $r_s$  = 0.03, p = 0.86), nor was there any association between parity and PZP concentration (ratio of geometric means [95% CI]: 1.034 [0.521, 2.054]; p = 0.92).

Considering that parity affects maternal plasma PZP concentration, logistic regression models to assess PZP's effect on pregnancy outcome were re-run and adjusted for both parity and BMI. The results showed that nulliparous women had 4-fold higher odds of developing PE compared to parous women but that PZP concentration was only weakly associated with pregnancy outcome (Table 3.3.2).

**Table 3.3.2:** Logistic regression model assessing the association between maternal plasma PZP concentration and pregnancy outcome in the St George Hospital cohort (n = 62; 31 normotensive [reference], 31 PE).

Variable	Odds ratio [95% CI]	p		
PZP (μg/mL)	0.996 [0.993, 0.999]	0.04		
Parity (nulliparous versus parous)	4.000 [1.189, 13.459]	0.03		
BMI	1.123 [0.975, 1.293]	0.11		

## 3.3.2 Nationwide Children's Hospital cohort

Given the limited sample size of the St George Hospital cohort (n = 62), samples from the Nationwide Children's Hospital, an independent cohort of 121 women, were subsequently analysed. In addition to analysing samples from normotensive and PE pregnancies, this cohort also included samples from women who had PE comorbid with IUGR (PE + IUGR) or sPTB. This cohort was generally younger, included more primigravid women, and blood plasma samples were collected earlier in gestation (late second to early third trimester) compared to the St George Hospital cohort (mid to late third trimester; Table S8). The overall proportion of nulliparous women was similar in both cohorts, except that the St George Hospital cohort had a bias toward nulliparity in the PE group, the Nationwide Children's Hospital cohort had a similar proportion of nulliparous mothers across all outcomes (Table 3.3.3). The frequency of parity and gravidity for each outcome group is available in Table S9. There was no significant difference in gestational age at sampling, maternal age, nor the distribution of primigravid mothers when comparing adverse pregnancy outcomes with the normotensive group (Table 3.3.3). Conversely, Caucasian women were underrepresented in the PE, PE + IUGR, and sPTB groups compared to normotensive pregnancy (Table 3.3.3).

**Table 3.3.3:** Maternal characteristics grouped by pregnancy outcome in the Nationwide Children's Hospital cohort. Maternal characteristics were collected at time of sampling.

	Normotensive	PE	р	PE + IUGR	р	sPTB	р
n	30	30		31		30	
GA at sampling (weeks)	28.38 ± 3.04	27.93 ± 3.00	1	27.47 ± 2.81	0.69	27.37 ± 2.88	0.6
Maternal age (years)	28.33 ± 4.48	27.50 ± 7.27	1	28.29 ± 7.13	1	26.10 ± 6.07	0.33
Nulliparous	16 (53.3)	16 (53.3)	1	21 (67.7)	0.9	14 (46.7)	1
Primigravida	13 (43.3)	12 (40)	1	16 (51.6)	1	9 (30)	1.26
Caucasian	23 (76.67)	10 (33.33)	0.006	13 (41.93)	0.03	9 (30)	0.003
Early onset (<34 weeks)	N/A	30 (100)	N/A	31 (100)	N/A	N/A	N/A

Normally distributed variables compared using Student's T-test and reported as mean  $\pm$  SD. Non-normally distributed variables compared using two-tailed Mann-Whitney U test and reported as median (IQR). Categorical variables compared using Fisher's exact test (2-sided) and reported as n (%), Fisher's exact test (2-sided). Reported p-value is adjusted using the Bonferroni correction for multiple comparisons and is compared to the normotensive group. Gravidity includes the current pregnancy.

## 3.3.2.1 Maternal plasma PZP concentration was not associated with adverse pregnancy outcomes

As observed in the St George Hospital cohort, maternal plasma PZP concentration in the Nationwide Children's Hospital cohort varied greatly between women of similar gestational age, ranging from 5.34 µg/mL to 750.96 µg/mL. There were no significant differences in median PZP concentration between normotensive pregnancies and pregnancies complicated by PE, PE + IUGR, or sPTB (Figure 3.3.4). To further assess the relationship between PZP and pregnancy outcome, logistic regression modelling adjusted for parity and gestational age at sampling was performed. The model was not adjusted for BMI as this information was not available for the participants in the Nationwide Children's Hospital cohort. There was no association between PZP or parity and pregnancy outcome in any of the models assessed (Table S10).

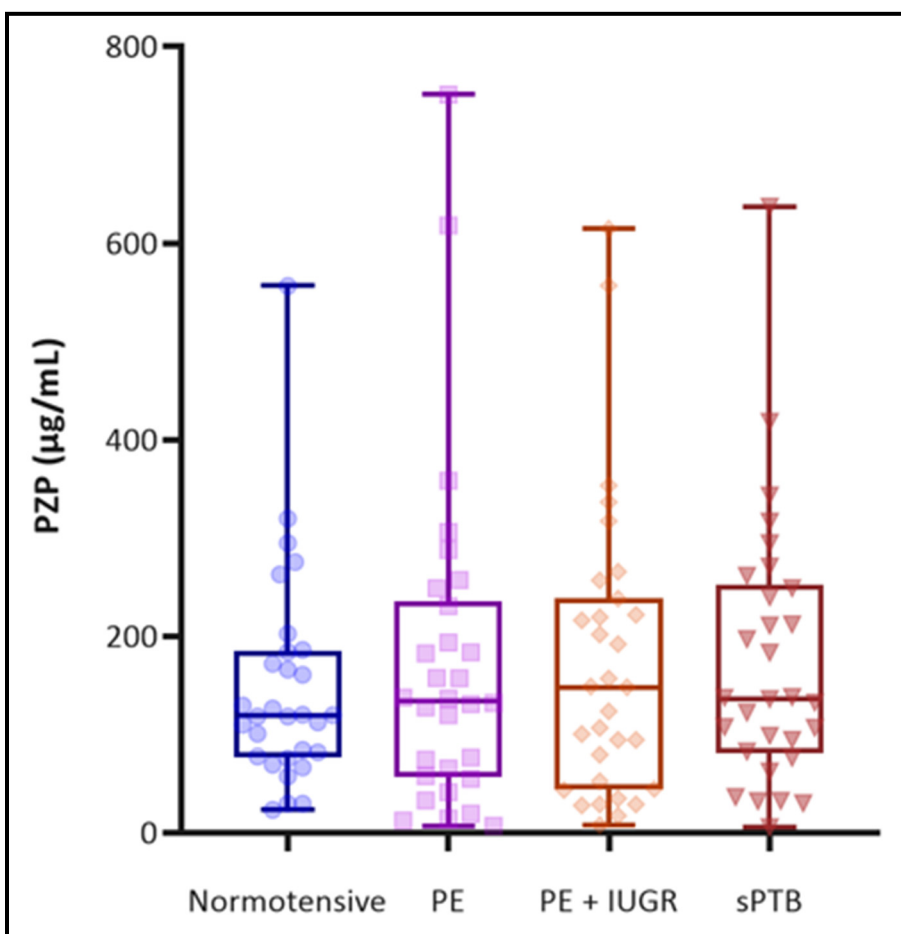


**Figure 3.3.4:** Unadjusted maternal plasma PZP concentration grouped by pregnancy outcome in the Nationwide Children's Hospital cohort. Kruskal-Wallis test with Dunn's post hoc multiple comparisons; no statistically significant differences were observed between groups. n = 121 (30 normotensive, 30 PE, 31 PE + IUGR, 30 sPTB).

## 3.3.2.2 Maternal plasma PZP concentration weakly correlated with parity and gravidity

Consistent with the main finding from the St George Hospital cohort, maternal plasma PZP concentration in the Nationwide Children's Hospital cohort showed a weak positive correlation with parity (Figure 3.3.5). Additionally, the correlation between PZP concentration and gravidity, though weaker, was statistically significant. No other variable was found to correlate with PZP concentration in this cohort (Table S11) and there was no difference in median PZP concentration between Caucasian and non-Caucasian women (p = 0.34; Figure S3).

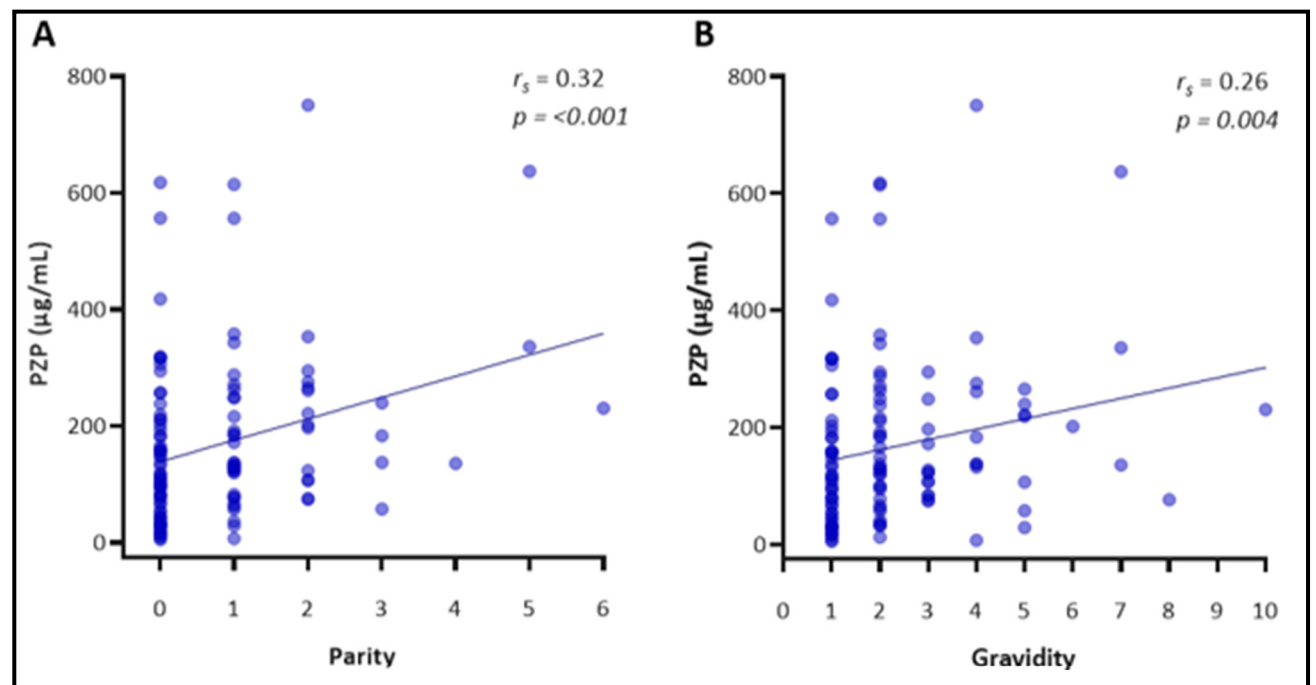


**Figure 3.3.5:** Correlation between maternal plasma PZP concentration and maternal characteristics in the Nationwide Children's Hospital cohort. **(A)** Parity; **(B)** gravidity. Spearman's rho; n =121.

## 3.3.2.3 Parity and gravidity were significantly associated with maternal plasma PZP concentration

Linear regression modelling was performed to further investigate the association between maternal plasma PZP concentration and parity or gravidity. Models to assess the influence of parity and gravidity on log-transformed PZP concentration were initially adjusted for gestational age at sampling but the AIC and BIC supported that univariate linear regression fit the data best (Table S12). Accordingly, being parous or multigravid was associated with 74.8% and 68.9% higher maternal plasma PZP concentration compared to being nulliparous or primigravida, respectively (Table 3.3.4). Consistent with these findings the median PZP concentration was higher in parous (177.82, IQR 107.35 – 263.67  $\mu$ g/mL) and multigravid (137.85, IQR 94.40 –

248.98  $\mu$ g/mL) women compared to nulliparous (106.94, IQR 43.34 – 183.11 $\mu$ g/mL, p = 0.001) or primigravid (105.37, IQR 34.28 – 182.61  $\mu$ g/mL, p = 0.005) women, respectively (Figure 3.3.6).

**Table 3.3.4:** Univariate linear regression analyses assessing the association between maternal characteristics and maternal plasma PZP concentration in the Nationwide Children's Hospital cohort (n = 121).

Characteristic	Ratio of geometric means [95% CI]	р
Parity (parous versus nulliparous)	1.748 [1.255, 2.437]	<0.001
Gravidity (multigravida versus primigravida)	1.689 [1.206, 2.367]	0.002

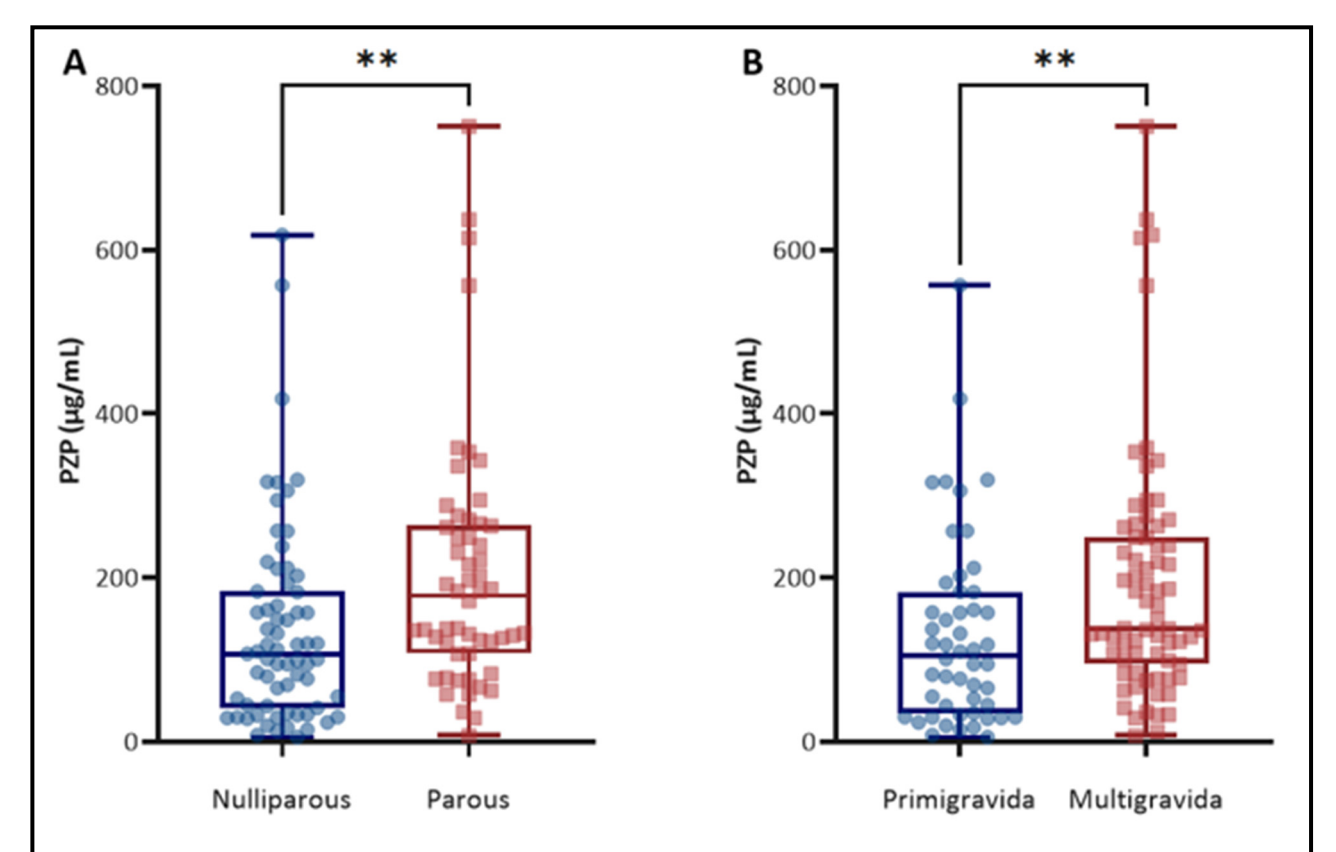


**Figure 3.3.6:** Unadjusted maternal plasma PZP concentration grouped by **(A)** parity and **(B)** gravidity in the Nationwide Children's Hospital cohort.

(A) Nulliparous (n = 67) versus parous (n = 54); (B) primigravida (n = 50) versus multigravida (n = 71). Two-tailed Mann-Whitney U, significance indicated with asterisks (\*\* p < 0.01).

When the data were separated by pregnancy outcome and further stratified by parity or gravidity, there was a general trend towards higher maternal plasma PZP concentrations in parous and multigravid pregnancy. However, the limited sample sizes in each subgroup precluded statistical analysis (Figure 3.3.7).

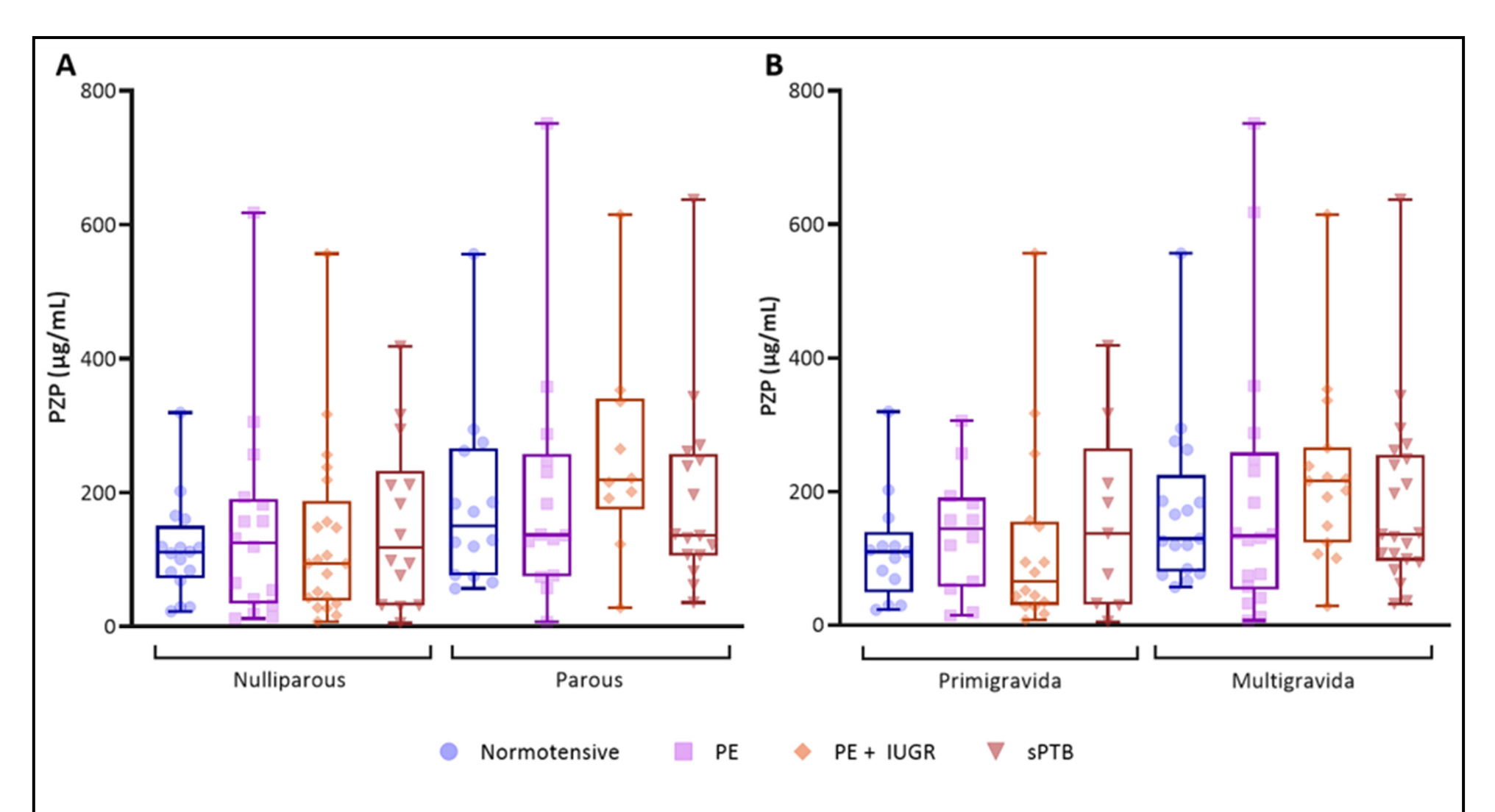


Figure 3.3.7: Unadjusted maternal plasma PZP concentration grouped by pregnancy outcome and stratified by (A) parity and (B) gravidity in the Nationwide Children's Hospital cohort.

No statistical analyses performed due to limited n in some groups.

## 3.3.3 Late STOP cohort

Data from both the St George Hospital and Nationwide Children's Hospital cohorts showed that maternal plasma PZP concentration is associated with parity. However, PZP concentration was only associated with gravidity in the Nationwide Children's Hospital cohort. Therefore, to further investigate the relationship between PZP and pregnancy outcome or maternal and neonatal characteristics, PZP concentration was measured in blood plasma samples collected from a cohort of nulliparous women during the mid third trimester. Compared to the previous cohorts analysed, the late STOP cohort was larger (n = 535) and included comprehensive clinical and demographic information for the participants. This cohort included samples from uncomplicated, PE, GH, GDM, SGA, sPTB, and otherwise complicated pregnancies. Relevant maternal and neonatal characteristics are presented in Table 3.3.5, with additional information regarding comorbidities available in Table S15. Women with PE, GH, or GDM had higher BMIs compared to those with uncomplicated pregnancies, and there were fewer Caucasian women with GDM. Birthweight was significantly lower for babies born to women with PE, SGA, or sPTB compared to the uncomplicated group. In the remaining pregnancy complications, there were no differences when compared to uncomplicated pregnancy in terms of BMI, ethnicity, or birthweight. There were also no significant differences between uncomplicated and adverse pregnancies in terms of gestational age at sampling, maternal age, smoking status, neonatal sex, or the proportion of primigravid mothers. The frequency of gravidity for each pregnancy outcome is available in Table S16.

**Table 3.3.5:** Maternal and neonatal characteristics grouped by pregnancy outcome in the late STOP cohort. Maternal characteristics collected at time of recruitment (11 – 16 weeks gestation).

	Uncomplicated	PE	р	GH	р	GDM	р	SGA	р	sPTB	р	Other	p
n	289	59		23		57		54		19		34	
GA at sampling (weeks)	34.0 (33.9 – 35.0)	34.0 (34.0 – 35.0)	1	34.0 (32.7 – 34.0)	0.70	34.0 (33.2 – 34.6)	1	34.0 (33.9 – 35.0)	1	34.0 (34.0 – 34.0)	0.89	34.0 (34.0 – 35.3)	1
Maternal age (years)	26.0 (23.0 – 29.0)	25.0 (23.0 – 29.0)	1	26.0 (23.0 – 31.0)	1	28.0 (23.0 – 32.0)	0.06	26.0 (23.0 – 29.0)	1	22.0 (20.0 – 29.0)	0.60	26.0 (22.8 – 29.0)	1
BMI (kg/m²)	25.5 (22.6 – 29.8)	29.6 (25.0 – 35.7)	0.006	29.5 (26.3 – 35.7)	0.02	29.3 (22.6 – 36.2)	0.03	28.3 (23.1 – 33.1)	0.48	25.4 (21.6 – 32.3)	1	27.9 (22.7 – 36.4)	0.44
Smoker (no)	244 (84.4)	50 (84.7)	1	17 (73.9)	1	48 (84.2)	1	42 (77.8)	1	15 (78.9)	1	28 (82.4)	1
Ethnicity (Caucasian)	248 (85.8)	55 (93.2)	0.84	21 (91.3)	1	40 (70.2)	0.04	50 (92.6)	1	17 (89.5)	1	30 (88.2)	1
Primigravida	222 (76.8)	42 (71.2)	1	16 (69.6)	1	38 (66.7)	0.64	34 (63.0)	0.19	13 (68.4)	1	25 (73.5)	1
Neonatal sex (F)	136 (47.1)	23 (39)	1	8 (34.8)	1	37 (64.9)	0.12	22 (40.7)	1	7 (36.8)	1	14 (41.2)	1
Birthweight (g)	3556 (3270 – 3790)	3114 (2726 – 3610)	0.006	3360 (3250 – 3615)	0.45	3435 (3246 – 3737)	1	2845 (2593 – 2995)	0.0006	2835 (2485 – 3235)	0.0006	3466 (3160 – 3714)	1
Early onset (<34 weeks)	N/A	1 (1.7)	N/A	N/A	N/A	N/A	N/A	N/A	N/A	N/A	N/A	N/A	N/A

Continuous variables compared using two-tailed Mann-Whitney U test and reported as median (IQR). Categorical variables compared using chi-square test and reported as n (%). All reported p-values are adjusted using the Bonferroni correction for multiple comparisons and are compared to the uncomplicated group.

## 3.3.3.1 Maternal plasma PZP concentration was not associated with adverse pregnancy outcomes

Consistent with the substantial inter-participant variation observed in the first two cohorts, maternal plasma PZP concentration ranged from 0.71  $\mu$ g/mL to 690.73  $\mu$ g/mL in mothers of similar gestational age. There was no significant difference in median PZP concentration between women with uncomplicated pregnancy and those with complications (Figure 3.3.8). To further investigate the relationship between PZP concentration and pregnancy outcome logistic regression modelling was performed. The AIC and BIC assessment supported that a model adjusted for BMI and gestational age at sampling provided the best fit (Table S17). However, PZP was not significantly associated with pregnancy outcomes in a model adjusted for these factors (Table S18). When mothers with PE + SGA were separated from those with PE + AGA there was no difference between median PZP concentration (p = 0.77), nor any association between PZP concentration and pregnancy outcome by logistic regression analysis (odds ratio [95% CI]: 0.999 [0.995, 1.002]; p = 0.47).

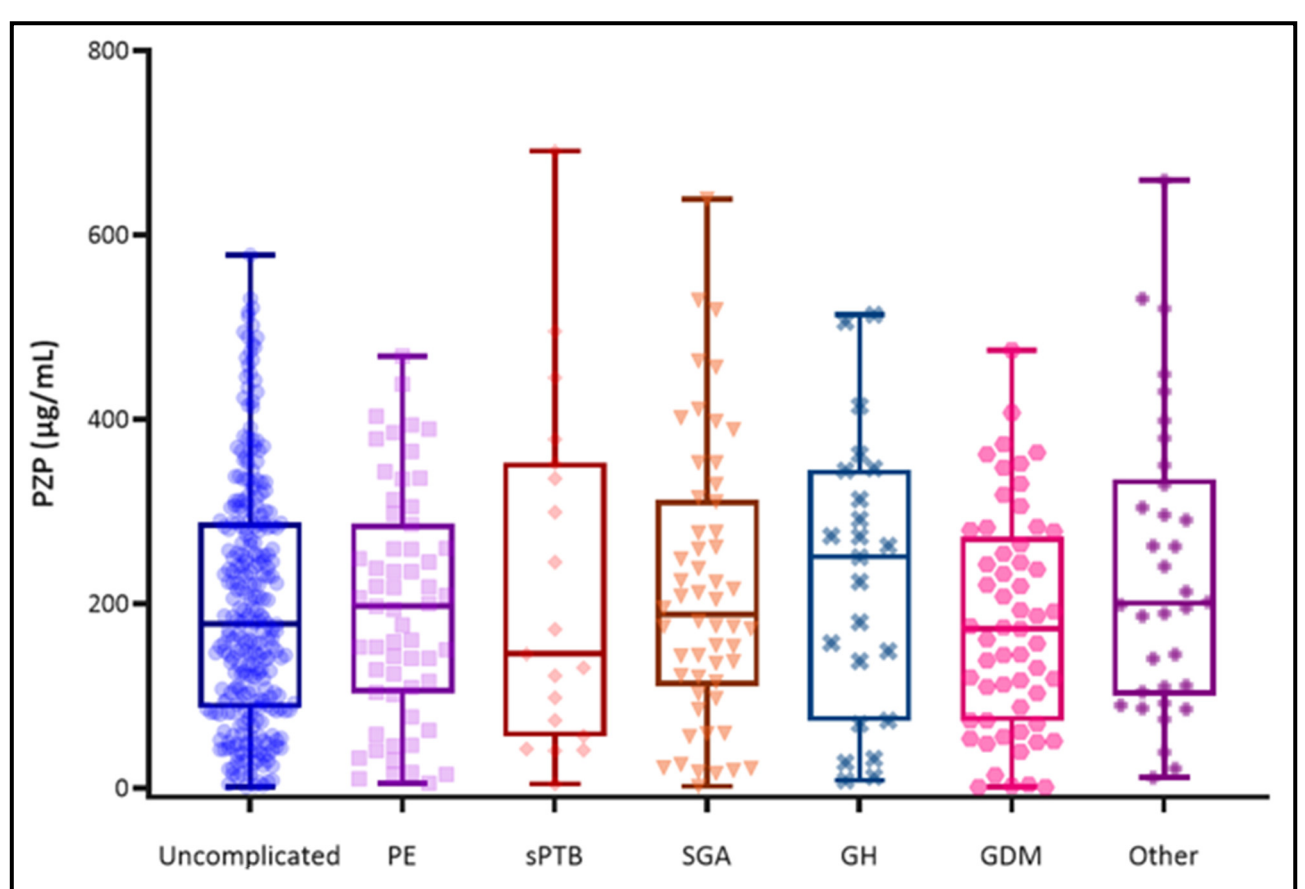


**Figure 3.3.8:** Unadjusted maternal plasma PZP concentration grouped by pregnancy outcome in the late STOP cohort. Kruskal-Wallis test with Dunn's post hoc multiple comparisons; no statistically significant differences were observed between groups. n = 535 (289 uncomplicated, 59 PE, 23 GH, 57 GDM, 54 SGA, 19 sPTB, 34 other).

## 3.3.3.2 Maternal plasma PZP concentration was lower in non-Caucasian mothers and weakly correlated with BMI

Ethnicity significantly influenced PZP concentration, with lower median PZP levels in non-Caucasian women (134.25, IQR 48.49 – 245.57 µg/mL) compared to Caucasian women (192.9, IQR 97.50 – 296.57 µg/mL, p = 0.001) (Figure 3.3.9). PZP did not differ by neonatal sex (p = 0.84), smoking status (p = 0.71) or gravidity (primigravida versus multigravida; p = 0.36).

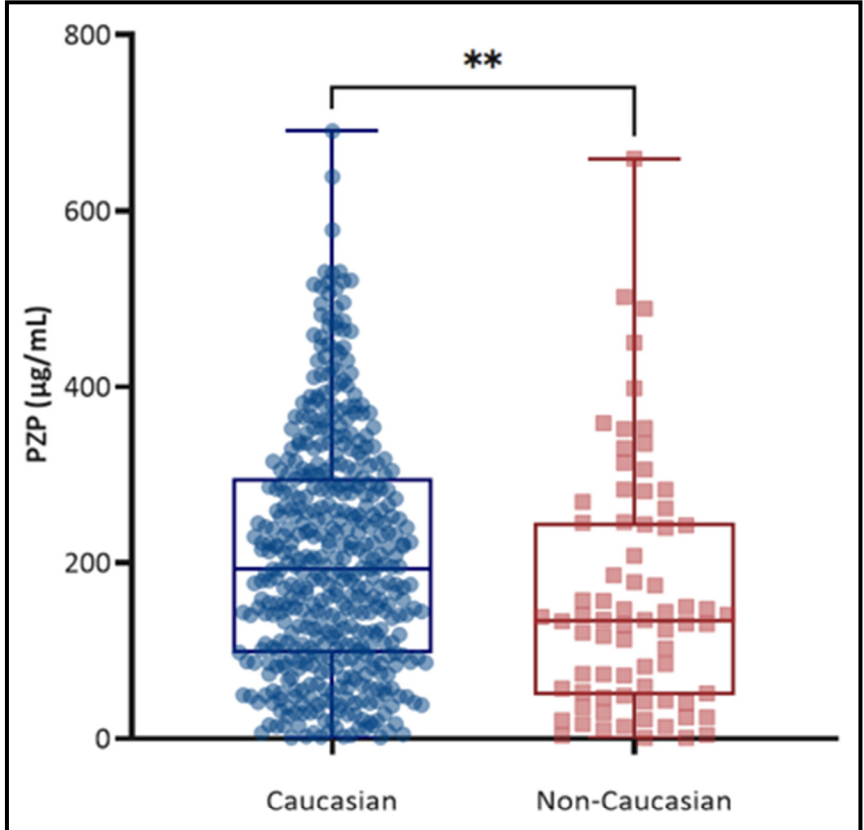


**Figure 3.3.9:** Unadjusted maternal plasma PZP concentration, grouped by ethnicity, in the late STOP cohort. Two-tailed Mann-Whitney U test; significance indicated with asterisks (\*\* p < 0.01). n = 535 (461 Caucasian, 74 non-Caucasian).

To assess the association between maternal plasma PZP concentration and continuous maternal or neonatal characteristics correlation analyses were performed. The only characteristic that correlated with PZP was BMI, which demonstrated a very weak positive correlation ( $r_s = 0.114$ , p = 0.008). PZP concentration did not significantly correlate with gestational age at sampling, maternal age, gravidity, nor birthweight (Table S19). To further investigate those characteristics that significantly correlated with maternal plasma PZP concentration quantile regression analyses at the 0.25, 0.5, and 0.75 quantiles were performed. The results showed that the association between BMI and PZP concentration was only significant at the 0.75 quantile (Table 3.3.6).

**Table 3.3.6:** Univariate quantile regression analyses assessing the association between maternal characteristics and maternal plasma PZP concentration in the late STOP cohort (n = 535).

	Quantile									
	0.25 (91.10 μg/ml	_)	0.5 (181.00 μg/mL	0.75 (288.31 μg/mL)						
	Coefficient [95% CI]	р	Coefficient [95% CI]	р	Coefficient [95% CI]	р				
BMI (kg/m²)	1.329 [-0.445, 3.103]	0.14	1.161 [-1.064, 3.385]	0.31	2.622 [0.195, 5.050]	0.03				

The coefficient represents the change in PZP concentration (µg/mL) per 1-unit increase in BMI at the specified quantile.

## 3.4 Discussion

The results of this study provide much needed insight regarding maternal plasma PZP concentrations in the third trimester of pregnancy and support the conclusion that PZP levels are influenced by parity. A key strength of this study is that PZP concentration was measured in blood samples from three independent pregnancy cohorts, enhancing the robustness and generalisability of findings that were consistent. While  $\alpha_2 M$  and PZP are relatively unstable once purified from blood plasma (Wyatt et al., 2015, Bonacci et al., 2000),  $\alpha_2 M$  has been shown to remain stable in plasma after long-term storage (Mendes et al., 2023). However, caution is needed when making cross-cohort comparison due to methodological differences, including the duration of plasma storage for each cohort, and differences in gestational age at sampling and participant demographic characteristics. A consistent finding across all cohorts, and in line with prior reports, there was remarkably wide variation in circulating PZP concentrations in women of similar gestational age. In some cases, PZP concentrations approached the mg/mL range, while in others only trace levels were detected.

Comparison of median PZP concentrations across the three cohorts supports that there is a relative peak in maternal plasma PZP during the middle of the third trimester (Figure S4). However, this increase may commonly be less pronounced than that reported in the foundational study by Ekelund and Laurell (1994), which examined plasma PZP concentration longitudinally across gestation in a small number of mothers. Combined, these findings underscore the need for further investigation into the factors that regulate PZP expression and its potential relevance to pregnancy-related physiology and complications.

# 3.4.1 Maternal plasma PZP concentration was lower in nulliparous versus parous pregnancy during mid-late gestation

The results presented in this chapter provide the first evidence that there is an association between maternal plasma PZP concentration and parity, whereby PZP concentration is

reduced in nulliparous mothers. A weak positive correlation between plasma PZP concentration and parity was identified in two independent pregnancy cohorts. However, only a small number of samples from mothers with parity ≥2 were available for analysis. Therefore, further studies are needed to more accurately describe the association between PZP concentration and parity ≥2. Although gravidity was associated with maternal plasma PZP concentration in the Nationwide Children's Hospital cohort, the results obtained from the nulliparous late STOP cohort confirmed that the number of births, rather than the number of pregnancies, is the key factor. The reasons for this are unclear but it suggests that PZP expression is influenced by biological processes that occur later in pregnancy, beyond the early stages when spontaneous miscarriage is most likely to occur.

It is generally agreed that parous women experience more favourable pregnancy outcomes compared to their nulliparous counterparts. However, the molecular mechanisms underpinning this association remain incompletely understood. A key distinction in parous pregnancies is the presence of pregnancy-trained decidual natural killer (PTdNK) cells, which are thought to enhance placental development and contribute to a lower incidence of obstetrical syndromes that have their basis in defects of placentation (Gamliel et al., 2018). These PTdNK cells secrete greater amounts of VEGFA and IFN-y, which promote vascularisation and placentation (Gamliel et al., 2018). Additionally, the persistence of trained immunity in subsequent pregnancies may allow for more efficient spiral artery remodelling and a more tolerogenic immune environment. Given PZP's putative immunomodulatory role, its elevated levels in parous pregnancies may help buffer excessive inflammation, complementing the posited pregnancy-induced immunological memory that promotes a more tolerogenic and anti-inflammatory maternal immune state in subsequent pregnancies (Huang et al., 2021).

## 3.4.2 Potential mechanism for the parity-associated increase in maternal plasma PZP concentration

The finding that maternal plasma PZP was elevated in multiparous mothers compared to nulliparous mothers challenges the idea that PZP is primarily upregulated by estrogen during pregnancy, as suggested by early research (Damber et al., 1976, Ottosson et al., 1981). Numerous studies have reported that estrogen levels are higher in nulliparous pregnancy compared to parous pregnancy (Schock et al., 2016, Bernstein et al., 1985, Arslan et al., 2006, Panagiotopoulou et al., 1990), thus alternative regulatory mechanisms must be responsible for the opposing relationship between parity and plasma PZP concentration. Additionally,

circulating PZP appears to peak in the middle of the third trimester, yet estrogen concentrations continuously increase throughout the entire duration of pregnancy (Schock et al., 2016). Given that PZP is upregulated in pregnancy-independent inflammatory states in both sexes (Smith et al., 2017, Shao et al., 2021, Nijholt et al., 2015, Huang et al., 2024), it is plausible that immunoregulation of PZP expression plays a more significant role in pregnancy than currently recognised. *In vitro* studies investigating the regulation of PZP production by placental cells in response to cytokines or other immunomodulatory factors would provide mechanistic insight into the specific pathways governing its expression.

Chromatin immunoprecipitation sequencing (ChIP-seq) has identified binding sites for signal transducers and activators of transcription (STATs) 3 and 5a on the PZP gene (Lachmann et al., 2010, Zhang et al., 2013, ENCODE Project Consortium, 2004), suggesting that STAT signalling may regulate PZP expression. In multiparous pregnancies, concentrations of STAT3 and STAT5a activators (Bai et al., 2021, Nguyen et al., 2015, Lin and Leonard, 2000, Platanias, 2005), including IL-8, IL-13, IL-15, IL-17 (Sanchez et al., 2021, Jarmund et al., 2021) and IFN-γ (Gamliel et al., 2018) are increased compared to nulliparous pregnancies. The biological mechanisms driving these cytokine differences remain unclear but may be influenced by immune tolerance to paternal antigens, whereby prior immune exposure leads to epigenetic and functional adaptations following a first pregnancy. Supporting this, mouse studies have shown that STAT binding sites, particularly those for STAT5a, become hypomethylated in subsequent pregnancies, allowing for more rapid activation of STAT-dependent genes (Dos Santos et al., 2015). Furthermore, both STAT5 signalling and maternal plasma PZP levels peak around 30 weeks gestation (Aghaeepour et al., 2017), lending additional support to the hypothesis that increased PZP in multiparous pregnancy may be driven by STAT signalling. Further work is needed to investigate this hypothesis, including in vitro experiments to assess the effect of STAT-activating cytokines on PZP expression in liver or placental cell lines and organoids. Additionally, measurement of STAT activation, cytokine profiles and PZP levels across gestation could help determine whether STAT signalling plays a role in regulating PZP in vivo. At present, though, this remains speculative and requires mechanistic validation.

Although immune responses may contribute to the regulation of maternal plasma PZP concentration, in the current study, there was no association between increased PZP concentration and adverse pregnancy outcomes involving inflammatory pathology, such as PE, IUGR, or PTB (Couture et al., 2024, Mei et al., 2022, Yin et al., 2021, Medina-Bastidas et al.,

2020). One potential explanation is the heterogeneity of these conditions. A major challenge for studying pregnancy complications is the substantial variation in their presentation. Even when cases share the same clinical diagnosis, the underlying pathophysiological processes can differ significantly – a key example being PE, which can manifest through distinct biological pathways (Torres-Torres et al., 2024). The presence of comorbidities further complicates the molecular landscape, making it difficult to isolate the contribution of individual factors such as PZP.

Other variables, such as ethnicity and BMI, also need to be considered. Racial differences in interferon responses have been reported (Reddy et al., 1999, Gaglio et al., 2004, Kimball et al., 2001), which may subsequently influence maternal plasma PZP concentration. In the current study, PZP was lower in non-Caucasian women compared to Caucasian women in the late STOP cohort but not in the Nationwide Children's Hospital cohort. However, this finding is provisional as sample sizes did not permit the analysis of individual ethnicities within the non-Caucasian groups that were biased toward Hispanic and African American in the Nationwide Children's Hospital cohort, and South, South East and Far East Asia in the late STOP cohort. Consistent with the prior study of Fosheim et al. (2023), a weak positive correlation between PZP and BMI was observed in the late STOP cohort. The results of regression modelling indicated that BMI was positively associated with PZP concentration but only at the upper end of the distribution (0.75 quantile), with no evidence of an association across the full range of PZP concentrations. These findings highlight the complexity of PZP regulation and underscore the need for further research to elucidate the precise genetic, environmental, and/or health-related factors that underpin these results.

# 3.4.3 There was no association between maternal plasma PZP concentration and LO-PE in the third trimester of nulliparous pregnancy

Consistent with the findings of Fosheim et al. (2023), data from the late STOP cohort support the conclusion that there is no association between circulating PZP concentration in the third trimester of pregnancy and LO-PE. A major strength of the current study, compared to Fosheim et al. (2023), is the use of plasma samples from a uniformly nulliparous cohort collected within a narrow gestational window, thereby reducing confounding related to parity and gestational age at sampling. A limitation, though, is the lack of corresponding samples from EO-PE, which is less common than LO-PE. In the light of new knowledge that parity is an important consideration, further studies are needed to validate the association between EO-PE and

circulating PZP concentration. Notably, nulliparity is known as a major risk factor for PE, regardless of time of onset (Bartsch et al., 2016, Lisonkova and Joseph, 2013). Therefore, its plausible that an over-representation of nulliparous mothers with PE compared to controls potentially underpins previous reports of lower circulating PZP concentration in PE (Horne et al., 1979, Rasanen et al., 2010, Liu et al., 2011, Fosheim et al., 2023).

In PE, elevated sFlt-1/PIGF ratio reflects an imbalance in angiogenic factors, skewing toward the anti-angiogenic state that contributes to placental dysfunction (Kwiatkowski et al., 2021). While it has been suggested that a negative correlation between PZP and the sFlt-1/PIGF ratio may link PZP deficiency to placental dysfunction (Fosheim et al., 2023), the regression analysis performed in this study provides little evidence that these two parameters affect one another. Given that the sFlt-1/PIGF ratio is elevated in nulliparous pregnancies compared to parous pregnancies (Law et al., 2010), further investigation is needed to clarify its relationship with circulating PZP concentration. This will help determine whether their association is independent or a reflects underlying factors such as parity.

## 3.4.4 Concluding remarks

Although the results presented in this chapter provide important new knowledge about the association between maternal plasma PZP concentration and parity, no evidence was found for any association between PZP concentration and pregnancy outcome in third trimester samples from nulliparous mothers. Notably, circulating levels of PZP decline during the third trimester (Ekelund and Laurell, 1994) but it is currently unknown if this relates to enhanced clearance, decreased expression, or a combination of these mechanisms. Regardless, it is plausible that the biological importance of PZP in pregnancy is relevant to the early stages of gestation when there is a rapid increase in circulating PZP concentration, rather than later in pregnancy when PZP concentrations decline. Studies utilising samples from earlier pregnancy, such as those described in the next chapter of this thesis, may therefore provide greater insight regarding the biological importance of PZP.

## **CHAPTER 4:**

# MEASUREMENT OF MATERNAL PLASMA PZP CONCENTRATION IN NULLIPAROUS PREGNANCY

## 4.1 Introduction

Parity influences maternal biology, inducing distinct differences in gene expression between parous and nulliparous women. These differences are mediated, in part, by epigenetic mechanisms such as changes in DNA methylation. In immune cells from women with multiple sclerosis (MS), parity has been associated with thousands of differentially methylated positions linked to pathways involved in axon guidance, immune regulation, developmental biology, and cell-cell communication (Mehta et al., 2019, Campagna et al., 2023). These epigenetic changes have been shown to persist for up to 44 years following pregnancy. Similar effects are also seen in women without any underlying disease, where 184 CpG sites have been identified as differentially methylated between parous and nulliparous women in DNA derived from peripheral blood. These changes are linked to genes involved in neuroplasticity, immune function, and metabolism (Chen et al., 2024). Additionally, pregnancy alters DNA methylation patterns in genes associated with T-cell differentiation and inflammatory pathways (Ross et al., 2020). These findings highlight parity's broader role in shaping maternal biology and its potential to influence maternal immune adaptation during pregnancy.

Differences between nulliparous and parous women are also reflected in the composition of maternal plasma. Early studies reported that, compared to nulliparous women, parous women had 4% higher total plasma protein levels at 10 weeks gestation (Macdonald and Good, 1972). The concentration of specific proteins, including albumin (Macdonald and Good, 1972), IgG (Tandon et al., 1985), and PAPP-A and -D (Lin et al., 1974, Lin et al., 1976), are also reportedly increased in the plasma of parous women compared to nulliparous women. While the findings of these early studies may have limited reliability due to the protein quantification methods available at the time, the results of contemporary studies also support the association between parity and changes in the maternal plasma proteome. For example, parity is reported to influence 50% of principal components representing groups of proteins that captured key patterns in the maternal plasma proteome (Tarca et al., 2022). Specific proteins, including fibrinogen (Dai et al., 2023a), trefoil factor 3 (TFF3), and serine/threonine-protein kinase (DCAK1) were found to be elevated in nulliparous women compared to parous women (Tarca et al., 2022). The effect of parity extends to hormone levels too, with significantly lower levels of progesterone, 17-OH progesterone, and estradiol reported in parous women, compared to nulliparous women, in the first trimester (Järvelä et al., 2012).

Parity-related physiological and molecular changes may explain why nulliparous women are at greater risk of several complications including GH, PE, PTB, SGA, PROM, postpartum haemorrhage (PPH), and stillbirth (Rurangirwa et al., 2012, Bai et al., 2002, Willinger et al., 2009, Dai et al., 2023b, Magee et al., 2022). For example, the relative risk or odds ratio reported for the association between nulliparity and PE ranges between 2 and 3 (Duckitt and Harrington, 2005, Bartsch et al., 2016, Misra and Kiely, 1997). However, the association between parity and risk of pregnancy complications is not always linear. The risk of antepartum haemorrhage (APH), GDM, GH, PROM, threatened preterm labour (TPL), PPH, or  $3^{rd}$  degree tears, is highest in nulliparous women and lowest in women with parity of 1-3 but the risk of these complications then increases again with parity  $\geq 4$  (grand multiparity; Bai et al., 2002). Furthermore, the influence of maternal characteristics such as age and ethnicity on pregnancy outcomes may vary with parity (Fretts, 2005, Misra and Kiely, 1997), highlighting the importance of accounting for this factor when characterising pregnancy-related molecules.

A limited number of studies have reliably quantified PZP in maternal pregnancy plasma (Table 3.1.1), and of these, none have included large, well-characterised cohorts that were matched by parity. Building on the previous chapter, which identified parity as a significant determinant of maternal plasma PZP concentration, it was hypothesised that restricting analyses to nulliparous mothers would reduce confounding and reveal associations that may have been obscured in mixed-parity cohorts. This chapter therefore characterised maternal plasma PZP concentration in two independent cohorts of nulliparous mothers.

The specific aims of this chapter were to:

- 1) Quantify maternal plasma PZP concentrations in nulliparous pregnancy using samples obtained from women who had uncomplicated and adverse pregnancies
- 2) Investigate the association between maternal plasma PZP concentration and maternal and neonatal characteristics, including pregnancy outcomes, in nulliparous women

## 4.2 Methods

## 4.2.1 Recruitment

Pregnancy plasma samples analysed in this chapter were obtained from participants recruited to the prospective cohort studies **Sc**reening for Pregnancy Endpoints (SCOPE) and Screening Tests to identify poor Outcomes of Pregnancy (STOP) (Figure 4.2.1; Table 4.2.1). SCOPE was a

multi-centre international study, and the samples used herein were exclusively from the South Australian arm of the study. STOP participants were largely recruited at the same hospital as the Australian arm of the SCOPE study (Table 4.2.1). PE was defined as systolic blood pressure ≥140 mmHg and/or diastolic blood pressure ≥90 mmHg after 20 weeks gestation on at least 2 occasions 4 h apart, along with proteinuria and/or any multi-system complication of PE. sPTB was defined as spontaneous preterm labour or preterm PROM resulting in birth <37 weeks. GH was defined as new-onset hypertension (systolic ≥140 mmHg and/or diastolic blood pressure ≥90 mmHg) after 20 weeks gestation. SGA was defined as birthweight <10<sup>th</sup> percentile using customised centiles adjusted for maternal weight, height, parity, ethnicity, and infant sex. GDM was diagnosed by a 75 g oral glucose tolerance test with fasting glucose ≥5.1 mmol/L and/or 2 h glucose ≥7.8 mmol/L (Mohammed et al., 2020, Jankovic-Karasoulos et al., 2021). If multiple complications were present a hierarchy was used to classify cases where PE > sPTB > GH > SGA > GDM. Women who experienced a complication other than those listed were classified as 'other'.

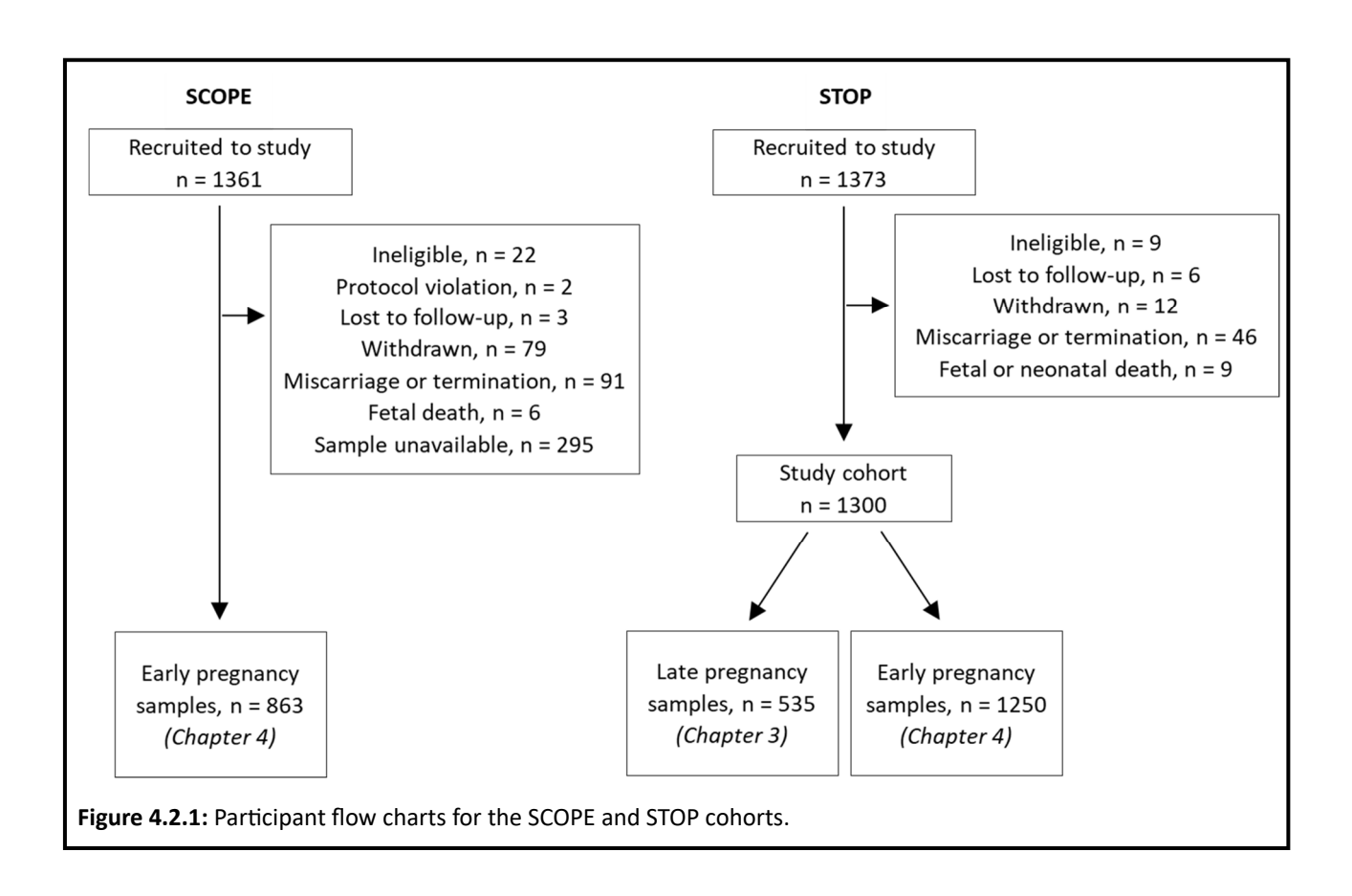


**Table 4.2.1:** Details for the recruitment of participants to the prospective cohort studies SCOPE and STOP.

Study	Recruitment Locations	Recruitment	Gestational Age	Eligibility	Exclusion Criteria				
	(within South Australia)	Dates	at Recruitment	Criteria					
					≥3 terminations or miscarriages				
					Major fetal or uterine anomalies				
					Abnormal karyotype				
					Treated hypertension pre-pregnancy				
				Healthy	Renal disease				
SCOPE	Lyell McEwin Hospital				Anti-phospholipid syndrome				
30012	(Elizabeth Vale)	2005 – 2008	14 – 16 weeks	Nulliparous	Sickle cell disease				
	(Elizabeth vale)				Systemic lupus erythematosus				
				Singleton	HIV positive				
					Long term steroids				
					Previous cervical cone biopsy or suture				
					Treatment with any of; low dose-aspirin, >1g/24h calcium, fish oil, ≥1000mg				
					vitamin C, ≥400iu vitamin E, heparin/low molecular weight heparin				
					≥3 terminations or miscarriages				
	Lyell McEwin Hospital				Major fetal or uterine anomalies				
	(Elizabeth Vale)			Healthy	Treated hypertension pre-pregnancy				
	(Liizabetii vale)				Renal disease				
STOP	Women's and Children's	2015 – 2018	9 – 16 weeks	Nulliparous	Anti-phospholipid syndrome				
	Hospital (North Adelaide)				Type I or II diabetes mellitus				
	Hospital (North Adelaide)			Singleton	Systemic lupus erythematosus				
					Previous cervical cone biopsy				

Australian and New Zealand Clinical Trials Registry: SCOPE - ACTRN12607000551493, STOP - ACTRN12614000985684.

## 4.2.2 Sample preparation and analysis

Heparinised blood samples were collected from SCOPE and STOP participants in early gestation and held on ice prior to processing. Plasma was isolated by centrifugation and stored at -80 °C in 250 µL aliquots for future analyses. Maternal plasma PZP concentrations were quantified using an ELISA kit and ancillary reagents (R&D Systems; cat# DY8280-05 and DY008) as per manufacturer's instructions. Briefly, plasma samples were thawed once, centrifuged (21,000 x g, 5 min, 4 °C), and serially diluted (~1:25,000 final) using PBS as the dilution matrix. A seven-point standard curve (156–10,000 pg/mL) was prepared in plasma-PBS, generated by a 25,000-fold dilution of normal plasma in PBS to match the sample matrix, with a blank included. Bound PZP was detected using a biotinylated anti-PZP antibody, streptavidin-HRP, and colorimetric detection with TMB substrate, read at 450 nm with 540/570 nm correction. The antibodies used have been confirmed by the manufacturer to exhibit no cross-reactivity with the natural protein  $\alpha_2M$  or the recombinant proteins CD109, LDL R,  $\alpha_2ML1$ , complement C3a and complement C5a. All assays were performed by the candidate to reduce inter-user variability, and a pooled plasma control sample was included on each plate to monitor interplate consistency. Samples were randomised across 96-well assay plates, together with the late STOP samples (Chapter 2), to avoid cohort bias and minimise potential plate effects. The inter-assay and intra-assay coefficients of variation were 11.3% and <10%, respectively. Duplicate samples with readings that differed by >10% coefficient of variation were re-analysed (in duplicate) as a quality control measure. C-reactive protein (CRP; mg/L), serum folate (nmol/L), vitamin B12 (pmol/L) and homocysteine (Hcy, µmol/L) were quantified by Clinpath Laboratories (Adelaide, South Australia) using chemiluminescent immunoassays on an Abbott Alinity automated immunoassay analyser at the time of recruitment. Parameters of folate status were included because participants in the SCOPE and STOP cohorts were recruited either side of the introduction of mandatory folic acid food fortification in Australia in 2009.

## 4.2.3 Statistical analysis

Maternal plasma PZP concentration was interpolated using a four-parameter logistic (4PL) curve fit using GraphPad Prism (version 9.0.0). Values below the detection threshold were assigned a minimum value of 0.001  $\mu$ g/mL. These comprised 1.8% and 0.46% of the STOP and SCOPE cohorts, respectively.

Descriptive statistics for maternal and neonatal characteristics are grouped by pregnancy outcome and reported separately for each cohort. Due to the small sample sizes within each ethnic group, participants were broadly categorised as 'Caucasian' and 'non-Caucasian' for all analyses. Categorical variables were compared using the chi squared test and are reported as n (%). Continuous skewed variables were compared using the Mann-Whitney U test adjusted using the Bonferroni correction to account for multiple comparisons or the Kruskal-Wallis test with Dunn's post-hoc comparisons and are reported as median (IQR). Spearman's rho was used to assess correlations between maternal plasma PZP concentration and relevant variables. Univariate quantile regression and generalised linear models were used to further assess the association between maternal and neonatal characteristics and PZP concentration.

Logistic regression models were used to assess the association between PZP concentration and pregnancy outcomes, treating PZP as both a continuous variable and a categorical variable based on the first quartile, median, and third quartile thresholds. Models were adjusted for gestational age at sampling and maternal BMI, as indicated. Unless otherwise specified, reported odds ratios reflect comparisons between adverse pregnancy outcomes and uncomplicated pregnancies.

## 4.3 Results

#### 4.3.1 STOP cohort

Although participants in the SCOPE cohort were recruited prior to those in the STOP cohort, results are presented for the STOP cohort first, as these samples were collected at an earlier gestational timepoint. Maternal plasma PZP concentrations were measured in blood plasma samples obtained during the late first trimester and grouped according to pregnancy outcome. Relevant maternal characteristics and neonatal outcomes are presented in Table 4.3.1, with additional information regarding comorbidities available in Table S20. All groups were similar in terms of the gestational age at sampling, smoking status, neonatal sex, and the percentage of primigravid mothers (Table 4.3.1). The frequency of gravidity for the overall cohort is provided in (Table S21). Maternal age and ethnicity were largely consistent between the groups, except for women with GDM who had higher median maternal age and a lower proportion of Caucasians, compared to uncomplicated pregnancies. Mothers with PE, GH, or GDM had significantly higher BMIs compared to those with uncomplicated pregnancy. As expected,

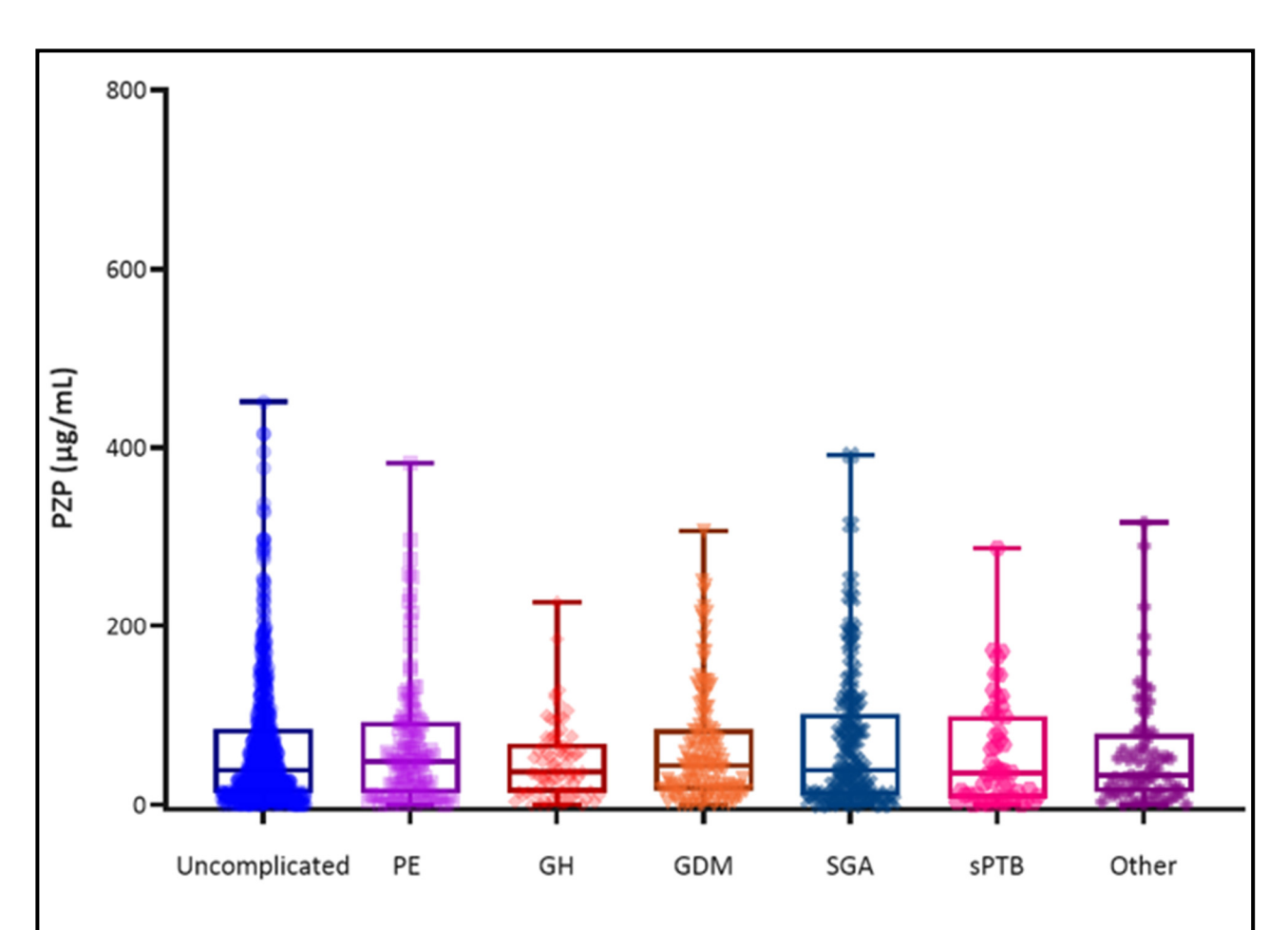
mothers with PE, SGA or sPTB gave birth to babies with significantly lower birthweight compared to those born from uncomplicated pregnancy (Table 4.3.1).

Table 4.3.1: Maternal and neonatal characteristics grouped by pregnancy outcome in the STOP cohort. Maternal characteristics collected at time of sampling.

	Uncomplicated	PE	p	GH	р	GDM	p	SGA	р	sPTB	p	Other	р
n	695	119		78		134		103		53		67	
Gestational age at sampling (weeks) <sup>a</sup>	11.1 (10.4 - 12.4)	11 (10.3 - 12.3)	0.82	11.1 (10.3 - 12.3)	1	11.1 (10.3 - 12.4)	1	11.1 (10.6 - 12.6)	1	10.9 (10.2 - 12)	0.54	11 (10.4 - 12.6)	1
Maternal age (years)	25 (22 - 29)	25 (21 - 28)	1	25.5 (23 - 29)	1	28 (23 - 31)	<0.001	26 (22 - 30)	1	24 (21 - 29.5)	1	26 (22 - 29)	1
BMI (kg/m²)b	25.3 (22.4 - 29.4)	29.9 (24.2 - 35.4)	<0.001	31.4 (25.8 - 38.3)	<0.001	28 (23.1 - 35.7)	<0.001	26.1 (22.7 - 31.4)	1	25.4 (21.4 - 32.2)	1	26 (22.1 - 32.6)	1
Non-smoker <sup>c</sup>	588 (85.2)	98 (82.4)	1	63 (80.8)	1	112 (83.6)	1	78 (75.7)	0.12	38 (71.7)	0.10	55 (82.1)	1
Ethnicity (Caucasian)	581 (83.5)	106 (89.1)	0.81	68 (87.2)	1	88 (65.7)	<0.001	87 (84.5)	1	45 (84.9)	1	58 (86.6)	1
Primigravida <sup>d</sup>	507 (73.7)	78 (66.1)	0.75	55 (72.4)	1	92 (68.7)	1	70 (68)	1	37 (71.2)	1	50 (74.6)	1
Neonatal sex (Female) <sup>e</sup>	353 (50.7)	51 (42.9)	0.82	35 (44.9)	1	77 (57.9)	0.79	44 (42.7)	0.84	21 (39.6)	0.92	31 (46.3)	1
Birthweight (g) <sup>f</sup>	3510 (3250 - 3790)	3100 (2595 - 3574)	<0.001	3355 (3148 - 3649)	0.14	3435 (3230 - 3755)	1	2800 (2520 - 2975)	<0.001	2546 (2080 - 2912)	<0.001	3422 (3095 - 3710)	0.22
Late-onset PE (≥34 weeks)	-	111 (93.3)	-	-	-	-	-	-	-	-	1	-	_

Continuous variables compared using two-tailed Mann-Whitney U test and reported as median (IQR). Categorical variables compared using chi-square test and reported as n (%). All reported p-values are adjusted using the Bonferroni correction for multiple comparisons and are compared to the uncomplicated group. Gravidity includes the current pregnancy. Missing data for  $^a$ n = 1 sPTB and 3 uncomplicated participants;  $^b$ n = 1 uncomplicated participants;  $^c$ n = 6 uncomplicated participants;  $^d$ n = 1 PE, 2 GH, 1 sPTB, and 8 uncomplicated participants;  $^e$ n = 1 GDM participant;  $^f$ n = 1 GDM participant.

There was large inter-participant variation in maternal plasma PZP concentration, with values ranging from 0.001 µg/mL (undetectable) to 450.85 µg/mL (Figure 4.3.1). There was no difference in the median PZP concentration between any of the pregnancy outcomes. To further investigate the relationship between PZP concentration and pregnancy outcome, logistic regression modelling, adjusted for maternal BMI and gestational age at sampling, was performed (Table S22). The results of logistic regression analyses using PZP concentration as a continuous independent variable showed that although the association between PZP and the odds of a woman having GH was statistically significant (p = 0.04), the effect size was very small (odds ratio [95% CI]: 0.995 [0.991, 0.999]). To complement this analysis, PZP was also modelled as a categorical variable using thresholds set at the first, second and third quartiles of PZP concentrations. Women with PZP  $\geq$ 84.12 µg/mL (third quartile) had 0.510 times lower odds of GH compared to those with lower concentrations, although the association was marginally significant (p = 0.046; Table S22). No other adverse pregnancy outcome was associated with PZP concentration.



**Figure 4.3.1:** Unadjusted maternal plasma PZP concentration grouped by pregnancy outcome in the STOP cohort. Kruskal-Wallis test with Dunn's post-hoc multiple comparisons; no statistically significant differences were observed between groups (n = 1250).

Correlation and Mann-Whitney U analyses were performed to explore the associations between maternal plasma PZP concentration and maternal and neonatal characteristics. PZP concentration positively correlated with gestational age at sampling, maternal age, BMI, CRP, and birthweight. Except for gestational age at sampling and BMI, all correlations were very weak. Additionally, very weak negative correlations between early pregnancy PZP and maternal B12 or homocysteine levels were identified. Gravidity, early pregnancy folate status, and gestational age at birth did not correlate with PZP concentration (Table 4.3.2). When stratified by maternal ethnicity or smoking status, median PZP concentration was lower in non-Caucasian women and smokers, respectively (Figure 4.3.2). The median PZP concentration did not differ when pregnancies were stratified by neonatal sex (p = 0.29).

**Table 4.3.2:** Correlations between maternal and neonatal characteristics and maternal plasma PZP concentration in the STOP cohort. Spearman's rho; n = 1,250.

	Correlation coefficient	р
Gestational age at sampling (weeks)	0.220	<0.001
Maternal age (years)	0.092	0.001
BMI (kg/m²)	0.139	<0.001
Gravidity	0.001	0.96
C-Reactive Protein (mg/L) <sup>a</sup>	0.092	0.001
Folate (nM) <sup>b</sup>	0.043	0.13
B12 (pM) <sup>c</sup>	-0.059	0.04
Homocysteine (μΜ) <sup>d</sup>	-0.061	0.03
Birthweight (g)	0.087	0.002
Gestational age at birth (weeks) <sup>e</sup>	0.012	0.67

Missing data for an = 3 GH, 1 PE, 1 sPTB, and 8 uncomplicated participants; bn = 3 GDM, 1 GH, 1 other complication, 1 SGA, 1 sPTB, and 2 uncomplicated participants; cn = 2 GDM, 1 GH, 1 other complication, 1 SGA, 1 sPTB, and 2 uncomplicated participants; dn = 2 GDM, 1 GH, 1 other complication, 1 SGA, 1 sPTB, and 4 uncomplicated participants; en = 1 GDM, 2 GH, 1 PE, 1 sPTB, and 8 uncomplicated participants.

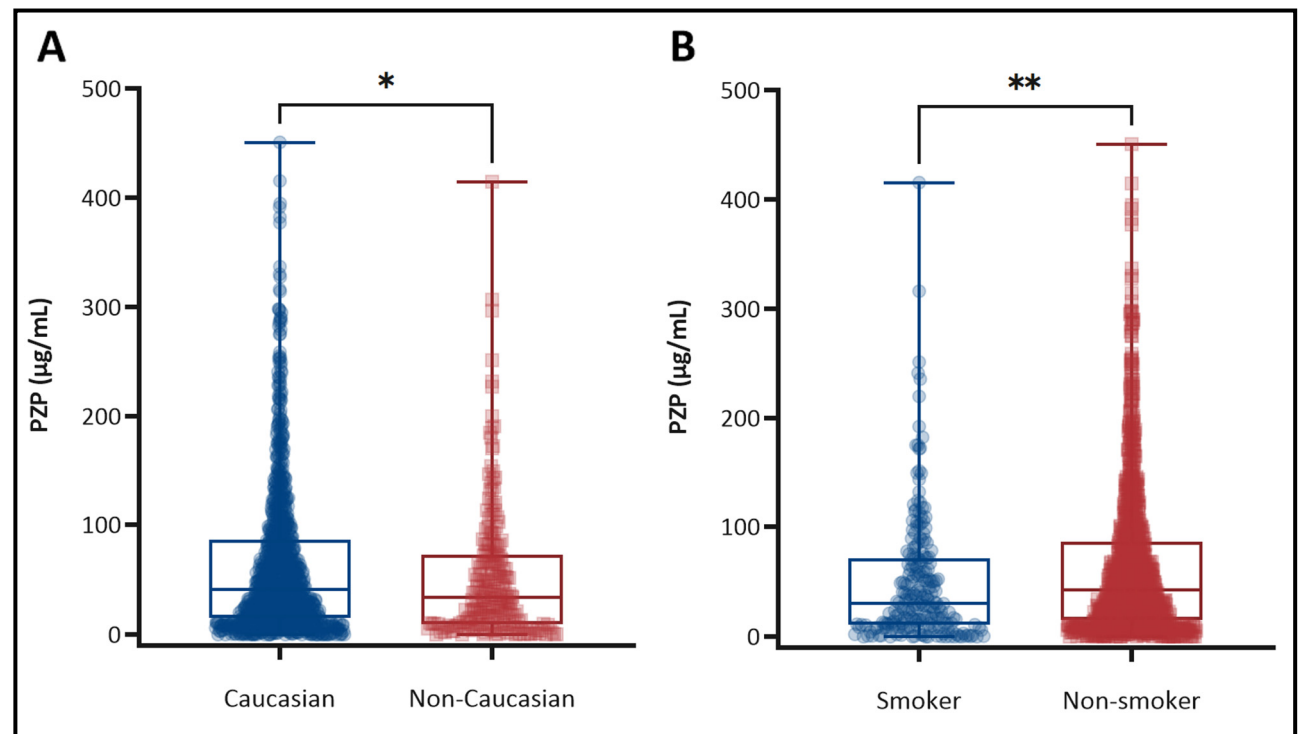


**Figure 4.3.2:** Unadjusted maternal plasma PZP concentration grouped by **(A)** ethnicity and **(B)** smoking status in the STOP cohort.

(A) Caucasian (n = 1033, median 41.16  $\mu$ g/mL, IQR 14.96 – 86.72  $\mu$ g/mL) versus non-Caucasian (n = 217, median 33.81  $\mu$ g/mL, IQR 9.60 – 72.76  $\mu$ g/mL) mothers and (B) smokers (n = 212, median 30.54  $\mu$ g/mL, IQR 10.62 – 71.40  $\mu$ g/mL) versus non-smokers (n = 1038, median 42.15  $\mu$ g/mL, IQR 15.13 – 86.53  $\mu$ g/mL). Two-tailed Mann-Whitney U test; significance indicated with asterisks (\* p <0.05, \*\* p <0.01).

To further investigate the relationship between maternal plasma PZP concentration and associated variables, regression analyses were performed. Quantile regression at the 0.25, 0.5, and 0.75 quantiles was used for models with PZP concentration as the dependent variable due to its non-normal distribution. The association between PZP and gestational age at sampling and BMI was significant across all quantiles with the association more pronounced as PZP concentration increased. Maternal age had the strongest association at the 0.5 quantile but was not significant at the 0.75 quantile (Table 4.3.3). Similarly, the relationship of PZP concentration with ethnicity and smoking status was not consistent across quantiles. Ethnicity was significantly associated with PZP concentrations at the 0.25 quantile, while smoking status was only significant at the 0.5 quantile (Table 4.3.3). Linear regression assessing the association between PZP concentration and birthweight (normally distributed) revealed a weak but significant positive association, with birthweight increasing by 0.556 grams for every 1  $\mu$ g/mL increase in PZP (coefficient [95% CI]: 0.556 [0.117, 0.996] p = 0.01). Despite reaching statistical significance, regression analyses were not performed for the association between PZP and B12 or homocysteine due to their very small effect sizes (Table 4.3.2).

Given that the direction of the relationship between PZP and CRP is unknown, both PZP and CRP were considered the dependent variables in separate regression models. Linear regression with CRP modelled as the dependent variable showed a very small but significant association between PZP and CRP concentration (coefficient [95% CI]: 0.007 [0.003, 0.012] p = 0.002). Quantile regression with PZP as the dependent variable indicated that the association between CRP and PZP was stronger in this model, and that the effect size increased with increasing PZP quantiles (Table 4.3.3).

**Table 4.3.3:** Univariate quantile regression analyses to assess the association between maternal characteristics and maternal plasma PZP concentration in the STOP cohort.

maternar plasma i zi concentrati							
	Quantile						
	0.25 (14.01 μg/r	0.5 (39.37 μg	/mL)	0.75 (84.12 μg/mL)			
Natara labora eta viatia	Coefficient	_	Coefficient		Coefficient	-	
Maternal characteristic	[95% CI]	р	[95% CI]	р	[95% CI]	р	
Gestational age at sampling	4.707	10.001	7.901	10.001	14.405	.0.004	
(weeks)*	[3.688, 5.726]	<0.001	[5.814 <i>,</i> 9.988]	<0.001	[10.572, 18.237]	<0.001	
Matanal and (varia)*	0.480	0.01	1.253	-0.001	1.256	0.08	
Maternal age (years)*	[0.116, 0.844]	0.01	[0.533, 1.973]	<0.001	[-0.167, 2.679]		
DA41 (1cm /mo21*	0.464	<0.001	0.718	0.006	1.272	0.006	
BMI (kg/m²)*	[0.202, 0.726]	<0.001	[0.203, 1.234]	0.006	[0.367, 2.177]		
CDD /mm // 1*	0.519	0.002	0.627	0.05	1.418	0.017	
CRP (mg/L)*	[0.178, 0.860]	0.003	[-0.006, 1.260]	0.05	[0.252, 2.584]		
Ethnicity (non-Caucasian	-5.360	0.02	-7.350	0.14	-14.150	0.122	
versus Caucasian)	[-10.267, -0.453]	0.03	[-17.025, 2.325]	0.14	[-32.067, 3.767]		
Smoking status (non-smoker	4.550	0.07	11.940	0.03	15.140	0.11	
versus smoker)	[-0.399, 9.499]	0.07	[2.071, 21.809]	0.02	[-3.369, 33.649]		

For continuous variables, the coefficient represents the change in PZP concentration ( $\mu g/mL$ ) per 1-unit increase in the maternal characteristic at the specified quantile. For categorical variables, the coefficient represents the difference in PZP concentration ( $\mu g/mL$ ) between groups at the specified quantile.

Although the observed association between higher maternal plasma PZP concentration and reduced odds of GH was adjusted for maternal BMI, results from quantile regression indicated that the relationship between PZP and BMI is non-linear. Given that BMI is one of the strongest risk factors for GH (Shin and Song, 2015, Lewandowska et al., 2020), to further explore the potential impact of BMI as a confounder the association between PZP concentration and pregnancy outcomes was examined in BMI-stratified groups:  $<25 \text{ kg/m}^2$  (underweight and healthy) and  $\ge25 \text{ kg/m}^2$  (overweight and obese). Due to the reduced sample size following stratification, no additional covariates were included in these models. More than half of participants in the STOP cohort had a BMI  $\ge25 \text{ kg/m}^2$  (58.6%), and PZP concentrations were significantly higher in these mothers compared to those with BMI  $<25 \text{ kg/m}^2$  (Figure 4.3.3).

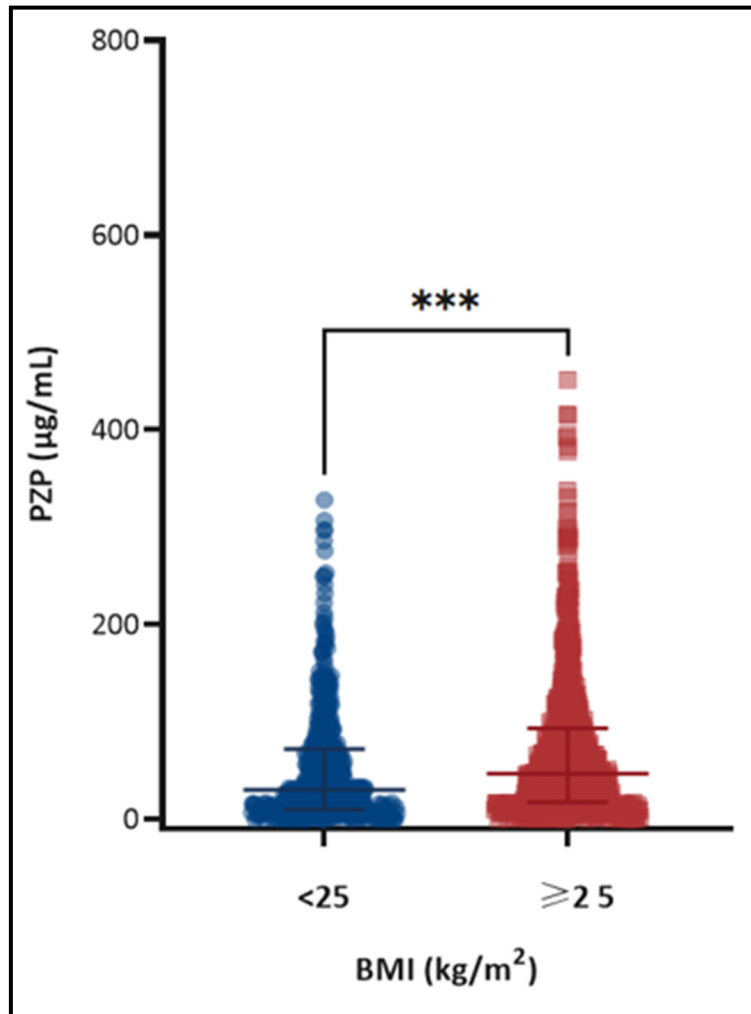


**Figure 4.3.3:** Unadjusted maternal plasma PZP concentration grouped by BMI in the STOP cohort. BMI <25 kg/m² includes underweight (n = 25) and healthy weight (n = 492) participants (median 29.94, IQR 9.56 − 71.84 μg/mL); BMI ≥25 kg/m² includes overweight (n = 351) and obese (n = 381) participants (median 46.77, IQR 17.09 − 93.06 μg/mL). Kruskal-Wallis test with Dunn's post-hoc multiple comparisons; significance indicated with asterisks (\*\*\*p <0.001).

Among women with a BMI <25 kg/m², the previously observed association between PZP concentration and GH was no longer significant. However, within this group, women with PZP concentrations ≥84.12 μg/mL (third quartile) had 2.31-fold higher odds of developing PE (95% CI: 1.09, 4.89) compared to those with lower PZP concentrations (Table S23). Additionally, those with PZP concentrations <14.01 μg/mL had 2.10-fold higher odds of delivering an SGA infant (95% CI: 1.08, 4.01; Table S23). No other significant associations between PZP concentration and adverse pregnancy outcomes were observed in this subgroup of mothers.

In contrast, among women with a BMI ≥25 kg/m², PZP concentration was not significantly associated with any pregnancy outcome except GH. In this group, a very small inverse association was detected, whereby each unit increase in PZP concentration was associated with a 0.99-fold decrease in the odds of GH (95% CI: 0.99, 1.00; Table S24).

Given that maternal plasma PZP concentration was associated with PE and GH, the relationship between plasma PZP and any pregnancy-associated hypertension (i.e., PE and GH combined) was explored further. To better capture potential non-linear effects and because modelling PZP as a continuous variable showed minimal effect sizes, the third quartile threshold was used to assess the odds of hypertensive versus normotensive pregnancy. Using this threshold, PZP concentration was not significantly associated with hypertensive pregnancy in the overall cohort (odds ratio [95% CI]: 0.901 [0.630, 1.289] p = 0.57), nor when stratified by BMI: BMI <25 kg/m² (odds ratio [95% CI]: 1.453 [0.745, 2.834] p = 0.27) and BMI ≥25 kg/m² (odds ratio [95% CI]: 0.750 [0.487, 1.154] p = 0.19).

#### 4.3.2 SCOPE cohort

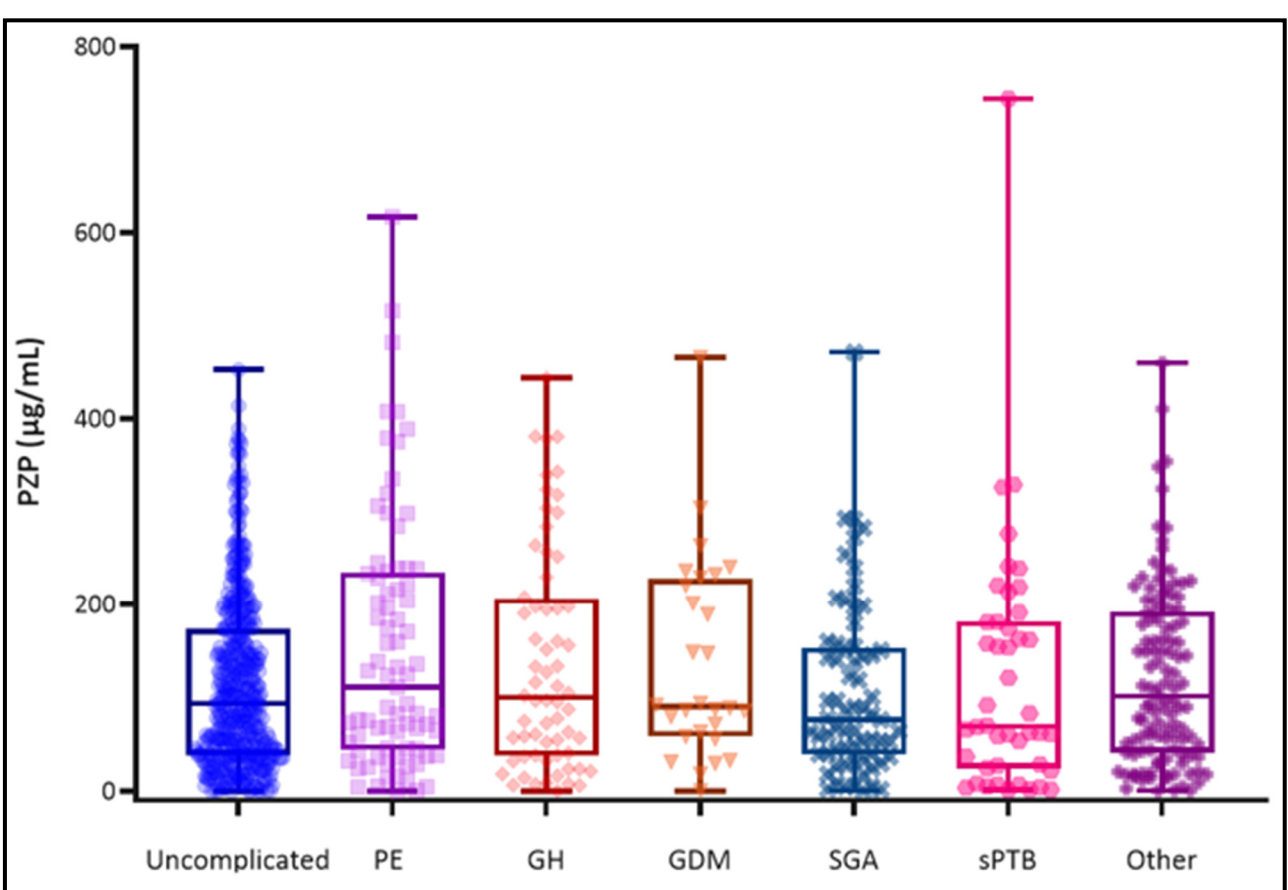
To further characterise maternal plasma PZP concentrations during pregnancy, samples from an independent cohort of nulliparous women were analysed. PZP concentration was measured in blood plasma samples collected from mothers during the early second trimester and grouped according to pregnancy outcome. Relevant maternal characteristics and neonatal outcomes are presented in Table 4.3.4, with additional information regarding comorbidities available in Table S25. All groups were similar in terms of gestational age at sampling, smoking status, ethnicity, neonatal sex and the percentage of primigravid mothers. The frequency of gravidity for the overall cohort is provided in Table S26. Maternal age and smoking status were consistent across all groups, except for mothers with GDM who were older, and a higher proportion of smokers in the SGA group. Consistent with what was observed in the STOP cohort, mothers with PE, GH, or GDM had significantly higher BMI compared to those with uncomplicated pregnancy. As expected, based on pathology, only mothers with PE, SGA or sPTB gave birth to babies with significantly lower birthweight compared to those with uncomplicated pregnancy.

Table 4.3.4: Maternal and neonatal characteristics grouped by pregnancy outcome in the SCOPE cohort. Maternal characteristics collected at time of sampling.

	Uncomplicated	PE	р	GH	р	GDM	р	SGA	р	sPTB	р	Other	p
n	464	79		64		28		67		44		117	
Gestational age at sampling (weeks)	15.6 (15.1 - 16)	15.6 (15.1 - 16)	1	15.4 (15.1 - 15.9)	1	15.5 (15 - 16.1)	1	15.4 (15 - 16)	1	15.6 (15.3 - 16.1)	0.93	15.4 (15.1 - 15.9)	1
Maternal age (years)	23 (20 - 26)	23 (20 - 27)	1	23 (19 - 26)	1	28.5 (25 - 33)	<0.001	22 (20 - 27)	1	22 (18 - 27)	1	22 (19 - 26)	0.13
BMI (kg/m²)	25.1 (22.1 - 28.8)	28.2 (24.3 - 33.9)	<0.001	28.5 (25.5 - 33.4)	<0.001	28.8 (23.1 - 35.9)	0.02	25.5 (22.5 - 31.9)	1	25.9 (21.6 - 31.6)	1	24.3 (20.2 - 28.9)	0.54
Non-smoker	362 (78)	65 (82.3)	1	51 (79.7)	1	27 (96.4)	0.12	31 (46.3)	<0.001	29 (65.9)	0.41	82 (70.1)	0.43
Ethnicity (Caucasian)	431 (92.9)	74 (93.7)	1	61 (95.3)	1	24 (85.7)	0.97	60 (89.6)	1	40 (90.9)	1	107 (91.5)	1
Primigravida	344 (74.1)	56 (70.9)	1	52 (81.3)	1	20 (71.4)	1	45 (67.2)	1	29 (65.9)	1	82 (70.1)	1
Neonatal sex (Female)	251 (54.1)	43 (54.4)	1	29 (45.3)	1	12 (42.9)	1	34 (50.7)	1	19 (43.2)	1	56 (47.9)	1
Birthweight (g)	3570 (3300 - 3845)	3020 (2590 - 3495)	<0.001	3425 (3222 - 3690)	0.10	3336 (3101 - 3764)	0.23	2760 (2570 - 2965)	<0.001	2422 (1944 - 2737)	<0.001	3330 (2962 - 3770)	<0.001
Late-onset PE (≥34 weeks)	-	72 (92.4)	-	-	-	-	-	-	-	-	-	-	-

Continuous variables compared using two-tailed Mann-Whitney U test and reported as median (IQR). Categorical variables compared using chi-square test and reported as n (%). All reported p-values are adjusted using the Bonferroni correction for multiple comparisons and are compared to the uncomplicated group. Gravidity includes the current pregnancy.

Maternal plasma PZP concentration showed considerable inter-individual variation, with values ranging from 0.001  $\mu$ g/mL (undetectable) to 743.91  $\mu$ g/mL. There were no significant differences in the median PZP concentration between any of the pregnancy outcome groups (Figure 4.3.4). To further investigate the relationship between PZP concentration and pregnancy outcome, logistic regression modelling, adjusted for BMI and gestational age at sampling, was performed (Table S27). The results of logistic regression analyses using PZP concentration as a continuous independent variable showed that there was a statistically significant (p = 0.01) but very small association with the odds of a woman having PE (odds ratio [95% CI]: 1.003 [1.001, 1.005]). The results of logistic regression models using thresholds set at each quartile of PZP concentration showed that mothers with PZP concentrations  $\geq$ 182.31  $\mu$ g/mL (third quartile) had 1.82-fold higher odds of developing PE compared to those with lower PZP concentrations (95% CI: 1.08, 3.06; Table S27).



**Figure 4.3.4:** Unadjusted maternal plasma PZP concentration grouped by pregnancy outcome in the SCOPE cohort. Kruskal-Wallis test with Dunn's post-hoc multiple comparisons; no statistically significant differences were observed between groups (n = 863).

Correlation and Mann-Whitney U analyses were performed to explore the associations between maternal plasma PZP concentration and maternal or neonatal characteristics. PZP concentration positively correlated with gestational age at sampling, maternal age, BMI, and CRP but all correlations were very weak (Table 4.3.5). No significant correlations were identified between PZP concentration and gravidity, folate, B12, homocysteine, birthweight, or gestational age at birth. When mothers were grouped based on ethnicity or smoking status, the median PZP concentration was lower in non-Caucasian women and smokers, respectively (Figure 4.3.5). The median PZP concentration did not differ when pregnancies were grouped by neonatal sex (p = 0.25).

**Table 4.3.5:** Correlations between maternal and neonatal characteristics and maternal plasma PZP concentration in the SCOPE cohort. Spearman's rho; n = 1,250.

	Correlation coefficient	p
Gestational age at sampling (weeks)	0.125	<0.001
Maternal age (years)	0.175	<0.001
BMI (kg/m²)	0.114	<0.001
Gravidity	-0.015	0.66
C-Reactive Protein (mg/L) <sup>a</sup>	0.199	<0.001
Folate <sup>b</sup>	0.024	0.48
B12 <sup>b</sup>	-0.001	0.97
Homocysteine <sup>b</sup>	0.016	0.65
Birthweight (g)	0.028	0.42
Gestational age at birth (weeks)	-0.022	0.51

Missing data for  $^{a}n = 2$  uncomplicated participants;  $^{b}n = 1$  GDM, 3 OC, 2 PE, and 10 uncomplicated participants.

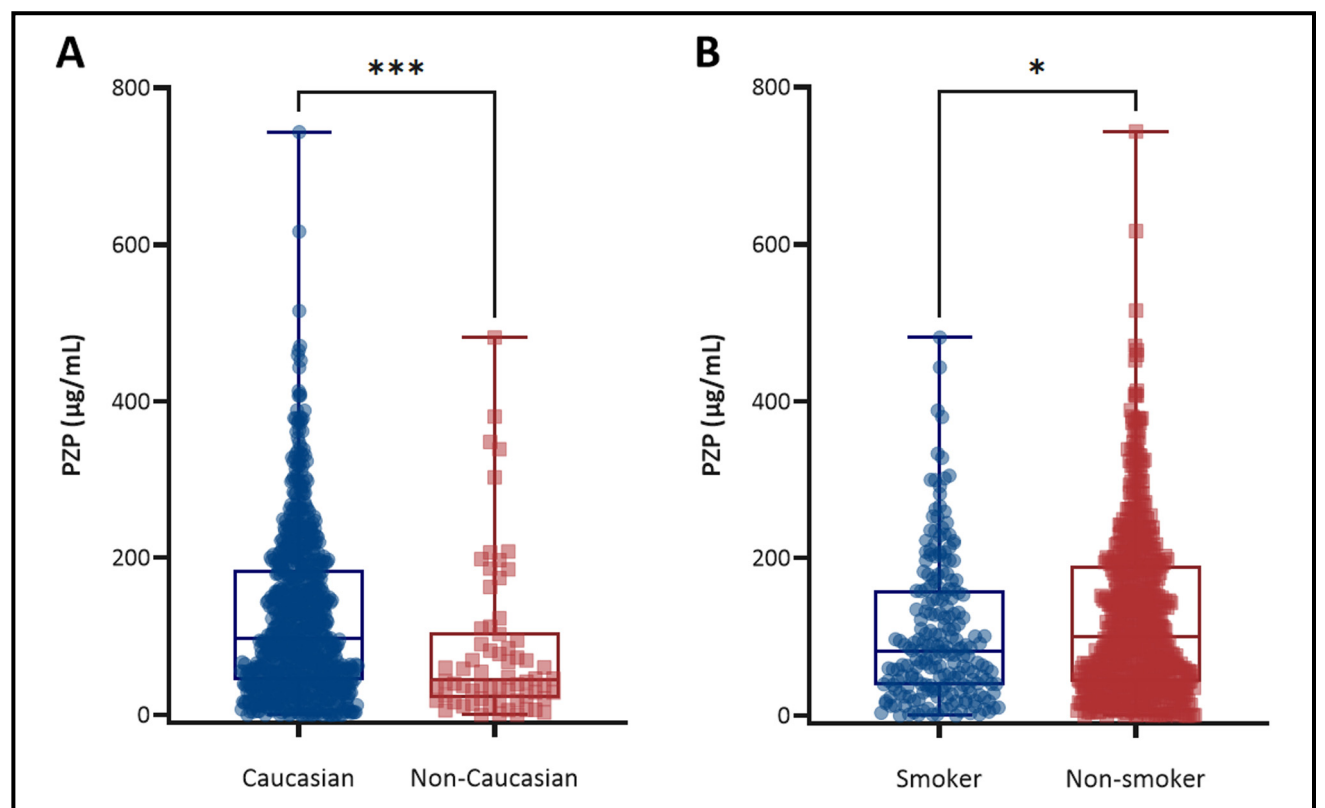


**Figure 4.3.5:** Unadjusted maternal plasma PZP concentration grouped by **(A)** ethnicity and **(B)** smoking status in the SCOPE cohort.

(A) Caucasian (n = 797, median 96.74  $\mu$ g/mL, IQR 43.91 – 184.51  $\mu$ g/mL) versus non-Caucasian (n = 66, median 44.49  $\mu$ g/mL, IQR 20.70 – 104.48  $\mu$ g/mL) mothers and (B) smokers (n = 216, median 82.27  $\mu$ g/mL, IQR 38.19 – 159.39  $\mu$ g/mL) versus non-smokers (n = 647, median 99.42  $\mu$ g/mL, IQR 41.86 – 190.41  $\mu$ g/mL). Two-tailed Mann-Whitney U test; significance indicated with asterisks (\* p <0.05, \*\* p <0.01).

To further investigate the relationship between maternal plasma PZP concentration and associated variables, regression analyses were performed. To assess the association between maternal characteristics and PZP concentration, quantile regression at the 0.25, 0.5, and 0.75 quantiles was performed. Gestational age at sampling and maternal age were significant across all quantiles, with the strength of their association more apparent as PZP concentration increased, whereas the association between BMI and PZP concentration was only significant at the 0.75 quantile (Table 4.3.6). Similarly to analyses in the STOP cohort, linear regression showed a very small but significant association between PZP and CRP concentration (coefficient [95% CI]: 0.011 [0.005, 0.016] p < 0.001). Quantile regression supported that there was a small increase in the strength of the association when PZP was modelled as the dependent variable. The association between ethnicity and PZP was significant at all quantiles, with the greatest disparity in PZP concentration observed at the 0.75 quantile. Conversely, smoking status was only significantly associated with PZP at the 0.75 quantile.

**Table 4.3.6:** Univariate quantile regression analyses to assess the association between maternal characteristics and maternal plasma PZP concentration in the SCOPE cohort.

			Quantile			
	0.25 (39.61 μg/	/mL)	0.5 (91.93 μg/n	nL)	0.75 (182.31 μg/mL)	
Maternal characteristic	Coefficient [95% CI]	р	Coefficient [95% CI]	р	Coefficient [95% CI]	р
Gestational age at	13.005		26.909		25.221	
sampling (weeks)	[4.717, 21.292]	0.002	[12.761, 41.056]	<0.001	[5.49, 44.951]	0.012
Maternal age (years)	2.109		3.628		4.52	
waternarage (years)	[1.124, 3.093]	<0.001	[1.861, 5.395]	<0.001	[2.124, 6.916]	<0.001
BMI (kg/m²)	0.695		1.449		3.567	
Bivii (kg/iii )	[-0.081, 1.471]	0.08	[-0.029, 2.926]	0.06	[1.869, 5.265]	<0.001
CDD (mg/L)	0.659		2.538		2.855	
CRP (mg/L)	[0.102, 1.216]	0.02	[1.441, 3.636]	<0.001	[1.575, 4.136]	<0.001
Ethnicity (non-Caucasian	-23.133		-54.165		-81.674	
vs Caucasian)	[-40.780, -5.486]	0.01	[-87.225, -21.106]	0.001	[-126.569, -36.779]	<0.001
Smoking status (non-	3.686		17.707		32.044	
smoker vs smoker)	[-7.556, 14.928]	0.52	[-3.289, 38.703]	0.10	[3.377, 60.712]	0.03

For continuous variables, the coefficient represents the change in PZP concentration ( $\mu g/mL$ ) per 1-unit increase in the maternal characteristic at the specified quantile. For categorical variables, the coefficient represents the difference in PZP concentration ( $\mu g/mL$ ) between groups at the specified quantile.

Consistent with analyses conducted in the STOP cohort, the influence of maternal BMI on the relationship between maternal plasma PZP concentration and pregnancy outcome was evaluated in the SCOPE cohort by stratifying the data into two BMI categories (<25 kg/m² and ≥25 kg/m²). This stratification accounts for the established association between elevated BMI and increased PE risk (Ulhaq et al., 2021, Mao et al., 2025, Sudjai, 2023, Bartsch et al., 2016). Given the reduced sample size within each subgroup, these models were not adjusted for additional covariates. As with the STOP cohort, more than half of the mothers in the SCOPE cohort had a BMI ≥25 kg/m² (54.9%) and PZP concentration was significantly higher in this group compared to those with BMI <25 kg/m² (Figure 4.3.6).

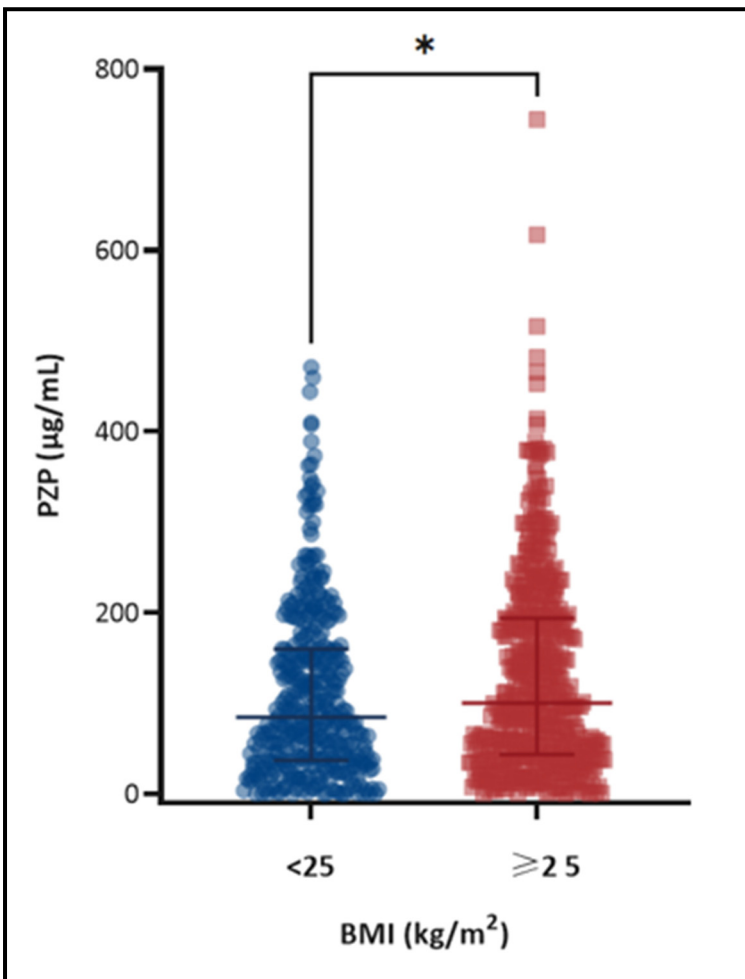


**Figure 4.3.6:** Unadjusted maternal plasma PZP concentration grouped by BMI in the SCOPE cohort. BMI <25 kg/m² includes underweight (n = 26) and healthy weight (n = 363) participants (median 84.57, IQR 36.99 − 159.89 μg/mL); BMI ≥25 kg/m² includes overweight (n = 248) and obese (n = 226) participants (median 100.21, IQR 43.54 − 193.95 μg/mL). Kruskal-Wallis test with Dunn's post-hoc multiple comparisons; significance indicated with asterisks (\*\*p <0.01).

Among women with BMI <25 kg/m², higher maternal plasma PZP concentration was significantly associated with increased odds of GH. Specifically, women with PZP concentrations ≥182.31 µg/mL (third quartile) had 2.95-fold higher odds of GH (95% CI: 1.02, 8.50) compared to those with lower concentrations of PZP (Table S28). No other pregnancy outcomes were significantly associated with PZP in this subgroup.

In contrast, among women with a BMI  $\ge 25 \text{ kg/m}^2$ , maternal plasma PZP concentration was not associated with GH but was significantly associated with PE. Specifically, mothers with PZP concentration  $\ge 182.31 \text{ µg/mL}$  had 2.03-fold increased odds of developing PE (95% CI: 1.07,

3.84) compared to those with lower concentrations (Table S29). No other associations between PZP and adverse pregnancy outcomes were identified (Table S29).

As in the STOP cohort, the association between maternal plasma PZP concentration and hypertensive pregnancy (PE and GH combined) was further examined using the third quartile (182.31 µg/mL) of PZP as a threshold. This approach was again chosen to better account for potential non-linear effects and the small effect sizes observed when PZP was modelled as a continuous variable. In the overall cohort, mothers with PZP concentrations  $\geq$ 182.32 µg/mL had significantly higher odds of hypertensive pregnancy compared to normotensive pregnancy (odds ratio [95% CI]: 1.808 [1.230, 2.658] p = 0.003). The strongest association was observed in mothers with BMI  $\leq$ 25 kg/cm², where PZP above the third quartile was associated with 2.04-fold increased odds of hypertensive pregnancy (odds ratio [95% CI]: 2.043 [1.024, 4.076] p = 0.02). A similar, though slightly weaker, association was observed in women with BMI  $\geq$ 25 kg/m² (odds ratio [95% CI]: 1.654 [1.027, 2.663] p = 0.04).

### 4.4 Discussion

This study is the first to report maternal plasma PZP concentration in large cohorts of nulliparous women, providing novel insights into the relationship between PZP, maternal characteristics and pregnancy outcomes. A major strength of this work is the analysis of two independent cohorts, which enhances the robustness of findings and increases confidence that the observed associations between circulating PZP levels and maternal age, BMI, smoking status, and ethnicity are real associations. The results of quantile regression analyses revealed nuanced, non-linear patterns in these associations, with effect sizes varying across the distribution of PZP concentrations. A summary of the main findings is presented in Table 4.4.1, highlighting both consistent and cohort-specific associations. The remainder of this discussion explores these associations in more detail, considers potential mechanisms, and addresses the limitations and implications of these findings for future research. While some effect sizes were small and may represent weak or chance associations, they are presented and interpreted here for completeness, as this information provides context and may be used to generate hypotheses for future investigation.

**Table 4.4.1:** Summary of the main findings following analysis of the associations between maternal or neonatal characteristics and maternal plasma PZP concentration in the STOP and SCOPE cohorts.

Finding	STOP	Associated by regression?	SCOPE	Associated by regression?
Positive association between PZP and:				
Gestational age at sampling	Yes	Yes, at 0.25, 0.5, & 0.75 quantiles	Yes	Yes, at 0.25, 0.5, & 0.75 quantiles
CRP (mg/L)	Yes	Yes, at 0.25, 0.5, & 0.75 quantiles	Yes	Yes, at 0.25, 0.5, & 0.75 quantiles
Maternal age	Yes	Yes, at 0.25 & 0.5 quantiles	Yes	Yes, at 0.25, 0.5, & 0.75 quantiles
ВМІ	Yes	Yes, at 0.25, 0.5, & 0.75 quantiles	Yes	Yes, at 0.75 quantile
Birthweight (g)	Yes	Yes	No	Not assessed
Negative association between PZP and:				
Homocysteine (μM)	Yes	Not assessed	No	Not assessed
B12 (pM)	Yes	Not assessed	No	Not assessed
PZP is higher in non-smokers	Yes	Yes, at 0.5 quantile	Yes	Yes, at 0.75 quantile
PZP is lower in non-Caucasian mothers	Yes	Yes, at 0.25 quantile Yes Yes, a		Yes, at 0.25, 0.5, & 0.75 quantiles

#### 4.4.1 Maternal plasma PZP concentration increased across early pregnancy

The results presented in this chapter show that gestational age at sampling is a primary determinant of maternal plasma PZP concentration, with levels increasing progressively throughout the late first trimester and early second trimester. However, this pattern varied depending on baseline PZP levels, highlighting individual differences in the upregulation of PZP during gestation and supporting the large variation between participants observed in previous studies (Ekelund and Laurell, 1994, Fosheim et al., 2023). In the STOP cohort, the association between gestational age and PZP concentration was most pronounced in the upper quantiles, suggesting that women with higher PZP concentrations tended to exhibit steeper increases across gestation, while those with lower concentrations showed more gradual changes. In the SCOPE cohort, this association plateaued at the moderate to high quantiles, suggesting that the trajectory of PZP's increasing concentration may stabilise beyond the first trimester in some individuals. Although individual trajectories could not be assessed due to the cross-sectional design, these findings imply non-linear regulation of PZP across gestation. Consistent with a seminal paper that showed a marked increase in PZP concentrations in early pregnancy for some women (Ekelund and Laurell, 1994), PZP levels in SCOPE participants were more than double that of STOP participants, likely reflecting the approximate 4-week difference in gestational age at sampling. The higher concentration was accompanied by broader variability in the SCOPE cohort, suggesting that as pregnancy progresses, plasma PZP concentration

becomes more heterogeneous. However, it is a limitation of the current study that PZP concentration was not analysed in longitudinally across gestation in the same participants.

In terms of concentration, approximately 10% of plasma proteins are modulated during pregnancy, with many immunoregulatory proteins (e.g., interleukin-1 receptor antagonist, complement components including C1q and C4BPA) showing elevated levels in the first trimester compared to pre-pregnancy (Romero et al., 2017, Tarca et al., 2022). The increase in PZP concentration with advancing gestation supports the idea that PZP contributes to maternal adaptations late in the first trimester, potentially influencing processes such as placentation or immunotolerance. Given that the only study measuring circulating PZP concentration across gestation is now over 30 years old (Ekelund and Laurell, 1994), reassessing PZP dynamics in a larger cohort using modern proteomic techniques would provide more precise insights into how PZP levels change throughout pregnancy. Furthermore, identification of the mechanisms that regulate PZP concentration during pregnancy is needed.

#### 4.4.2 Maternal characteristics influenced plasma PZP concentration

BMI, maternal age, ethnicity, and smoking status were all associated with maternal plasma PZP concentration in both the STOP and SCOPE cohorts. Of the findings reported herein, BMI is the only maternal characteristic previously reported to correlate with circulating PZP concentration, with a positive correlation identified in the control group only (normotensive and euglycemic throughout pregnancy) (Fosheim et al., 2023). In this chapter, correlations between maternal characteristics and PZP were assessed using data from the overall cohort (including mothers with pregnancy complications) to maximise statistical power and to capture general physiological trends. Additionally, this is the first study to use regression modelling to provide a more comprehensive analysis of the relationship between PZP and the aforementioned factors.

Obesity and advancing maternal age are both associated with elevated circulating inflammatory markers, such as IL-6 and CRP (Ramsay et al., 2002, Stewart et al., 2007, Westergaard et al., 2024, Ferrucci et al., 2005, Giuliani et al., 2001, Franceschi et al., 2000). Consistent with reports that PZP is upregulated in a range of pregnancy-independent inflammatory states (see Section 1.2.2.3), a positive association between plasma levels of PZP and CRP was identified in both cohorts assessed in this study. While the direction of the relationship between PZP and CRP was assessed, there was no strong evidence that one

protein influenced the other more substantially. This suggests that both are likely to be concomitantly upregulated in response to the pro-inflammatory environment of pregnancy. Although the effect sizes were modest, the positive associations between maternal age and BMI with maternal plasma PZP concentration may reflect a compensatory response to systemic low-grade inflammation that broadly affects these mothers.

The observed increase in maternal plasma PZP concentration with higher BMI may also reflect broader changes in lipid metabolism and HDL functionality. Obesity is typically associated with an unfavourable lipid profile, including reduced HDL cholesterol and a predominance of smaller, less protective HDL particles (Stadler et al., 2021). During pregnancy, obesity is also linked to altered HDL functionality, reflected by increased cholesterol efflux capacity and reduced serum antioxidant capacity in overweight/obese mothers compared to mothers with BMI <25 kg/cm² (Stadler et al., 2023). Proteomic analyses have shown that PZP becomes increasingly associated with HDL particles during pregnancy, with a specific enrichment on large HDL subclasses (Melchior et al., 2021), which are functionally distinct from the smaller HDL subclasses (Fazio and Pamir, 2016). Given PZP's anti-inflammatory and immunomodulatory properties, its integration into HDL may help preserve or enhance specific HDL functions that may become otherwise compromised in the context of maternal obesity.

Although it was a consistent finding that maternal plasma PZP concentration is decreased in non-Caucasian mothers, it is important to note that the non-Caucasian groups in both cohorts included a range of ethnicities broadly encompassing Indigenous, Black, Asian, Hispanic/Latino, Middle Eastern/North African, and Pacific peoples. Ethnicity-dependent inflammatory responses are widely reported (Westergaard et al., 2024), including during pregnancy (Gillespie et al., 2016, Gyllenhammer et al., 2021, Christian et al., 2013). Therefore, as with BMI and maternal age, immune responses may underpin differences in PZP concentration between Caucasian and non-Caucasian mothers. This highlights the need for more stratified analyses in future research to determine whether these differences reflect biological variation or sampling biases. Furthermore, the smaller sample size of non-Caucasian mothers compared to Caucasian mothers in both cohorts limits statistical power and reinforces the need for larger ethnically diverse groups to fully elucidate the relationship between ethnicity and PZP concentration.

An unexpected but consistent finding was that maternal plasma PZP concentration is lower in mothers who smoked cigarettes in early pregnancy, which is well-known to promote low-grade systemic inflammation (Yanbaeva et al., 2007, Shiels et al., 2014). One possible explanation for reduced PZP levels in smokers may relate to the negative effect of smoking on nitric oxide (NO) bioavailability. Supporting this idea, plasma PZP concentration is positively correlated with NO bioavailability in children with chronic kidney disease (Chen et al., 2023b). Additionally, PZP is downregulated in Nrf-2-deficient mice (Gao et al., 2020), a transcription factor that is activated by NO (Um et al., 2011). These mechanistic links suggest that reduced NO bioavailability in smokers may contribute to lower circulating PZP. It should be acknowledged that in the current study, the disparity in sample size between smokers and non-smokers may limit statistical power. Additionally, smoking was self-reported by participants and no objective information regarding the level of smoking was available.

Although maternal plasma PZP concentration was consistently associated with BMI, maternal age, ethnicity, and smoking status in both cohorts, it is important to acknowledge that these maternal characteristics are interrelated and likely influence one another – and PZP levels – in complex ways. For example, both BMI and smoking prevalence can vary across ethnic groups and tend to shift with advancing maternal age. As such, it is difficult to attribute changes in PZP concentration to any one factor in isolation. Additionally, the large variability and highly skewed distribution of PZP levels limits the utility of conventional statistical approaches, such as linear regression, for disentangling these effects. This was reflected in the quantile regression results, which showed that the associations between maternal factors and PZP varied across the distribution. Addressing these complexities will require larger, more diverse cohorts and the use of advanced statistical modelling approaches capable of accounting for confounding, effect modification, and interactions, particularly in the context of a non-normally distributed variable like PZP concentration.

## 4.4.3 Maternal plasma PZP concentration was associated with adverse pregnancy outcomes

In addition to uncovering novel associations between maternal plasma PZP concentration and maternal characteristics, this study was the first to evaluate the relationship between PZP concentrations and adverse pregnancy outcomes exclusively in nulliparous women. Although median PZP concentrations did not differ significantly between women with uncomplicated pregnancies and those with adverse outcomes, logistic regression modelling revealed an

association between plasma PZP concentration and the odds of a mother developing PE, GH, or delivering an SGA infant (Table 4.4.2). Given the substantial variability in PZP concentration between individuals, comparing means or medians alone offers limited insights. The associations detected were generally modest, and their biological significance remains uncertain. However, they were most evident in categorical regression models, which are better suited to identifying non-linear or threshold-dependent effects. Regression analyses, where sample size permits, are therefore crucial for gaining a deeper understanding of these associations, and an approach that is distinctly lacking in previous studies.

**Table 4.4.2:** Summary of how **increasing** maternal plasma PZP concentration affects the odds of adverse pregnancy outcomes. Arrows and dashes indicate direction of change.

Outcome	Whole cohort		BMI <2	5 kg/m²	BMI ≥25 kg/m²		
	STOP	SCOPE	STOP	SCOPE	STOP	SCOPE	
PE (versus uncomplicated)	-	<b>↑</b> ‡	<b>↑</b> <sup>†</sup>	-	-	<b>↑</b> ‡	
GH (versus uncomplicated)	<b>↓</b> <sup>‡</sup>	-	-	<b>↑</b> ‡	<b>*</b>	-	
Hypertensive (versus normotensive)	-	<b>↑</b> †	-	<b>↑</b> †	-	<b>↑</b> †	
SGA (versus uncomplicated)	-	-	$\mathbf{\psi}^{\dagger}$	_	-	_	

<sup>\*</sup>associated with PZP as a continuous variable, †associated with PZP using a threshold, †associated with PZP as both a continuous variable and using a threshold.

# 4.4.3.1 Higher maternal plasma PZP concentration in early-mid gestation was associated with increased odds of pregnancy-induced hypertension

When assessing the association between maternal plasma PZP concentration and hypertensive disorders of pregnancy, inconsistent trends were observed between the STOP and SCOPE cohorts (Table 4.4.2). The reasons for this can only be speculated and may relate to important cohort differences, such as time of sampling, which are discussed in more detail below (see Section 4.4.4). Regardless, the findings presented in this chapter regarding the association between maternal plasma PZP concentration and pregnancy outcomes must be interpreted cautiously. Increased maternal plasma PZP concentration was generally associated with higher odds of hypertensive disorders of pregnancy (i.e., GH or PE), particularly for mothers with BMI <25 kg/m². It is important to note, though, that stratifying the data according to BMI reduced the sample size available for analysis and hypertensive disorders of pregnancy occurred in only a small fraction of mothers with BMI <25 kg/m². Therefore, validation of this finding in a larger cohort of mothers is needed. It is plausible that the metabolic pathways influencing PZP expression or activity – such as those related to adiposity,

inflammation, or lipid metabolism (discussed further in Chapter 5) – may be more prominent in mothers with higher BMI, thereby altering the association between PZP and pregnancy outcomes. This may also explain why no association was observed between PZP and hypertensive pregnancy overall in STOP, as opposing trends for GH and PE could obscure effects when combined.

The finding that increased maternal plasma PZP concentration is associated with increased odds of PE contrasts with much of the existing literature, where lower PZP concentrations have typically been reported among women with PE (Horne et al., 1979, Rasanen et al., 2010, Liu et al., 2011, Fosheim et al., 2023). Several factors may explain the discrepancies between these findings. Most previous studies sampled maternal plasma later in pregnancy, often in the third trimester, and did not account for BMI or gestational age at sampling (Fosheim et al., 2023). Given the demonstrated influence of BMI and gestational age on PZP levels in this chapter, failure to account for these factors in previous work may have led to confounded results. Additionally, previous cohorts included mothers with mixed parity. Thus, uneven parity distributions across the outcome groups in prior studies may have compromised the results.

Although the precise role of PZP in the development of PE remains unclear, its association with this syndrome suggests that it may be involved in maternal physiological changes that precede or accompany PE onset. While the cohorts analysed in this thesis were predominantly comprised of mothers with LO-PE, recent updates to the two-stage model of PE propose that LO-PE also originates from placental pathology. Specifically, as the placenta reaches its structural or functional limits, intraplacental malperfusion and hypoxia may occur, triggering the release of pathogenic factors (Staff, 2019). In this context, PZP concentrations may rise markedly in early pregnancy in an attempt to support the critical immunological shift from the pro-inflammatory environment required for early placentation, to the more anti-inflammatory state of mid-pregnancy that promotes fetal tolerance (reviewed by Narayan and Nelson-Piercy (2020) & Dutta et al. (2024)). Supporting this idea, PZP has been shown to inhibit proinflammatory Th1 responses, particularly in synergy with glycodelin A (Skornicka et al., 2004). Given that dysregulated immune adaptation is a hallmark of PE, elevated PZP may reflect a compensatory response aimed at restoring immune tolerance (Couture et al., 2024, Stewart et al., 2007, Mihu et al., 2015). Alternatively, increased PZP levels may contribute to the regulation of heightened proteolytic activity observed in PE (Gu et al., 2009, Wang et al., 2010), which is discussed further in Chapter 5.

GH and PE exist on a clinical continuum, and some cases of GH can rapidly progress to PE if the pregnancy were to continue or if maternal monitoring is delayed (Brown et al., 2018, Rana et al., 2019). Misclassification may occur particularly if PE diagnosis relied heavily on the presence of proteinuria, as was historically standard. However, updated diagnostic criteria acknowledge that proteinuria is not required for a PE diagnosis if there is other evidence of maternal organ dysfunction (Brown et al., 2018). It is therefore plausible that the observed association with GH in mothers from the SCOPE cohort with BMI <25 kg/m² includes cases that did not meet traditional diagnostic criteria for PE but were pathophysiologically similar. Alternatively, it's possible that GH in leaner mothers reflects a biologically distinct subtype, potentially sharing more overlap with PE in terms of pathology. Given these complexities, the observed association warrants further investigation in cohorts with detailed phenotyping.

### 4.4.3.2 Increased maternal plasma PZP concentration was associated with decreased odds of delivering an SGA infant

Interestingly, in the STOP cohort among mothers with BMI <25 kg/m², increased maternal plasma PZP concentration was associated with both increased odds of PE and decreased odds of delivering an SGA infant. While these outcomes often co-occur, cases with both PE and SGA were hierarchically assigned to the PE group in this study, such that the SGA group excludes comorbid cases. The divergent directions of association suggest that PZP may influence distinct biological pathways underlying these complications. One possibility is that elevated PZP in PE reflects a compensatory response to maternal systemic changes, particularly in the context of LO-PE which was the predominant phenotype in both STOP and SCOPE. In contrast, the inverse association with SGA may reflect a more localised role for PZP in supporting placentation and healthy fetal growth. To date, PZP has not been associated with SGA, IUGR, or FGR in the literature. One study that used immunohistochemical analysis of placental tissue to detect PZP specifically reported no association between PZP expression and IUGR (Löb et al., 2022), although it is important to note that not all SGA infants result from IUGR/FGR. Although the association between elevated plasma PZP concentration and reduced odds of SGA may represent a novel finding, it should be interpreted with caution. This association was limited to mothers with BMI <25 kg/m<sup>2</sup> in a single cohort (STOP) and was not observed in other analyses. However, a positive association between plasma PZP concentration and infant birthweight was also observed in STOP, highlighting the need for further research to clarify the validity and biological relevance of a potential link between PZP and fetal growth.

#### 4.4.4 Differences between the STOP & SCOPE cohorts

The differing results observed between the STOP and SCOPE cohorts may reflect a combination of biological, methodological, and environmental factors. The association between maternal characteristics and maternal plasma PZP concentration appeared stronger in the SCOPE cohort, which comprised samples obtained later in gestation (~15 weeks) compared to the STOP cohort (~11 weeks). This may reflect a more dynamic phase of maternal adaptation in early gestation, during which physiological processes influencing PZP may still be fluctuating. Combined with a higher proportion of mothers with BMI ≥25 kg/m² in STOP, this could have obscured or skewed associations in the whole-cohort analyses. These findings underscore the importance of considering maternal BMI not only as a covariate but as a potential effect modifier in the relationship between PZP and pregnancy outcomes. Stratified analyses of larger cohorts are therefore essential to uncover associations that are otherwise masked in heterogeneous populations. Analyses of the pooled data from STOP and SCOPE using complex modelling that is designed to account for variables such as gestational age may help to further clarify the relationships between maternal characteristics and PZP concentration. However, given the quality and quantity of data available this was not undertaken in the current study.

Differences between the cohort populations may also contribute to the inconsistent results. Participants in STOP were recruited after the introduction of the folate food fortification mandate in Australia in 2009, whereas the SCOPE cohort were recruited prior to this. While maternal plasma PZP concentration did not show any meaningful correlations with markers of blood folate status (i.e., B12, folate, homocysteine), folate levels have been demonstrated to alter the expression of several plasma proteins involved in immune function, inflammation, and coagulation. For example, the expression of complement proteins (e.g., C3, C4),  $\alpha_2$ M,  $\alpha_1$ ACT, and apoA1 are altered with changes in blood folate status (Duthie et al., 2010). While it is possible that the changes in the circulating immune proteome associated with altered folate exposure may indirectly influence PZP concentrations, this interpretation is speculative and requires further investigation to establish its validity.

In addition to biological and environmental factors, it is important to acknowledge that technical considerations may have contributed to the inconsistent findings across cohorts. Of the samples requiring re-analysis to meet quality control criteria (<10% coefficient of variation between duplicates), 78.6% originated from the STOP cohort. The same dilution protocol was used across both cohorts, but the inherently lower PZP concentrations observed in early

pregnancy meant that many STOP samples fell close to the lower limit of assay detection, increasing their susceptibility to variation. This challenge reflects both the dynamic changes in PZP across gestation and the wide inter-individual variation in maternal concentrations, which together complicate accurate quantification of PZP. To mitigate technical sources of error, all assays were performed by a single operator (the candidate), vials were thawed only once and immediately aliquoted to minimise freeze-thaw cycles, and the dilution protocol was designed to maximise pipetting precision by favouring the use of smaller, more accurate pipettes. Samples with high duplicate variation were reanalysed, and results were only accepted once precision criteria were met. While the potential impact of PZP complexation with endogenous proteases was not examined, and a full independent validation of the assay was not performed, the specificity of the assay is supported by manufacturer data and its prior use in publications (Cater, 2021, Cater et al., 2019, Fosheim et al., 2023). Collectively, these measures increase the reliability of the assay and help preserve the overall integrity and robustness of the data, as far as was feasible within the constraints of this work.

Despite these precautions, ELISA may not represent the optimal approach for quantifying PZP in pregnancy. The DuoSet kit used herein is the only commercially available assay for PZP, but it reports concentrations in the pg/mL range, which may be appropriate for non-pregnant women or males but is poorly suited for the markedly higher concentrations observed in pregnancy. This necessitates large dilutions of maternal plasma, introducing additional opportunities for pipetting error and loss of precision. Moreover, the restricted dynamic range of ELISA, determined by the standard curve, limits the ability to capture the wide span of physiological PZP concentrations across gestation. Future studies may benefit from alternative approaches such as immunoassays with extended dynamic range, bead-based multiplex platforms, or targeted mass spectrometry, which could provide greater accuracy and reproducibility across the concentration range encountered in pregnancy.

### 4.4.5 Concluding remarks

In summary, this chapter presents the first comprehensive analysis of maternal plasma PZP concentration in early pregnancy across two large, well-characterised cohorts of nulliparous women. These findings confirm that PZP levels vary considerably between individuals and are influenced by a range of maternal characteristics. Importantly, quantile regression revealed that these associations differ across the PZP distribution, highlighting the limitations of typical statistical tests and the need for more nuanced analyses. Moreover, maternal plasma PZP

concentration was associated with hypertensive disorders of pregnancy and SGA, with preliminary evidence suggesting that these associations may be more apparent in lean mothers. This raises the possibility that PZP contributes to distinct pathophysiological pathways underlying adverse pregnancy outcomes, although further validation in larger cohorts is needed. While these findings provide valuable new insights, they also raise important questions regarding the mechanisms regulating PZP expression, its functional relevance in pregnancy, and its potential role in disease pathogenesis. The final chapter explores these questions in greater detail, integrating biochemical and epidemiological findings to propose a model for the context-dependent functions of PZP in pregnancy.

# **CHAPTER 5:**

# FINAL DISCUSSION

### 5.1 Summary

Pregnancy is fundamentally important for all mammals, yet the maternal adaptions required to successfully navigate this life-stage remain incompletely understood. The work described in this thesis advances our understanding of the maternal factors contributing to variability in circulating PZP concentrations during pregnancy and underscores how these factors may drive cohort-dependent associations with adverse pregnancy outcomes such as PE. Additionally, by comparing and contrasting the actions of PZP and  $\alpha_2 M$  on chymase activity *in vitro*, the work presented in this thesis provides new knowledge of how the quaternary structure of these proteins is fundamentally important to their role in modulating biological processes. The final chapter of this thesis attempts to integrate the main findings reported herein and proposes a theoretical framework by which PZP-chymase interactions may contribute to pregnancy-associated maternal adaptations. Additionally, this model proposes that imbalance between the normal functions of PZP and  $\alpha_2 M$ , including their clearance via LRP1, may contribute to adverse pregnancy outcomes.

# 5.2 A framework for the distinct roles of PZP and $\alpha_2M$ in the regulation of chymase activity

The available evidence suggests that tight regulation of chymase activity is critically important for a successful pregnancy, reflecting its potential roles in supporting spiral artery remodelling locally and modulating vascular tone systemically (Tchougounova et al., 2003, Roy et al., 2014, Saarinen et al., 1994, Groschwitz et al., 2013, Tchougounova et al., 2005, Fu et al., 2017, Zhao et al., 2005, Bulmer et al., 2012, Zhang et al., 2022, Leskinen et al., 2001, Leskinen et al., 2003, Meyer et al., 2017, Takai et al., 1997, Urata et al., 1990b, Caughey et al., 2000, Urata et al., 1990a). Yet our understanding of the mechanisms responsible for these functions is limited. Thus, the findings presented in this thesis – demonstrating that chymase activity is modulated in fundamentally different ways depending on whether it binds to pregnancy-associated PZP or constitutively abundant  $\alpha_2 M$  – are highly intriguing and expand our understanding of how their divergent quaternary structures give rise to distinct functional outcomes. It is posited that the biological importance of PZP will be revealed by deepening our understanding of how its actions differ to those of  $\alpha_2 M$ .

### 5.2.1 Preferential binding to PZP over α2M may prolong chymase activity via reduced LRP1-mediated clearance

Previous studies using chymotrypsin as a model protease show that α<sub>2</sub>M-protease complexes bind LRP1 with 8-fold greater affinity than PZP-protease complexes in vitro (Chiabrando et al., 2002). If this difference in receptor affinity is not simply a consequence of the protease substrate involved, it would suggest that a₂M-chymase complexes are preferentially cleared from circulation relative to PZP-chymase complexes (Figure 5.2.1A). The rise in circulating PZP concentrations during pregnancy may allow it to outcompete  $\alpha_2 M$  for interaction with chymase, leading to the formation of PZP-chymase complexes with lower affinity for LRP1 and slower clearance, thereby sustaining chymase activity in circulation (Figure 5.2.1i). Such a mechanism may enable chymase to perform important pregnancy-specific functions that might otherwise be attenuated by the more rapid clearance of a<sub>2</sub>M-chymase. However, the overall regulation of chymase is likely influenced by additional factors. PZP-bound chymase can still be targeted by endogenous inactivators such as α1AT, which is also upregulated during pregnancy (Abbassi-Ghanavati et al., 2009); Figure 5.2.1ii). Moreover, chymase that binds to the heparin proteoglycan matrix of mast cells – which may sometimes occur upon mast cell degranulation – is protected from endogenous inactivators/inhibitors, including α1AT and α₂M (Lindstedt et al., 2001). These findings highlight the multifaceted nature of chymase regulation and suggest that its net activity depends on the relative abundance and availability of binding partners that modulate its function and clearance. A layered regulatory model, involving competition between clearance and inactivation pathways, may explain how appropriate chymase activity is maintained during pregnancy (Figure 5.2.1). This framework could also partially explain why PZP is upregulated in pregnancy, but high levels are not necessarily essential for successful gestation.

## 5.2.2 PZP may cooperate with other molecular inactivators to control chymase activity when LRP1-mediated clearance is overwhelmed

LRP1 is a multifunctional and highly promiscuous receptor that binds over 100 ligands, including LDL, and plays a critical role in lipid homeostasis during pregnancy (Guay et al., 2020). Under conditions of high ligand load, disease stress, or altered expression, such as metabolic dysfunction LRP1-mediated endocytosis is overwhelmed (Hofmann et al., 2007, Hamlin et al., 2016)(Figure 5.2.1B). Under these conditions, the clearance of  $\alpha_2$ M-chymase complexes via LRP1 may be impaired, potentially prolonging protease activity due to  $\alpha_2$ M's capacity to shield chymase from endogenous inactivators (Figure 5.2.1iii). In this scenario,

elevated PZP concentrations may act as a compensatory mechanism because, although PZP-chymase complexes are less efficiently cleared, they remain susceptible to inhibition by circulating inactivators such as  $\alpha$ 1AT (Figure 5.2.1ii). Thus, PZP may serve as a 'safety net', limiting protease activity when the clearance of  $\alpha_2$ M-protease complexes is impaired. It should be noted that this represents a hypothesis that requires empirical testing. Further studies incorporating *in situ* measurement of PZP,  $\alpha_2$ M, and chymase complex formation, as well as direct assessment of their differential clearance *in vivo*, would help determine the validity of this model.

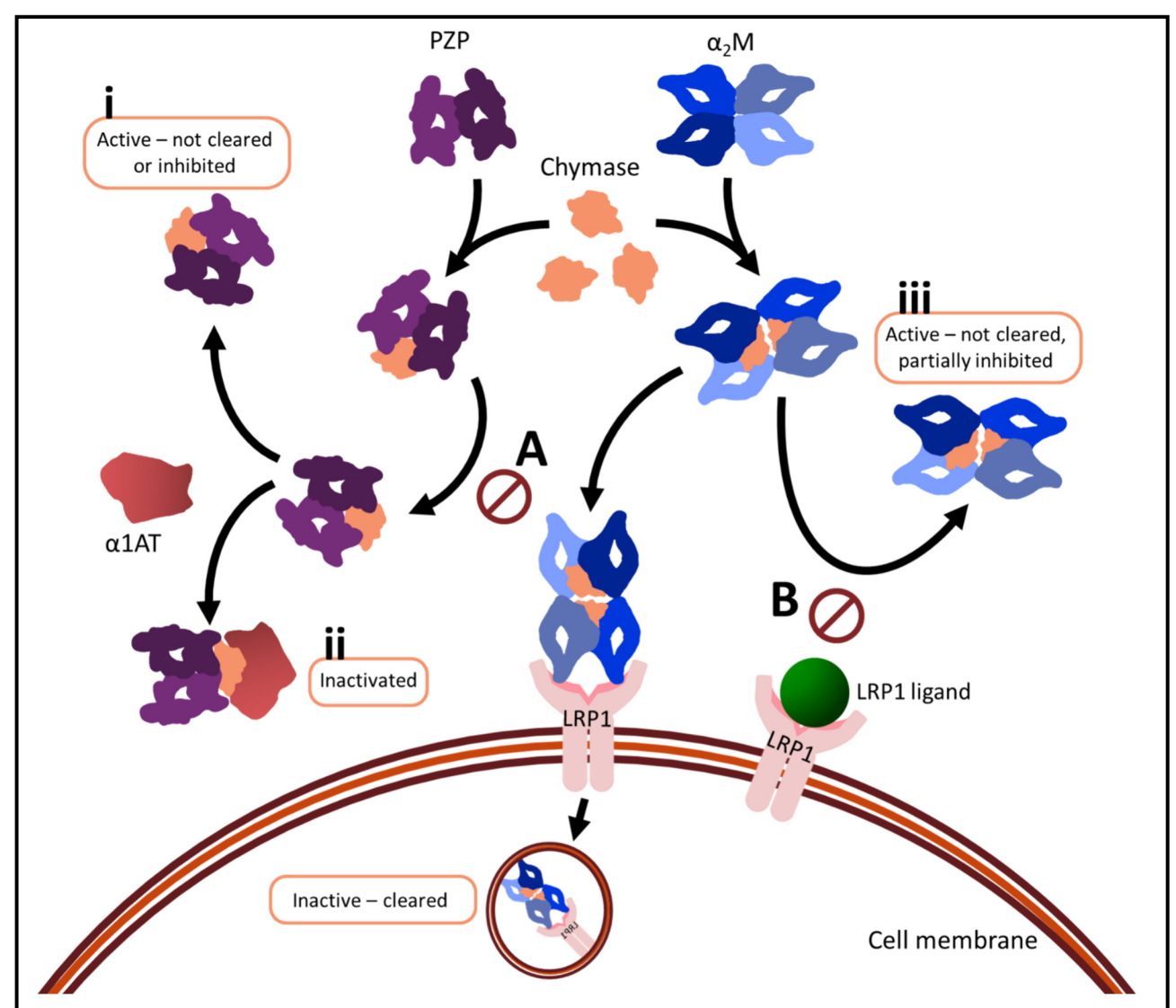


**Figure 5.2.1:** Proposed model of context-dependent regulation of chymase activity (status indicated in orange boxes) by PZP and  $\alpha_2M$  through differential clearance and susceptibility to endogenous inactivators. **(A)** When LRP1 is readily available,  $\alpha_2M$ -chymase complexes outcompete PZP-chymase for clearance via LRP1, resulting in the persistence of PZP-chymase complexes in circulation. **(B)** Under conditions where LRP1 is saturated by other ligands, neither  $\alpha_2M$ -chymase nor PZP-chymase complexes are efficiently cleared. Thus, chymase activity may be **(i)** fully preserved when bound to PZP, **(ii)** neutralised when targeted by endogenous inactivators such as  $\alpha_1AT$ , or **(iii)** prolonged but attenuated when bound to  $\alpha_2M$ .

# 5.3 PZP may play a role in protecting HDL from chymase-mediated degradation

During pregnancy, PZP becomes enriched on large HDL particles (Melchior et al., 2021) but the functional significance of this enrichment remains unclear. One possibility is that PZP is recruited to HDL to protect HDL-associated ApoA1 from chymase-mediated degradation (Lee et al., 2003). By binding chymase and limiting its access to ApoA1, PZP may help preserve HDL integrity and function during pregnancy. Although there is no direct evidence that PZP influences cholesterol efflux capacity, it is plausible that by maintaining HDL functionality, PZP indirectly supports this process. Consistent with this idea, cholesterol efflux capacity is reportedly increased during pregnancy (Melchior et al., 2021), and further increased in pregnant mothers with BMI ≥25 kg/cm² (Stadler et al., 2023). Elevated PZP levels in mothers with higher BMI may therefore reflect a compensatory response aimed at preserving HDL functionality and promoting metabolic homeostasis under physiologically stressful conditions. An alternate hypothesis is that elevated concentrations of PZP in obese mothers is the result of reduced clearance via LRP1 due to saturation of the receptor. It could also be posited that increased plasma PZP levels in mothers with BMI >25 kg/cm<sup>2</sup> reflect higher systemic inflammation. In the cohorts analysed, the association between PZP and CRP was weak, which does not strongly support this explanation. However, it is important to note that CRP was measured at the time of cohort recruitment by a commercial pathology laboratory. Therefore, differences in sample storage, timing, and handling, as well as the dynamic nature of both acute-phase proteins and PZP, mean that direct correlation between these measures is inherently limited.

# 5.4 A link between maternal plasma PZP concentration and maternal BMI suggests a possible metabolic role for PZP

Recent evidence points to a possible role for PZP in metabolic regulation. In murine models, PZP has been shown to promote thermogenesis through the activation of BAT (Lin et al., 2021). Further, adipose-specific overexpression of PZP protected against diet-induced obesity by enhancing the browning of white adipose tissue (WAT), increasing thermogenic gene expression, and improving glucose tolerance and insulin sensitivity (Jiang et al., 2022). While the findings of these studies raise the possibility that increased PZP may be upregulated in overweight and obese mothers to buffer metabolic stress. It is a limitation that they were derived from mouse models. However, proteomic analyses of human adipose-derived stem

cells identified PZP as one of several proteins that are upregulated during adipogenesis (Zvonic et al., 2007). This suggests that adipose tissue may contribute to circulating PZP levels – a source not typically considered in pregnancy – and that PZP itself may play a role in adipose tissue development or function. Together, these findings support a model in which PZP contributes to lipid handling and energy homeostasis in pregnancy, not only through protease regulation but also via direct effects on adipose tissue biology and thermogenic activity. Further studies are warranted to explore these mechanisms in more detail in the context of pregnancy.

# 5.5 Elevated maternal plasma PZP concentration and increased odds of hypertensive pregnancy

Several studies have linked PZP gene variants to an increased risk of hypertensive pregnancy disorders (Tyrmi et al., 2022, Tyrmi et al., 2023, Ardissino et al., 2024), including evidence from integrative genetic analyses that genetically determined higher circulating PZP is causally associated with greater risk of PE (Ardissino et al., 2024, Tyrmi et al., 2023). While some methodological limitations are acknowledged, this thesis presents the first evidence that elevated maternal plasma PZP is associated with increased odds of pregnancy-associated hypertension in nulliparous mothers. It remains unclear whether the upregulation of PZP contributes to the pathogenesis of hypertensive pregnancy or is merely a consequence of underlying inflammatory pathology, either of which are possible. While it is tempting to speculate that the interaction between PZP and chymase described in this thesis may be directly important to the association between increased maternal plasma PZP concentration and increased odds of pregnancy-associated hypertension, further work is needed to more deeply understand the role of PZP in controlling chymase in physiological settings. Specifically, a deeper understanding of the relationship between maternal plasma PZP concentration and the excessive chymase activity observed in the placenta and maternal serum of women with PE (Wang et al., 2007, Wang et al., 2010, Gu et al., 2017) is needed.

Nulliparous mothers with BMI  $\geq$ 25 kg/m² had elevated maternal plasma PZP levels compared to those with BMI  $\leq$ 25 kg/m². While the observed association between PZP and hypertensive disorders of pregnancy in this group should be interpreted cautiously, it raises the possibility that PZP participates in biological processes common to maternal adiposity and susceptibility to hypertension. Given that elevated BMI is a well-established risk factor for GH and PE, particularly LO-PE (Ulhaq et al., 2021, Sudjai, 2023, Bartsch et al., 2016, Mao et al., 2025), it

remains unclear whether the association between PZP and PE in overweight and obese mothers is primarily driven by maternal adiposity itself.

The finding that maternal plasma PZP concentration was positively associated with PE and/or GH in nulliparous mothers with BMI <25 kg/m² is highly intriguing. In contrast, to overweight or obese nulliparous mothers, who are typically subject to increased clinical surveillance, prediction of PE risk in nulliparous mothers with healthy BMI remains a clinical challenge. While the small sample sizes generated when stratifying by BMI limit statistical power, these results suggest that elevated PZP may be linked to underlying biological processes that increase susceptibility to PE in nulliparous women. Further studies are required to validate this association and to assess whether it reflects a meaningful biological relationship, particularly in prospective models stratified by BMI and other maternal characteristics.

### 5.6 Final remarks

PZP is a protein that has long remained in the shadow of its closely related counterpart,  $\alpha_2 M$ . However, methodological advances that now enable accurate discrimination between the two proteins are helping to reveal PZP as a distinct biological entity with unique functions, including the differential regulation of shared substrates such as chymase. This thesis deepens our understanding of how quaternary structure shapes the functional properties of these proteins – including their ability to sterically hinder substrates – and, in doing so, provides new insight into the biological significance of this important protein family.

By leveraging access to samples from multiple pregnancy cohorts and implementing quality control measures to minimise technical variability, this research identified several previously undescribed associations between PZP, maternal characteristics, and pregnancy outcomes. Notably, these findings challenge the longstanding assumption that PZP expression is primarily estrogen-dependent, instead highlighting the potential roles of parity, immunoregulation, and epigenetic control. The identification of parity as a novel determinant of circulating PZP concentrations informed the first attempt to characterise maternal plasma PZP levels exclusively in nulliparous mothers, confirming its positive association with BMI. These results underscore that PZP should not be considered in isolation but rather as one component of a broader regulatory network in which redundancy and compensation by other factors likely influence pregnancy outcomes.

While the positive association between elevated PZP in early pregnancy and pregnancy-associated hypertension measured in this study suggests a possible link, the findings were not consistent between STOP and SCOPE and requires further validation.

The work presented in this thesis provides the foundations for future investigations to elucidate the biological functions of PZP. Given the wide variation in circulating PZP concentration measured in pregnant mothers, it is evident that high levels of maternal plasma PZP are not essential to successful pregnancy. On one hand, this may be the result of PZP sharing functions with other molecules that render it redundant. Proteomic studies to comprehensively identify endogenous substrates for PZP are needed to reveal which molecular networks PZP participates in. On the other hand, it is possible that the importance of PZP is context-dependent or linked to a functional state that is dependent on post-translational regulation, such as proteolytic cleavage. Thus, selective measurement of native PZP versus the proteolytically cleaved form may also help to inform its role. Additionally, the development of methods to establish human placental organoids (Schäffers et al., 2025, Wessel et al., 2024, Zhou et al., 2025) represent an exciting opportunity to more fully understand the function of this enigmatic protein in the context of placental biology.

# SUPPLEMENTARY INFORMATION

### **6.1 List of Supplementary Figures**

Figure S1: Annotated Western blot image showing how the relative migration of PZP species
were calculated162
Figure S2: Fluorescence intensity curve of bisANS binding to PZP alone and PZP co-incubated
with chymotrypsin163
Figure S3: Unadjusted maternal plasma PZP concentration grouped by ethnicity in the
Nationwide Children's Hospital cohort167
Figure S4: Unadjusted maternal plasma PZP concentration by gestational age at sampling fo
each cohort170

### **6.2 List of Supplementary Tables**

Table S1: Reported substrates for human chymase    160
Table S2: Comorbidities among participants from the St George Hospital cohort.         164
Table S3: Frequency of parity and gravidity in the St George Hospital cohort
Table S4: Logistic regression models assessing the association between maternal plasma PZP
concentration and pregnancy outcome in the St George Hospital cohort164
Table S5: Correlations between maternal plasma PZP concentration and maternal and
neonatal characteristics
Table S6: Univariate linear regression analyses assessing the relationship between maternal
plasma PZP concentration and clinical characteristics that significantly correlated with PZP in
the St George Hospital cohort
Table S7: Linear regression models assessing the effect of parity on maternal plasma PZP
concentration in the St George hospital cohort
Table S8:         Maternal characteristics grouped by cohort in the St George Hospital and Nationwide
Children's Hospital cohorts
Table S9: Frequency of parity and gravidity in the Nationwide Children's Hospital cohort 165
Table S10: Logistic regression models assessing the association between maternal plasma
PZP concentration and pregnancy outcome in the Nationwide Children's Hospital cohort 166
Table S11: Correlations between maternal characteristics and maternal plasma PZP
concentration in the Nationwide Children's Hospital cohort
Table S12: Linear regression models assessing the effect of parity and gravidity on maternal
plasma PZP concentration in the Nationwide Children's Hospital cohort
Table S13: Correlation of parity and gravidity with maternal plasma PZP concentration within
each pregnancy outcome group in the Nationwide Children's Hospital cohort
Table S14: Individual linear regression models assessing the effect of parity and gravidity on
maternal plasma PZP concentration within each pregnancy outcome group in the Nationwide
Children's Hospital cohort
Table S15: Comorbidities among participants in the late STOP cohort
Table S16: Frequency of gravidity in the late STOP cohort.    168
Table S17: AIC and BIC for logistic regression models used to assess the effect of maternal
plasma PZP concentration on pregnancy outcome in the late STOP cohort
Table S18: Logistic regression models assessing the association between maternal plasma
PZP concentration and pregnancy outcome in the late STOP cohort

Table S19: Correlations between maternal plasma PZP concentration and maternal and
neonatal characteristics in the late STOP cohort
Table S20: Comorbidities for participants in the STOP cohort.    171
Table S21: Frequency of gravidity in the STOP cohort
Table S22: Logistic regression analyses, adjusted for gestational age at sampling and BMI, to
assess the effect of PZP on the odds of a woman having a pregnancy complication compared
to uncomplicated pregnancy in the STOP cohort
Table S23: Logistic regression analyses to assess the effect of PZP on the odds of a woman
having a pregnancy complication compared to uncomplicated pregnancy in mothers from the
STOP cohort with BMI <25 kg/cm²
Table S24: Logistic regression analyses to assess the effect of PZP on the odds of a woman
having a pregnancy complication compared to uncomplicated pregnancy in mothers from the
STOP cohort with BMI ≥25 kg/cm²174
Table S25:    Comorbidities for participants in the SCOPE cohort.    175
Table S26: Frequency of gravidity in the SCOPE cohort
Table S27: Logistic regression analyses, adjusted for gestational age at sampling and BMI, to
assess the effect of PZP on the odds of a woman having a pregnancy complication compared
to uncomplicated pregnancy in the SCOPE cohort
Table S28: Logistic regression analyses to assess the effect of PZP on the odds of a woman
having a pregnancy complication compared to uncomplicated pregnancy in mothers from the
SCOPE cohort with BMI <25 kg/cm²
Table S29: Logistic regression analyses to assess the effect of PZP on the odds of a woman
having a pregnancy complication compared to uncomplicated pregnancy in mothers from the
SCOPE cohort with BMI ≥25 kg/cm <sup>2</sup> 178

# **6.3 Chapter 2 Supplementary Information**

**Table S1:** Reported substrates for human chymase.

Substrate	Substrate function	Study type	Supporting results	Reference
Fibronectin	Component of ECM. Involved in cellular interactions with ECM (e.g., cell migration, adhesion, differentiation, growth)	In vitro	Degradation of fibronectin in smooth muscle cells visible.	(Leskinen et al., 2003)
Biglycan	ECM component. Released as an alarmin.	In vitro	Degradation of biglycan within 60 min	(Roy et al., 2014)
Pro-MMP-1 (procollagenase)	Inactive precursor of MMP-1. Active form involved in ECM degradation.	In vitro	Time- and concentration-dependent activation of MMP-1. Enhanced by presence of heparin.	(Saarinen et al., 1994)
Pro-MMP-2	Inactive precursor of MMP-2. Active form involved in ECM degradation.	In vitro	Time- and concentration-dependent activation of MMP-2. Enhanced by presence of heparin.	(Groschwitz et al., 2013)
Albumin	Osmotic pressure regulation. Carrier protein.	In vitro	Cleavage of albumin into two fragments that remain disulfide linked	(Raymond et al., 2003)
Membrane-bound stem cell factor (SCF)	Supports development of stem cells, germ cells, mast cells, and melanocytes.  Promotes haematopoiesis.	In vitro	Cleavage of SCF near membrane to produce soluble bioactive form	(Longley et al., 1997)
IL-6	Pro-inflammatory cytokine.	In vitro	Cleavage of IL-6	(Fu et al., 2017, Zhao et al., 2005)
IL-13	Pro-inflammatory cytokine.	In vitro	Degradation of IL-13	(Zhao et al., 2005)
IL-15	Pro-inflammatory cytokine.	In vitro	Cleavage of IL-15	(Fu et al., 2017)
Pro-IL-18	Inactive precursor of IL-18.	In vitro	Time-dependent cleavage of pro-IL-18 to a truncated, biologically active IL-18 species.	(Omoto et al., 2006)
IL-18	Pro-inflammatory cytokine	In vitro	Degradation of IL-18	(Fu et al., 2017)
Pro-IL-33	Inactive precursor of IL-33.	In vitro	Cleavage of IL-33 to an active form	(Fu et al., 2017)

IL-33	Pro-inflammatory cytokine.	In vitro	Degradation of IL-33	(Roy et al., 2014, Fu et al., 2017)
Pro-IL-1β	Inactive precursor of IL-1β. Active form is a pro-inflammatory cytokine.	In vitro	Time-dependent cleavage of pro-IL-1β to a truncated, biologically active IL-1β species.	(Morales- Maldonado et al., 2024, Mizutani et al., 1991)
Pro-IL-1α	Inactive precursor of IL- $1\alpha$ . Active form is a pro-inflammatory cytokine.	In vitro	Dose-dependent cleavage of pro-IL-1 $\alpha$ to a truncated, biologically active IL-1 $\alpha$ species.	(Afonina et al., 2011)
IFN-γ	Pro-inflammatory cytokine.	In vitro	Cleavage of IFN-γ	(Fu et al., 2017)
Latent TGF-β1	Inactive precursor form of TGF-β1. Active TGF-β1 can control cell growth, proliferation, differentiation, and apoptosis.	In vitro	Chymase-specific inhibitor reduced active TGF-β1 compared to control and tryptase inhibitor.	(Cho et al., 2015)
Connective tissue growth factor (CTGF)	Involved in tissue/bone development and repair, fibrosis, angiogenesis and tumorigenesis.	In vitro	Cleavage of CTGF	(Fu et al., 2017)
Insulin-like growth factor 1 (IGF-1)	Mediator of growth hormone stimulated somatic growth, and independent anabolic processes in cells/tissue.	In vitro	Degradation of IGF-1	(Fu et al., 2017, Tejada et al., 2016)
Human and virulent Hsp70	Intracellular chaperone. Released as an alarmin.	In vitro	Degradation of Hsp70 within 60 min, can be blocked by chymostatin	(Roy et al., 2014)
HMGB1	Signalling molecule, involved in gene regulation.  Released as an alarmin.	In vitro	Degradation of HMGB1	(Roy et al., 2014)
Angiotensin I	Precursor to Angiotensin II, a potent vasoconstrictor.	In vitro, ex vivo	Purified chymase cleaved Ang I to Ang II	(Takai et al., 1997, Urata et al., 1990b, Caughey et al., 2000, Raymond et al., 2009)

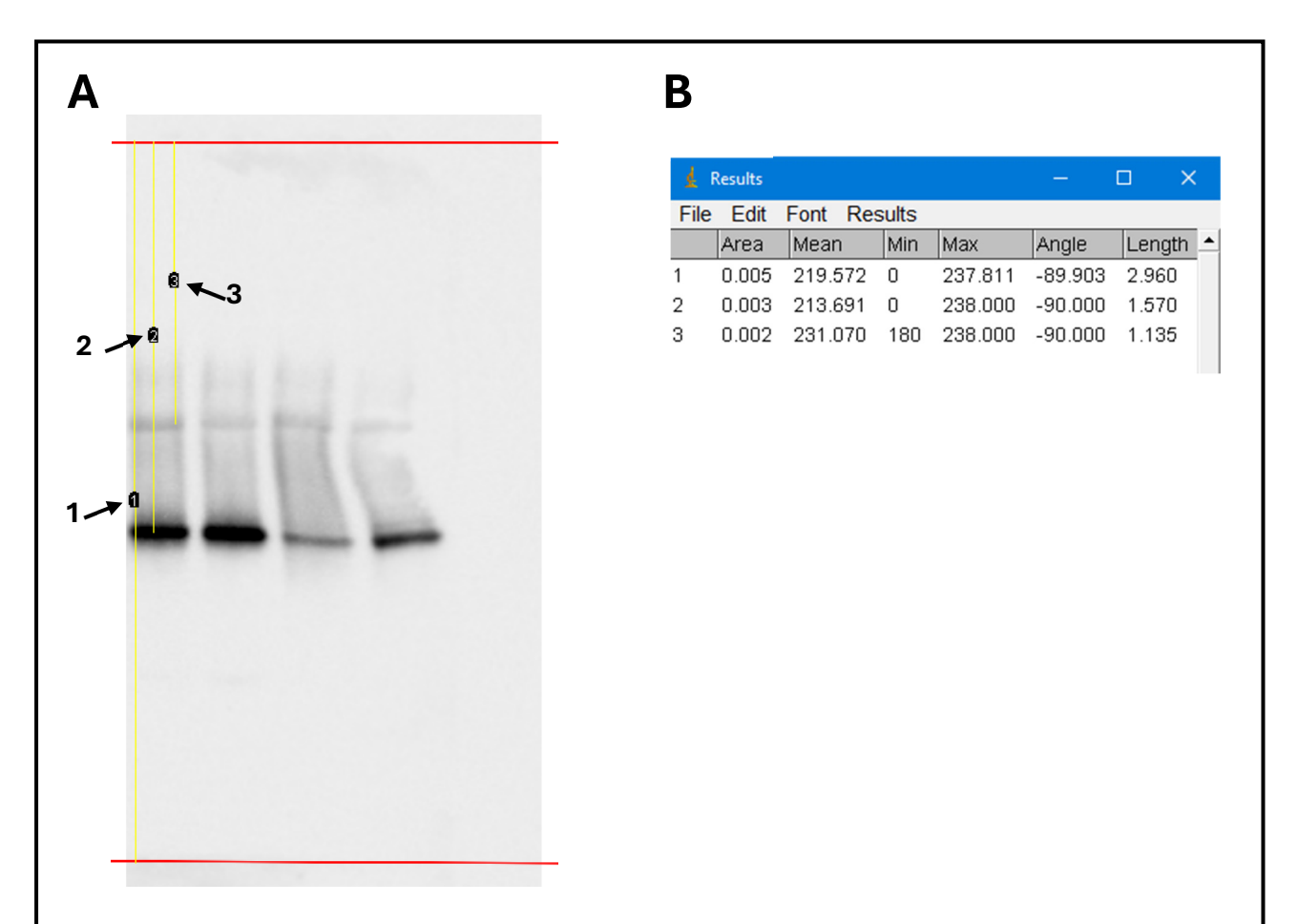


**Figure S1:** Annotated Western blot image showing how the relative migration (Rf) of PZP species were calculated. The equivalent of 1 μL of human pregnancy plasma was separated on a NuPAGE Tris-Acetate 3-8% mini protein gel, transferred to a nitrocellulose membrane and probed with an anti-PZP antibody. **(A)** The edges of the blot were marked by adjusting the contrast as needed. ImageJ was then used to measure the length of the blot (1), from the top of the blot to the lower band (2), and from the top of the blot to the upper band (3). **(B)** Measurements obtained from ImageJ corresponding to **(A)**. Rf was calculated by dividing the distance to the band of interest by the overall length of the blot e.g., 1.570/2.960 = 0.53 for the lower band, and 1.135/2.960 = 0.38 for the upper band.

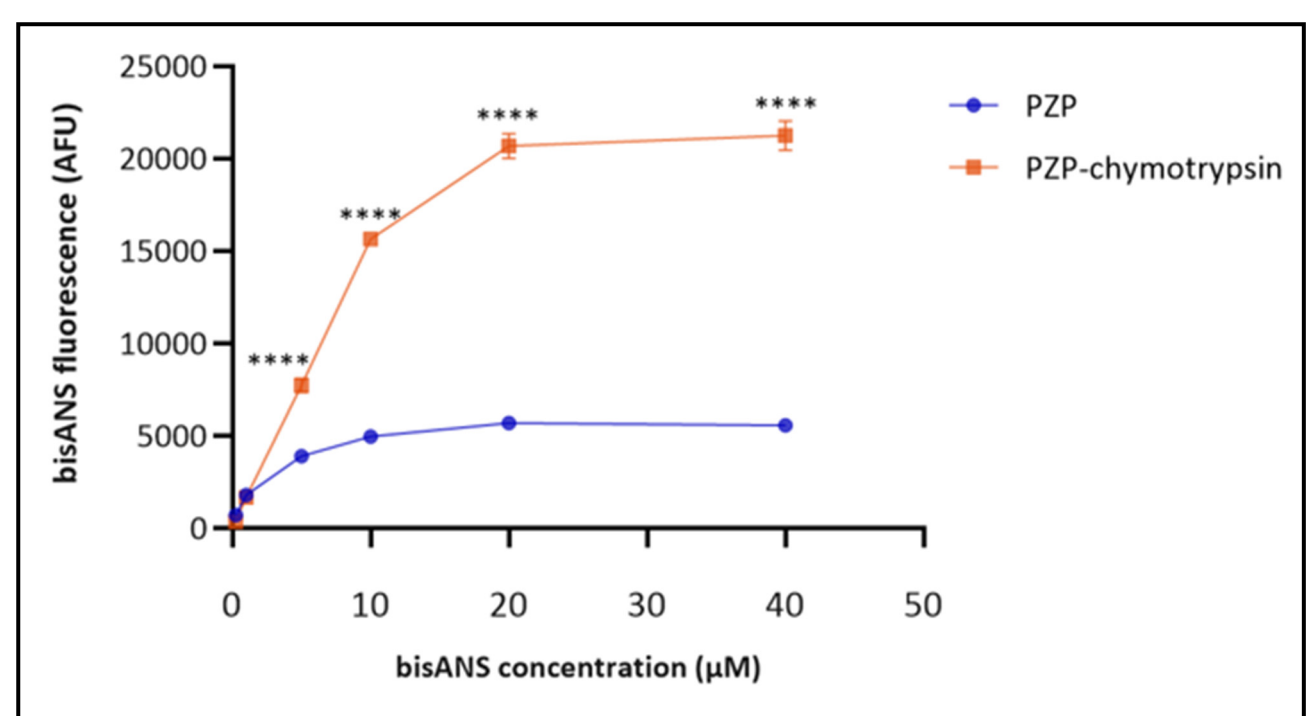


**Figure S2:** Fluorescence intensity curve of bisANS binding to PZP alone and PZP co-incubated with chymotrypsin. PZP (1  $\mu$ M) was incubated alone or with chymotrypsin at a 1:1 molar ratio for 45 min at 37 °C. bisANS was added at final concentrations indicated by x-axis. Data are mean bisANS fluorescence  $\pm$  SD (n = 3) expressed in arbitrary fluorescence units (AFU) and are representative of two independent experiments. One-way ANOVA with post-hoc Tukey's HSD for each timepoint, significance indicated by asterisks (\*\*\*\* p <0.0001).

## **6.4 Chapter 3 Supplementary Information**

## 6.4.1 St George Hospital

 Table S2: Comorbidities among participants from the St George Hospital cohort.

	Control	Preeclampsia
n	31	31
Comorbidities		
Gestational diabetes mellitus	1 (3.2)	7 (22.6)
Chronic/essential hypertension	0 (0)	4 (12.9)
Gestational hypertension	0 (0)	4 (12.9)
Antepartum haemorrhage (>20 weeks)	2 (6.4)	0 (0)
Threatened pre-term labour	0 (0)	7 (22.6)
Thrombocytopaenia	0 (0)	8 (25.8)
HELLP syndrome	0 (0)	2 (6.4)

Reported as n (%).

**Table S3:** Frequency of parity and gravidity in the St George Hospital cohort.

	Parity			Grav	vidity (incl	udes curre	ent pregna	ncy)	
	0	1	2	3	1	2	3	4	5
Normotensive	17	9	2	3	5	16	6	3	1
Preeclampsia	7	20	4	0	10	11	3	5	2
Total	24	29	6	3	15	27	9	8	3

**Table S4:** Logistic regression models assessing the association between maternal plasma PZP concentration and pregnancy outcome in the St George Hospital cohort (n = 62; 31 normotensive [reference] and 31 PE).

Model [AIC, BIC]	Variable	Odds ratio [95% CI]	p
1 [85.4, 84.6]	PZP (μg/mL)	0.996 [0.996, 0.999]	0.01
	Gestational age at sampling (weeks)	0.968 [ 0.796, 1.177]	0.74
	BMI (kg/m²)	1.088 [0.962, 1.231]	0.18
2 [83.5, 82.9]	PZP (μg/mL)	0.996 [0.992, 0.999]	0.01
	BMI (kg/m²)	1.088 [0.962, 1.230]	0.18
3 [85.3, 84.7]	PZP (μg/mL)	0.996 [0.993, 0.999]	0.02
	Gestational age at sampling (weeks)	0.969 [0.799, 1.177]	0.75
4 [83.4, 83.0]	PZP (μg/mL)	0.996 [0.993, 0.999]	0.02

**Table S5:** Correlations between maternal plasma PZP concentration and maternal and neonatal characteristics. Spearman's rho; n = 535.

Characteristic	Correlation coefficient	p
BMI (kg/m²)	0.14	0.30
Maternal age (years)	-0.01	0.94
Gestational age at time of sampling (weeks)	-0.07	0.59
Systolic BP (mmHg)	-0.20	0.11
Diastolic BP (mmHg)	-0.19	0.15
Gestational age at birth (weeks)	0.26	0.049
Neonatal birthweight (g)	0.23	0.08
Parity	0.28	0.03
Gravidity	0.23	0.07

**Table S6:** Univariate linear regression analyses assessing the relationship between maternal plasma PZP concentration and clinical characteristics that significantly correlated with PZP in the St George Hospital cohort.

Predictor (n)	Dependent Variable	Ratio of geometric means [95% CI]	р
sFlt-1:PIGF (40)	Log[PZP (μg/mL)]	0.997 [0.994, 0.999]	0.03
PZP (μg/mL) (40)	sFlt-1:PlGF	0.997 [0.994, 0.999]	0.02
PZP (μg/ml) (62)	Gestational age at birth (weeks) <sup>a</sup>	1.003 [1.000, 1.007]	0.05

<sup>&</sup>lt;sup>a</sup>Missing data for n = 2 normotensive participants.

**Table S7:** Linear regression models assessing the association between parity and maternal plasma PZP concentration in the St George hospital cohort (n = 62).

Model [AIC, BIC]	Variable	Ratio of geometric means [95% CI]	р	
1 [173.3, 179.7]	Parity (parous versus nulliparous)	1.748 [1.085, 2.814]	0.02	
2 [174.8, 183.3]	Parity (parous versus nulliparous)	1.747 [1.087, 2.808]	0.02	
	Gestational age at sampling	0.969 [0.890, 2.808]	0.48	
3 [175.0, 183.5]	Parity (parous versus nulliparous)	1.720 [1.065, 2.778]	0.03	
	BMI	1.013 [0.963, 1.066]	0.61	
4 [176.5, 187.7]	Parity (parous versus nulliparous)	1.720 [1.067, 2.773]	0.03	
	Gestational age at sampling	0.970 [0.890, 1.056]	0.48	
	BMI	1.013 [0.963, 1.065]	0.62	

#### 6.4.2 Nationwide Children's Hospital

**Table S8:** Maternal characteristics grouped by cohort in the St George Hospital and Nationwide Children's Hospital cohorts.

	Nationwide Children's Hospital	St George Hospital	р
n	121	62	
Maternal age (years)	28.04 ± 6.37	32.27 ± 4.90	<0.0001
Gestational age at sampling (weeks)	27.92 ± 2.94	35.80 ± 2.70	<0.0001
Nulliparous	53 (43.8)	24 (38.7)	0.46
Primigravida	50 (41.3)	15 (24.2)	0.02

Continuous variables compared using Student's T-test and reported as mean  $\pm$  SD. Categorical variables compared using Fisher's exact test and reported as n (%).

Table S9: Frequency of parity and gravidity in the Nationwide Children's Hospital cohort.

	Parity						Gravidity (includes current pregnancy)										
	0	1	2	3	4	5	6	1	2	3	4	5	6	7	8	9	10
Normotensive	16	11	3	0	0	0	0	13	12	4	1	0	0	0	0	0	0
PE	16	8	2	3	0	0	1	12	8	3	4	1	0	0	1	0	1
PE + IUGR	21	4	5	0	0	1	0	16	6	2	1	4	1	1	0	0	0
sPTB	14	9	4	1	1	1	0	9	10	4	3	2	0	2	0	0	0
Total	67	32	14	4	1	2	1	50	36	13	9	7	1	3	1	0	1

**Table S10:** Logistic regression models assessing the association between maternal plasma PZP concentration and pregnancy outcome in the Nationwide Children's Hospital cohort (n = 121; 30 normotensive [reference]).

Model [AIC, BIC]	Outcome	Variable	Odds Ratio [95% CI]	р
1 [338.7, 338.2]	PE	PZP (μg/mL)	1.001 [0.998, 1.005]	0.48
	PE + IUGR	PZP (μg/mL)	1.001 [0.998, 1.005]	0.48
	sPTB	PZP (μg/mL)	1.002 [0.998, 1.005]	0.43
2 [337.4, 336.7]	PE	PZP (μg/mL)	1.002 [0.998, 1.006]	0.46
		Parity (parous versus nulliparous)	0.905 [0.316, 2.586]	0.85
	PE + IUGR	PZP (μg/mL)	1.002 [0.998, 1.006]	0.32
		Parity (parous versus nulliparous)	0.474 [0.161, 1.97]	0.18
	sPTB	PZP (μg/mL)	1.001 [0.997, 1.005]	0.49
		Parity (parous versus nulliparous)	1.190 [0.417, 3.396]	0.75
3 [338.3, 337.7]	PE	PZP (μg/mL)	1.001 [0.998, 1.005]	0.47
		Gestational age at sampling (weeks)	0.947 [0.796, 1.128]	0.54
	PE + IUGR	PZP (μg/mL)	1.001 [0.998, 1.005]	0.46
		Gestational age at sampling (weeks)	0.896 [0.752, 1.067]	0.90
	sPTB	PZP (μg/mL)	1.002 [0.998, 1.005]	0.41
		Gestational age at sampling (weeks)	0.885 [0.741, 1.057]	0.18
4 [336.8, 335.9]	PE	PZP (μg/mL)	1.002 [0.998, 1.006]	0.44
		Parity (parous versus nulliparous)	0.868 [0.300, 2.508]	0.79
		Gestational age at sampling (weeks)	0.945 [0.793, 1.126]	0.53
	PE + IUGR	PZP (μg/mL)	1.002 [0.998, 1.006]	0.28
		Parity (parous versus nulliparous)	0.434 [0.144, 1.302]	0.14
		Gestational age at sampling (weeks)	0.882 [0.738, 1.054]	0.17
	sPTB	PZP (μg/mL)	1.002 [0.998, 1.006]	0.44
		Parity (parous versus nulliparous)	1.091 [0.376, 3.166]	0.87
		Gestational age at sampling (weeks)	0.887 [0.743, 1.060]	0.89

**Table S11:** Correlations between maternal characteristics and maternal plasma PZP concentration in the Nationwide Children's Hospital cohort. Spearman's rho; n = 121.

Characteristic	Correlation coefficient	p
Maternal age (years)	0.12	0.19
Gestational age at time of sampling (weeks)	0.04	0.63
Parity	0.32	<0.001
Gravidity	0.26	0.004

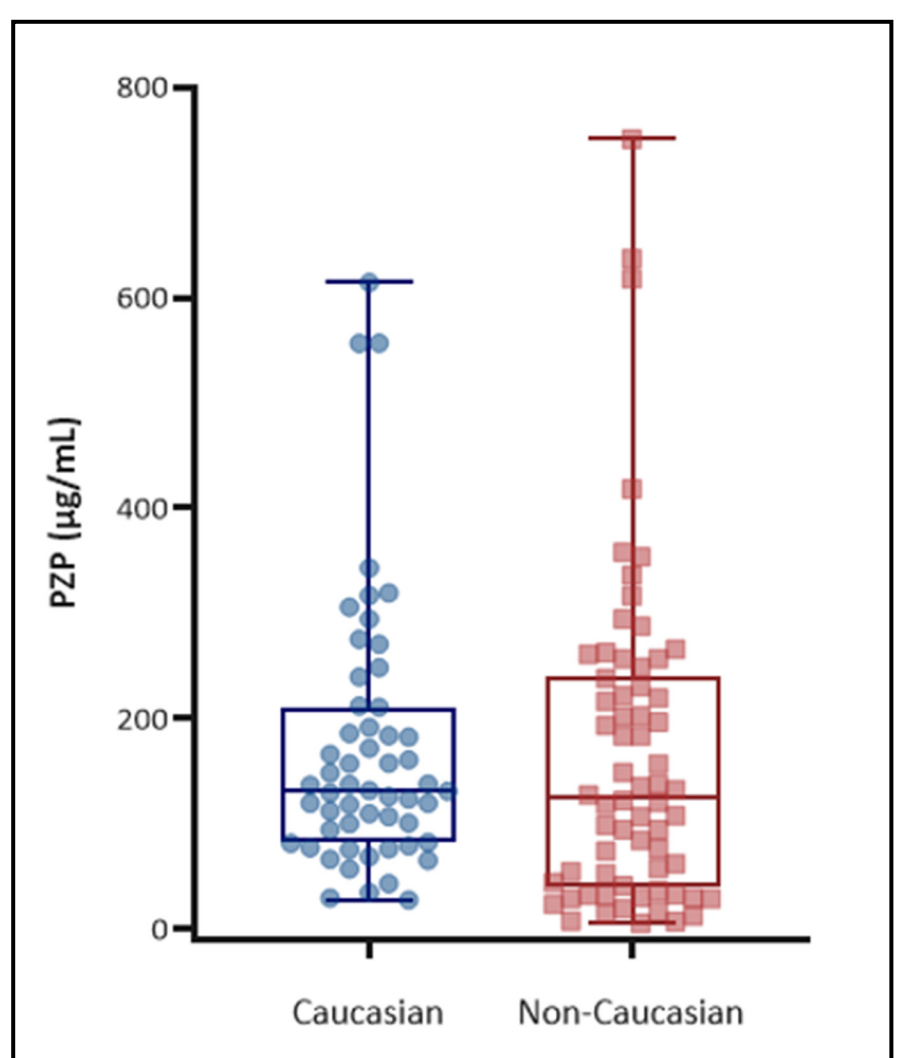


**Figure S3:** Unadjusted maternal plasma PZP concentration grouped by ethnicity in the Nationwide Children's Hospital cohort. Two-tailed Mann-Whitney U test; no statistically significant differences were observed between groups. n = 121 (55 Caucasian, 66 non-Caucasian).

**Table S12:** Linear regression models assessing the association between parity or gravidity and maternal plasma PZP concentration in the Nationwide Children's Hospital cohort (n = 121).

Model [AIC, BIC]	Variable	Odds ratio [95% CI]	р
1 [331.9, 343.1]	Parity (parous versus nulliparous)	1.774 [1.273, 2.474]	<0.001
	Gestational age at sampling (weeks)	1.027 [0.970, 1.087]	0.361
2 [330.8, 339.1]	Parity (parous versus nulliparous)	1.748 [1.255, 2.437]	<0.001
3 [332.8, 343.9]	Gravidity (multigravida versus primigravida)	1.760 [1.251, 2.477]	0.001
	Gestational age at sampling (weeks)	1.036 [0.978, 1.098]	0.225
4 [332.2, 340.61]	Gravidity (multigravida versus primigravida)	1.689 [1.206, 2.367]	0.002

**Table S13:** Correlation of parity and gravidity with maternal plasma PZP concentration within each pregnancy outcome group in the Nationwide Children's Hospital cohort. Spearman's rho.

Outcome	Variable	Correlation coefficient	р
Normotensive (n = 30)	Parity	0.33	0.07
	Gravidity	0.33	0.08
PE (n = 30)	Parity	0.20	0.29
	Gravidity	0.03	0.86
PE + IUGR (n = 31)	Parity	0.46	0.01
	Gravidity	0.47	0.008
sPTB (n = 30)	Parity	0.25	0.19
	Gravidity	0.18	0.34

**Table S14:** Individual linear regression models assessing the association between parity or gravidity and maternal plasma PZP concentration within each pregnancy outcome group in the Nationwide Children's Hospital cohort.

Outcome	Variable	Ratio of geometric means [95% CI]	р
Normotensive (n = 30)	Parity (parous versus nulliparous)	1.607 [0.998, 2.586]	0.05
	Gravidity (multigravida versus primigravida)	1.628 [1.009, 2.625]	0.05
PE (n = 30)	Parity (parous versus nulliparous)	1.534 [0.707, 3.331]	0.28
	Gravidity (multigravida versus primigravida)	1.098 [0.491, 2.452]	0.82
PE + IUGR (n = 31)	Parity (parous versus nulliparous)	2.442 [1.193, 4.997]	0.02
	Gravidity (multigravida versus primigravida)	2.677 [1.406, 5.097]	0.003
sPTB (n = 30)	Parity (parous versus nulliparous)	1.631 [0.834, 3.189]	0.15
	Gravidity (multigravida versus primigravida)	1.661 [0.799, 3.455]	0.17

#### 6.4.3 Late STOP

 Table S15: Comorbidities among participants in the late STOP cohort

	PE	sPTB	GH	SGA
n (%)	59 (100)	19 (100)	23 (100)	54 (100)
Comorbidities				
Spontaneous preterm birth n (%)	2 (3.4)	-	-	-
Gestational hypertension n (%)	1 (1.7)	2 (10.5)	-	-
Small for gestational age n (%)	18 (30.5)	3 (15.8)	0 (0)	-
Gestational diabetes mellitus n (%)	11 (18.6)	4 (21.1)	4 (17.4)	5 (9.3)

Women with multiple comorbidities were included in the count for both categories.

**Table S16:** Frequency of gravidity in the late STOP cohort.

		Gravidity (includes current pregnancy)			
	1	2	3	4	5
Uncomplicated	222	49	14	3	1
Preeclampsia	28	10	3	0	0
Small for gestational age	34	11	6	3	0
PE + SGA	14	3	1	0	0
Gestational hypertension	16	7	0	0	0
Gestational diabetes mellitus	38	17	2	0	0
Spontaneous preterm birth	13	3	2	1	0
Other complication	25	6	3	0	0
Total	390	106	31	7	1

**Table S17:** AIC and BIC for logistic regression models used to assess the association between maternal plasma PZP concentration and pregnancy outcome in the late STOP cohort.

Model	AIC	BIC
PZP (μg/mL)	1576.5	1576.1
PZP (μg/mL), gestational age at sampling (weeks)	1571.6	1570.9
PZP (μg/mL), BMI (kg/m²)	1549.8	1549.2
PZP (μg/mL), gestational age at sampling (weeks), BMI (kg/m²)	1545.5	1544.7

**Table S18:** Logistic regression models assessing the association between maternal plasma PZP concentration and pregnancy outcome in the late STOP cohort (n = 535; n = 289 uncomplicated [reference]).

Outcome	Variable	Odds ratio [95% CI]	p
Preeclampsia (n = 59)	PZP (μg/mL)	1.000 [0.998, 1.002]	0.76
	GA (weeks)	1.123 [0.892, 1.413]	0.32
	BMI (kg/m²)	1.068 [1.029, 1.108]	<0.001
Gestational hypertension (n = 23)	PZP (μg/mL)	1.001 [0.998, 1.004]	0.40
, , , , , , , , , , , , , , , , , , ,	GA (weeks)	0.818 [0.569, 1.177]	0.28
	BMI (kg/m²)	1.089 [1.036, 1.144]	<0.001
Gestational diabetes mellitus (n = 57)	PZP (μg/mL)	0.999 [0.996, 1.001]	0.24
Gestational diabetes meintus (n = 37)	GA (weeks)	0.929 [0.735, 1.176]	0.54
	BMI (kg/m²)	1.070 [1.031, 1.109]	<0.001
Spontaneous preterm birth (n = 19)	PZP (μg/mL)	1.001 [0.998, 1.005]	0.49
. ,	GA (weeks)	0.759 [0.516, 1.118]	0.16
	BMI (kg/m²)	0.998 [0.930, 1.072]	0.96
Small for gestational age (n = 54)	PZP (μg/mL)	1.001 [0.999, 1.003]	0.50
omain for gestational age (ii. 5.1)	GA (weeks)	1.073 [0.846, 1.361]	0.56
	BMI (kg/m²)	1.044 [1.003, 1.087]	0.03
Other conglication (n = 24)	PZP (μg/mL)	1.002 [0.999, 1.004]	0.18
Other complication (n = 34)	GA (weeks)	1.141 [0.851, 1.528]	0.18
	BMI (kg/m²)	1.051 [1.001, 1.102]	0.04

**Table S19:** Correlations between maternal plasma PZP concentration and maternal and neonatal characteristics in the late STOP cohort. Spearman's rho; n = 535.

	Correlation coefficient	p
Gestational age at sampling (weeks)	-0.01	0.78
Maternal age (years)	0.05	0.25
BMI (kg/m²)	0.11	0.008
Gravidity	-0.05	0.23
Birthweight (g)	-0.01	0.87

#### 6.4.4 Additional

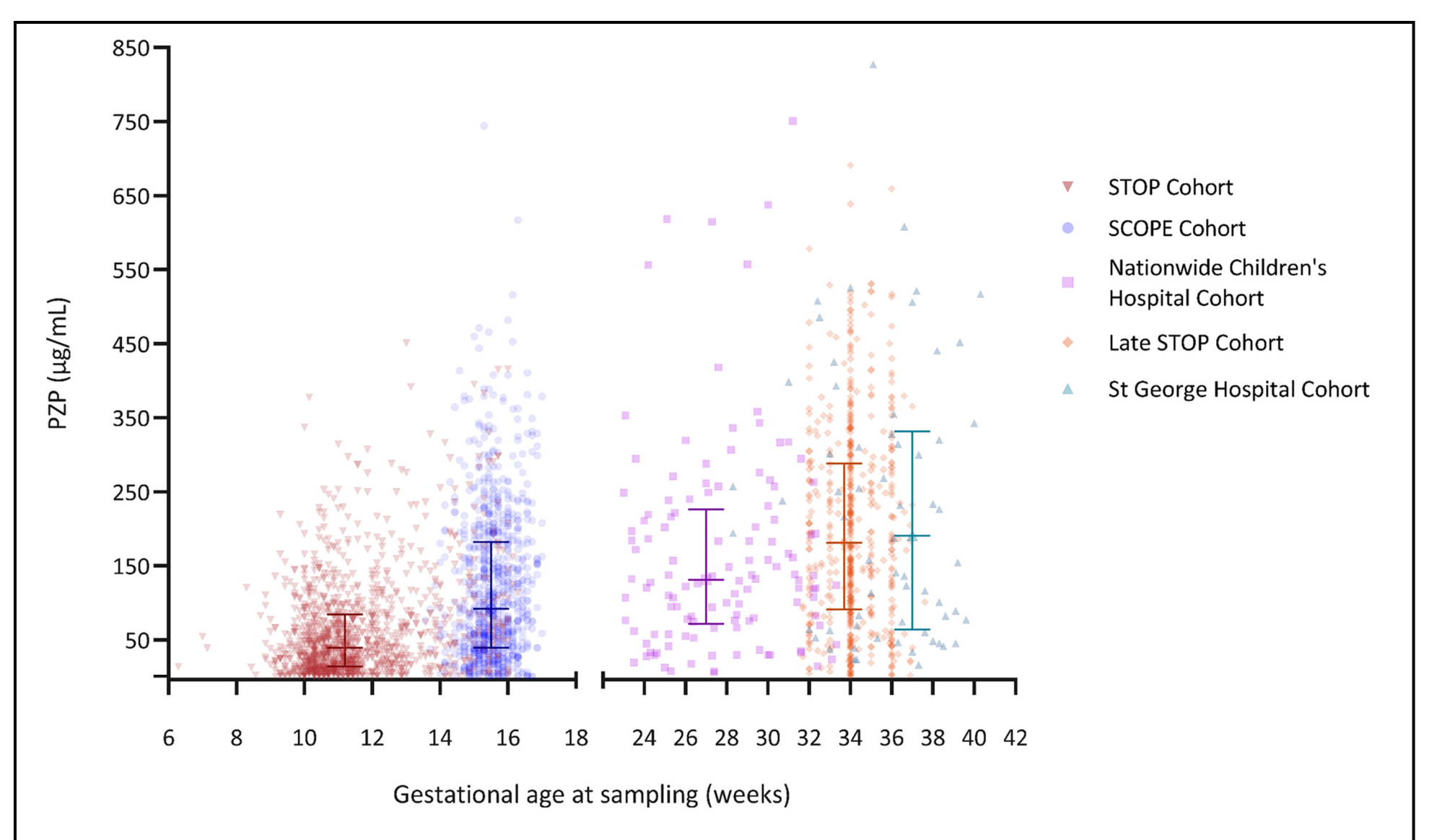


Figure S4: Unadjusted maternal plasma PZP concentration by gestational age at sampling (weeks) for the STOP (n = 1250) and SCOPE (n = 863), Nationwide Children's Hospital (n = 121), late STOP (n = 535), and St George Hospital Cohorts (n = 62). Bars represent median, Q1, and Q3.

## 6.5 Chapter 4 Supplementary Information

### 6.5.1 STOP

**Table S20:** Comorbidities for participants in the STOP cohort.

	Preeclampsia	Spontaneous preterm birth	Gestational hypertension	Small for gestational age
n (%)	119 (100)	53 (100)	78 (100)	103 (100)
Comorbidities				
Spontaneous preterm birth n (%)	5 (4.2)	-	-	-
Gestational hypertension n (%)	1 (0.8)	5 (9.4)	-	-
Small for gestational age n (%)	38 (31.9)	7 (13.2)	0 (0)	-
Gestational diabetes mellitus n (%)	19 (16.0)	12 (22.6)	17 (21.8)	11 (10.7)

Women with multiple comorbidities were included in the count for both categories.

**Table S21:** Frequency of gravidity in the STOP cohort.

		Gravidity (includes current pregnancy)			
	1	2	3	4	5
Uncomplicated <sup>a</sup>	496	138	46	5	2
Preeclampsia <sup>b</sup>	77	31	8	2	0
Gestational hypertension	55	17	6	0	0
Gestational diabetes mellitus	104	23	6	1	0
Small for gestational age	75	20	8	0	0
Spontaneous preterm birth	40	10	3	0	0
Other complication <sup>c</sup>	42	15	6	2	0
Total	889	254	83	10	2

Missing data for <sup>a</sup>n = 9, <sup>b</sup>n = 1, <sup>c</sup>n = 2 participants.

**Table S22:** Logistic regression analyses, adjusted for gestational age at sampling and BMI, to assess the association between PZP and the odds of a woman having a pregnancy complication compared to uncomplicated pregnancy (n = 695) in the **STOP cohort.** 

Outcome	Contrasts (PZP μg/mL)	Odds ratio [95% CI]	p
Preeclampsia (n = 119)	None	1.001 [0.998, 1.004]	0.44
	≥14.01 / <14.01 (first quartile)	0.957 [0.605, 1.515]	0.85
	≥39.37 / <39.37 (median)	1.408 [0.938, 2.115]	0.10
	≥84.12 / <84.12 (third quartile)	1.228 [0.785, 1.922]	0.37
Gestational hypertension (n = 78)	None	0.995 [0.991, 0.999]	0.04
,,,,,,,,,,,,,,,,,,,,,,,,,,,,,,,,,,,,,,,	≥14.01 / <14.01 (first quartile)	0.998 [0.562, 1.774]	0.99
	≥39.37 / <39.37 (median)	0.838 [0.512, 1.373]	0.49
	≥84.12 / <84.12 (third quartile)	0.510 [0.264, 0.988]	0.046
Gestational diabetes mellitus (n = 134)	None	1.000 [0.997, 1.003]	0.96
	≥14.01 / <14.01 (first quartile)	1.389 [0.862, 2.237]	0.18
	≥39.37 / <39.37 (median)	1.107 [0.754, 1.626]	0.60
	≥84.12 / <84.12 (third quartile)	0.960 [0.617, 1.494]	0.86
Small for gestational age (n = 103)	None	1.001 [0.998, 1.004]	0.60
Small for gestational age (II 103)	≥14.01 / <14.01 (first quartile)	0.818 [0.511, 1.311]	0.40
	≥39.37 / <39.37 (median)	0.964 [0.628, 1.478]	0.87
	≥84.12 / <84.12 (third quartile)	1.262 [0.791, 2.014]	0.33
Constant of the contract of th	None	0.999 [0.994, 1.004]	0.77
Spontaneous preterm birth (n = 53)	≥14.01 / <14.01 (first quartile)	0.693 [0.378, 1.271]	0.69
	≥39.37 / <39.37 (median)	0.848 [0.473, 1.520]	0.58
	≥84.12 / <84.12 (third quartile)	1.155 [0.595, 2.241]	0.67
011 ( 67)	None	0.000 [0.004 1.003]	0.40
Other complication (n = 67)	None	0. 999 [0.994, 1.003]	0.49
	≥14.01 / <14.01 (first quartile)	1.028 [0.566, 1.867]	0.93
	≥39.37 / <39.37 (median)	0.843 [0.502, 1.416]	0.52
	≥84.12 / <84.12 (third quartile)	0.765 [0.408, 1.432]	0.40

**Table S23:** Logistic regression analyses to assess the association between PZP and the odds of a woman having a pregnancy complication compared to uncomplicated pregnancy (n = 328) in mothers from the **STOP cohort with BMI** <25 kg/cm<sup>2</sup>.

Outcome	Contrasts (PZP μg/mL)	Odds ratio [95% CI]	p
Preeclampsia (n = 32)	None	1.005 [1.000, 1.010]	0.054
	≥14.01 / <14.01 (first quartile)	1.352 [0.537, 3.404]	0.52
	≥39.37 / <39.37 (median)	1.815 [0.859, 3.834]	0.12
	≥84.12 / <84.12 (third quartile)	2.308 [1.089, 4.891]	0.03
Gestational hypertension (n = 12)	None	0.990 [0.973, 1.006]	0.22
destational hypertension (ii 12)	≥14.01 / <14.01 (first quartile)	0.936 [0.247, 3.543]	0.92
	≥39.37 / <39.37 (median)	1.089 [0.344, 3.447]	0.88
	≥84.12 / <84.12 (third quartile)	0.307 [0.039, 2.414]	0.26
Gestational diabetes mellitus (n = 47)	None	1.004 [0.999, 1.008]	0.13
	≥14.01 / <14.01 (first quartile)	1.021 [0.496, 2.101]	0.95
	≥39.37 / <39.37 (median)	1.755 [0.938, 3.284]	0.08
	≥84.12 / <84.12 (third quartile)	1.431 [0.728, 2.814]	0.30
Small for gestational age (n = 43)	None	1.002 [0.996, 1.007]	0.58
entange geometria age (ii ie,	≥14.01 / <14.01 (first quartile)	0.477 [0.246, 0.925]	0.03
	≥39.37 / <39.37 (median)	0.784 [0.412, 1.492]	0.46
	≥84.12 / <84.12 (third quartile)	1.306 [0.639, 2.668]	0.46
Spontaneous preterm birth (n = 26)	None	1.000 [0.992, 1.007]	0.92
Spontaneous preterm birth (II – 20)	≥14.01 / <14.01 (first quartile)	0.589 [0.253, 1.375]	0.22
	≥39.37 / <39.37 (median)	0.799 [0.356, 1.791]	0.59
	≥84.12 / <84.12 (third quartile)	1.499 [0.627, 3.585]	0.36
		1 004 [0 001 1 007]	0.55
Other complication (n = 29)	None	1.001 [0.994, 1.007]	0.83
	≥14.01 / <14.01 (first quartile)	1.498 [0.553, 4.057]	0.43
	≥39.37 / <39.37 (median)	1.543 [0.714, 3.333]	0.27
	≥84.12 / <84.12 (third quartile)	0.880 [0.346, 2.241]	0.79

**Table S24:** Logistic regression analyses to assess the association between PZP and the odds of a woman having a pregnancy complication compared to uncomplicated pregnancy (n = 367) in mothers from the **STOP cohort with BMI** ≥25 kg/cm².

Outcome	Contrasts (PZP μg/mL)	Odds ratio [95% CI]	p
Preeclampsia (n = 87)	None	0.999 [0.995, 1.002]	0.39
	≥14.01 / <14.01 (first quartile)	0.944 [0.555, 1.607]	0.83
	≥39.37 / <39.37 (median)	0.987 [0.618, 1.576]	0.96
	≥84.12 / <84.12 (third quartile)	0.797 [0.460, 1.381]	0.42
Gestational hypertension (n = 66)	None	0.995 [0.990, 1.000]	0.03
Gestational hypertension (ii = 66)	≥14.01 / <14.01 (first quartile)	0.978 [0.537, 1.782]	0.94
	≥39.37 / <39.37 (median)	0.816 [0.483, 1.380]	0.45
	≥84.12 / <84.12 (third quartile)	0.593 [0.305, 1.155]	0.12
Gestational diabetes mellitus (n = 87)	None	0.998 [0.995, 1.001]	0.25
destational diabetes memers (n = 67)	≥14.01 / <14.01 (first quartile)	1.137 [0.655, 1.975]	0.65
	≥39.37 / <39.37 (median)	0.715 [0.446, 1.144]	0.16
	≥84.12 / <84.12 (third quartile)	0.797 [0.460, 1.381]	0.42
Small for gestational age (n = 60)	None	1.001 [0.997, 1.004]	0.76
	≥14.01 / <14.01 (first quartile)	1.512 [0.755, 3.029]	0.24
	≥39.37 / <39.37 (median)	1.126 [0.651, 1.949]	0.67
	≥84.12 / <84.12 (third quartile)	0.971 [0.524, 1.799]	0.93
Spontaneous preterm birth (n = 27)	None	0.998 [0.992, 1.004]	0.49
. , , ,	≥14.01 / <14.01 (first quartile)	0.806 [0.341, 1.903]	0.62
	≥39.37 / <39.37 (median)	0.634 [0.286, 1.402]	0.26
	≥84.12 / <84.12 (third quartile)	1.124 [0.477, 2.650]	0.79
Other complication (n = 38)	None	0.998 [0.993, 1.003]	0.38
Other complication (II – 36)	≥14.01 / <14.01 (first quartile)	0.833 [0.398, 1.745]	0.63
	≥39.37 / <39.37 (median)	0.746 [0.381, 1.460]	0.39
	≥84.12 / <84.12 (third quartile)	0.603 [0.257, 1.413]	0.24

### 6.5.2 SCOPE

**Table S25:** Comorbidities for participants in the SCOPE cohort.

	Preeclampsia	Spontaneous preterm birth	Gestational hypertension	Small for gestational age
n (%)	79 (100)	44 (100)	64 (100)	67 (100)
Comorbidities				
Spontaneous preterm birth n (%)	5 (4.2)	-	-	-
Gestational hypertension n (%)	0 (0)	1 (2.3)	-	-
Small for gestational age n (%)	35 (44.3)	4 (9.1)	0 (0)	-
Gestational diabetes mellitus n (%)	6 (7.6)	0 (0)	2 (3.1)	3 (4.5)

Women with multiple comorbidities were included in the count for both categories.

**Table S26:** Frequency of gravidity in the SCOPE cohort.

	Gravidity (includes current pregnancy)			
	1	2	3	4
Uncomplicated	344	90	26	4
Preeclampsia	56	19	4	0
Gestational hypertension	52	10	2	0
Gestational diabetes mellitus	20	7	1	0
Small for gestational age	45	18	3	1
Spontaneous preterm birth	29	12	2	1
Other complication	82	23	10	2
Total	628	179	48	8

**Table S27:** Logistic regression analyses, adjusted for gestational age at sampling and BMI, to assess the association between PZP and the odds of a woman having a pregnancy complication compared to uncomplicated pregnancy (n = 464) in the **SCOPE cohort.** 

Outcome	Contrasts (PZP μg/mL)	Odds ratio [95% CI]	р
Preeclampsia (n = 79)	None	1.003 [1.001, 1.005]	0.01
	≥39.61 / <39.61 (first quartile)	1.071 [0.600, 1.912]	0.82
	≥91.93 / <91.93 (median)	0.984 [0.603, 1.605]	0.95
	≥182.31 / <182.31 (third quartile)	1.819 [1.083, 3.057]	0.02
Gestational hypertension (n = 64)	None	1.002 [0.999, 1.004]	0.16
	≥39.61 / <39.61 (first quartile)	0.871 [0.475, 1.594]	0.65
	≥91.93 / <91.93 (median)	1.104 [0.646, 1.887]	0.72
	≥182.31 / <182.31 (third quartile)	1.538 [0.864, 2.738]	0.14
Gestational diabetes mellitus (n = 28)	None	1.002 [0.998, 1.005]	0.30
	≥39.61 / <39.61 (first quartile)	1.504 [0.554, 4.085]	0.42
	≥91.93 / <91.93 (median)	0.814 [0.374, 1.770]	0.60
	≥182.31 / <182.31 (third quartile)	1.785 [0.790, 4.030]	0.16
Small for gestational age (n = 67)	None	0.999 [0.996, 1.002]	0.46
	≥39.61 / <39.61 (first quartile)	1.004 [0.554, 1.820]	0.99
	≥91.93 / <91.93 (median)	0.718 [0.425, 1.216]	0.22
	≥182.31 / <182.31 (third quartile)	0.759 [0.390, 1.479]	0.42
Consistence of the second block (c. 44)	N	4.000 [0.007, 4.002]	0.05
Spontaneous preterm birth (n = 44)	None	1.000 [0.997, 1.003]	0.85
	≥39.61 / <39.61 (first quartile)	0.655 [0.333, 1.288]	0.22
	≥91.93 / <91.93 (median)	0.675 [0.358, 1.272]	0.22
	≥182.31 / <182.31 (third quartile)	0.959 [0.455, 2.019]	0.91
Other complication (n = 117)	None	1.001 [0.999, 1.003]	0.29
	≥39.61 / <39.61 (first quartile)	1.135 [0.703, 1.831]	0.60
	≥91.93 / <91.93 (median)	1.198 [0.792, 1.812]	0.39
	≥182.31 / <182.31 (third quartile)	1.361 [0.850, 2.179]	0.20

**Table S28:** Logistic regression analyses to assess the association between PZP and the odds of a woman having a pregnancy complication compared to uncomplicated pregnancy (n = 227) in mothers from the **SCOPE cohort with BMI** <25 kg/cm<sup>2</sup>.

Outcome	Contrasts (PZP μg/mL)	Odds ratio [95% CI]	р
Preeclampsia (n = 24)	None	1.002 [0.998, 1.006]	0.40
	≥39.61 / <39.61 (first quartile)	0.686 [0.269, 1.747]	0.43
	≥91.93 / <91.93 (median)	1.027 [0.443, 2.382]	0.95
	≥182.31 / <182.31 (third quartile)	1.683 [0.682, 4.153]	0.26
Gestational hypertension (n = 15)	None	1.005 [1.001, 1.010]	0.03
· · · · ·	≥39.61 / <39.61 (first quartile)	0.777 [0.237, 2.545]	0.68
	≥91.93 / <91.93 (median)	2.054 [0.680, 6.198]	0.20
	≥182.31 / <182.31 (third quartile)	2.945 [1.020, 8.504]	0.046
Gestational diabetes mellitus (n = 9)	None	1.001 [0.994, 1.008]	0.85
	≥39.61 / <39.61 (first quartile)	0.565 [0.136, 2.340]	0.43
	≥91.93 / <91.93 (median)	1.283 [0.336, 4.903]	0.72
	≥182.31 / <182.31 (third quartile)	1.683 [0.407, 6.962]	0.47
Small for gestational age (n = 31)	None	0.999 [0.994, 1.003]	0.58
<u> </u>	≥39.61 / <39.61 (first quartile)	0.514 [0.231, 1.143]	0.10
	≥91.93 / <91.93 (median)	0.742 [0.347, 1.585]	0.44
	≥182.31 / <182.31 (third quartile)	0.647 [0.237, 1.770]	0.40
Spontaneous preterm birth (n = 18)	None	0.007 [0.004_4_002]	0.24
Spontaneous preterm birtir (ii = 10)	≥39.61 / <39.61 (first quartile)	0.997 [0.991, 1.003]	0.31
	≥91.93 / <91.93 (median)	0.444 [0.164, 1.205]	0.11
	≥182.31 / <182.31 (third quartile)	0.395 [0.136, 1.144] 0.962 [0.303, 3.047]	0.09
	2102.31 / \102.31 (time quartile)	0.902 [0.303, 3.047]	0.95
Other complication (n = 65)	None	1.001 [0.998, 1.004]	0.44
	≥39.61 / <39.61 (first quartile)	0.942 [0.488, 1.816]	0.86
	≥91.93 / <91.93 (median)	1.357 [0.778, 2.365]	0.28

**Table S29:** Logistic regression analyses to assess the association between PZP and the odds of a woman having a pregnancy complication compared to uncomplicated pregnancy (n = 237) in mothers from the **SCOPE cohort with BMI** ≥25 kg/cm².

Outcome	Contrasts (PZP μg/mL)	Odds ratio [95% CI]	p
Preeclampsia (n = 55)	None	1.003 [1.001, 1.006]	0.01
	≥39.61 / <39.61 (first quartile)	1.270 [0.629, 2.563]	0.51
	≥91.93 / <91.93 (median)	1.034 [0.574, 1.860]	0.91
	≥182.31 / <182.31 (third quartile)	2.025 [1.069, 3.835]	0.03
Gestational hypertension (n = 49)	None	1.001 [0.998, 1.004]	0.57
, , ,	≥39.61 / <39.61 (first quartile)	0.886 [0.447, 1.756]	0.73
	≥91.93 / <91.93 (median)	0.755 [0.407, 1.401]	0.37
	≥182.31 / <182.31 (third quartile)	1.693 [0.854, 3.355]	0.13
Gestational diabetes mellitus (n = 19)	None	1.002 [0.998, 1.006]	0.25
Gestational diabetes meintas (n = 15)	≥39.61 / <39.61 (first quartile)	3.011 [0.676, 13.409]	0.15
	≥91.93 / <91.93 (median)	0.674 [0.262, 1.735]	0.41
	≥182.31 / <182.31 (third quartile)	2.238 [0.837, 5.986]	0.11
Small for gestational age $(n = 36)$	None	0.999 [0.995, 1.003]	0.57
	≥39.61 / <39.61 (first quartile)	1.240 [0.537, 2.865]	0.61
	≥91.93 / <91.93 (median)	0.590 [0.288, 1.208]	0.15
	≥182.31 / <182.31 (third quartile)	0.926 [0.383, 2.240]	0.86
Spontaneous preterm birth (n = 26)	None	1.002 [0.999, 1.006]	0.22
• • • • • • • • • • • • • • • • • • • •	≥39.61 / <39.61 (first quartile)	0.962 [0.386, 2.398]	0.93
	≥91.93 / <91.93 (median)	1.081 [0.480, 2.436]	0.85
	≥182.31 / <182.31 (third quartile)	1.151 [0.439, 3.021]	0.78
Oth liti ( 52)	Name	4.004 [0.000 4.004]	0.66
Other complication (n = 52)	None	1.001 [0.998, 1.004]	0.66
	≥39.61 / <39.61 (first quartile)	1.063 [0.532, 2.122]	0.86
	≥91.93 / <91.93 (median) 1.001 [0.549, 1.825]		1.00
	≥182.31 / <182.31 (third quartile)	1.555 [0.790, 3.062]	0.20

#### REFERENCES

- Abalos, E., Cuesta, C., Grosso, A. L., Chou, D. & Say, L. 2013. Global and regional estimates of preeclampsia and eclampsia: a systematic review. *European Journal of Obstetrics and Gynecology and Reproductive Biology,* 170, 1-7.
- Abbassi-Ghanavati, M., Greer, L. G. & Cunningham, F. G. 2009. Pregnancy and Laboratory Studies: A Reference Table for Clinicians. *Obstetrics & Gynecology*, 114.
- AbdAlla, S., Lother, H., el Massiery, A. & Quitterer, U. 2001. Increased AT(1) receptor heterodimers in preeclampsia mediate enhanced angiotensin II responsiveness. *Nat Med*, 7, 1003-9.
- Abu-Raya, B., Michalski, C., Sadarangani, M. & Lavoie, P. M. 2020. Maternal Immunological Adaptation During Normal Pregnancy. *Frontiers in Immunology*, 11.
- ACOG 2002. ACOG practice bulletin. Diagnosis and management of preeclampsia and eclampsia. Number 33, January 2002. *Obstet Gynecol*, 99, 159-67.
- ACOG 2013. ACOG Practice bulletin no. 134: fetal growth restriction. *Obstet Gynecol*, 121, 1122-1133.
- ACOG 2020. Gestational Hypertension and Preeclampsia: ACOG Practice Bulletin, Number 222. *Obstetrics & Gynecology,* 135.
- Afonina, I. S., Tynan, G. A., Logue, S. E., Cullen, S. P., Bots, M., Lüthi, A. U., Reeves, E. P., McElvaney, N. G., Medema, J. P., Lavelle, E. C. & Martin, S. J. 2011. Granzyme B-Dependent Proteolysis Acts as a Switch to Enhance the Proinflammatory Activity of IL-1. *Molecular Cell*, 44, 265-278.
- Aghababaei, M., Perdu, S., Irvine, K. & Beristain, A. G. 2014. A disintegrin and metalloproteinase 12 (ADAM12) localizes to invasive trophoblast, promotes cell invasion and directs column outgrowth in early placental development. *Mol Hum Reprod*, 20, 235-49.
- Aghaeepour, N., Ganio, E. A., McIlwain, D., Tsai, A. S., Tingle, M., Van Gassen, S., Gaudilliere, D. K., Baca, Q., McNeil, L., Okada, R., Ghaemi, M. S., Furman, D., Wong, R. J., Winn, V. D., Druzin, M. L., El-Sayed, Y. Y., Quaintance, C., Gibbs, R., Darmstadt, G. L., Shaw, G. M., Stevenson, D. K., Tibshirani, R., Nolan, G. P., Lewis, D. B., Angst, M. S. & Gaudilliere, B. 2017. An immune clock of human pregnancy. *Sci Immunol*, 2.
- Aluvihare, V. R., Kallikourdis, M. & Betz, A. G. 2004. Regulatory T cells mediate maternal tolerance to the fetus. *Nature Immunology*, 5, 266-271.
- Andersson, M. K., Enoksson, M., Gallwitz, M. & Hellman, L. 2008. The extended substrate specificity of the human mast cell chymase reveals a serine protease with well-defined substrate recognition profile. *International Immunology*, 21, 95-104.
- Arandjelovic, S., Dragojlovic, N., Li, X., Myers, R. R., Campana, W. M. & Gonias, S. L. 2007. A derivative of the plasma protease inhibitor α2-macroglobulin regulates the response to peripheral nerve injury. *Journal of neurochemistry*, 103, 694-705.
- Arbeláez, L. F., Bergmann, U., Tuuttila, A., Shanbhag, V. P. & Stigbrand, T. 1997. Interaction of Matrix Metalloproteinases-2 and -9 with Pregnancy Zone Protein and α2-Macroglobulin. *Archives of Biochemistry and Biophysics*, 347, 62-68.
- Arbelaez, L. F., Jensen, P. E. H. & Stigbrand, T. 1995. Proteinases from the fibrinolytic and coagulation systems: Analyses of binding to pregnancy zone protein, a pregnancy-associated plasma proteinase inhibitor. *Fibrinolysis*, 9, 41-47.
- Ardissino, M., Truong, B., Slob, E. A. W., Schuermans, A., Yoshiji, S., Morley, A. P., Burgess, S., Ng, F. S., de Marvao, A., Natarajan, P., Nicolaides, K., Gaziano, L., Butterworth, A. & Honigberg, M. C. 2024. Proteome- and Transcriptome-Wide Genetic Analysis Identifies

- Biological Pathways and Candidate Drug Targets for Preeclampsia. *Circ Genom Precis Med*, 17, e004755.
- Armstrong, N. P., Teisner, B., Redman, C. W., Westergaard, J. G., Folkersen, J. & Grudzinskas, J. G. 1986. Complement activation, circulating protease inhibitors and pregnancy-associated proteins in severe pre-eclampsia. *Br J Obstet Gynaecol*, 93, 811-4.
- Armstrong, P. B., Mangel, W. F., Wall, J. S., Hainfield, J. F., Van Holde, K. E., Ikai, A. & Quigley, J. P. 1991. Structure of alpha 2-macroglobulin from the arthropod Limulus polyphemus. *Journal of Biological Chemistry*, 266, 2526-2530.
- Arslan, A. A., Zeleniuch-Jacquotte, A., Lukanova, A., Afanasyeva, Y., Katz, J., Levitz, M., Del Priore, G. & Toniolo, P. 2006. Effects of Parity on Pregnancy Hormonal Profiles Across Ethnic Groups with a Diverse Incidence of Breast Cancer. *Cancer Epidemiology, Biomarkers & Prevention*, 15, 2123-2130.
- Asplin, I. R., Wu, S. M., Mathew, S., Bhattacharjee, G. & Pizzo, S. V. 2001. Differential regulation of the fibroblast growth factor (FGF) family by α2-macroglobulin: evidence for selective modulation of FGF-2–induced angiogenesis. *Blood, The Journal of the American Society of Hematology*, 97, 3450-3457.
- Bai, J., Wong, F. W. S., Bauman, A. & Mohsin, M. 2002. Parity and pregnancy outcomes. American Journal of Obstetrics and Gynecology, 186, 274-278.
- Bai, Y., Li, H. & Lv, R. 2021. Interleukin-17 activates JAK2/STAT3, PI3K/Akt and nuclear factor-κB signaling pathway to promote the tumorigenesis of cervical cancer. *Exp Ther Med*, 22, 1291.
- Bartsch, E., Medcalf, K. E., Park, A. L. & Ray, J. G. 2016. Clinical risk factors for pre-eclampsia determined in early pregnancy: systematic review and meta-analysis of large cohort studies. *BMJ*, 353, i1753.
- Beckman, L., Bergdahl, K., Cedergren, B., Damber, M. G., Lidén, S., von Schoultz, B. & Stigbrand, T. 1977. Increased serum levels of the pregnancy zone protein in psoriasis. *Acta Derm Venereol*, 57, 403-6.
- Bernhard, O. K., Kapp, E. A. & Simpson, R. J. 2007. Enhanced Analysis of the Mouse Plasma Proteome Using Cysteine-Containing Tryptic Glycopeptides. *Journal of Proteome Research*, 6, 987-995.
- Bernstein, L., Pike, M. C., Ross, R. K., Judd, H. L., Brown, J. B. & Henderson, B. E. 1985. Estrogen and Sex Hormone-Binding Globulin Levels in Nulliparous and Parous Women2. *JNCI: Journal of the National Cancer Institute*, 74, 741-745.
- Biadasiewicz, K., Fock, V., Dekan, S., Proestling, K., Velicky, P., Haider, S., Knöfler, M., Fröhlich, C. & Pollheimer, J. 2014. Extravillous trophoblast-associated ADAM12 exerts proinvasive properties, including induction of integrin beta 1-mediated cellular spreading. *Biol Reprod*, 90, 101.
- Birkenmeier, G., Müller, R., Huse, K., Forberg, J., Gläser, C., Hedrich, H., Nicklisch, S. & Reichenbach, A. 2003. Human α2-macroglobulin: genotype–phenotype relation. *Experimental Neurology,* 184, 153-161.
- Björk, I. & Fish, W. W. 1982. Evidence for similar conformational changes in α2-macroglobulin on reaction with primary amines or proteolytic enzymes. *Biochemical Journal*, 207, 347-356.
- Blennow, K., Ricksten, A., Prince, J. A., Brookes, A. J., Emahazion, T., Wasslavik, C., Bogdanovic, N., Andreasen, N., Båtsman, S., Marcusson, J., Nägga, K., Wallin, A., Regland, B., Olofsson, H., Hesse, C., Davidsson, P., Minthon, L., Jansson, A., Palmqvist, L. & Rymo, L. 2000. No association between the α2-macroglobulin (A2M) deletion and Alzheimer's disease, and no change in A2M mRNA, protein, or protein expression. *Journal of Neural Transmission*, 107, 1065-1079.

- Blumenstein, M., McMaster, M. T., Black, M. A., Wu, S., Prakash, R., Cooney, J., McCowan, L. M. E., Cooper, G. J. S. & North, R. A. 2009. A proteomic approach identifies early pregnancy biomarkers for preeclampsia: Novel linkages between a predisposition to preeclampsia and cardiovascular disease. *PROTEOMICS*, 9, 2929-2945.
- Bonacci, G., Sánchez, M. C., Gonzalez, M., Ceschin, D., Fidelio, G., Vides, M. A. & Chiabrando, G. 2000. Stabilization of homogeneous preparations of pregnancy zone protein lyophilized in the presence of saccharose. Structural and functional studies. *J Biochem Biophys Methods*, 46, 95-105.
- Bonacci, G. R., Cáceres, L. C., Sánchez, M. C. & Chiabrando, G. A. 2007. Activated α2-macroglobulin induces cell proliferation and mitogen-activated protein kinase activation by LRP-1 in the J774 macrophage-derived cell line. *Archives of Biochemistry and Biophysics*, 460, 100-106.
- Brown, D., Khan, J., Copeland, G. & Jewell, D. 1980. Alpha 2-macroglobulin in patients with inflammatory bowel disease. *Journal of Clinical & Laboratory Immunology*, 4, 53-57.
- Brown, M. A., Magee, L. A., Kenny, L. C., Karumanchi, S. A., McCarthy, F. P., Saito, S., Hall, D. R., Warren, C. E., Adoyi, G. & Ishaku, S. 2018. The hypertensive disorders of pregnancy: ISSHP classification, diagnosis & management recommendations for international practice. *Pregnancy Hypertension*, 13, 291-310.
- Budd, A., Blandin, S., Levashina, E. A. & Gibson, T. J. 2004. Bacterial α2-macroglobulins: colonization factors acquired by horizontal gene transfer from the metazoan genome? *Genome Biology*, 5, R38.
- Buhimschi, I. A., Nayeri, U. A., Zhao, G., Shook, L. L., Pensalfini, A., Funai, E. F., Bernstein, I. M., Glabe, C. G. & Buhimschi, C. S. 2014. Protein misfolding, congophilia, oligomerization, and defective amyloid processing in preeclampsia. *Science Translational Medicine*, 6, 245ra92.
- Bulmer, J. N., Innes, B. A., Levey, J., Robson, S. C. & Lash, G. E. 2012. The role of vascular smooth muscle cell apoptosis and migration during uterine spiral artery remodeling in normal human pregnancy. *The FASEB Journal*, 26, 2975-2985.
- Burton, G. J., Redman, C. W., Roberts, J. M. & Moffett, A. 2019. Pre-eclampsia: pathophysiology and clinical implications. *BMJ*, 366, l2381.
- Cáceres, L. C., Bonacci, G. R., Sánchez, M. C. & Chiabrando, G. A. 2010. Activated α2 macroglobulin induces matrix metalloproteinase 9 expression by low-density lipoprotein receptor-related protein 1 through MAPK-ERK1/2 and NF-κB activation in macrophage-derived cell lines. *Journal of Cellular Biochemistry*, 111, 607-617.
- Campagna, M. P., Xavier, A., Stankovich, J., Maltby, V. E., Slee, M., Yeh, W. Z., Kilpatrick, T., Scott, R. J., Butzkueven, H., Lechner-Scott, J., Lea, R. A. & Jokubaitis, V. G. 2023. Parity is associated with long-term differences in DNA methylation at genes related to neural plasticity in multiple sclerosis. *Clinical Epigenetics*, 15, 20.
- Carlsson-Bosted, L., Moestrup, S. K., Gliemann, J., Sottrup-Jensen, L. & Stigbrand, T. 1988. Three different conformational states of pregnancy zone protein identified by monoclonal antibodies. *J Biol Chem*, 263, 6738-41.
- Cater, J. H. 2021. Investigations of the roles of pregnancy zone protein and plasminogen activator inhibitor type-2 in extracellular proteostasis. Doctor of Philosophy, University of Wollongong.
- Cater, J. H., Kumita, J. R., Zeineddine Abdallah, R., Zhao, G., Bernardo-Gancedo, A., Henry, A., Winata, W., Chi, M., Grenyer, B. S. F., Townsend, M. L., Ranson, M., Buhimschi, C. S., Charnock-Jones, D. S., Dobson, C. M., Wilson, M. R., Buhimschi, I. A. & Wyatt, A. R. 2019. Human pregnancy zone protein stabilizes misfolded proteins including

- preeclampsia- and Alzheimer's-associated amyloid beta peptide. *Proceedings of the National Academy of Sciences of the United States of America*, 116, 6101-6110.
- Caughey, G. H., Raymond, W. W. & Wolters, P. J. 2000. Angiotensin II generation by mast cell α-and β-chymases. *Biochimica et Biophysica Acta (BBA) Protein Structure and Molecular Enzymology,* 1480, 245-257.
- Chalasani, N., Guo, X., Loomba, R., Goodarzi, M. O., Haritunians, T., Kwon, S., Cui, J., Taylor, K. D., Wilson, L., Cummings, O. W., Chen, Y. D. & Rotter, J. I. 2010. Genome-wide association study identifies variants associated with histologic features of nonalcoholic Fatty liver disease. *Gastroenterology*, 139, 1567-76, 1576.e1-6.
- Chen, G.-f., Xu, T.-h., Yan, Y., Zhou, Y.-r., Jiang, Y., Melcher, K. & Xu, H. E. 2017. Amyloid beta: structure, biology and structure-based therapeutic development. *Acta Pharmacologica Sinica*, 38, 1205-1235.
- Chen, H., Li, Z., liu, N., Zhang, W. & Zhu, G. 2014. Influence of Alpha-2-Macroglobulin 5 bp I/D and Ile1000Val Polymorphisms on the Susceptibility of Alzheimer's disease: A Systematic Review and Meta-analysis of 52 Studies. *Cell Biochemistry and Biophysics*, 70, 511-519.
- Chen, K., Zheng, T., Chen, C., Liu, L., Guo, Z., Peng, Y., Zhang, X. & Yang, Z. 2023a. Pregnancy Zone Protein Serves as a Prognostic Marker and Favors Immune Infiltration in Lung Adenocarcinoma. *Biomedicines*, 11, 1978.
- Chen, L., Baum, L., Ng, H.-K., Chan, L. Y. S., Sastre, I., Artíga, M. a. J., Valdivieso, F., Bullido, M. a. J., Chiu, H. F. K. & Pang, C.-P. 1999. Apolipoprotein E promoter and α2-Macroglobulin polymorphisms are not genetically associated with Chinese late onset Alzheimer's disease. *Neuroscience Letters*, 269, 173-177.
- Chen, S., Johs, M., Karmaus, W., Holloway, J. W., Kheirkhah Rahimabad, P., Goodrich, J. M., Peterson, K. E., Dolinoy, D. C., Arshad, S. H. & Ewart, S. 2024. Assessing the effect of childbearing on blood DNA methylation through comparison of parous and nulliparous females. *Epigenetics Communications*, 4, 2.
- Chen, W.-L., Liao, W.-T., Hsu, C.-N. & Tain, Y.-L. 2023b. Pregnancy Zone Protein as an Emerging Biomarker for Cardiovascular Risk in Pediatric Chronic Kidney Disease. *Journal of Clinical Medicine*, 12.
- Cheng, S., Banerjee, S., Daiello, L. A., Nakashima, A., Jash, S., Huang, Z., Drake, J. D., Ernerudh, J., Berg, G., Padbury, J., Saito, S., Ott, B. R. & Sharma, S. 2021. Novel blood test for early biomarkers of preeclampsia and Alzheimer's disease. *Scientific Reports*, 11, 15934.
- Chiabrando, G., Bonacci, G., Sanchez, C., Ramos, A., Zalazar, F. & Vides, M. A. 1997. A procedure for human pregnancy zone protein (and human alpha 2-macroglobulin) purification using hydrophobic interaction chromatography on phenyl-sepharose CL-4B column. *Protein Expr Purif*, 9, 399-406.
- Chiabrando, G. A., Vides, M. A. & Sánchez, M. C. 2002. Differential Binding Properties of Human Pregnancy Zone Protein—and α2-Macroglobulin—Proteinase Complexes to Low-Density Lipoprotein Receptor-Related Protein. *Archives of Biochemistry and Biophysics*, 398, 73-78.
- Cho, S. H., Lee, S. H., Kato, A., Takabayashi, T., Kulka, M., Shin, S. C. & Schleimer, R. P. 2015. Cross-Talk between Human Mast Cells and Bronchial Epithelial Cells in Plasminogen Activator Inhibitor-1 Production via Transforming Growth Factor-β1. American Journal of Respiratory Cell and Molecular Biology, 52, 88-95.
- Christensen, U., Simonsen, M., Harrit, N. & Sottrup-Jensen, L. 1989. Pregnancy zone protein, a proteinase-binding macroglobulin. Interactions with proteinases and methylamine. *Biochemistry*, 28, 9324-31.

- Christensen, U., Sottrup-Jensen, L. & Harrit, N. 1991. Pregnancy zone protein, a proteinase binding alpha-macroglobulin. Stopped-flow kinetic studies of its interaction with chymotrypsin. *Biochim Biophys Acta*, 1076, 91-6.
- Christian, L. M., Glaser, R., Porter, K. & Iams, J. D. 2013. Stress-induced inflammatory responses in women: effects of race and pregnancy. *Psychosom Med*, 75, 658-69.
- Cohn, E. J., Strong, L. E., Hughes, W. L., Mulford, D. J., Ashworth, J. N., Melin, M. & Taylor, H. L. 1946. Preparation and Properties of Serum and Plasma Proteins. IV. A System for the Separation into Fractions of the Protein and Lipoprotein Components of Biological Tissues and Fluids. *Journal of the American Chemical Society*, 68, 459-475.
- Constantinescu, P. 2016. *The Role of proteases and chaperones in extracellular proteostasis.*University of Wollongong.
- Couture, C., Caron, M., St-Onge, P., Brien, M.-E., Sinnett, D., Dal Soglio, D. & Girard, S. 2024. Identification of divergent placental profiles in clinically distinct pregnancy complications revealed by the transcriptome. *Placenta*, 154, 184-192.
- Cox, B. E., Word, R. A. & Rosenfeld, C. R. 1996. Angiotensin II receptor characteristics and subtype expression in uterine arteries and myometrium during pregnancy. *The Journal of Clinical Endocrinology & Metabolism*, 81, 49-58.
- Crookston, K. P., Webb, D. J., Wolf, B. B. & Gonias, S. L. 1994. Classification of alpha 2-macroglobulin-cytokine interactions based on affinity of noncovalent association in solution under apparent equilibrium conditions. *Journal of Biological Chemistry*, 269, 1533-1540.
- Dai, J., Mao, P., Pu, C., Wang, X. & Liu, X. 2023a. Trimester-specific reference intervals and profile of coagulation parameters for Chinese pregnant women with diverse demographics and obstetric history: a cross-sectional study. *BMC Pregnancy and Childbirth*, 23, 421.
- Dai, J., Shi, Y., Wu, Y., Guo, L., Lu, D., Chen, Y., Wang, Y., Lai, H. & Kong, X. 2023b. The interaction between age and parity on adverse pregnancy and neonatal outcomes. *Front Med (Lausanne)*, 10, 1056064.
- Damber, M. G., von Schoultz, B., Solheim, F. & Stigbrand, T. 1976. A quantitative study of the pregnancy zone protein in sera of woman taking oral contraceptives. *Am J Obstet Gynecol*, 124, 289-92.
- Danielli, M., Thomas, R. C., Gillies, C. L., Hu, J., Khunti, K. & Tan, B. K. 2022. Blood biomarkers to predict the onset of pre-eclampsia: A systematic review and meta-analysis. *Heliyon*, 8, e11226.
- Delforce, S. J., Lumbers, E. R., Morosin, S. K., Wang, Y. & Pringle, K. G. 2019. The Angiotensin II type 1 receptor mediates the effects of low oxygen on early placental angiogenesis. *Placenta*, 75, 54-61.
- Devriendt, K., Van Den Berghe, H., Cassiman, J.-J. & Marynen, P. 1991. Primary structure of pregnancy zone protein. Molecular cloning of a full-length PZP cDNA clone by the polymerase chain reaction. *Biochimica et Biophysica Acta (BBA) Gene Structure and Expression*, 1088, 95-103.
- Devriendt, K., Zhang, J., van Leuven, F., van den Berghe, H., Cassiman, J.-J. & Marynen, P. 1989. A cluster of α2-macroglobulin-related genes (α2M) on human chromosome 12p: cloning of the pregnancy-zone protein gene and an α2M pseudogene. *Gene*, 81, 325-334.
- Dimitriadis, E., Rolnik, D. L., Zhou, W., Estrada-Gutierrez, G., Koga, K., Francisco, R. P. V., Whitehead, C., Hyett, J., da Silva Costa, F., Nicolaides, K. & Menkhorst, E. 2023. Preeclampsia. *Nature Reviews Disease Primers*, 9, 8.
- Dos Santos, C. O., Dolzhenko, E., Hodges, E., Smith, A. D. & Hannon, G. J. 2015. An epigenetic memory of pregnancy in the mouse mammary gland. *Cell Rep*, 11, 1102-9.

- Duckitt, K. & Harrington, D. 2005. Risk factors for pre-eclampsia at antenatal booking: systematic review of controlled studies. *Bmj*, 330, 565.
- Duthie, S. J., Horgan, G., de Roos, B., Rucklidge, G., Reid, M., Duncan, G., Pirie, L., Basten, G. P. & Powers, H. J. 2010. Blood Folate Status and Expression of Proteins Involved in Immune Function, Inflammation, and Coagulation: Biochemical and Proteomic Changes in the Plasma of Humans in Response to Long-Term Synthetic Folic Acid Supplementation. *Journal of Proteome Research*, 9, 1941-1950.
- Dutta, S., Sengupta, P. & Liew, F. F. 2024. Cytokine landscapes of pregnancy: mapping gestational immune phases. *Gynecology and Obstetrics Clinical Medicine*, **4**, e000011.
- Ekelund, L. & Laurell, C. B. 1994. The pregnancy zone protein response during gestation: A metabolic challenge. *Scandinavian Journal of Clinical and Laboratory Investigation*, 54, 623-629.
- El-Sherbiny, W., Nasr, A. & Soliman, A. 2012. Metalloprotease (ADAM12-S) as a Predictor of Preeclampsia: Correlation with Severity, Maternal Complications, Fetal Outcome, and Doppler Parameters. *Hypertension in Pregnancy*, 31, 442-450.
- Elawad, T., Scott, G., Bone, J. N., Elwell, H., Lopez, C. E., Filippi, V., Green, M., Khalil, A., Kinshella, M.-L. W., Mistry, H. D., Pickerill, K., Shanmugam, R., Singer, J., Townsend, R., Tsigas, E. Z., Vidler, M., Volvert, M.-L., von Dadelszen, P., Magee, L. A. & the, P. N. 2024. Risk factors for pre-eclampsia in clinical practice guidelines: Comparison with the evidence. *BJOG: An International Journal of Obstetrics & Gynaecology*, 131, 46-62.
- ENCODE Project Consortium 2004. The ENCODE (ENCyclopedia Of DNA Elements) Project. *Science*, 306, 636-40.
- Evans, R., O'Neill, M., Pritzel, A., Antropova, N., Senior, A., Green, T., Žídek, A., Bates, R., Blackwell, S., Yim, J., Ronneberger, O., Bodenstein, S., Zielinski, M., Bridgland, A., Potapenko, A., Cowie, A., Tunyasuvunakool, K., Jain, R., Clancy, E., Kohli, P., Jumper, J. & Hassabis, D. 2022. Protein complex prediction with AlphaFold-Multimer. *bioRxiv*, 2021.10.04.463034.
- Fabrizi, C., Businaro, R., Lauro, G. M. & Fumagalli, L. 2001. Role of α2-macroglobulin in regulating amyloid β-protein neurotoxicity: protective or detrimental factor? *Journal of Neurochemistry*, 78, 406-412.
- Fazio, S. & Pamir, N. 2016. HDL Particle Size and Functional Heterogeneity. *Circ Res,* 119, 704-7.
- Feldman, S. R., Gonias, S. L. & Pizzo, S. V. 1985a. Model of alpha 2-macroglobulin structure and function. *Proceedings of the National Academy of Sciences*, 82, 5700-5704.
- Feldman, S. R., Rosenberg, M. R., Ney, K. A., Michalopoulos, G. & Pizzo, S. V. 1985b. Binding of α2-macroglobulin to hepatocytes: mechanism of in vivo clearance. *Biochemical and biophysical research communications*, 128, 795-802.
- Feng, J. K., Lu, Y. F., Li, J., Qi, Y. H., Yi, M. L. & Ma, D. Y. 2015. Upregulation of salivary α2 macroglobulin in patients with type 2 diabetes mellitus. *Genet Mol Res*, 14, 2268-74.
- Ferrucci, L., Corsi, A., Lauretani, F., Bandinelli, S., Bartali, B., Taub, D. D., Guralnik, J. M. & Longo, D. L. 2005. The origins of age-related proinflammatory state. *Blood*, 105, 2294-2299.
- Finch, S., Shoemark, A., Dicker, A. J., Keir, H. R., Smith, A., Ong, S., Tan, B., Choi, J.-Y., Fardon, T. C., Cassidy, D., Huang, J. T. J. & Chalmers, J. D. 2019. Pregnancy Zone Protein Is Associated with Airway Infection, Neutrophil Extracellular Trap Formation, and Disease Severity in Bronchiectasis. American journal of respiratory and critical care medicine, 200, 992-1001.
- Fong, M. & Crane, J. 2023. Histology, Mast Cells. *StatPearls*. Treasure Island (FL): StatPearls Publishing.

- Fosheim, I. K., Jacobsen, D. P., Sugulle, M., Alnaes-Katjavivi, P., Fjeldstad, H. E. S., Ueland, T., Lekva, T. & Staff, A. C. 2023. Serum amyloid A1 and pregnancy zone protein in pregnancy complications and correlation with markers of placental dysfunction. *American Journal of Obstetrics & Gynecology MFM*, 5, 100794.
- Franceschi, C., BonafÈ, M., Valensin, S., Olivieri, F., De Luca, M., Ottaviani, E. & De Benedictis, G. 2000. Inflamm-aging: An Evolutionary Perspective on Immunosenescence. *Annals of the New York Academy of Sciences*, 908, 244-254.
- French, K., Yerbury, J. J. & Wilson, M. R. 2008. Protease Activation of α2-Macroglobulin Modulates a Chaperone-like Action with Broad Specificity. *Biochemistry*, 47, 1176-1185.
- Fretts, R. C. 2005. Etiology and prevention of stillbirth. *American Journal of Obstetrics & Gynecology*, 193, 1923-1935.
- Fu, Z., Thorpe, M., Alemayehu, R., Roy, A., Kervinen, J., de Garavilla, L., Åbrink, M. & Hellman, L. 2017. Highly Selective Cleavage of Cytokines and Chemokines by the Human Mast Cell Chymase and Neutrophil Cathepsin G. *The Journal of Immunology,* 198, 1474-1483.
- Gaglio, P. J., Rodriguez-Torres, M., Herring, R., Anand, B., Box, T., Rabinovitz, M., Brown, R. S., Jr. & the Infergen Study, G. 2004. Racial Differences in Response Rates to Consensus Interferon in HCV Infected Patients Naive to Previous Therapy. *Journal of Clinical Gastroenterology*, 38.
- Gallwitz, M. & Hellman, L. 2006. Rapid lineage-specific diversification of the mast cell chymase locus during mammalian evolution. *Immunogenetics*, 58, 641-654.
- Gamliel, M., Goldman-Wohl, D., Isaacson, B., Gur, C., Stein, N., Yamin, R., Berger, M., Grunewald, M., Keshet, E., Rais, Y., Bornstein, C., David, E., Jelinski, A., Eisenberg, I., Greenfield, C., Ben-David, A., Imbar, T., Gilad, R., Haimov-Kochman, R., Mankuta, D., Elami-Suzin, M., Amit, I., Hanna, J. H., Yagel, S. & Mandelboim, O. 2018. Trained Memory of Human Uterine NK Cells Enhances Their Function in Subsequent Pregnancies. *Immunity*, 48, 951-962.e5.
- Ganrot, P. O. & Scherstén, B. 1967. Serum α2-macroglobulin concentration and its variation with age and sex. *Clinica Chimica Acta*, 15, 113-120.
- Gao, L., Kumar, V., Vellichirammal, N. N., Park, S. Y., Rudebush, T. L., Yu, L., Son, W. M., Pekas, E. J., Wafi, A. M., Hong, J., Xiao, P., Guda, C., Wang, H. J., Schultz, H. D. & Zucker, I. H. 2020. Functional, proteomic and bioinformatic analyses of Nrf2- and Keap1- null skeletal muscle. *J Physiol*, 598, 5427-5451.
- Gillespie, S. L., Porter, K. & Christian, L. M. 2016. Adaptation of the inflammatory immune response across pregnancy and postpartum in Black and White women. *Journal of Reproductive Immunology*, 114, 27-31.
- Giriyappagoudar, M., Vastrad, B., Horakeri, R. & Vastrad, C. 2023. Study on Potential Differentially Expressed Genes in Idiopathic Pulmonary Fibrosis by Bioinformatics and Next-Generation Sequencing Data Analysis. *Biomedicines*, 11, 3109.
- Giuliani, N., Sansoni, P., Girasole, G., Vescovini, R., Passeri, G., Passeri, M. & Pedrazzoni, M. 2001. Serum interleukin-6, soluble interleukin-6 receptor and soluble gp130 exhibit different patterns of age- and menopause-related changes. *Exp Gerontol*, 36, 547-57.
- Gobezie, R., Kho, A., Krastins, B., Sarracino, D. A., Thornhill, T. S., Chase, M., Millett, P. J. & Lee, D. M. 2007. High abundance synovial fluid proteome: distinct profiles in health and osteoarthritis. *Arthritis Research & Therapy*, 9, R36.
- Gomathy, E., Akurati, L. & Radhika, K. 2018. Early onset and late onset preeclampsia-maternal and perinatal outcomes in a rural teritiary health center. *International Journal of Reproduction, Contraception, Obstetrics and Gynecology,* 7, 2266+.
- Gonias, S. L., Carmichael, A., Mettenburg, J. M., Roadcap, D. W., Irvin, W. P. & Webb, D. J. 2000. Identical or overlapping sequences in the primary structure of human α2-macroglobulin

- are responsible for the binding of nerve growth factor-β, platelet-derived growth factor-BB, and transforming growth factor-β. *Journal of Biological Chemistry*, 275, 5826-5831.
- Greenwood, J. D., Minhas, K., di Santo, J. P., Makita, M., Kiso, Y. & Croy, B. A. 2000. Ultrastructural Studies of Implantation Sites from Mice Deficient in Uterine Natural Killer Cells. *Placenta*, 21, 693-702.
- Griffin, J. F. T. 1983. Pregnancy-Associated Plasma Protein Levels at Term in Normal Pregnancy, Preeclampsia and Essential Hypertension. *Australian and New Zealand Journal of Obstetrics and Gynaecology*, 23, 11-14.
- Groschwitz, K. R., Wu, D., Osterfeld, H., Ahrens, R. & Hogan, S. P. 2013. Chymase-mediated intestinal epithelial permeability is regulated by a protease-activating receptor/matrix metalloproteinase-2-dependent mechanism. *American Journal of Physiology-Gastrointestinal and Liver Physiology*, 304, G479-G489.
- Gu, Y., Lewis, D. F., Alexander, J. S. & Wang, Y. 2009. Placenta-derived chymotrypsin-like protease (CLP) disturbs endothelial junctional structure in preeclampsia. *Reprod Sci*, 16, 479-88.
- Gu, Y., Lewis, D. F., Alexander, J. S. & Wang, Y. 2017. Upregulation of cathepsin C expression contributes to endothelial chymase activation in preeclampsia. *Hypertension Research*, 40, 976-981.
- Guay, S.-P., Houde, A.-A., Breton, E., Baillargeon, J.-P., Perron, P., Gaudet, D., Hivert, M.-F., Brisson, D. & Bouchard, L. 2020. DNA methylation at LRP1 gene locus mediates the association between maternal total cholesterol changes in pregnancy and cord blood leptin levels. *Journal of Developmental Origins of Health and Disease*, 11, 369-378.
- Gupta, A. K., Pokhriyal, R., Khan, M. I., Kumar, D. R., Gupta, R., Chadda, R. K., Ramachandran, R., Goyal, V., Tripathi, M. & Hariprasad, G. 2019. Cerebrospinal Fluid Proteomics For Identification Of α2-Macroglobulin As A Potential Biomarker To Monitor Pharmacological Therapeutic Efficacy In Dopamine Dictated Disease States Of Parkinson's Disease And Schizophrenia. Neuropsychiatr Dis Treat, 15, 2853-2867.
- Güzel, C., van den Berg, C. B., Koopman, S., van Krugten, R. J., Stoop, M., Stingl, C., Duvekot, J. J. & Luider, T. M. 2020. Cerebrospinal Fluid of Preeclamptic and Normotensive Pregnant Women Compared to Nonpregnant Women Analyzed with Mass Spectrometry. ACS omega, 5, 32256-32266.
- Gyllenhammer, L. E., Entringer, S., Buss, C., Simhan, H. N., Grobman, W. A., Borders, A. E. & Wadhwa, P. D. 2021. Racial differences across pregnancy in maternal pro-inflammatory immune responsivity and its regulation by glucocorticoids. *Psychoneuroendocrinology*, 131, 105333.
- Hamlin, A. N., Basford, J. E., Jaeschke, A. & Hui, D. Y. 2016. LRP1 Protein Deficiency Exacerbates Palmitate-induced Steatosis and Toxicity in Hepatocytes. *Journal of Biological Chemistry*, 291, 16610-16619.
- Han, L., Holland, O. J., Da Silva Costa, F. & Perkins, A. V. 2023. Potential biomarkers for late-onset and term preeclampsia: A scoping review. *Frontiers in Physiology,* 14.
- Hanover, J. A., Willingham, M. C. & Pastan, I. 1983. Receptor-mediated endocytosis of alpha 2-macroglobulin: solubilization and partial purification of the fibroblast alpha 2-macroglobulin receptor. *Ann N Y Acad Sci*, 421, 410-23.
- Harmon, Q. E., Huang, L., Umbach, D. M., Klungsøyr, K., Engel, S. M., Magnus, P., Skjærven, R., Zhang, J. & Wilcox, A. J. 2015. Risk of fetal death with preeclampsia. *Obstetrics and gynecology*, 125, 628-635.
- Harpel, P. C., Hayes, M. B. & Hugli, T. E. 1979. Heat-induced fragmentation of human alpha 2-macroglobulin. *J Biol Chem*, 254, 8669-78.

- Hartgill, T. W., Bergersen, T. K. & Pirhonen, J. 2011. Core body temperature and the thermoneutral zone: a longitudinal study of normal human pregnancy. *Acta Physiologica*, 201, 467-474.
- Harwood, S. L. & Enghild, J. J. 2024. Engineering New Protease Inhibitors Using α2-Macroglobulin. *In:* SANTAMARIA, S. (ed.) *Proteases and Cancer: Methods and Protocols*. New York, NY: Springer US.
- Harwood, S. L., Lyngsø, J., Zarantonello, A., Kjøge, K., Nielsen, P. K., Andersen, G. R., Pedersen, J. S. & Enghild, J. J. 2021a. Structural Investigations of Human A2M Identify a Hollow Native Conformation That Underlies Its Distinctive Protease-Trapping Mechanism. *Mol Cell Proteomics*, 20, 100090.
- Harwood, S. L., Nielsen, N. S., Diep, K., Jensen, K. T., Nielsen, P. K., Yamamoto, K. & Enghild, J. J. 2021b. Development of selective protease inhibitors via engineering of the bait region of human  $\alpha_2$ -macroglobulin. *The Journal of biological chemistry*, 297, 100879-100879.
- Heidemann, B. H. & McClure, J. H. 2003. Changes in maternal physiology during pregnancy. British journal of anaesthesia CEPD reviews, 3, 65-68.
- Hellman, L. & Thorpe, M. 2014. Granule proteases of hematopoietic cells, a family of versatile inflammatory mediators an update on their cleavage specificity, in vivo substrates, and evolution. *Biological Chemistry*, 395, 15-49.
- Herse, F., Dechend, R., Harsem, N. K., Wallukat, G., Janke, J., Qadri, F., Hering, L., Muller, D. N., Luft, F. C. & Staff, A. C. 2007. Dysregulation of the Circulating and Tissue-Based Renin-Angiotensin System in Preeclampsia. *Hypertension*, 49, 604-611.
- Hirai, C., Sugimura, M., Makino, S. & Takeda, S. 2016. Chymotrypsin Enhances Soluble Fms-Like Tyrosine Kinase 1 Production Through Protease-Activated Receptor 2 in Placenta-Derived Immortalized Human Trophoblast Cells. *Reproductive Sciences*, 23, 1542-1550.
- Hod, T., Cerdeira, A. S. & Karumanchi, S. A. 2015. Molecular Mechanisms of Preeclampsia. Cold Spring Harbor Perspectives in Medicine, 5, a023473.
- Hofmann, S. M., Zhou, L., Perez-Tilve, D., Greer, T., Grant, E., Wancata, L., Thomas, A., Pfluger, P. T., Basford, J. E., Gilham, D., Herz, J., Tschöp, M. H. & Hui, D. Y. 2007. Adipocyte LDL receptor–related protein–1 expression modulates postprandial lipid transport and glucose homeostasis in mice. *The Journal of Clinical Investigation*, 117, 3271-3282.
- Horne, C. H., Briggs, J. D., Howie, P. W. & Kennedy, A. C. 1972. Serum α-macroglobulins in renal disease and preeclampsia. *J Clin Pathol*, 25, 590-3.
- Horne, C. H., Thomson, A. W., Hunter, C. B., Tunstall, A. M., Towler, C. M. & Billingham, M. E. 1979. Pregnancy-associated alpha 2-glycoprotein (alpha 2-PAG) and various acute phase reactants in rheumatoid arthritis and osteoarthritis. *Biomedicine*, 30, 90-4.
- Hu, Z., Zhang, M., Fan, J., Hu, J., Lin, G., Piao, S., Liu, P., Liu, J., Fu, S., Sun, W., Gygi, S. P., Zhang, J. & Zhou, C. 2023. High-Level Secretion of Pregnancy Zone Protein Is a Novel Biomarker of DNA Damage-Induced Senescence and Promotes Spontaneous Senescence. *Journal of Proteome Research*, 22, 3570-3579.
- Huang, C., AlSubki, L., Yamaya, A., Sung, N. & Kwak-Kim, J. 2023. Poor ovarian response in assisted reproductive technology cycles is associated with anti-ovarian antibody and pro-inflammatory immune responses. *Journal of Reproductive Immunology*, 160, 104152.
- Huang, J., Xu, Y., Chen, Y., Shen, J., Qiu, Y., Li, X., Chen, X. & Ma, S. 2024. Revisiting the role of pregnancy zone protein (PZP) as a cancer biomarker in the immunotherapy era. *Journal of Translational Medicine*, 22, 500.
- Huang, X., Wang, L., Zhao, S., Liu, H., Chen, S., Wu, L., Liu, L., Ding, J., Yang, H., Maxwell, A., Yin, Z., Mor, G. & Liao, A. 2021. Pregnancy Induces an Immunological Memory

- Characterized by Maternal Immune Alterations Through Specific Genes Methylation. *Frontiers in Immunology,* Volume 12 2021.
- Huang, X., Wang, Y., Yu, C., Zhang, H., Ru, Q., Li, X., Song, K., Zhou, M. & Zhu, P. 2022. Cryo-EM structures reveal the dynamic transformation of human alpha-2-macroglobulin working as a protease inhibitor. *Science China Life Sciences*, 65, 2491-2504.
- Huang, Z., Zhang, P., Chen, R., Sun, L., Wang, J., Yan, R., Liu, M., Ding, Y., Wang, J., Wei, J., Yin, W., Lu, X., Wang, G., Yang, X. & Li, R. 2025. Targeting A2M-LRP1 reverses uterine spiral artery remodeling disorder and alleviates the progression of preeclampsia. *Cell Communication and Signaling*, 23, 107.
- Huerta, V., Toledo, P., Fleitas, N., Martín, A., Pupo, D., Yero, A., Sarría, M., Sánchez, A., Besada, V., Ramos, Y., Márquez, G., Guirola, O. & Chinea, G. 2014. Receptor-activated human α2-macroglobulin interacts with the envelope protein of dengue virus and protects virions from temperature-induced inactivation through multivalent binding. *Journal of General Virology*, 95, 2668-2676.
- Hughes, S. R., Khorkova, O., Goyal, S., Knaeblein, J., Heroux, J., Riedel, N. G. & Sahasrabudhe, S. 1998. α2-macroglobulin associates with β-amyloid peptide and prevents fibril formation. *Proceedings of the National Academy of Sciences*, 95, 3275-3280.
- Huntington, J. A. 2011. Serpin structure, function and dysfunction. *Journal of thrombosis and haemostasis.*, 9 Suppl 1, 26-34.
- Ijsselstijn, L., Dekker, L. J. M., Stingl, C., van der Weiden, M. M., Hofman, A., Kros, J. M., Koudstaal, P. J., Sillevis Smitt, P. A. E., Ikram, M. A., Breteler, M. M. B. & Luider, T. M. 2011. Serum Levels of Pregnancy Zone Protein are Elevated in Presymptomatic Alzheimer's Disease. *Journal of Proteome Research*, 10, 4902-4910.
- Imber, M. J. & Pizzo, S. V. 1981. Clearance and binding of two electrophoretic "fast" forms of human alpha 2-macroglobulin. *Journal of Biological Chemistry*, 256, 8134-8139.
- Ino, K., Uehara, C., Kikkawa, F., Kajiyama, H., Shibata, K., Suzuki, T., Khin, E. E., Ito, M., Takeuchi, M., Itakura, A. & Mizutani, S. 2003. Enhancement of Aminopeptidase A Expression during Angiotensin II-Induced Choriocarcinoma Cell Proliferation through AT1 Receptor Involving Protein Kinase C- and Mitogen-Activated Protein Kinase-Dependent Signaling Pathway. The Journal of Clinical Endocrinology & Metabolism, 88, 3973-3982.
- Ishimatsu, S., Itakura, A., Okada, M., Kotani, T., Iwase, A., Kajiyama, H., Ino, K. & Kikkawa, F. 2006. Angiotensin II Augmented Migration and Invasion of Choriocarcinoma Cells Involves PI3K Activation Through the AT1 Receptor. *Placenta*, 27, 587-591.
- Jarmund, A. H., Giskeødegård, G. F., Ryssdal, M., Steinkjer, B., Stokkeland, L. M. T., Madssen, T. S., Stafne, S. N., Stridsklev, S., Moholdt, T., Heimstad, R., Vanky, E. & Iversen, A. C. 2021. Cytokine Patterns in Maternal Serum From First Trimester to Term and Beyond. *Front Immunol*, 12, 752660.
- Järvelä, I. Y., Žáčková, T., Laitinen, P., Ryynänen, M. & Tekay, A. 2012. Effect of parity and fetal sex on placental and luteal hormones during early first trimester. *Prenatal Diagnosis*, 32, 160-167.
- Jensen, P. E., Hägglöf, E. M., Arbelaez, L. F., Stigbrand, T. & Shanbhag, V. P. 1993. Comparison of conformational changes of pregnancy zone protein and human alpha 2-macroglobulin, a study using hydrophobic affinity partitioning. *Biochim Biophys Acta*, 1164, 152-8.
- Jensen, P. E. & Sottrup-Jensen, L. 1986. Primary structure of human alpha 2-macroglobulin. Complete disulfide bridge assignment and localization of two interchain bridges in the dimeric proteinase binding unit. *Journal of Biological Chemistry*, 261, 15863-15869.
- Jensen, P. E. & Stigbrand, T. 1992. Differences in the proteinase inhibition mechanism of human alpha 2-macroglobulin and pregnancy zone protein. *Eur J Biochem*, 210, 1071-7.

- Jiang, X., Lin, J., Dong, M., Liu, X., Huang, Y., Zhang, H., Ye, R., Zhou, H., Yan, C., Yuan, S., Chen, L., Jiang, R., Zheng, K. & Jin, W. 2022. Overexpression of Pregnancy Zone Protein in Fat Antagonizes Diet-Induced Obesity Under an Intermittent Fasting Regime. Front Physiol, 13, 950619.
- Jumper, J., Evans, R., Pritzel, A., Green, T., Figurnov, M., Ronneberger, O., Tunyasuvunakool, K., Bates, R., Žídek, A., Potapenko, A., Bridgland, A., Meyer, C., Kohl, S. A. A., Ballard, A. J., Cowie, A., Romera-Paredes, B., Nikolov, S., Jain, R., Adler, J., Back, T., Petersen, S., Reiman, D., Clancy, E., Zielinski, M., Steinegger, M., Pacholska, M., Berghammer, T., Bodenstein, S., Silver, D., Vinyals, O., Senior, A. W., Kavukcuoglu, K., Kohli, P. & Hassabis, D. 2021. Highly accurate protein structure prediction with AlphaFold. Nature, 596, 583-589.
- Kandhaya-Pillai, R., Miro-Mur, F., Alijotas-Reig, J., Tchkonia, T., Kirkland, J. L. & Schwartz, S. 2017. TNFα-senescence initiates a STAT-dependent positive feedback loop, leading to a sustained interferon signature, DNA damage, and cytokine secretion. *Aging (Albany NY)*, 9, 2411-2435.
- Kang, D. E., Pietrzik, C. U., Baum, L., Chevallier, N., Merriam, D. E., Kounnas, M. Z., Wagner, S. L., Troncoso, J. C., Kawas, C. H., Katzman, R. & Koo, E. H. 2000. Modulation of amyloid β-protein clearance and Alzheimer's disease susceptibility by the LDL receptor–related protein pathway. *The Journal of Clinical Investigation*, 106, 1159-1166.
- Karlsson, M., Zhang, C., Méar, L., Zhong, W., Digre, A., Katona, B., Sjöstedt, E., Butler, L., Odeberg, J., Dusart, P., Edfors, F., Oksvold, P., von Feilitzen, K., Zwahlen, M., Arif, M., Altay, O., Li, X., Ozcan, M., Mardinoglu, A., Fagerberg, L., Mulder, J., Luo, Y., Ponten, F., Uhlén, M. & Lindskog, C. 2021. A single–cell type transcriptomics map of human tissues. Science Advances, 7, eabh2169.
- Kashiwagi, H., Ishimoto, H., Izumi, S.-i., Seki, T., Kinami, R., Otomo, A., Takahashi, K., Kametani, F., Hirayama, N., Sasaki, E., Shiina, T., Sakabe, K., Mikami, M. & Kametani, Y. 2020. Human PZP and common marmoset A2ML1 as pregnancy related proteins. *Scientific Reports*, 10, 5088.
- Kimball, P., Elswick, R. K. & Shiffman, M. 2001. Ethnicity and cytokine production gauge response of patients with hepatitis C to interferon-alpha therapy. *J Med Virol*, 65, 510-6.
- Krause, K., Azouz, F., Nakano, E., Nerurkar, V. R. & Kumar, M. 2019. Deletion of Pregnancy Zone Protein and Murinoglobulin-1 Restricts the Pathogenesis of West Nile Virus Infection in Mice. *Frontiers in Microbiology,* 10.
- Krimbou, L., Tremblay, M., Davignon, J. & Cohn, J. S. 1998. Association of apolipoprotein E with α2-macroglobulin in human plasma. *Journal of lipid research*, 39, 2373-2386.
- Kumar, R., Kuligina, E., Sokolenko, A., Siddiqui, Q., Gardi, N., Gupta, S., Varma, A. K. & Hasan, S. K. 2021. Genetic ablation of pregnancy zone protein promotes breast cancer progression by activating TGF-β/SMAD signaling. *Breast Cancer Research and Treatment*, 185, 317-330.
- Kunori, Y., Koizumi, M., Masegi, T., Kasai, H., Kawabata, H., Yamazaki, Y. & Fukamizu, A. 2002. Rodent α-chymases are elastase-like proteases. *European Journal of Biochemistry*, 269, 5921-5930.
- Kunori, Y., Yumiko, M., Minako, I., Hiroaki, M., Takashi, K. & and Fukamizu, A. 2005. Species Differences in Angiotensin II Generation and Degradation by Mast Cell Chymases. *Journal of Receptors and Signal Transduction*, 25, 35-44.
- Kwak-Kim, J. Y. H., Chung-Bang, H. S., Ng, S. C., Ntrivalas, E. I., Mangubat, C. P., Beaman, K. D., Beer, A. E. & Gilman-Sachs, A. 2003. Increased T helper 1 cytokine responses by circulating T cells are present in women with recurrent pregnancy losses and in infertile women with multiple implantation failures after IVF. *Human Reproduction*, 18, 767-773.

- Kwiatkowski, S., Bednarek-Jędrzejek, M., Kwiatkowska, E., Cymbaluk-Płoska, A. & Torbè, A. 2021. Diagnosis of placental insufficiency independently of clinical presentations using sFlt-1/PLGF ratio, including SGA patients. *Pregnancy Hypertension*, 25, 244-248.
- Labbadia, J. & Morimoto, R. I. 2015. The Biology of Proteostasis in Aging and Disease. *Annual Review of Biochemistry*, 84, 435-464.
- Lachmann, A., Xu, H., Krishnan, J., Berger, S. I., Mazloom, A. R. & Ma'ayan, A. 2010. ChEA: transcription factor regulation inferred from integrating genome-wide ChIP-X experiments. *Bioinformatics*, 26, 2438-44.
- Lagrange, J., Lecompte, T., Knopp, T., Lacolley, P. & Regnault, V. 2022. Alpha-2-macroglobulin in hemostasis and thrombosis: An underestimated old double-edged sword. *Journal of Thrombosis and Haemostasis*, 20, 806-815.
- Lai, J., Syngelaki, A., Nicolaides, K. H., von Dadelszen, P. & Magee, L. A. 2021. Impact of new definitions of preeclampsia at term on identification of adverse maternal and perinatal outcomes. *American Journal of Obstetrics and Gynecology*, 224, 518.e1-518.e11.
- LaMarre, J., Wollenberg, G., Gonias, S. & Hayes, M. 1991. Cytokine binding and clearance properties of proteinase-activated alpha 2-macroglobulins. *Laboratory investigation; a journal of technical methods and pathology,* 65, 3-14.
- LaMarre, J., Wollenberg, G. K., Gauldie, J. & Hayes, M. A. 1990. Alpha 2-macroglobulin and serum preferentially counteract the mitoinhibitory effect of transforming growth factor-beta 2 in rat hepatocytes. *Laboratory investigation; a journal of technical methods and pathology,* 62, 545-551.
- Lauer, D., Reichenbach, A. & Birkenmeier, G. 2001. α2-Macroglobulin-Mediated Degradation of Amyloid β1–42: A Mechanism to Enhance Amyloid β Catabolism. *Experimental Neurology*, 167, 385-392.
- Law, L. W., Sahota, D. S., Chan, L. W., Chen, M., Lau, T. K. & Leung, T. Y. 2010. Effect of long-term storage on placental growth factor and fms-like tyrosine kinase 1 measurements in samples from pregnant women. *J Matern Fetal Neonatal Med*, 23, 1475-80.
- Leaños-Miranda, A., Inova, C.-G., Méndez-Aguilar, F., Molina-Pérez, C. J., Ramírez-Valenzuela, K. L., Sillas-Pardo, L. J., Uraga-Camacho, N. C., Isordia-Salas, I. & Berumen-Lechuga, M. G. 2018. Lower circulating angiotensin II levels are related to the severity of preeclampsia and its risk as disclosed by a specific bioassay. *Medicine*, 97.
- Lee, C. H. 2017. A Simple Outline of Methods for Protein Isolation and Purification. *Endocrinol Metab (Seoul)*, 32, 18-22.
- Lee, M., Kovanen, P. T., Tedeschi, G., Oungre, E., Franceschini, G. & Calabresi, L. 2003. Apolipoprotein composition and particle size affect HDL degradation by chymase: effect on cellular cholesterol efflux. *J Lipid Res*, 44, 539-46.
- Leskinen, M., Wang, Y., Leszczynski, D., Lindstedt, K. A. & Kovanen, P. T. 2001. Mast Cell Chymase Induces Apoptosis of Vascular Smooth Muscle Cells. *Arteriosclerosis, Thrombosis, and Vascular Biology,* 21, 516-522.
- Leskinen, M. J., Lindstedt, K. A., Wang, Y. & Kovanen, P. T. 2003. Mast Cell Chymase Induces Smooth Muscle Cell Apoptosis by a Mechanism Involving Fibronectin Degradation and Disruption of Focal Adhesions. *Arteriosclerosis, Thrombosis, and Vascular Biology,* 23, 238-243.
- Lewandowska, M., Więckowska, B., Sajdak, S. & Lubiński, J. 2020. Pre-Pregnancy Obesity vs. Other Risk Factors in Probability Models of Preeclampsia and Gestational Hypertension. *Nutrients*, 12, 2681.
- Lim, K. J. H., Odukoya, O. A., Ajjan, R. A., Li, T.-C., Weetman, A. P. & Cooke, I. D. 2000. The role of T-helper cytokines in human reproduction. *Fertility and Sterility*, 73, 136-142.

- Lin, J.-X. & Leonard, W. J. 2000. The role of Stat5a and Stat5b in signaling by IL-2 family cytokines. *Oncogene*, 19, 2566-2576.
- Lin, J., Jiang, X., Dong, M., Liu, X., Shen, Q., Huang, Y., Zhang, H., Ye, R., Zhou, H., Yan, C., Yuan, S., Wu, X., Chen, L., Wang, Y., He, M., Tao, Y., Zhang, Z. & Jin, W. 2021. Hepatokine Pregnancy Zone Protein Governs the Diet-Induced Thermogenesis Through Activating Brown Adipose Tissue. *Advanced Science*, 8, 2101991.
- Lin, T.-M., Halbert, S. P. & Spellacy, W. N. 1974. Measurement of Pregnancy-Associated Plasma Proteins during Human Gestation. *The Journal of Clinical Investigation*, 54, 576-582.
- Lin, T.-M., Halbert, S. P. & Spellacy, W. N. 1976. Relation of obstetric parameters to the concentrations of four pregnancy-associated plasma proteins at term in normal gestation. *American Journal of Obstetrics and Gynecology*, 125, 17-24.
- Lin, T. M. & Halbert, S. P. 1976. Placental localization of human pregnancy--associated plasma proteins. *Science*, 193, 1249.
- Lindstedt, L., Lee, M. & Kovanen, P. T. 2001. Chymase bound to heparin is resistant to its natural inhibitors and capable of proteolyzing high density lipoproteins in aortic intimal fluid. *Atherosclerosis*, 155, 87-97.
- Lisonkova, S. & Joseph, K. S. 2013. Incidence of preeclampsia: risk factors and outcomes associated with early- versus late-onset disease. *American Journal of Obstetrics and Gynecology*, 209, 544.e1-544.e12.
- Liu, C., Zhang, N., Yu, H., Chen, Y., Liang, Y., Deng, H. & Zhang, Z. 2011. Proteomic analysis of human serum for finding pathogenic factors and potential biomarkers in preeclampsia. *Placenta*, 32, 168-174.
- Liu, X., Sun, J., Wen, X., Duan, J., Xue, D., Pan, Y., Sun, J., Zhang, W., Cheng, X. & Wang, C. 2020. Proteome profiling of gestational diabetes mellitus at 16-18 weeks revealed by LC-MS/MS. *J Clin Lab Anal*, 34, e23424.
- Löb, S., Vattai, A., Kuhn, C., Mittelberger, J., Herbert, S.-L., Wöckel, A., Schmoeckel, E., Mahner, S. & Jeschke, U. 2022. The Pregnancy Zone Protein (PZP) is significantly downregulated in the placenta of preeclampsia and HELLP syndrome patients. *Journal of Reproductive Immunology*, 153, 103663.
- Löb, S., Vattai, A., Kuhn, C., Schmoeckel, E., Mahner, S., Wöckel, A., Kolben, T., Keil, C., Jeschke, U. & Vilsmaier, T. 2021. Pregnancy Zone Protein (PZP) is significantly upregulated in the decidua of recurrent and spontaneous miscarriage and negatively correlated to Glycodelin A (GdA). *Journal of Reproductive Immunology*, 143, 103267.
- Loechel, F., Fox, J. W., Murphy, G., Albrechtsen, R. & Wewer, U. M. 2000. ADAM 12-S Cleaves IGFBP-3 and IGFBP-5 and Is Inhibited by TIMP-3. *Biochemical and Biophysical Research Communications*, 278, 511-515.
- Longley, B. J., Tyrrell, L., Ma, Y., Williams, D. A., Halaban, R., Langley, K., Lu, H. S. & Schechter, N. M. 1997. Chymase cleavage of stem cell factor yields a bioactive, soluble product. *Proceedings of the National Academy of Sciences*, 94, 9017-9021.
- Lumbers, E. R. 1970. Peripheral vascular reactivity to angiotensin and noradrenaline in pregnant and non-pregnant women. *Aust J Exp Biol Med Sci*, 48, 493-500.
- Lumbers, E. R., Delforce, S. J., Arthurs, A. L. & Pringle, K. G. 2019. Causes and Consequences of the Dysregulated Maternal Renin-Angiotensin System in Preeclampsia. *Frontiers in Endocrinology*, 10.
- Lumbers, E. R. & Pringle, K. G. 2013. Roles of the circulating renin-angiotensin-aldosterone system in human pregnancy. *American Journal of Physiology-Regulatory, Integrative and Comparative Physiology*, 306, R91-R101.

- Luo, Z.-C., An, N., Xu, H.-R., Larante, A., Audibert, F. & Fraser, W. D. 2007. The effects and mechanisms of primiparity on the risk of pre-eclampsia: a systematic review. *Paediatric and Perinatal Epidemiology*, 21, 36-45.
- Luque, D., Goulas, T., Mata, C. P., Mendes, S. R., Gomis-Rüth, F. X. & Castón, J. R. 2022. Cryo-EM structures show the mechanistic basis of pan-peptidase inhibition by human α2macroglobulin. *Proceedings of the National Academy of Sciences*, 119, e2200102119.
- Macdonald, H. N. & Good, W. 1972. THE EFFECT OF PARITY ON PLASMA TOTAL PROTEIN, ALBUMIN, UREA AND α-AMINO NITROGEN LEVELS DURING PREGNANCY. *BJOG: An International Journal of Obstetrics & Gynaecology*, 79, 518-525.
- MacDonald, T. M., Walker, S. P., Hannan, N. J., Tong, S. & Kaitu'u-Lino, T. u. J. 2022. Clinical tools and biomarkers to predict preeclampsia. *eBioMedicine*, 75.
- Magee, L. A., Brown, M. A., Hall, D. R., Gupte, S., Hennessy, A., Karumanchi, S. A., Kenny, L. C., McCarthy, F., Myers, J., Poon, L. C., Rana, S., Saito, S., Staff, A. C., Tsigas, E. & von Dadelszen, P. 2022. The 2021 International Society for the Study of Hypertension in Pregnancy classification, diagnosis & management recommendations for international practice. *Pregnancy Hypertens*, 27, 148-169.
- Mao, J., Sun, H., Shen, Q., Zou, C., Yang, Y. & Du, Q. 2025. Impact of pre-pregnancy body mass index on preeclampsia. *Front Med (Lausanne)*, 12, 1529966.
- Mariani, E., Seripa, D., Ingegni, T., Nocentini, G., Mangialasche, F., Ercolani, S., Cherubini, A., Metastasio, A., Pilotto, A., Senin, U. & Mecocci, P. 2006. Interaction of CTSD and A2M polymorphisms in the risk for Alzheimer's disease. *Journal of the Neurological Sciences*, 247, 187-191.
- Marino-Puertas, L., Del Amo-Maestro, L., Taulés, M., Gomis-Rüth, F. X. & Goulas, T. 2019. Recombinant production of human α2-macroglobulin variants and interaction studies with recombinant G-related α2-macroglobulin binding protein and latent transforming growth factor-β2. *Scientific Reports*, 9.
- Marrero, A., Duquerroy, S., Trapani, S., Goulas, T., Guevara, T., Andersen, G. R., Navaza, J., Sottrup-Jensen, L. & Gomis-Rüth, F. X. 2012. The Crystal Structure of Human α2-Macroglobulin Reveals a Unique Molecular Cage. *Angewandte Chemie International Edition*, 51, 3340-3344.
- Martos, L., Ramón, L. A., Oto, J., Fernández-Pardo, Á., Bonanad, S., Cid, A. R., Gruber, A., Griffin, J. H., España, F., Navarro, S. & Medina, P. 2018. α2-Macroglobulin Is a Significant In Vivo Inhibitor of Activated Protein C and Low APC:α2M Levels Are Associated with Venous Thromboembolism. *Thromb Haemost*, 118, 630-638.
- Matthijs, G., Devriendt, K., Cassiman, J.-J., Van den Berghe, H. & Marynen, P. 1992. Structure of the human alpha-2 macroglobulin gene and its promotor. *Biochemical and Biophysical Research Communications*, 184, 596-603.
- Maxfield, F. R., Willingham, M. C., Haigler, H. T., Dragsten, P. & Pastan, I. H. 1981. Binding, surface mobility, internalization, and degradation of rhodamine-labeled alpha 2-macroglobulin. *Biochemistry*, 20, 5353-8.
- McMahon, M. J., Bowen, M., Mayer, A. D. & Cooper, E. H. 1984. Relation of α2-macroglobulin and other antiproteases to the clinical features of acute pancreatitis. *The American journal of surgery*, 147, 164-170.
- Medina-Bastidas, D., Guzmán-Huerta, M., Borboa-Olivares, H., Ruiz-Cruz, C., Parra-Hernández, S., Flores-Pliego, A., Salido-Guadarrama, I., Camargo-Marín, L., Arambula-Meraz, E. & Estrada-Gutierrez, G. 2020. Placental Microarray Profiling Reveals Common mRNA and IncRNA Expression Patterns in Preeclampsia and Intrauterine Growth Restriction. *International Journal of Molecular Sciences*, 21, 3597.

- Mehta, D., Wani, S., Wallace, L., Henders, A. K., Wray, N. R. & McCombe, P. A. 2019. Cumulative influence of parity-related genomic changes in multiple sclerosis. *Journal of Neuroimmunology*, 328, 38-49.
- Mei, Y., Ran, Y., Liu, Z., Zhou, Y., He, J., Yin, N. & Qi, H. 2022. IL-27 Mediates Th1 Cells Infiltration in Fetal Membranes in Preterm Labor. *Reproductive Sciences*, 29, 1764-1775.
- Melchior, J. T., Swertfeger, D. K., Morris, J., Street, S. E., Warshak, C. R., Welge, J. A., Remaley, A. T., Catov, J. M., Davidson, W. S. & Woollett, L. A. 2021. Pregnancy is accompanied by larger high density lipoprotein particles and compositionally distinct subspecies. *J Lipid Res*, 62, 100107.
- Mendes, S. R., Gomis-Rüth, F. X. & Goulas, T. 2023. Frozen fresh blood plasma preserves the functionality of native human α2-macroglobulin. *Scientific Reports*, 13, 4579.
- Merrill, D. C., Karoly, M., Chen, K., Ferrario, C. M. & Brosnihan, K. B. 2002. Angiotensin-(1–7) in normal and preeclamptic pregnancy. *Endocrine*, 18, 239-245.
- Meyer, N., Woidacki, K., Knöfler, M., Meinhardt, G., Nowak, D., Velicky, P., Pollheimer, J. & Zenclussen, A. C. 2017. Chymase-producing cells of the innate immune system are required for decidual vascular remodeling and fetal growth. *Scientific Reports*, 7, 45106.
- Mihu, D., Razvan, C., Malutan, A. & Mihaela, C. 2015. Evaluation of maternal systemic inflammatory response in preeclampsia. *Taiwanese Journal of Obstetrics and Gynecology*, 54, 160-166.
- Mishra, J. S., Gopalakrishnan, K. & Kumar, S. 2018. Pregnancy upregulates angiotensin type 2 receptor expression and increases blood flow in uterine arteries of rats. *Biol Reprod*, 99, 1091-1099.
- Misra, D. P. & Kiely, J. L. 1997. The Association Between Nulliparity and Gestational Hypertension. *Journal of Clinical Epidemiology*, 50, 851-855.
- Mizutani, H., Schechter, N., Lazarus, G., Black, R. A. & Kupper, T. S. 1991. Rapid and specific conversion of precursor interleukin 1 beta (IL-1 beta) to an active IL-1 species by human mast cell chymase. *Journal of Experimental Medicine*, 174, 821-825.
- Mor, G., Aldo, P. & Alvero, A. B. 2017. The unique immunological and microbial aspects of pregnancy. *Nature Reviews Immunology,* 17, 469-482.
- Mor, G. & Cardenas, I. 2010. The immune system in pregnancy: a unique complexity. *Am J Reprod Immunol*, 63, 425-33.
- Morales-Maldonado, A., Humphry, M., Figg, N. & Clarke, M. C. H. 2024. Human vascular smooth muscle cells utilise chymase for the atypical cleavage and activation of Interleukin-1β. *Atherosclerosis*, 390, 117308.
- Narayan, B. & Nelson-Piercy, C. 2020. Physiological Changes of the Immune System During Pregnancy. *In:* EINAV, S., WEINIGER, C. F. & LANDAU, R. (eds.) *Principles and Practice of Maternal Critical Care.* Cham: Springer International Publishing.
- Narita, M., Holtzman, D. M., Schwartz, A. L. & Bu, G. 1997. α2-Macroglobulin Complexes with and Mediates the Endocytosis of β-Amyloid Peptide via Cell Surface Low-Density Lipoprotein Receptor-Related Protein. *Journal of Neurochemistry*, 69, 1904-1911.
- Navajas, R., Ramos-Fernandez, A., Herraiz, I., Galindo, A., Bartha, J. L., Corrales, F. & Paradela, A. 2022. Quantitative proteomic analysis of serum-purified exosomes identifies putative pre-eclampsia-associated biomarkers. *Clinical Proteomics*, 19, 5.
- Naveau, S., Poynard, T., Benattar, C., Bedossa, P. & Chaput, J.-C. 1994. Alpha-2-macroglobulin and hepatic fibrosis. *Digestive Diseases and Sciences*, 39, 2426-2432.
- Nguyen, P. M., Putoczki, T. L. & Ernst, M. 2015. STAT3-Activating Cytokines: A Therapeutic Opportunity for Inflammatory Bowel Disease? *J Interferon Cytokine Res*, 35, 340-50.
- Nielsen, N. S., Zarantonello, A., Harwood, S. L., Jensen, K. T., Kjøge, K., Thøgersen, I. B., Schauser, L., Karlsen, J. L., Andersen, G. R. & Enghild, J. J. 2022. Cryo-EM structures of

- human A2ML1 elucidate the protease-inhibitory mechanism of the A2M family. *Nature Communications*, 13, 3033.
- Nijholt, D. A. T., Ijsselstijn, L., van der Weiden, M. M., Zheng, P.-P., Sillevis Smitt, P. A. E., Koudstaal, P. J., Luider, T. M. & Kros, J. M. 2015. Pregnancy Zone Protein is Increased in the Alzheimer's Disease Brain and Associates with Senile Plaques. *Journal of Alzheimer's Disease*, 46, 227-238.
- O'Connor-McCourt, M. D. & Wakefield, L. M. 1987. Latent transforming growth factor-beta in serum. A specific complex with alpha 2-macroglobulin. *Journal of Biological Chemistry*, 262, 14090-14099.
- Ødegård, R. A., Vatten, L. J., Nilsen, S. T., Salvesen, K. Å. & Austgulen, R. 2000. Preeclampsia and fetal growth. *Obstetrics & Gynecology*, 96, 950-955.
- Oh, J. W., Kim, S. K., Cho, K.-C., Kim, M.-S., Suh, C. S., Lee, J. R. & Kim, K. P. 2017. Proteomic analysis of human follicular fluid in poor ovarian responders during in vitro fertilization. *PROTEOMICS*, 17, 1600333.
- Omoto, Y., Tokime, K., Yamanaka, K., Habe, K., Morioka, T., Kurokawa, I., Tsutsui, H., Yamanishi, K., Nakanishi, K. & Mizutani, H. 2006. Human Mast Cell Chymase Cleaves Pro-IL-18 and Generates a Novel and Biologically Active IL-18 Fragment1. *The Journal of Immunology*, 177, 8315-8319.
- Oshima, T., Hashimoto, I., Hiroshima, Y., Kimura, Y., Tanabe, M. I. E., Onuma, S., Morita, J., Nagasawa, S., Kanematsu, K., Aoyama, T., Yamada, T., Ogata, T., Rino, Y., Saito, A. Y. A. & Miyagi, Y. 2024. Clinical Significance of Pregnancy Zone Protein Expression in Patients With Locally Advanced Gastric Cancer After Curative Resection. *Anticancer Research*, 44, 369.
- Ottosson, U. B., Damber, J. E., Damber, M. G., Selstam, G., Solheim, F., Stigbrand, T., Södergård, R. & Von Schoultz, B. 1981. Effects on sex hormone binding globulin capacity and pregnancy zone protein of treatment with combinations of ethinyl-oestradiol and norethisterone. *Maturitas*, 3, 295-300.
- Panagiotopoulou, K., Katsouyanni, K., Petridou, E., Garas, Y., Tzonou, A. & Trichopoulos, D. 1990. Maternal age, parity, and pregnancy estrogens. *Cancer Causes Control*, 1, 119-24.
- Paréj, K., Dobó, J., Závodszky, P. & Gál, P. 2013. The control of the complement lectin pathway activation revisited: Both C1-inhibitor and antithrombin are likely physiological inhibitors, while α2-macroglobulin is not. *Molecular Immunology*, 54, 415-422.
- Peslova, G., Petrak, J., Kuzelova, K., Hrdy, I., Halada, P., Kuchel, P. W., Soe-Lin, S., Ponka, P., Sutak, R., Becker, E., Huang, M. L.-H., Suryo Rahmanto, Y., Richardson, D. R. & Vyoral, D. 2009. Hepcidin, the hormone of iron metabolism, is bound specifically to α-2-macroglobulin in blood. *Blood*, 113, 6225-6236.
- Petersen, C. M. 1993. Alpha 2-macroglobulin and pregnancy zone protein. Serum levels, alpha 2-macroglobulin receptors, cellular synthesis and aspects of function in relation to immunology. *Dan Med Bull*, 40, 409-46.
- Petersen, C. M., Jensen, P. H., Bukh, A., Sunder, T. L., Lamm, L. U. & Ingerslev, J. 1990. Pregnancy zone protein: a re-evaluation of serum levels in healthy women and in women suffering from breast cancer or trophoblastic disease. *Scandinavian Journal of Clinical and Laboratory Investigation*, 50, 479-485.
- Philip, A., Bostedt, L., Stigbrand, T. & O'Connor-Mccourt, M. D. 1994. Binding of transforming growth factor-beta (TGF-beta) to pregnancy zone protein (PZP). Comparison to the TGF-beta-alpha2-macroglobulin interaction. *European Journal of Biochemistry*, 221, 687-693.

- Platanias, L. C. 2005. Mechanisms of type-I- and type-II-interferon-mediated signalling. *Nature Reviews Immunology*, **5**, 375-386.
- Pongpaew, P., Boonyakarnkul, N., Schelp, F.-P., Changbumrung, S., Supawan, V., Tawprasert, S. & Migasena, P. 1994. Serum concentrations of alpha-2-macroglobulin and other serum proteinase inhibitors in Thai vegetarians and omnivores. *Nutrition Research*, 14, 337-345.
- Pongpaew, P., Schelp, F.-P., Supawan, V., Prayurahong, B., Mahaweerawat, U., Intarakhao, C., Sriboonlue, P. & Migasena, P. 1991. Influence of dietary intake on alpha-2-macroglobulin and other biochemical parameters in healthy thai males. *Nutrition Research*, 11, 559-565.
- Qiu, G., Cao, L. & Chen, Y.-J. 2023. Novel heterozygous mutation in alpha-2-macroglobulin (A2M) suppressing the binding of amyloid-β (Aβ). *Frontiers in Neurology*, 13.
- Quinn, K. A., Pye, V. J., Dai, Y.-P., Chesterman, C. N. & Owensby, D. A. 1999. Characterization of the Soluble Form of the Low Density Lipoprotein Receptor-Related Protein (LRP). *Experimental Cell Research*, 251, 433-441.
- Ramsay, J. E., Ferrell, W. R., Crawford, L., Wallace, A. M., Greer, I. A. & Sattar, N. 2002. Maternal Obesity Is Associated with Dysregulation of Metabolic, Vascular, and Inflammatory Pathways. *The Journal of Clinical Endocrinology & Metabolism*, 87, 4231-4237.
- Rana, S., Lemoine, E., Granger, J. P. & Karumanchi, S. A. 2019. Preeclampsia. *Circulation Research*, 124, 1094-1112.
- Rasanen, J., Girsen, A., Lu, X., Lapidus, J. A., Standley, M., Reddy, A., Dasari, S., Thomas, A., Jacob, T., Pouta, A., Surcel, H.-M., Tolosa, J. E., Gravett, M. G. & Nagalla, S. R. 2010. Comprehensive Maternal Serum Proteomic Profiles of Preclinical and Clinical Preeclampsia. *Journal of Proteome Research*, 9, 4274-4281.
- Raymond, W. W., Ruggles, S. W., Craik, C. S. & Caughey, G. H. 2003. Albumin Is a Substrate of Human Chymase: PREDICTION BY COMBINATORIAL PEPTIDE SCREENING AND DEVELOPMENT OF A SELECTIVE INHIBITOR BASED ON THE ALBUMIN CLEAVAGE SITE. *Journal of Biological Chemistry*, 278, 34517-34524.
- Raymond, W. W., Su, S., Makarova, A., Wilson, T. M., Carter, M. C., Metcalfe, D. D. & Caughey, G. H. 2009. Alpha 2-macroglobulin capture allows detection of mast cell chymase in serum and creates a reservoir of angiotensin II-generating activity. *J Immunol*, 182, 5770-7.
- Reddy, K. R., Hoofnagle, J. H., Tong, M. J., Lee, W. M., Pockros, P., Heathcote, E. J., Albert, D. & Joh, T. 1999. Racial differences in responses to therapy with interferon in chronic hepatitis C. Consensus Interferon Study Group. *Hepatology*, 30, 787-93.
- Reddy, V. Y., Desorchers, P. E., Pizzo, S. V., Gonias, S. L., Sahakian, J. A., Levine, R. L. & Weiss, S. J. 1994. Oxidative dissociation of human alpha 2-macroglobulin tetramers into dysfunctional dimers. *J Biol Chem*, 269, 4683-91.
- Reddy, V. Y., Pizzo, S. V. & Weiss, S. J. 1989. Functional Inactivation and Structural Disruption of Human α2-Macroglobulin by Neutrophils and Eosinophils. *Journal of Biological Chemistry*, 264, 13801-13809.
- Rehman, A. A., Ahsan, H. & Khan, F. H. 2013. Alpha-2-macroglobulin: A physiological guardian. Journal of Cellular Physiology, 228, 1665-1675.
- Rolnik, D. L., Wright, D., Poon, L. C. Y., Syngelaki, A., O'Gorman, N., de Paco Matallana, C., Akolekar, R., Cicero, S., Janga, D., Singh, M., Molina, F. S., Persico, N., Jani, J. C., Plasencia, W., Papaioannou, G., Tenenbaum-Gavish, K. & Nicolaides, K. H. 2017. ASPRE trial: performance of screening for preterm pre-eclampsia. *Ultrasound Obstet Gynecol*, 50, 492-495.

- Romero, R., Erez, O., Maymon, E., Chaemsaithong, P., Xu, Z., Pacora, P., Chaiworapongsa, T., Done, B., Hassan, S. S. & Tarca, A. L. 2017. The maternal plasma proteome changes as a function of gestational age in normal pregnancy: a longitudinal study. *Am J Obstet Gynecol*, 217, 67.e1-67.e21.
- Ross, K. M., Carroll, J., Horvath, S., Hobel, C. J., Coussons-Read, M. E. & Dunkel Schetter, C. 2020. Immune epigenetic age in pregnancy and 1 year after birth: Associations with weight change. *American Journal of Reproductive Immunology*, 83, e13229.
- Roy, A., Ganesh, G., Sippola, H., Bolin, S., Sawesi, O., Dagälv, A., Schlenner, S. M., Feyerabend, T., Rodewald, H.-R., Kjellén, L., Hellman, L. & Åbrink, M. 2014. Mast Cell Chymase Degrades the Alarmins Heat Shock Protein 70, Biglycan, HMGB1, and Interleukin-33 (IL-33) and Limits Danger-induced Inflammation \*. Journal of Biological Chemistry, 289, 237-250.
- Rubenstein, D. S., Thøgersen, I. B., Pizzo, S. V. & Enghild, J. J. 1993. Identification of monomeric alpha-macroglobulin proteinase inhibitors in birds, reptiles, amphibians and mammals, and purification and characterization of a monomeric alpha-macroglobulin proteinase inhibitor from the American bullfrog Rana catesbeiana. *Biochem J*, 290 ( Pt 1), 85-95.
- Rugsarash, W., Tungtrongchitr, R., Petmitr, S., Phonrat, B., Pongpaew, P., Harnroongroj, T. & Tungtrongchitr, A. 2006. The genetic association between alpha-2-macroglobulin (A2M) gene deletion polymorphism and low serum A2M concentration in overweight/obese Thais. *Nutr Neurosci*, 9, 93-8.
- Rurangirwa, A. A., Gaillard, R., Steegers, E. A., Hofman, A. & Jaddoe, V. W. 2012. Hemodynamic Adaptations in Different Trimesters Among Nulliparous and Multiparous Pregnant Women; The Generation R Study. *American Journal of Hypertension*, 25, 892-899.
- Saarinen, J., Kalkkinen, N., Welgus, H. G. & Kovanen, P. T. 1994. Activation of human interstitial procollagenase through direct cleavage of the Leu83-Thr84 bond by mast cell chymase. *Journal of Biological Chemistry*, 269, 18134-18140.
- Saito, S., Hashimoto, H., Yonemasu, K. & Ichijo, M. 1990. Pregnancy zone protein inhibits production of interleukin-2 but does not affect interleukin-2 receptor expression on T cell activation. *Journal of Reproductive Immunology,* 17, 115-126.
- Saito, S., Sakai, M., Sasaki, Y., Tanebe, K., Tsuda, H. & Michimata, T. 1999. Quantitative analysis of peripheral blood Th0, Th1, Th2 and the Th1:Th2 cell ratio during normal human pregnancy and preeclampsia. *Clin Exp Immunol*, 117, 550-5.
- Sanchez, A., Gandhi, K., Garza, J., Gibson, A., Manales, N. & Ventolini, G. 2021. Variations in cytokine profiles between parous and nulliparous adult women. 3, 39-44.
- Sánchez, M. C., Chiabrando, G. A., Guglielmone, H. A., Bonacci, G. R., Rabinovich, G. A. & Vides, M. A. 1998. Interaction of Human Tissue Plasminogen Activator (t-PA) with Pregnancy Zone Protein: A Comparative Study with t-PA- α2 -Macroglobulin Interaction1. *The Journal of Biochemistry*, 124, 274-279.
- Sánchez, M. C., Chiabrando, G. A. & Vides, M. A. 2001. Pregnancy Zone Protein–Tissue-Type Plasminogen Activator Complexes Bind to Low-Density Lipoprotein Receptor-Related Protein (LRP). *Archives of Biochemistry and Biophysics*, 389, 218-222.
- Sand, O., Folkersen, J., Westergaard, J. G. & Sottrup-Jensen, L. 1985. Characterization of human pregnancy zone protein. Comparison with human alpha 2-macroglobulin. *Journal of Biological Chemistry*, 260, 15723-15735.
- Sarcione, E. J. & Biddle, W. C. 2001. Elevated serum pregnancy zone protein levels in HIV-1-infected men. *AIDS*, 15.
- Saunders, A. J., Bertram, L., Mullin, K., Sampson, A. J., Latifzai, K., Basu, S., Jones, J., Kinney, D., MacKenzie-Ingano, L., Yu, S., Albert, M. S., Moscarillo, T. J., Go, R. C. P., Bassett, S. S., Daly, M. J., Laird, N. M., Wang, X., Velicelebi, G., Wagner, S. L., Becker, D. K., Tanzi, R.

- E. & Blacker, D. 2003. Genetic association of Alzheimer's disease with multiple polymorphisms in alpha-2-macroglobulin. *Human Molecular Genetics*, 12, 2765-2776.
- Schäffers, O. J. M., Gribnau, J., van Rijn, B. & Bunnik, E. M. 2025. Ethical considerations for advancing research using organoid models derived from the placenta. *Human Reproduction Update*, 31, 392-401.
- Schechter, N. M., Plotnick, M., Selwood, T., Walter, M. & Rubin, H. 1997. Diverse Effects of pH on the Inhibition of Human Chymase by Serpins. *Journal of Biological Chemistry*, 272, 24499-24507.
- Schneider, C. A., Rasband, W. S. & Eliceiri, K. W. 2012. NIH Image to ImageJ: 25 years of image analysis. *Nature Methods*, 9, 671-675.
- Schock, H., Zeleniuch-Jacquotte, A., Lundin, E., Grankvist, K., Lakso, H., Idahl, A., Lehtinen, M., Surcel, H. M. & Fortner, R. T. 2016. Hormone concentrations throughout uncomplicated pregnancies: a longitudinal study. *BMC Pregnancy Childbirth*, 16, 146.
- Sekiguchi, R., Fujito, N. T. & Nonaka, M. 2012. Evolution of the thioester-containing proteins (TEPs) of the arthropoda, revealed by molecular cloning of TEP genes from a spider, Hasarius adansoni. *Developmental & Comparative Immunology*, 36, 483-489.
- Shao, J., Jin, Y., Shao, C., Fan, H., Wang, X. & Yang, G. 2021. Serum exosomal pregnancy zone protein as a promising biomarker in inflammatory bowel disease. *Cellular & Molecular Biology Letters*, 26.
- Shen, L., Zhao, D., Chen, Y., Zhang, K., Chen, X., Lin, J., Li, C., Iqbal, J., Zhao, Y., Liang, Y., Wei, Y. & Feng, C. 2019. Comparative Proteomics Analysis of Serum Proteins in Gestational Diabetes during Early and Middle Stages of Pregnancy. *Proteomics Clin Appl*, 13, e1800060.
- Shi, L., Buckley, N. J., Bos, I., Engelborghs, S., Sleegers, K., Frisoni, G. B., Wallin, A., Lléo, A., Popp, J., Martinez-Lage, P., Legido-Quigley, C., Barkhof, F., Zetterberg, H., Visser, P. J., Bertram, L., Lovestone, S. & Nevado-Holgado, A. J. 2021. Plasma Proteomic Biomarkers Relating to Alzheimer's Disease: A Meta-Analysis Based on Our Own Studies. Frontiers in Aging Neuroscience, 13.
- Shiels, M. S., Katki, H. A., Freedman, N. D., Purdue, M. P., Wentzensen, N., Trabert, B., Kitahara, C. M., Furr, M., Li, Y., Kemp, T. J., Goedert, J. J., Chang, C. M., Engels, E. A., Caporaso, N. E., Pinto, L. A., Hildesheim, A. & Chaturvedi, A. K. 2014. Cigarette Smoking and Variations in Systemic Immune and Inflammation Markers. *JNCI: Journal of the National Cancer Institute*, 106, dju294.
- Shimomura, R., Nezu, T., Hosomi, N., Aoki, S., Sugimoto, T., Kinoshita, N., Araki, M., Takahashi, T., Maruyama, H. & Matsumoto, M. 2018. Alpha-2-macroglobulin as a Promising Biological Marker of Endothelial Function. *Journal of Atherosclerosis and Thrombosis*, 25, 350-358.
- Shin, D. & Song, W. O. 2015. Prepregnancy body mass index is an independent risk factor for gestational hypertension, gestational diabetes, preterm labor, and small- and large-forgestational-age infants. *J Matern Fetal Neonatal Med*, 28, 1679-86.
- Skornicka, E. L., Kiyatkina, N., Weber, M. C., Tykocinski, M. L. & Koo, P. H. 2004. Pregnancy zone protein is a carrier and modulator of placental protein-14 in T-cell growth and cytokine production. *Cellular Immunology*, 232, 144-156.
- Smith, A., Choi, J.-Y., Finch, S., Ong, S., Keir, H., Dicker, A. & Chalmers, J. 2017. Sputum Pregnancy Zone Protein (PZP) a potential biomarker of bronchiectasis severity. *European Respiratory Journal*, 50, OA1969.
- Smithies, O. 1959. Zone electrophoresis in starch gels and its application to studies of serum proteins. *Adv Protein Chem,* 14, 65-113.

- Soma-Pillay, P., Nelson-Piercy, C., Tolppanen, H. & Mebazaa, A. 2016. Physiological changes in pregnancy. *Cardiovascular Journal of Africa*, 27, 89-94.
- Sottrup-Jensen, L. 1989. α-Macroglobulins: structure, shape, and mechanism of proteinase complex formation. *Journal of Biological Chemistry*, 264, 11539-11542.
- Sottrup-Jensen, L., Borth, W., Hall, M., Quigleys, J. P. & Armstrong, P. B. 1990. Sequence similarity between α2-macroglobulin from the horseshoe crab, Limulus polyphemus, and proteins of the α2-macroglobulin family from mammals. *Comparative Biochemistry and Physiology Part B: Comparative Biochemistry*, 96, 621-625.
- Sottrup-Jensen, L., Folkersen, J., Kristensen, T. & Tack, B. F. 1984. Partial primary structure of human pregnancy zone protein: extensive sequence homology with human alpha 2-macroglobulin. *Proc Natl Acad Sci U S A*, 81, 7353-7.
- Sottrup-Jensen, L., Petersen, T. E. & Magnusson, S. 1980. A thiol-ester in α2-macroglobulin cleaved during proteinase complex formation. *FEBS Letters*, 121, 275-279.
- Sottrup-Jensen, L., Sand, O., Kristensen, L. & Fey, G. H. 1989. The α-Macroglobulin Bait Region: Sequence diversity and localization of cleavage sites for proteinases in five mammalian α-macroglobulins. *Journal of Biological Chemistry*, 264, 15781-15789.
- Sottrup-Jensen, L., Stepanik, T. M., Kristensen, T., Lønblad, P. B., Jones, C. M., Wierzbicki, D. M., Magnusson, S., Domdey, H., Wetsel, R. A. & Lundwall, A. 1985. Common evolutionary origin of alpha 2-macroglobulin and complement components C3 and C4. *Proceedings of the National Academy of Sciences*, 82, 9-13.
- Spycher, S., Arya, S., Isenman, D. & Painter, R. 1987. A functional, thioester-containing alpha 2-macroglobulin homologue isolated from the hemolymph of the American lobster (Homarus americanus). *Journal of Biological Chemistry*, 262, 14606-14611.
- Stadler, J. T., Lackner, S., Mörkl, S., Trakaki, A., Scharnagl, H., Borenich, A., Wonisch, W., Mangge, H., Zelzer, S., Meier-Allard, N., Holasek, S. J. & Marsche, G. 2021. Obesity Affects HDL Metabolism, Composition and Subclass Distribution. *Biomedicines*, 9.
- Stadler, J. T., van Poppel, M. N. M., Wadsack, C., Holzer, M., Pammer, A., Simmons, D., Hill, D., Desoye, G., Marsche, G. & Group, D. C. I. 2023. Obesity Affects Maternal and Neonatal HDL Metabolism and Function. *Antioxidants* [Online], 12.
- Staff, A. C. 2019. The two-stage placental model of preeclampsia: An update. *Journal of Reproductive Immunology,* 134-135, 1-10.
- Steiner, J. P., Bhattacharya, P. & Strickland, D. K. 1985. Thrombin-induced conformational changes of human alpha 2-macroglobulin: evidence for two functional domains. *Biochemistry*, 24, 2993-3001.
- Stewart, F. M., Freeman, D. J., Ramsay, J. E., Greer, I. A., Caslake, M. & Ferrell, W. R. 2007. Longitudinal Assessment of Maternal Endothelial Function and Markers of Inflammation and Placental Function throughout Pregnancy in Lean and Obese Mothers. *The Journal of Clinical Endocrinology & Metabolism*, 92, 969-975.
- Su, L., Zhang, G. & Kong, X. 2020. Prognostic Significance of Pregnancy Zone Protein and Its Correlation with Immune Infiltrates in Hepatocellular Carcinoma. *Cancer Management and Research*, Volume 12, 9883-9891.
- Sudjai, D. 2023. Association of pre-pregnancy body mass index with early- and late-onset severe preeclampsia. *European Journal of Obstetrics & Gynecology and Reproductive Biology: X,* 19, 100223.
- Takai, S., Shiota, N., Sakaguchi, M., Muraguchi, H., Matsumura, E. & Miyazaki, M. 1997. Characterization of chymase from human vascular tissues. *Clin Chim Acta*, 265, 13-20.
- Tandon, S. N., Siddiqui, J. S., Sahu, S., Kapoor, A. K., Bhushan, V., Gupta, A. K. & Khanna, D. N. 1985. Serum protein profile in normal pregnancy and in relation to parity. *Indian J Physiol Pharmacol*, 29, 227-33.

- Tarca, A. L., Romero, R., Bhatti, G., Gotsch, F., Done, B., Gudicha, D. W., Gallo, D. M., Jung, E., Pique-Regi, R., Berry, S. M., Chaiworapongsa, T. & Gomez-Lopez, N. 2022. Human Plasma Proteome During Normal Pregnancy. *Journal of Proteome Research*, 21, 2687-2702.
- Tayade, C., Esadeg, S., Fang, Y. & Croy, B. A. 2005. Functions of alpha 2 macroglobulins in pregnancy. *Molecular and Cellular Endocrinology*, 245, 60-66.
- Tchougounova, E., Lundequist, A., Fajardo, I., Winberg, J.-O., Åbrink, M. & Pejler, G. 2005. A Key Role for Mast Cell Chymase in the Activation of Pro-matrix Metalloprotease-9 and Promatrix Metalloprotease-2. *Journal of Biological Chemistry*, 280, 9291-9296.
- Tchougounova, E., Pejler, G. & Abrink, M. 2003. The chymase, mouse mast cell protease 4, constitutes the major chymotrypsin-like activity in peritoneum and ear tissue. A role for mouse mast cell protease 4 in thrombin regulation and fibronectin turnover. *J Exp Med*, 198, 423-31.
- Tejada, T., Tan, L., Torres, R. A., Calvert, J. W., Lambert, J. P., Zaidi, M., Husain, M., Berce, M. D., Naib, H., Pejler, G., Abrink, M., Graham, R. M., Lefer, D. J., Naqvi, N. & Husain, A. 2016. IGF-1 degradation by mouse mast cell protease 4 promotes cell death and adverse cardiac remodeling days after a myocardial infarction. *Proceedings of the National Academy of Sciences*, 113, 6949-6954.
- Teka, H., Yemane, A., Abraha, H. E., Berhe, E., Tadesse, H., Gebru, F., Yahya, M., Tadesse, Y., Gebre, D., Abrha, M., Tesfay, B., Tekle, A., Gebremariam, T., Amare, B., Ebrahim, M. M., Zelelow, Y. B. & Mulugeta, A. 2023. Clinical presentation, maternal-fetal, and neonatal outcomes of early-onset versus late onset preeclampsia-eclampsia syndrome in a teaching hospital in a low-resource setting: A retrospective cohort study. *PLOS ONE*, 18, e0281952.
- Than, G. N., Csaba, I. F., Szabó, D. G., Karg, N. J. & Novák, P. F. 1976. Quantitative Immunological study of pregnancy-associated alpha2-globulin antigen. *Vox Sang*, 30, 134-8.
- Thøgersen, I. B., Salvesen, G., Brucato, F. H., Pizzo, S. V. & Enghild, J. J. 1992. Purification and characterization of an α-macroglobulin proteinase inhibitor from the mollusc Octopus vulgaris. *Biochemical Journal*, 285, 521-527.
- Thul, P. J., Åkesson, L., Wiking, M., Mahdessian, D., Geladaki, A., Ait Blal, H., Alm, T., Asplund, A., Björk, L., Breckels, L. M., Bäckström, A., Danielsson, F., Fagerberg, L., Fall, J., Gatto, L., Gnann, C., Hober, S., Hjelmare, M., Johansson, F., Lee, S., Lindskog, C., Mulder, J., Mulvey, C. M., Nilsson, P., Oksvold, P., Rockberg, J., Schutten, R., Schwenk, J. M., Sivertsson, Å., Sjöstedt, E., Skogs, M., Stadler, C., Sullivan, D. P., Tegel, H., Winsnes, C., Zhang, C., Zwahlen, M., Mardinoglu, A., Pontén, F., von Feilitzen, K., Lilley, K. S., Uhlén, M. & Lundberg, E. 2017. A subcellular map of the human proteome. Science, 356, eaal3321.
- Tomoto, M., Mineharu, Y., Sato, N., Tamada, Y., Nogami-Itoh, M., Kuroda, M., Adachi, J., Takeda, Y., Mizuguchi, K., Kumanogoh, A., Natsume-Kitatani, Y. & Okuno, Y. 2024. Idiopathic pulmonary fibrosis-specific Bayesian network integrating extracellular vesicle proteome and clinical information. *Scientific Reports*, 14, 1315.
- Torres-Torres, J., Espino-y-Sosa, S., Martinez-Portilla, R., Borboa-Olivares, H., Estrada-Gutierrez, G., Acevedo-Gallegos, S., Ruiz-Ramirez, E., Velasco-Espin, M., Cerda-Flores, P., Ramirez-Gonzalez, A. & Rojas-Zepeda, L. 2024. A Narrative Review on the Pathophysiology of Preeclampsia. *International Journal of Molecular Sciences* [Online], 25.
- Travis, J. & Salvesen, G. S. 1983. Human plasma proteinase inhibitors. *Annu Rev Biochem*, 52, 655-709.

- Tycko, B. & Maxfield, F. R. 1982. Rapid acidification of endocytic vesicles containing alpha 2-macroglobulin. *Cell*, 28, 643-51.
- Tyrmi, J. S., Kaartokallio, T., Lokki, A. I., Jääskeläinen, T., Kortelainen, E., Ruotsalainen, S., Karjalainen, J., Ripatti, S., FINNPEC Study Group, FinnGen Project, Estonian Biobank Research Team, Laisk, T., Kettunen, J., Pouta, A., Kivinen, K., Kajantie, E., Heinonen, S., Kere, J. & Laivuori, H. 2022. GWAS of preeclampsia and hypertensive disorders of pregnancy uncovers genes related to cardiometabolic, endothelial and placental function. *medRxiv*, 2022.05.19.22275002.
- Tyrmi, J. S., Kaartokallio, T., Lokki, A. I., Jääskeläinen, T., Kortelainen, E., Ruotsalainen, S., Karjalainen, J., Ripatti, S., Kivioja, A., Laisk, T., Kettunen, J., Pouta, A., Kivinen, K., Kajantie, E., Heinonen, S., Kere, J., Laivuori, H., FINNPEC Study Group, F. P. & Team, t. E. B. R. 2023. Genetic Risk Factors Associated With Preeclampsia and Hypertensive Disorders of Pregnancy. *JAMA Cardiology*, 8, 674-683.
- Uhlén, M., Fagerberg, L., Hallström, B. M., Lindskog, C., Oksvold, P., Mardinoglu, A., Sivertsson, Å., Kampf, C., Sjöstedt, E., Asplund, A., Olsson, I., Edlund, K., Lundberg, E., Navani, S., Szigyarto, C. A.-K., Odeberg, J., Djureinovic, D., Takanen, J. O., Hober, S., Alm, T., Edqvist, P.-H., Berling, H., Tegel, H., Mulder, J., Rockberg, J., Nilsson, P., Schwenk, J. M., Hamsten, M., von Feilitzen, K., Forsberg, M., Persson, L., Johansson, F., Zwahlen, M., von Heijne, G., Nielsen, J. & Pontén, F. 2015. Tissue-based map of the human proteome. Science, 347, 1260419.
- Ulhaq, R. A., Anis, W., Fatmaningrum, W. & Akbar, M. I. A. 2021. Association between prepregnancy body mass index and gestational weight gain and the risk of preeclampsia: A systematic review and meta-analysis. *Asian Pacific Journal of Reproduction*, 10.
- Um, H.-C., Jang, J.-H., Kim, D.-H., Lee, C. & Surh, Y.-J. 2011. Nitric oxide activates Nrf2 through S-nitrosylation of Keap1 in PC12 cells. *Nitric Oxide*, 25, 161-168.
- Urata, H., Healy, B., Stewart, R. W., Bumpus, F. M. & Husain, A. 1990a. Angiotensin II-forming pathways in normal and failing human hearts. *Circ Res*, 66, 883-90.
- Urata, H., Kinoshita, A., Misono, K. S., Bumpus, F. M. & Husain, A. 1990b. Identification of a highly specific chymase as the major angiotensin II-forming enzyme in the human heart. *Journal of Biological Chemistry*, 265, 22348-22357.
- Valnickova, Z., Thøgersen, I. B., Christensen, S., Chu, C. T., Pizzo, S. V. & Enghild, J. J. 1996. Activated Human Plasma Carboxypeptidase B Is Retained in the Blood by Binding to α2-Macroglobulin and Pregnancy Zone Protein. *Journal of Biological Chemistry*, 271, 12937-12943.
- Van Gool, D., de Strooper, B., Van Leuven, F., Triau, E. & Dom, R. 1993. α2-macroglobulin expression in neuritic-type plaques in patients with Alzheimer's disease. *Neurobiology of Aging*, 14, 233-237.
- Van Leuven, F. & Cassiman, J. J. 1980. Receptor-mediated Uptake of α2Macroglobulin-protease Complexes by Cultured Cells. *In:* DE BRABANDER, M., MAREEL, M. & DE RIDDER, L. (eds.) *Cell Movement and Neoplasia*. Pergamon.
- Van Rompaey, L. & Marynen, P. 1994. Temperature-Dependent Biosynthesis of Thiol Esters in Baculovirus Recombinant α2M and PZP. *Annals of the New York Academy of Sciences*, 737, 506-509.
- Vandooren, J. & Itoh, Y. 2021. Alpha-2-Macroglobulin in Inflammation, Immunity and Infections. *Frontiers in Immunology*, 12.
- Varadi, M., Anyango, S., Deshpande, M., Nair, S., Natassia, C., Yordanova, G., Yuan, D., Stroe, O., Wood, G., Laydon, A., Žídek, A., Green, T., Tunyasuvunakool, K., Petersen, S., Jumper, J., Clancy, E., Green, R., Vora, A., Lutfi, M., Figurnov, M., Cowie, A., Hobbs, N., Kohli, P., Kleywegt, G., Birney, E., Hassabis, D. & Velankar, S. 2021. AlphaFold Protein Structure

- Database: massively expanding the structural coverage of protein-sequence space with high-accuracy models. *Nucleic Acids Research*, 50, D439-D444.
- Varma, V. R., Varma, S., An, Y., Hohman, T. J., Seddighi, S., Casanova, R., Beri, A., Dammer, E. B., Seyfried, N. T., Pletnikova, O., Moghekar, A., Wilson, M. R., Lah, J. J., O'Brien, R. J., Levey, A. I., Troncoso, J. C., Albert, M. S., Thambisetty, M., Predictors of Cognitive Decline Among Normal, I. & the Alzheimer's Disease Neuroimaging Initiative, s. 2017. Alpha-2 macroglobulin in Alzheimer's disease: a marker of neuronal injury through the RCAN1 pathway. *Molecular Psychiatry*, 22, 13-23.
- von Dadelszen, P., Syngelaki, A., Akolekar, R., Magee, L. A. & Nicolaides, K. H. 2023. Preterm and term pre-eclampsia: Relative burdens of maternal and perinatal complications. *Bjog*, 130, 524-530.
- von Schoultz, B. 1974. A quantitative study of the pregnancy zone protein in the sera of pregnant and puerperal women. *American Journal of Obstetrics and Gynecology*, 119, 792-797.
- Vreeke, G. J. C., Vincken, J.-P. & Wierenga, P. A. 2023. The path of proteolysis by bovine chymotrypsin. *Food Research International*, 165, 112485.
- Wajapeyee, N., Wang, S. Z., Serra, R. W., Solomon, P. D., Nagarajan, A., Zhu, X. & Green, M. R. 2010. Senescence induction in human fibroblasts and hematopoietic progenitors by leukemogenic fusion proteins. *Blood*, 115, 5057-60.
- Wallukat, G., Homuth, V., Fischer, T., Lindschau, C., Horstkamp, B., Jüpner, A., Baur, E., Nissen, E., Vetter, K., Neichel, D., Dudenhausen, J. W., Haller, H. & Luft, F. C. 1999. Patients with preeclampsia develop agonistic autoantibodies against the angiotensin AT1 receptor. *The Journal of Clinical Investigation*, 103, 945-952.
- Walter, M., Sutton, R. M. & Schechter, N. M. 1999. Highly Efficient Inhibition of Human Chymase by α(2)-Macroglobulin. *Archives of Biochemistry and Biophysics*, 368, 276-284.
- Wang, J., Zhang, P., Liu, M., Huang, Z., Yang, X., Ding, Y., Liu, J., Cheng, X., Xu, S., He, M., Zhang, F., Wang, G., Li, R. & Yang, X. 2023. Alpha-2-macroglobulin is involved in the occurrence of early-onset pre-eclampsia via its negative impact on uterine spiral artery remodeling and placental angiogenesis. *BMC Med*, 21, 90.
- Wang, S., Wei, X., Zhou, J., Zhang, J., Li, K., Chen, Q., Terek, R., Fleming, B. C., Goldring, M. B., Ehrlich, M. G., Zhang, G. & Wei, L. 2014. Identification of α2-Macroglobulin as a Master Inhibitor of Cartilage-Degrading Factors That Attenuates the Progression of Posttraumatic Osteoarthritis. Arthritis & Rheumatology, 66, 1843-1853.
- Wang, Y., Gu, Y., Lewis, D. F., Alexander, J. S. & Granger, D. N. 2010. Elevated Plasma Chymotrypsin-like Protease (Chymase) Activity in Women with Preeclampsia. *Hypertension in Pregnancy*, 29, 253-261.
- Wang, Y., Gu, Y., Zhang, Y., Lewis, D. F., Alexander, J. S. & Granger, D. N. 2007. Increased Chymotrypsin-like Protease (chymase) Expression and Activity in Placentas from Women with Preeclampsia. *Placenta*, 28, 263-269.
- Wavrant-DeVrièze, F., Rudrasingham, V., Lambert, J.-C., Chakraverty, S., Kehoe, P., Crook, R., Amouyel, P., Wu, W., Holmans, P., Rice, F., Pérez-Tur, J., Frigard, B., Morris, J. C., Carty, S., Cottel, D., Tunstall, N., Lovestone, S., Petersen, R. C., Chartier-Harlin, M.-C., Goate, A., Owen, M. J., Williams, J. & Hardy, J. 1999. No association between the alpha-2 macroglobulin I1000V polymorphism and Alzheimer's disease. *Neuroscience Letters*, 262, 137-139.
- Webster, K., Fishburn, S., Maresh, M., Findlay, S. C. & Chappell, L. C. 2019. Diagnosis and management of hypertension in pregnancy: summary of updated NICE guidance. *Bmj*, 366, l5119.
- Wei, Y., He, A., Huang, Z., Liu, J. & Li, R. 2022. Placental and plasma early predictive biomarkers for gestational diabetes mellitus. *PROTEOMICS Clinical Applications*, 16, 2200001.

- Wessel, B. M., Castro, J. N. & Roberts, V. H. J. 2024. Trophoblast Organoids: Capturing the Complexity of Early Placental Development In Vitro. *Organoids*, 3, 174-193.
- Westergaard, D., Lundgaard, A. T., Vomstein, K., Fich, L., Hviid, K. V. R., Egerup, P., Christiansen, A.-M. H., Nielsen, J. R., Lindman, J., Holm, P. C., Hartwig, T. S., Jørgensen, F. S., Zedeler, A., Kolte, A. M., Westh, H., Jørgensen, H. L., la Cour Freiesleben, N., Banasik, K., Brunak, S. & Nielsen, H. S. 2024. Immune changes in pregnancy: associations with pre-existing conditions and obstetrical complications at the 20th gestational week—a prospective cohort study. *BMC Medicine*, 22, 583.
- Westergaard, J. G., Bach, A., Teisner, B., Hau, J. & Grudzinskas, J. G. 1982. Circulating human pregnancy zone protein and oestriol in twin pregnancies. *Reproduction*, 66, 695-698.
- Widmer, M., Cuesta, C., Khan, K. S., Conde-Agudelo, A., Carroli, G., Fusey, S., Karumanchi, S. A., Lapaire, O., Lumbiganon, P., Sequeira, E., Zavaleta, N., Frusca, T., Gülmezoglu, A. M. & Lindheimer, M. D. 2015. Accuracy of angiogenic biomarkers at ≤20weeks' gestation in predicting the risk of pre-eclampsia: A WHO multicentre study. *Pregnancy Hypertension: An International Journal of Women's Cardiovascular Health*, 5, 330-338.
- Williams, P. J., Mistry, H. D., Innes, B. A., Bulmer, J. N. & Broughton Pipkin, F. 2010. Expression of AT1R, AT2R and AT4R and Their Roles in Extravillous Trophoblast Invasion in the Human. *Placenta*, 31, 448-455.
- Willinger, M., Ko, C.-W. & Reddy, U. M. 2009. Racial disparities in stillbirth risk across gestation in the United States. *American Journal of Obstetrics and Gynecology*, 201, 469.e1-469.e8.
- Woidacki, K., Popovic, M., Metz, M., Schumacher, A., Linzke, N., Teles, A., Poirier, F., Fest, S., Jensen, F., Rabinovich, G. A., Maurer, M. & Zenclussen, A. C. 2013. Mast cells rescue implantation defects caused by c-kit deficiency. *Cell Death & Disease*, 4, e462-e462.
- Wollenberg, G. K., LaMarre, J., Rosendal, S., Gonias, S. L. & Hayes, M. A. 1991. Binding of tumor necrosis factor alpha to activated forms of human plasma alpha 2 macroglobulin. *Am J Pathol*, 138, 265-72.
- Wu, M., Lan, H., Ye, Z. & Wang, Y. 2021. Hypermethylation of the PZP gene is associated with hepatocellular carcinoma cell proliferation, invasion and migration. FEBS Open Bio, 11, 826-832.
- Wu, S. M., Boyer, C. M. & Pizzo, S. V. 1997. The Binding of Receptor-recognized α2-Macroglobulin to the Low Density Lipoprotein Receptor-related Protein and the α2M Signaling Receptor Is Decoupled by Oxidation\*. *Journal of Biological Chemistry,* 272, 20627-20635.
- Wu, S. M., Patel, D. D. & Pizzo, S. V. 1998. Oxidized α2-macroglobulin (α2M) differentially regulates receptor binding by cytokines/growth factors: Implications for tissue injury and repair mechanisms in inflammation. *Journal of Immunology*, 161, 4356-4365.
- Wyatt, A. R., Constantinescu, P., Ecroyd, H., Dobson, C. M., Wilson, M. R., Kumita, J. R. & Yerbury, J. J. 2013a. Protease-activated alpha-2-macroglobulin can inhibit amyloid formation via two distinct mechanisms. *FEBS Letters*, 587, 398-403.
- Wyatt, A. R., Kumita, J. R., Farrawell, N. E., Dobson, C. M. & Wilson, M. R. 2015. Alpha-2-Macroglobulin Is Acutely Sensitive to Freezing and Lyophilization: Implications for Structural and Functional Studies. *PLOS ONE*, 10, e0130036.
- Wyatt, A. R., Kumita, J. R., Mifsud, R. W., Gooden, C. A., Wilson, M. R. & Dobson, C. M. 2014. Hypochlorite-induced structural modifications enhance the chaperone activity of human 2-macroglobulin. *Proceedings of the National Academy of Sciences*, 111, E2081-E2090.
- Wyatt, A. R. & Wilson, M. R. 2013. Acute phase proteins are major clients for the chaperone action of α2-macroglobulin in human plasma. *Cell Stress and Chaperones*, 18, 161-170.

- Wyatt, A. R., Yerbury, J. J., Berghofer, P., Greguric, I., Katsifis, A., Dobson, C. M. & Wilson, M. R. 2011. Clusterin facilitates in vivo clearance of extracellular misfolded proteins. *Cell Mol Life Sci*, 68, 3919-31.
- Wyatt, A. R., Yerbury, J. J., Ecroyd, H. & Wilson, M. R. 2013b. Extracellular Chaperones and Proteostasis. *Annual Review of Biochemistry*, 82, 295-322.
- Xu, X., Wang, Y., Wang, L., Liao, Q., Chang, L., Xu, L., Huang, Y., Ye, H., Xu, L., Chen, C., Shen, X., Zhang, F., Ye, M., Wang, Q. & Duan, S. 2013. Meta-Analyses of 8 Polymorphisms Associated with the Risk of the Alzheimer's Disease. *PLOS ONE*, 8, e73129.
- Xuan, C., Li, H., Li, L.-L., Tian, Q.-W., Wang, Q., Zhang, B.-B., Guo, J.-J., He, G.-W. & Lun, L.-M. 2019. Screening and Identification of Pregnancy Zone Protein and Leucine-Rich Alpha-2-Glycoprotein as Potential Serum Biomarkers for Early-Onset Myocardial Infarction using Protein Profile Analysis. *PROTEOMICS Clinical Applications*, 13, 1800079.
- Yan, Q., Blue, N. R., Truong, B., Zhang, Y., Guerrero, R. F., Liu, N., Honigberg, M. C., Parry, S., McNeil, R. B., Simhan, H. N., Chung, J., Mercer, B. M., Grobman, W. A., Silver, R., Greenland, P., Saade, G. R., Reddy, U. M., Wapner, R. J. & Haas, D. M. 2024. Genetic Associations with Placental Proteins in Maternal Serum Identify Biomarkers for Hypertension in Pregnancy. *medRxiv*.
- Yanbaeva, D. G., Dentener, M. A., Creutzberg, E. C., Wesseling, G. & Wouters, E. F. M. 2007. Systemic Effects of Smoking. *Chest*, 131, 1557-1566.
- Yang, J., Fang, W., Wu, W., Tian, Z., Gao, R., Yu, L., Chen, D., Weng, X., Zhu, S. & Yang, C. 2021a. A Novel Diagnostic Biomarker, PZP, for Detecting Colorectal Cancer in Type 2 Diabetes Mellitus Patients Identified by Serum-Based Mass Spectrometry. Frontiers in Molecular Biosciences, 8.
- Yang, J., Yang, C., Shen, H., Wu, W., Tian, Z., Xu, Q., Cao, C., Ye, S., Ban, L., Tong, X. & Mei, J. 2021b. Discovery and validation of PZP as a novel serum biomarker for screening lung adenocarcinoma in type 2 diabetes mellitus patients. *Cancer Cell International*, 21, 162.
- Yart, L., Roset Bahmanyar, E., Cohen, M. & Martinez de Tejada, B. 2021. Role of the Uteroplacental Renin-Angiotensin System in Placental Development and Function, and Its Implication in the Preeclampsia Pathogenesis. *Biomedicines*, 9.
- Yerbury, J. J., Kumita, J. R., Meehan, S., Dobson, C. M. & Wilson, M. R. 2009. α2-Macroglobulin and Haptoglobin Suppress Amyloid Formation by Interacting with Prefibrillar Protein Species. *Journal of Biological Chemistry*, 284, 4246-4254.
- Yerbury, J. J. & Wilson, M. R. 2010. Extracellular chaperones modulate the effects of Alzheimer's patient cerebrospinal fluid on Aβ1-42 toxicity and uptake. *Cell Stress and Chaperones*, 15, 115-121.
- Yin, Y., Qu, L., Zhu, D., Wu, Y. & Zhou, X. 2021. Effect of SOCS3 on apoptosis of human trophoblasts via adjustment of the JAK2/STAT3 signaling pathway in preterm birth. *Transl Pediatr*, 10, 1637-1646.
- Yoshino, S., Fujimoto, K., Takada, T., Kawamura, S., Ogawa, J., Kamata, Y., Kodera, Y. & Shichiri, M. 2019. Molecular form and concentration of serum α2-macroglobulin in diabetes. *Scientific Reports*, 9, 12927.
- Zeisler, H., Llurba, E., Chantraine, F., Vatish, M., Staff, A. C., Sennström, M., Olovsson, M., Brennecke, S. P., Stepan, H., Allegranza, D., Dilba, P., Schoedl, M., Hund, M. & Verlohren, S. 2016. Predictive Value of the sFlt-1:PlGF Ratio in Women with Suspected Preeclampsia. *N Engl J Med*, 374, 13-22.
- Zenclussen, A. C. & Hämmerling, G. J. 2015. Cellular Regulation of the Uterine Microenvironment That Enables Embryo Implantation. *Frontiers in Immunology,* 6.

- Zhang, H., Liu, D., Duan, Y., Liu, Y., Liu, J., Bai, N., Zhou, Q., Xu, Z., Li, L. & Liu, H. 2023a. Alpha 2-Macroglobulin Polymorphisms and Susceptibility to Alzheimer's Disease: A Comprehensive Meta-Analysis Based on 62 Studies. *J Alzheimers Dis Rep*, 7, 1351-1370.
- Zhang, J. X., Zhang, J., Yan, W., Wang, Y. Y., Han, L., Yue, X., Liu, N., You, Y. P., Jiang, T., Pu, P. Y. & Kang, C. S. 2013. Unique genome-wide map of TCF4 and STAT3 targets using ChIP-seq reveals their association with new molecular subtypes of glioblastoma. *Neuro Oncol*, 15, 279-89.
- Zhang, L., Li, W., Chi, X., Sun, Q., Li, Y., Xing, W. & Ding, G. 2025. Predictive performance of sFlt-1, PlGF and the sFlt-1/PlGF ratio for preeclampsia: A systematic review and meta-analysis. *J Gynecol Obstet Hum Reprod*, 54, 102925.
- Zhang, L., Liu, J., Feng, X. & Lash, G. E. 2023b. Unraveling the mysteries of spiral artery remodeling. *Placenta*, 141, 51-56.
- Zhang, N., Schumacher, A., Fink, B., Bauer, M., Zenclussen, A. C. & Meyer, N. 2022. Insights into Early-Pregnancy Mechanisms: Mast Cells and Chymase CMA1 Shape the Phenotype and Modulate the Functionality of Human Trophoblast Cells, Vascular Smooth-Muscle Cells and Endothelial Cells. *Cells*, 11, 1158.
- Zhang, Y., Wei, X., Browning, S., Scuderi, G., Hanna, L. S. & Wei, L. 2017. Targeted designed variants of alpha-2-macroglobulin (A2M) attenuate cartilage degeneration in a rat model of osteoarthritis induced by anterior cruciate ligament transection. *Arthritis Research & Therapy*, 19, 175.
- Zhao, D., Shen, L., Wei, Y., Xie, J., Chen, S., Liang, Y., Chen, Y. & Wu, H. 2017. Identification of candidate biomarkers for the prediction of gestational diabetes mellitus in the early stages of pregnancy using iTRAQ quantitative proteomics. *PROTEOMICS Clinical Applications*, 11, 1600152.
- Zhao, W., Oskeritzian, C. A., Pozez, A. L. & Schwartz, L. B. 2005. Cytokine Production by Skin-Derived Mast Cells: Endogenous Proteases Are Responsible for Degradation of Cytokines 1. *The Journal of Immunology,* 175, 2635-2642.
- Zhou, J., Sheridan, M. A., Tian, Y., Dahlgren, K. J., Messler, M., Peng, T., Zhao, A., Ezashi, T., Schulz, L. C., Ulery, B. D., Roberts, R. M. & Schust, D. J. 2025. Development of apical out trophoblast stem cell derived organoids to model early human pregnancy. *iScience*, 28.
- Zhu, M., Zhao, B., Wei, L. & Wang, S. 2021. alpha-2-Macroglobulin, a Native and Powerful Proteinase Inhibitor, Prevents Cartilage Degeneration Disease by Inhibiting Majority of Catabolic Enzymes and Cytokines. *Current Molecular Biology Reports*, 7, 1-7.
- Zvonic, S., Lefevre, M., Kilroy, G., Floyd, Z. E., DeLany, J. P., Kheterpal, I., Gravois, A., Dow, R., White, A., Wu, X. & Gimble, J. M. 2007. Secretome of Primary Cultures of Human Adipose-derived Stem Cells: Modulation of Serpins by Adipogenesis. *Molecular & Cellular Proteomics*, 6, 18-28.